



3 1176 00116 7387

NACA RM A55F16

~~CONFIDENTIAL~~

Copy 14

RM A55F16

C.10



# RESEARCH MEMORANDUM

AERODYNAMIC PRINCIPLES FOR THE DESIGN OF  
JET-ENGINE INDUCTION SYSTEMS

By Wallace F. Davis and Richard Scherrer

Ames Aeronautical Laboratory  
Moffett Field, Calif.

CLASSIFICATION CHANGED

UNCLASSIFIED

Notice of N.A.S.A. Class. Change  
Notices No. 13, dtd Apr. 14, 1965.  
HAR-5-12-65.

CLASSIFIED DOCUMENT

This material contains information affecting the National Defense of the United States within the meaning of the espionage laws, Title 18, U.S.C., Secs. 793 and 794, the transmission or revelation of which in any manner to an unauthorized person is prohibited by law.

**NATIONAL ADVISORY COMMITTEE  
FOR AERONAUTICS**

**WASHINGTON**

February 27, 1956

~~CONFIDENTIAL~~

64/94

TABLE OF CONTENTS

	Page
I. INTRODUCTION . . . . .	1
II. DEFINITIONS . . . . .	3
AIR-INDUCTION SYSTEM . . . . .	3
DIVISION OF FORCES . . . . .	4
PERFORMANCE PARAMETERS . . . . .	9
PRESSURE RECOVERY . . . . .	9
DRAG . . . . .	11
MASS FLOW . . . . .	12
III. PRELIMINARY CONSIDERATIONS . . . . .	13
AIRCRAFT REQUIREMENTS . . . . .	13
AIRFRAME-INDUCTION-SYSTEM COMBINATION . . . . .	14
ENGINE-INDUCTION-SYSTEM COMBINATION . . . . .	15
MATCHING . . . . .	16
OPTIMIZATION . . . . .	19
FLOW UNIFORMITY AND STEADINESS . . . . .	20
IV. DETAIL CONSIDERATIONS . . . . .	22
INDUCTION . . . . .	22
PRESSURE RECOVERY AND FLOW UNIFORMITY . . . . .	23
Ducts . . . . .	23
Area ratio . . . . .	23
Skin friction losses . . . . .	24
Flow separation . . . . .	25
Design . . . . .	27
Subsonic Flight . . . . .	31
Lip design . . . . .	33
Angle of attack . . . . .	36
Inlet asymmetry . . . . .	37
Supersonic Flight . . . . .	37
Supersonic compression . . . . .	38
Limiting internal contraction . . . . .	40
Limiting inlet Mach number . . . . .	43
Boundary-layer shock-wave interaction . . . . .	45
Lip design . . . . .	47
Mass-flow variation . . . . .	48
Angle of attack . . . . .	51
DRAG . . . . .	52
Subsonic Flight . . . . .	53
Supersonic Flight . . . . .	56
External wave drag with no spillage . . . . .	57
External profile . . . . .	61
Additive drag . . . . .	63
Change in external wave drag . . . . .	64
Lip bluntness . . . . .	65
Net wave drag . . . . .	66

## TABLE OF CONTENTS - Concluded

	Page
FLOW STEADINESS . . . . .	68
Subsonic Flight . . . . .	68
Choked flow . . . . .	68
Duct rumble . . . . .	69
Twin-duct instability . . . . .	70
Supersonic Flight . . . . .	71
Causes of unsteadiness . . . . .	71
Character of unsteadiness . . . . .	73
Prevention of unsteadiness . . . . .	74
INTERFERENCE . . . . .	76
AIRCRAFT-INDUCTION SYSTEM . . . . .	77
Effects of Inlet Location . . . . .	77
Subsonic flight . . . . .	77
Supersonic flight . . . . .	79
Induced Effects of Angle of Attack . . . . .	81
Bodies . . . . .	81
Wings . . . . .	84
Effects of Forebody Boundary Layer . . . . .	86
Boundary-Layer Removal . . . . .	87
Suction . . . . .	88
Diversion . . . . .	89
Submerged inlets . . . . .	92
Combined Effects . . . . .	93
Scoop incremental drag . . . . .	93
Wakes . . . . .	94
INDUCTION-SYSTEM AIRCRAFT . . . . .	94
Drag . . . . .	95
Skin friction and separation . . . . .	95
Transonic drag rise . . . . .	95
Wave drag . . . . .	96
Lift and Pitching Moment . . . . .	98
Wing leading-edge inlets . . . . .	99
Wing-root inlets . . . . .	99
Scoops . . . . .	100
Nacelles . . . . .	101
APPENDIX A - SYMBOLS . . . . .	104
APPENDIX B . . . . .	108
REFERENCES . . . . .	113
BIBLIOGRAPHY . . . . .	138
FIGURES . . . . .	171

NACA RM A55F16

## NATIONAL ADVISORY COMMITTEE FOR AERONAUTICS

RESEARCH MEMORANDUMAERODYNAMIC PRINCIPLES FOR THE DESIGN OF  
JET-ENGINE INDUCTION SYSTEMS

By Wallace F. Davis and Richard Scherrer

## I. INTRODUCTION

An air-induction system conveys air from the atmosphere to the engine of an aircraft. Its purpose is to supply, under all flight conditions, the air needed for best operation of the engine with the least disturbance to the external flow. In other words, to avoid penalties in engine size, weight, and fuel consumption, an induction system must supply air at the maximum pressure and with the least drag and adverse interference possible. The flow to the engine must be sufficiently uniform and steady to maintain engine performance and to avoid vibration and structural failure. The significance of the air-induction system in high-speed-aircraft design has been well illustrated by Sulkin in reference 1. It is shown that for fighter aircraft flying at Mach numbers less than about 1.1, the pressure losses through a typical normal-shock inlet cause a loss in engine thrust that is equivalent to less than 10 percent of the wing drag; whereas, at a Mach number of 1.6, these pressure losses reduce the engine thrust force by an amount equal to the wing drag.

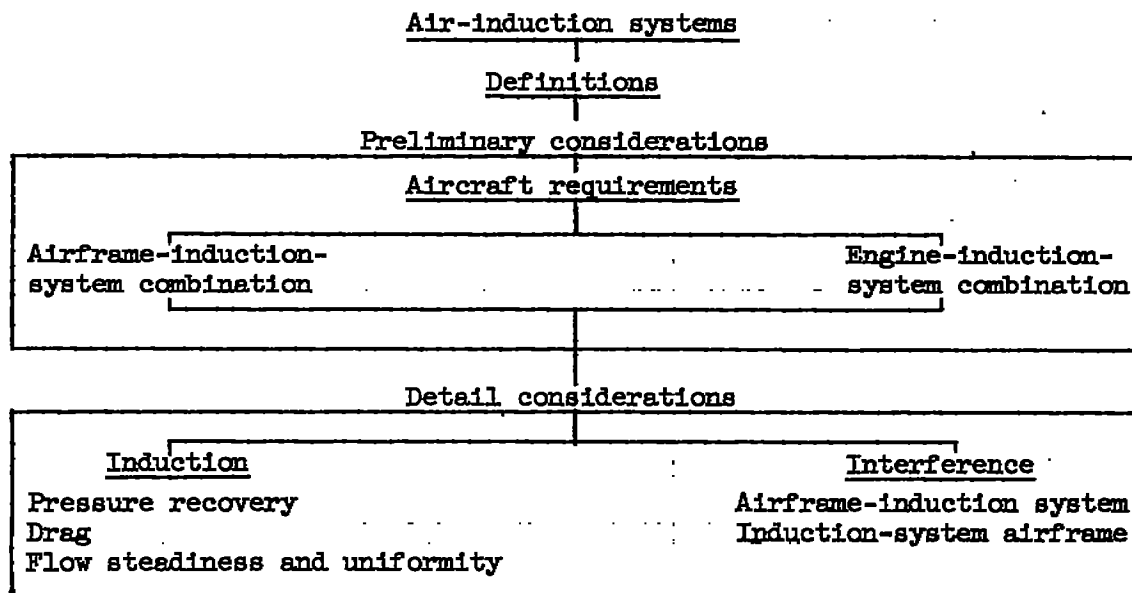
A sizable quantity of research has been directed toward finding solutions to the problems of air-induction systems, particularly in the Mach number range from 0 to 2; but the results have not been consolidated into an organized group of design principles. Küchemann and Weber have written a textbook on propulsion (ref. 2) and present some discussion of air induction. However, further consolidation of information is required, particularly for supersonic aircraft. It is the purpose of this report to assemble principles of induction-system design for flight to a Mach number of 2 and to use existing data to show the consequences of compromising them. In order to accomplish this task it was necessary to make an extensive search of existing literature on air-induction systems. A bibliography based on this search is appended to the present report. The bibliography lists reports published since 1948 and thus extends the bibliography of reference 3. The authors acknowledge with gratitude the assistance given by Mr. Emmet A. Mossman, Mr. Forrest E. Gowen, and Mr. Warren E. Anderson in carrying out the literature search and in making other contributions to this report.



The design of an air-induction system for an aircraft is greatly influenced by the design of both the airframe and the engine, and the performance of airframe and engine can be seriously affected by the induction system. Therefore, the problems of air induction must be considered from an over-all viewpoint, and a broad outline must be selected to relate design principles. In this report, the problems of air-induction systems are arranged according to the following outline, and the principles that have been established for their solution are presented under the appropriate problem headings.

- A. Definitions are presented to describe the forces involved and the terminology used in air-induction-system design.
- B. The relationships of the induction system to both airframe and engine are discussed to indicate the preliminary design considerations.
- C. The detail design problems of ensuring high performance of an isolated air-induction system and then of maintaining this performance when in combination with other aircraft components are discussed under two headings:
  1. Induction, that is, the pressure-recovery, drag, flow-uniformity, and flow-steadiness problems encountered in supplying air to an engine.
  2. Interference, or how other parts of an airframe affect the induction system and vice versa.

This arrangement is illustrated by the following chart:

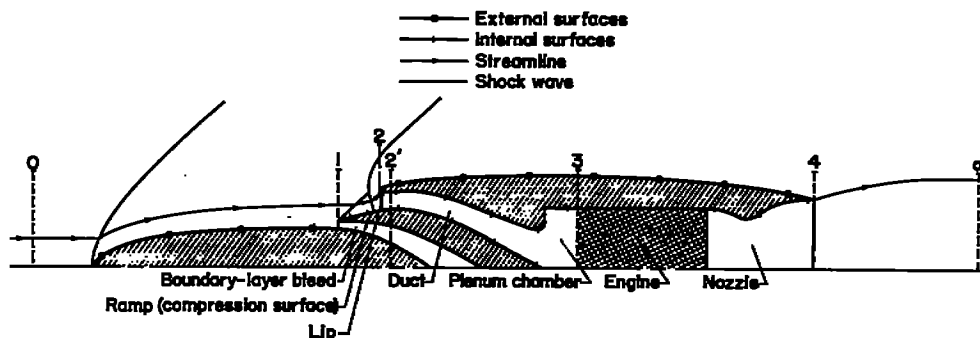


## II. DEFINITIONS

In order to discuss induction-system design over a wide range of operating conditions, it is necessary to have a consistent terminology. The definitions that have been selected for use in this report have all been used previously; and in the many instances where several terms have been used by various investigators to indicate the same concept, the choice made here is based upon considerations of consistency, popular usage, and convenience.

### AIR-INDUCTION SYSTEM

To define the major factors involved, consider the general arrangement of the following sketch:



Sketch (1)

The air-induction system (stations 1 to 3) is a part of the propulsion system (stations 1 to 4) and is defined to be that portion of an aircraft whose purpose is to convey air from the atmosphere to an engine. The induction system includes any measures taken to compress or divide the oncoming air stream that eventually flows through the engine, such as the ramp and boundary-layer bleed (stations 1 to 2) shown in the sketch. The inlet is at station 2, and the inlet area is measured in a plane tangent to the most upstream point of the lip and normal to the mean flow direction in this plane at maximum mass flow and zero angle of attack. If the entire cowl lip does not lie in the inlet plane, the inlet area is taken as the area outlined by the forwardmost points on the lips projected onto the inlet plane. For particularly distorted inlet shapes, these definitions are not always applicable; in such cases, an area should be

chosen which is the most representative in terms of induction-system performance. Many specific definitions of inlet area have been employed in the literature; two of these which are particularly useful are the capture area, the axial projection of the inlet area and compression-surface frontal area onto the plane of station 1, and the minimum cross-section area, station 2'. Each of these definitions is convenient in certain cases, and they are identical for sharp-lip normal-shock inlets. The duct (stations 2' to 3) in the general case includes an area and shape variation along its length, bends, and a plenum chamber. The engine intake is at station 3 and is considered to be upstream of all components that are normally supplied with an engine and that are present when static tests of the engine are made. It is thus ahead of screens and swirl vanes. The inlet lip and the fairing of external surfaces into other parts of the aircraft are considered to be problems of the induction system.

Generally speaking, there are two characteristics used to identify air-induction systems; namely, the location of the inlet on an aircraft and the method used to produce compression upstream of the inlet. For example, induction systems are denoted by such terms as nose, side scoop, wing-root, conical-shock, or internal-contraction inlets; and these expressions are combined for more complete designations.

#### DIVISION OF FORCES

The division of forces between a propulsive unit and other parts of an aircraft must be carefully defined to ensure consistency. (See ref. 4, for example.) The air that flows through a jet-propulsion system is compressed, heated, and then expanded to atmospheric pressure with the reaction from the ensuing acceleration of the gases used to overcome the restraining forces of pressure and friction and to accelerate the aircraft. The division of the component forces that are included in these thrust and drag forces is, to a large extent, arbitrary, but for practical reasons specific definitions must be selected. The engine designer, having no knowledge of the airframes in which an engine might be installed, defines engine thrust with quantities that are independent of installation conditions. The term used to describe the propelling force of an isolated engine is the "net thrust" which is the rate of change of total momentum (pressure plus momentum flux) of the gases handled by the engine from the free stream to the tail-pipe exit. The aircraft designer defines the force available to accelerate an aircraft, that is, the net propulsive force, as the sum of all the forces, friction and pressure, in the flight direction that act on all the surfaces of the aircraft (both internal and external) that are exposed to the flow of air. In using engine information to calculate this net propulsive force, the designer must be consistent because it is assumed in the engine data that the propulsive system receives air with free-stream momentum, but in an aircraft installation this is generally not so. A correction must be made for the difference

between the free-stream and inlet total momentum in order to obtain the net propulsive force. The following discussion illustrates the considerations which are involved.

The net thrust force of an engine is defined as (see Appendix A for definitions of symbols and sketch (1) for the positions indicated by the numerical subscripts)

$$F_n = m_4 V_4 - m_0 V_0 + A_4(p_4 - p_0) \quad (1)$$

It is assumed in this equation that the velocity and pressure distribution at stations 0 and 4 are uniform and steady and that  $A_4$  is normal to the flight direction. The net propulsive force of an aircraft is defined as

$$F_{np} = \left[ \int_{A_{in}} (p - p_0) dA - Dv_{in} \right] - \left[ \int_{A_{ex}} (p - p_0) dA + Dv_{ex} \right] \quad (2)$$

Here, the pressure forces  $\int (p - p_0) dA$  and the viscous forces  $(Dv)$  are the components in the flight direction, and they are divided between internal and external surfaces,  $A_{in}$  and  $A_{ex}$ . A force tending to accelerate in the flight direction is considered positive; thus the reaction from the accelerated gases of a jet engine causes a positive pressure difference and a resultant positive force on the internal surfaces  $A_{in}$ . The internal surfaces include those of the air-induction system (that is, from the stagnation point on the leading edge of the ramp and from the stagnation point on the inlet lip to the engine intake, station 3, in sketch (1)) and the engine and nozzle passages to the exit. The external surfaces  $A_{ex}$  are those in sketch (1) from the forebody nose to station 1 and from the stagnation point on the lip to station 4.

The first bracketed term of equation (2) less the force on the ramp is, according to the momentum theorem, equal to the rate of momentum change between the exit and the plane which includes the stagnation points on the inlet lip (for a three-dimensional inlet)

$$\left[ \int_{A_{in}} (p - p_0) dA - Dv_{in} \right] - (-F_r) = m_4 V_4 + A_4(p_4 - p_0) - M_I \quad (3)$$

where

$$M_I = \int_{A_I} \rho_I V_I^2 dA + \int_{A_I} (p_I - p_0) dA$$

$A_I$  area in the plane through the entry section enclosed by the stagnation points of the internal flow on the lip; this plane is here assumed normal to the flight direction, and flow-inclination angles are assumed to be negligibly small

$F_r$  sum of the pressure and friction forces in the flight direction acting on the ramp; it is a negative force.

To utilize  $F_n$  in determining  $F_{np}$ , the equation for the former can be rewritten as the sum of the rates of momentum change of the gases handled by the engine between the exit and station  $A_I$  and from  $A_I$  to the free stream

$$F_n = m_4 V_4 + A_4 (p_4 - p_0) - M_I + M_I - m_0 V_0 \quad (4)$$

From equation (3),

$$F_n = \left[ \int_{A_{in}} (p - p_0) dA - Dv_{in} \right] + F_r + M_I - m_0 V_0$$

so, substituting in equation (2)

$$F_{np} = F_n - (M_I - m_0 V_0) - F_r - \left[ \int_{A_{ex}} (p - p_0) dA + Dv_{ex} \right]$$

or

$$F_{np} = F_n - \left[ \int_{A_{ex}} (p - p_0) dA + Dv_{ex} + (M_I - m_0 V_0) + F_r \right] \quad (5)$$

According to the momentum theorem, the rate of change of momentum through the boundary about a definite volume of fluid is equal to the resultant of the pressure integral over the free-fluid surface and the forces acting on the fluid due to solid surfaces. (This statement of the theorem assumes steady flow and no shear forces on the free-fluid surface.) For the streamtube between  $A_I$  and the free stream,

$$\int_{A_I} \rho_I V_I^2 dA + \int_{A_I} (p_I - p_0) dA - m_0 V_0 = \int_0^{A_I} (p - p_0) dA - F_B - F_r$$

F

NACA RM A55F16.

7

or

$$M_I - m_0 V_0 = \int_0^{A_I} (p - p_0) dA - F_B - F_r \quad (6)$$

where  $F_B$  is the body force between the nose and station 1 in sketch (1) acting on the air which eventually flows through the engine. If the air-induction system has a boundary-layer bleed, as in sketch (1), which prevents the boundary layer from the forebody from entering the inlet,  $M_I$  would not include any of the momentum decrement of this boundary layer, so  $F_B$  should then represent only the pressure drag on the strip of external body surface which is affected by the flow to the engine. Substituting equation (6) into equation (5) gives the final relationship

$$F_{np} = F_n - \left[ \int_{A_{ex}} (p - p_0) dA + D_{V_{ex}} + \int_0^{A_I} (p - p_0) dA - F_B \right] \quad (7)$$

In subsonic flight, when the flow is neither separated nor anywhere supersonic, the determination of net propulsive force is somewhat simplified. For such conditions, the flow outside the boundary layer can be considered irrotational, and D'Alembert's theorem states that for a body about which the streamlines close, the component of the pressure integral in the flight direction must be zero over a bounding streamtube from the upstream station at which the flow is undisturbed to the similar downstream station provided, in the case of a three-dimensional body, that it carries no lift. Assuming for ease of explanation that the external flow reaches ambient pressure at station 4 and that sketch (1) is axially symmetric, it follows that

$$\int_0^{A_I} (p - p_0) dA + \int_{A_I}^4 (p - p_0) dA = 0$$

Restating the terms of equation (7) in smaller components

$$F_{np} = F_n - \left[ \int_B (p - p_0) dA + \int_{A_I}^4 (p - p_0) dA + D_{V_{ex}} + \int_0^{A_I} (p - p_0) dA - \int_B (p - p_0) dA - D_{V_B} \right]$$

(the integral designated B is the pressure force on the forebody from the nose to station 1) so

$$F_{np} = F_n - Dv_{ex} + Dv_B \quad (8)$$

where  $Dv_B$  is the friction force on the forebody surface that affects the flow to the engine. In equation (8)  $Dv_B$  (and in equation (7)  $\int_0^{A_I} (p - p_0) dA - F_B$  for the case of rotational flow) is the corrective term required by the definition of the component forces of  $F_{np}$ . The engine net thrust is the rate of momentum change from the free stream to the tail-pipe exit (eq. (1)), but part of this momentum change  $Dv_B$  cannot be charged to the internal flow because it is accounted for in the external flow as a part of  $Dv_{ex}$ . To avoid the inclusion of  $Dv_B$  twice in  $F_{np}$ , the momentum at the initial station of the internal flow must be corrected to local conditions, which means that  $Dv_B$  must be added into the equation for  $F_{np}$  because the true inlet momentum is less than that as defined ( $m_0 V_0$ ) and thus tends to increase  $F_{np}$ . In the event the boundary layer from external surfaces is removed from the engine flow by a boundary-layer bleed such as that of sketch (1),  $F_n$  is not affected by this loss in stream momentum, and the correction  $Dv_B$  is unnecessary. Then

$$F_{np} = F_n - Dv_{ex} \quad (9)$$

Taking boundary layer into an induction system does not, of course, result in only an additive correction, for  $F_n$  decreases because of the loss in pressure at the engine face and the decrease in  $m_4$  and  $V_4$  which must be suffered by an engine with a limiting design temperature. However, if  $Dv_B$  increases faster than  $F_n$  decreases, there can be an improvement in  $F_{np}$  as boundary layer is taken into the induction system. Quick in reference 5 shows that for a certain engine a decrease in specific fuel consumption and an increase in available thrust can be produced by taking boundary layer from a forebody into the engine at flight speeds less than about 300 mph. At greater speeds, the thrust decreased rapidly relative to that of an engine taking in no boundary layer because of the increasing compressor inlet temperature and because of the loss in dynamic compression ahead of the engine. (See also ref. 2, p. 205.)

If the pressure at station 4 is not equal to ambient pressure, then

$$\int_0^{A_I} (p - p_0) dA + \int_{A_I}^4 (p - p_0) dA + \int_4^{\infty} (p - p_0) dA = 0$$

and

$$F_{np} = F_n + \int_4^{\infty} (p - p_o) dA - Dv_{ex} + Dv_B \quad (10)$$

In other words, a correction must be made for the momentum change occurring in the jet which affects the flow and thus the forces, as previously defined, which act on the system. This correction is a pressure-drag force which acts on the external surfaces. (See ref. 6.) The fact that symmetry is not a necessary condition for the preceding equations for subsonic potential flow has been demonstrated in reference 7. It can also be seen from the fact that if a closed body, which according to the assumed flow conditions can have no pressure drag, is added to the system, the symmetry is destroyed and the total pressure drag must still be zero if the flow remains irrotational.

#### PERFORMANCE PARAMETERS

The basic terms used in describing the performance of air-induction systems are pressure recovery, drag, and mass flow. A description of each of these concepts follows.

#### PRESSURE RECOVERY

Several terms have been used to describe the performance of air-induction systems in regard to their effectiveness in providing an engine with high-pressure air. The total-pressure ratio  $p_{t_3}/p_{t_0}$  is the average total pressure at the engine intake  $p_{t_3}$  divided by the total pressure available from flight. (Methods of measurement and the determination of the effective  $p_{t_3}$  in nonuniform flow are discussed in Appendix B.) This ratio is used when an air-induction system is being considered in relation to an engine-airframe combination because it is directly related to the net thrust and the fuel consumption. Küchemann and Weber show by a simplified analysis of turbojet engines in reference 2 (p. 197) that

$$\frac{\Delta F_n}{F_{n1}} = \frac{F_{n1} - F_{na}}{F_{n1}} = L \left( 1 - \frac{p_{t_3}}{p_{t_0}} \right) \quad (11)$$

$$\frac{\Delta(Q/F_n)}{(Q/F_n)_1} = \frac{(Q/F_n)_1 - (Q/F_n)_a}{(Q/F_n)_1} = (1 - L) \left( 1 - \frac{p_{t_3}}{p_{t_0}} \right) \quad (12)$$



where

$$L \approx 1 + \frac{1 - \frac{\eta_{J1}}{2}}{1 - \eta_{J1}} \left[ \frac{\frac{\gamma - 1}{2\gamma} \left( \frac{p_o}{p_{tn}} \right)_1^{\frac{\gamma-1}{\gamma}}}{1 - \left( \frac{p_o}{p_{tn}} \right)_1^{\frac{\gamma-1}{\gamma}}} \right]$$

$\eta_J$  jet efficiency,  $\frac{2}{1 + (V_J/V_O)}$

$\frac{p_o}{p_{tn}}$  pressure ratio across the engine exit nozzle

a actual installation with induction-system losses

i ideal installation without induction-system losses

Q fuel consumption

Thus  $L$  depends on engine design and flight conditions and is greater than 1. A decrease in total-pressure ratio reduces the engine net thrust and increases the specific fuel consumption with a greater effect on the thrust reduction. This occurs because the net thrust decreases with both the mass flow and the jet velocity while the fuel that can be burned decreases only as the mass flow for a fixed turbine inlet temperature. (See also refs. 8 and 9.)

Ram-recovery ratio  $(p_{t3} - p_o)/(p_{t0} - p_o)$  is the ratio of differences in total pressure as measured at the engine face and ambient static pressure  $p_{t3} - p_o$  and the total pressure and static pressure in the undisturbed stream  $p_{t0} - p_o$ . This parameter is useful because experience has demonstrated it to be only a weak function of Mach number for well-designed systems in subsonic flow at a fixed mass-flow ratio. (See ref. 10.) Thus, the results of low-speed wind-tunnel tests can be extrapolated to high subsonic Mach numbers (of the order of 0.9) for conditions in which the total-pressure profile at the inlet in flight is simulated in the tests.<sup>1</sup> Conversion from ram-recovery ratio to total-pressure ratio is accomplished by the formula:

---

<sup>1</sup>See reference 11 for a discussion of equivalent mass-flow ratios to be used in low-speed tests simulating high-speed conditions. The equivalent mass-flow ratio is one which produces the same pressure rise ahead of an inlet at low speed as occurs at high speed and thus is useful in simulating conditions for configurations which have a boundary layer growing on surfaces ahead of the inlet.

---

$$\frac{p_{t3}}{p_{t0}} = \frac{\frac{p_{t3} - p_0}{p_{t0} - p_0} \left[ \left( 1 + \frac{\gamma - 1}{2} M_0^2 \right)^{\frac{\gamma}{\gamma - 1}} - 1 \right] + 1}{\left( 1 + \frac{\gamma - 1}{2} M_0^2 \right)^{\frac{\gamma}{\gamma - 1}}} \quad (13)$$

Curves of this variation for  $\gamma = 1.4$  are presented in figure 1. (Throughout this report  $\gamma$  is assumed to be equal to 1.4.)

The parameter  $1 - [(p_{t3} - p_{t0})/q_2]$  has frequently been used to describe losses in duct systems. As with ram-recovery ratio, tests of subsonic diffusers with unseparated flow have shown little variation of this parameter with Mach number; but, also, it is not directly related to engine performance. With air-induction systems,  $q_2$  can be estimated for most operating conditions without resorting to detailed flow measurements at the inlet. At the high mass-flow ratios which occur in take-off, the major losses in pressure occur at the inlet lips, and it is a fair assumption that  $p_{t2} \approx p_{t3}$ . Then,  $q_2$  can be calculated from the measured mass-flow,  $A_2$ , and  $p_{t3}$ . However, at mass-flow ratios of the order of 1, the major losses occur in the duct and  $p_{t2} \approx p_{t0}$  under which conditions it is more reasonable to calculate  $q_2$  on the basis of  $p_{t0}$ . If the parameter is used, the conditions for the determination of  $q_2$  must be specifically stated to avoid confusion.

#### DRAG

The drag coefficient of an air-induction system is the dimensionless ratio of force in the flight direction caused by an air-induction system being added to an airframe-engine combination to the product of the dynamic pressure of flight and a characteristic area of the induction system. As indicated in the previous discussion, it is necessary to be consistent in defining drag; the bracketed term of equation (7), the net drag  $D_n$ , can be regarded as the drag force which is consistent with the definition of net thrust  $F_n$  usually used in computing net propulsive force  $F_{np}$ . The bracketed term of equation (7), in the general case, includes much more than the drag force of the air-induction system, for the drag of basic body, wing, tail, etc., must, of course, be included in the net propulsive force. However, for the present discussion, it is assumed that only a scoop arrangement such as that of sketch (1) is being considered. The force on the air-induction system is the pressure and friction forces caused by adding the scoop to a basic body plus the pressure integral on the free surface of the engine-flow streamtube minus

the body forces acting on this streamtube.<sup>2</sup> This difference of pressure integral and body force has been called the "scoop incremental drag." (See refs. 7 and 12.) In the present development, the ramp was considered part of the air-induction system, and the force on it does not appear in the scoop incremental drag. However, if a ramp (possibly because it is a portion of a canopy) is considered not a part of the internal system, but to contribute an external force, then the portion of it affecting the engine flow must be included in  $F_B$  of the scoop incremental drag. If the configuration has a nose inlet and there is no forebody acting on the engine flow, then only the pressure integral from the inlet to the free stream is effective; this force has been called the "additive drag." (See refs. 7, 12, and 13.) The "external drag" of an air-induction system is the sum of the pressure and viscous forces in the flight direction acting on the external surfaces of the air-induction system. Many reports on inlets define "external drag" as the sum of external pressure, friction, and scoop-incremental drag forces; to prevent confusion, this sum is called "net drag" in the subsequent discussion.

#### MASS FLOW

The mass-flow ratio used to describe the flow through air-induction systems is the mass of air that flows through an inlet divided by a reference flow rate

$$\frac{m_2}{m_{\text{ref}}} = \frac{\int_{A_2} \rho V dA}{\int_{A_{\text{ref}}} \rho V dA} \quad (14)$$

(A discussion of mass-flow measurements is presented in Appendix B.) Many choices of the reference can be made, each having some advantage for particular conditions. In this report, two reference rates are usually used:

1. The mass-flow ratio  $m_2/m_0$  is based on the reference  $m_0 = \rho_0 V_0 A_2$  which can be readily determined. In subsonic, incompressible flow,  $m_2/m_0$  reduces to inlet-velocity ratio  $V_2/V_0$  which has often been used to describe air-induction-system performance. This definition of mass-flow ratio has the disadvantage that in supersonic flight it can be greater than 1 if the inlet is located in a compression field whereas a definition based on capture area has a maximum possible value of 1 if local flow

---

<sup>2</sup>As indicated perviously, if a boundary-layer bleed removes all the boundary layer from the streamtube entering the inlet, the body viscous force  $D_{VP}$  is part of the external flow and must not be included in the body force acting on the engine streamtube.

properties are used. However, in the general case,  $m_0$  is easier to evaluate than  $m_c = \int_{A_{c1}} \rho V dA$ , and in subsonic flow both ratios can be greater than 1. (See p. 4 for definition of capture area  $A_{c1}$ .)

2. The mass-flow ratio  $m_{2^*}/m_{2^*}^*$  is used for the static condition when  $V_0=0$ . This ratio is based on the flow rate for choked flow at station  $2^*$ . The mass flow,  $m_{2^*}^*$ , is equal to  $\rho^* V^* A_{2^*}$  where  $\rho^*$  and  $V^*$  are the density and velocity for flow at a Mach number of 1 at the prescribed ambient pressure and temperature. This ratio has been found to correlate data well, and it indicates how near the flow quantity is to the maximum possible. As will be shown later, it is a criterion of the excellence of lip design for low-speed flight. For flight speeds other than zero and for isentropic flow, the two definitions of mass-flow ratio are related by the equation

$$\frac{m_0}{m_{2^*}^*} = \frac{0.579 \frac{m_{2^*}}{m_{2^*}^*} \frac{A_{2^*}}{A_2} \left(1 + \frac{\gamma-1}{2} M_0^2\right)^{\frac{\gamma+1}{2(\gamma-1)}}}{M_0} \quad (15)$$

which is plotted in figure 2 for  $\frac{A_{2^*}}{A_2} = 1.0$ . The choking limit for a sharp lip inlet, from reference 14, is also shown in figure 2.

### III. PRELIMINARY CONSIDERATIONS

#### AIRCRAFT REQUIREMENTS

As discussed in reference 15, aircraft requirements are the basis for the choice of both airframe and engine. Since one of the considerations of airframe design is that of the induction system and since the engine performance is affected by the internal aerodynamic problems of induction, the considerations of the air-induction system enter into the preliminary layout of aircraft; and they must be viewed from the standpoint of the flight requirements. Aircraft range and endurance, for instance, are dictated by fuel consumption, which is affected by the drag and pressure recovery of the induction system. Similarly, take-off distance, rate of climb, maneuvering accelerations, etc., depend upon net propulsive force and hence on induction-system drag and pressure recovery. Aside from these performance requirements that vary with aircraft purpose, there are other, less tangible, requirements that must be taken into account in any design. For example, safety, vulnerability, and serviceability considerations affect engine location and thus the type of air-induction system. The emphasis on any particular requirement

depends upon the intended mission. Thus, the design of an air-induction system must be adapted by compromises to suit many requirements in various degrees.

#### AIRFRAME-INDUCTION-SYSTEM COMBINATION

To illustrate some of the problems encountered in fitting an induction system to an airframe and to introduce some of the types of inlets that have been developed for various engine locations, the progression of design problems with increasing size of airplane is briefly discussed. Current design practice for high-speed turbojet-powered aircraft can be indicated by the following compilation:

Airplane	Fuselage length	Number of engines	Inlet type and location	Duct length
	Engine diameter			Engine diameter
F-86F	14	1	Fuselage open nose	5.5
F-86D	14.5	1	Fuselage nose scoop	5.5
F4D-1	15	1	Wing root	4.5 <sup>1</sup>
F8U-1	16	1	Fuselage nose scoop	9
F7U-1	17	2	Fuselage side scoops	6
F-100	17	1	Fuselage open nose	9
F-84E	17	1	Fuselage open nose	6
XF-104	18	1	Fuselage side scoops	5.7 <sup>1</sup>
XF-105	18	1	Extended wing root	7 <sup>1</sup>
F-89	20	2	Fuselage side scoops	2
F4D-2	20.5	1	Extended wing root	5
F-101	21.5	2	Wing root	3
B-57	22	2	Nacelles, open nose	1.5
A3D-1	23	2	Nacelles, open nose	1.5
F-102A	24	1	Fuselage side scoops	10 <sup>1</sup>
X-3	30	2	Fuselage side scoops	3.5
B-47	40	6	Nacelles, open nose	1.5
B-52	44	8	Nacelles, open nose	1.5

<sup>1</sup>These airplanes have two inlets for one engine, and the ratio of duct length to engine diameter is for a reference diameter corresponding to half the engine frontal area.

Airplane size relative to the engine is indicated by the ratio of fuselage length to engine diameter. For small airplanes with one engine, in which this ratio is less than 18, an inlet located in the fuselage nose or underslung just behind the nose has been used most frequently. From the induction-system standpoint, such locations are desirable because the problems associated with boundary layer flowing into the inlet are either eliminated or minimized. The underslung inlet, in addition, maintains

performance at off-design positive angles of attack because the flow is deflected into the inlet by the nose. As the ratio of fuselage-to-engine size increases, or if nose volume is required for equipment, scoops further back on the fuselage or wing-root inlets are used. From the induction standpoint, an underslung scoop position is again desirable because of the off-design angle-of-attack performance and because the body boundary layer is the thinnest on the windward side. This position has, however, been avoided because of the possibility of foreign-object damage to engines during run-up, taxiing, or take-off.<sup>8</sup> The wing-root inlet has a possible advantage over scoops in that the portion of the inlet perimeter adjacent to the body can be relatively short, thereby reducing the proportion of body boundary layer flowing into the inlet. Furthermore, with multiple engines the ducts can be short and the flow unimpeded by bends. For mid-wing aircraft, the wing-root inlet is in a region of large induced flow angles, both from the body and wing at subsonic speeds, so special precautions must be taken to insure adequate performance at off-design angles of attack. For a high-wing airplane, a design problem of the wing-root inlet at angle of attack is the thick boundary layer on the leeward side of the body.

For aircraft of greater relative size (fuselage-length-to-engine-diameter ratio  $> 22$ ) there are several possible locations with the choice depending on many considerations. For engines clustered in the fuselage, scoop inlets can be used; for engines in the wing-root or buried in the wing, wing-root, wing-leading-edge, or, for very large aircraft, underslung wing scoops are possibilities. However, nacelles with a simple nose inlet have been used most frequently. Such arrangements are desirable from the air-induction standpoint because the ducts are short and straight and the problems of aircraft-induction-system interference are generally reduced.

#### ENGINE-INDUCTION-SYSTEM COMBINATION

The performance of a propulsive system depends not only on the individual characteristics of the air-induction system and of the engine,

<sup>8</sup>The studies of references 16 and 17 indicate that the flow into an airplane induction system can seldom lift damaging objects by itself. For instance, an inlet whose center line is two inlet diameters above the ground and through which the flow velocity is 700 feet per second cannot pick up sand particles larger than about 0.02 inch in diameter unless a vortex forms between the inlet and the ground. However, such a vortex can form under the proper conditions, and if the damaging objects on the ground are restrained laterally, as they would be if lodged in a crack in a runway, the vortex will suck them into the engine; or, if objects which can do damage (see ref. 18) are thrown into the air by some other means, the engine can easily draw them into the inlet. Foreign-object damage to engines is generally considered to be an operational problem, that is, one of using screens, of policing ramps and runways and of proper taxiing procedures, rather than a factor affecting inlet location and airframe design.

but also on the compatibility of these characteristics through the range of flight conditions. This problem of compatibility arises because ram-jet or turbojet engines require a specific schedule of air flow to achieve rated thrust through the flight Mach number and altitude ranges. The flow through a nonadjustable inlet combined with an engine varies with flight conditions and deviates from the optimum conditions selected for the critical design point. If the range of operating conditions is sufficiently wide, the air-induction system is complicated by adjustments that must be provided to maintain its performance near optimum.

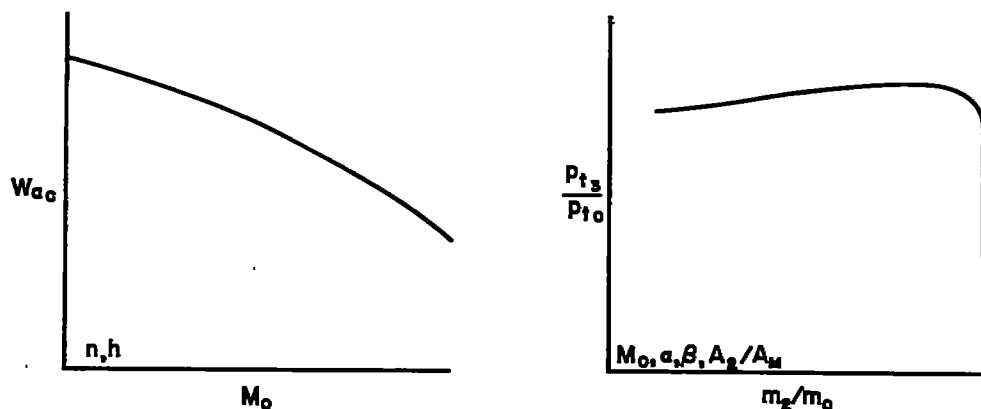
The general problem of combining an air-induction system with an engine can be divided into three parts: (1) matching, (2) optimization, (3) evaluation. Matching is the determination of the mutually compatible operating point for an engine and air-induction system at each flight condition; it consists simply of relating the engine flow requirements to the air-induction-system characteristics by means of the continuity equation to determine inlet area or mass-flow ratio for prescribed operating conditions. Optimization is the determination of the matching conditions for maximum net propulsive force or minimum specific fuel consumption. This can consist of the calculation of the optimum inlet area or mass-flow ratio for fixed systems or of the proper variation of inlet dimensions for variable systems. The two problems, matching and optimization, are presented in some detail in the following discussion. Evaluation is the comparison of several possible propulsive systems on an airframe to determine the best system for a certain mission. Evaluations can involve many considerations in addition to those of aerodynamics, such as structure, weight, mechanical complexity, etc. However, by restricting the propulsion-system variables to net propulsive force and fuel consumption for prescribed flight plans, many valuable results can be obtained from an evaluation study. For example, Fradenburgh and Kremzier in reference 19 describe an evaluation of the effects of various propulsive systems on aircraft range. Another approach, which is similar to that used by Woodworth and Kelber in comparing jet engines (ref. 20), is to determine the allowable weights for the installation of each of several air-induction systems on an airframe having a prescribed range. Such an evaluation provides the designer with the information necessary to select possible mechanical arrangements. These studies are part of the general problem of power-plant-aircraft optimization discussed in reference 15.

#### MATCHING

The problem of matching an air-induction system and an engine requires knowledge of the performance characteristics of each, and the problem of optimizing the design for a special airplane requires knowledge of the

characteristics through a wide range of flight conditions.<sup>4</sup> These characteristics are determined by analysis and tests, but since in the preliminary stages the air-induction system has not yet been designed, its performance must be assumed from past experience or by determining what performance is necessary and then striving to design and develop an arrangement that will accomplish the goal.

To illustrate a method for matching a turbojet engine and an air-induction-system combination, the variation of corrected weight flow of air for an engine ( $W_{ac} = W_{a\sqrt{\theta/8}}$ ) as a function of Mach number and the variation of the pressure recovery of the air-induction system with mass-flow ratio as shown in sketch (2) are assumed to be known.



Sketch (2)

For a complete analysis, this information must be available for each parameter indicated on the sketch; that is, the flow variation must be known for the expected range of engine rotational speed  $n$  and of flight altitude  $h$ . The induction-system variation must be known for the Mach number  $M_0$ , angle-of-attack  $\alpha$ , and angle-of-sideslip  $\beta$  ranges, and possibly for a range of the ratio of inlet area to body frontal area  $A_2/A_M$ , although in the usual case changes in this ratio are small and their effects are negligible. Transposing the continuity equation

$$\rho_0 V_0 A_0 = \rho_2 V_2 A_2 = \rho_3 V_3 A_3$$

(assuming uniform flow at all stations) into engine-inlet terminology by

<sup>4</sup>See reference 21 for a discussion of engine performance parameters; reference 22 for an analysis of turbojet-engine-inlet matching; references 8, 23, and 24 for relationships between engine and induction-system performance and methods of determining optimum performance conditions; and references 25 and 26 for studies of the penalties associated with mismatching.



defining  $\delta \equiv p_{t_3}/p_{SL}$ ,  $\delta_0 \equiv p_{t_0}/p_{SL}$ , and  $\sqrt{\theta} \equiv \sqrt{T_{t_3}/T_{SL}}$

$$\frac{m_2}{m_0} \equiv \frac{\rho_2 V_2 A_2}{\rho_0 V_0 A_2} = \frac{A_0}{A_2}$$

gives

$$\begin{aligned} \frac{W_2 \sqrt{\theta}}{A_2 \delta} \frac{p_{t_3}}{p_{t_0}} &= g \rho_{SL} a_{SL} \frac{m_2}{m_0} \left[ \frac{M_0}{\left(1 + \frac{\gamma - 1}{2} M_0^2\right)^{\frac{\gamma+1}{2(\gamma-1)}}} \right] \\ &= 85.4 \frac{m_2}{m_0} \left[ \frac{M_0}{(1 + 0.2 M_0^2)^3} \right] \end{aligned} \quad (16)$$

when

$$\gamma \quad 1.4$$

$$g \quad 32.17 \text{ ft/sec}^2$$

$$\rho_{SL} \quad 0.002376 \text{ slugs/ft}^3$$

$$a_{SL} \quad 1117 \text{ ft/sec}$$

This relationship can be represented graphically so that from the known engine and air-induction system characteristics the inlet area required to match the engine at the selected induction-system conditions can be readily determined as illustrated in figure 3. Thus, for a given flight condition of Mach number and altitude (sketch (2)), a mass-flow ratio is selected and the corresponding pressure ratio determined from the air-induction-system performance data; the corrected engine weight flow is determined from the engine curve; and the proper inlet area is determined by the intersection of the corresponding horizontal and vertical lines in the third quadrant of figure 3. This inlet area furnishes the engine the proper volume rate of flow at the chosen mass-flow ratio, but, this is, of course, not necessarily the mass-flow ratio that produces the maximum net propulsive force or the minimum fuel consumption.

A similar method can also be used to study matching at static conditions where the mass-flow ratio  $m_2/m_0$  has no significance. Defining

inlet Mach number  $M_2'$  as that which would exist if the flow to station 2 were isentropic,<sup>5</sup>

$$\frac{W_a \sqrt{\theta}}{A_2 \delta} \frac{P_{t3}}{P_{t0}} = \frac{85.4 M_2'}{(1 + 0.2 M_2'^2)^3} \quad (17)$$

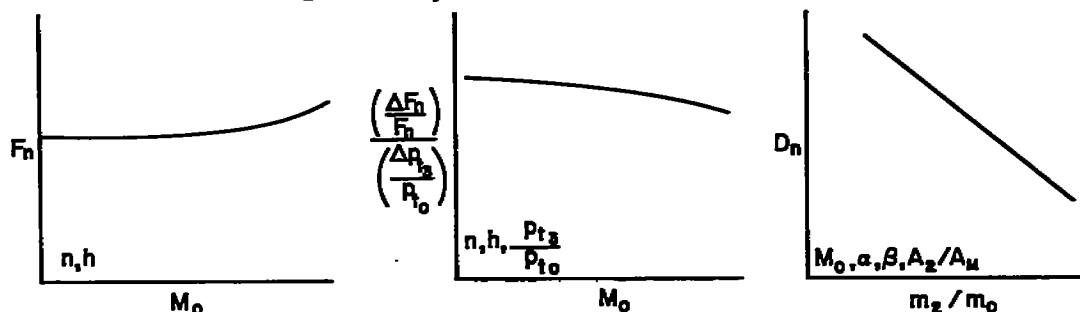
This equation corresponds to equation (16) if  $m_2/m_0=1$  and  $M_2'$  is substituted for  $M_0$ . With these changes, figure 3 can be adapted to static conditions. Information on  $P_{t3}/P_{t0}$  as a function of  $m_2/m_2^*$  can be converted to a function of  $M_2'$  by the relation

$$\frac{m_2}{m_2^*} = 1.728 M_2' (1 + 0.2 M_2'^2)^{-3} \quad (18)$$

and this variation together with the known engine characteristics can be used to determine the inlet area required to match the engine or the penalties resulting from mismatching.

### OPTIMIZATION

To determine the inlet areas for maximum net propulsive force over a range of flight conditions, the net thrust of the engine  $F_n$ , the correction to engine net thrust due to pressure losses upstream of the engine  $\frac{\Delta F_n}{F_n}$  (see ref. 24) and the net drag of the air-induction system, as  $\frac{\Delta P_{t3}}{P_{t3}}$  shown in the following sketch, must be known:



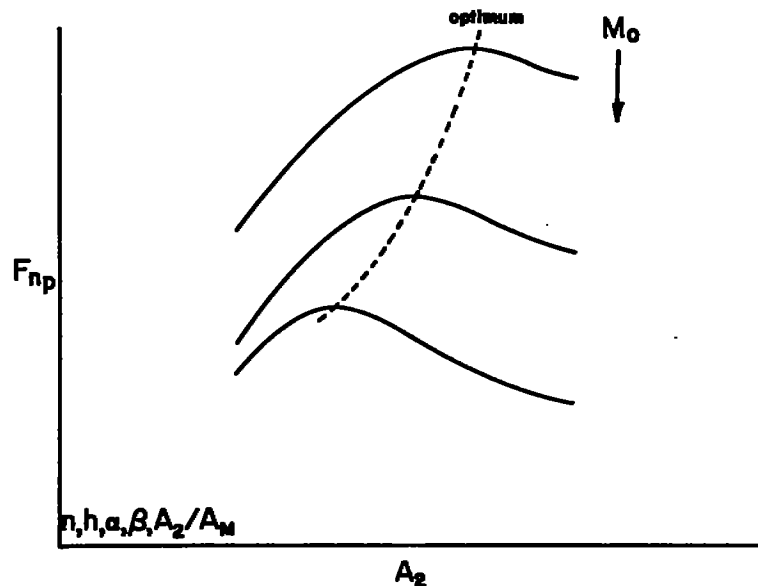
Sketch (3)

<sup>5</sup>A prime symbol is used here with  $M_2$  to indicate that the number represents a fictitious condition and is used only for convenience. As will be shown later, the flow through inlets with practical lip shapes is not isentropic at take-off.

Then, for the conditions for which  $A_2$  was calculated to match the engine, the net propulsive force can be determined as

$$F_{np} = F_n - \Delta F_n - D_n \quad (19)$$

The optimum inlet areas for a Mach number range at a constant altitude, engine speed, and airplane attitude are determined by curves of net propulsive force as a function of inlet area as shown in the following sketch:



Sketch (4)

Such curves provide the information required in final evaluation, that is, the penalties in net propulsive force that would result from flight with a constant inlet area or any other deviation from the ideal variable-area system that might be required by mechanical, structural, or flight considerations. Of course, to optimize for a prescribed mission the other variables, such as altitude and angle of attack, must be taken into account.

Maximum net propulsive force is important, but it is not always the critical design consideration. For instance, with long-range aircraft the fuel consumption per pound of net thrust might be more important. The procedure for optimizing this parameter is similar to that just described; fuel flow rates corresponding to the calculated net propulsive forces are determined from engine performance curves, and the ratio  $W_f/F_n$  is plotted as a function of inlet area for the range of flight conditions to determine the optimums. The inlet area for minimum specific

fuel consumption is, in general, different from that for maximum net propulsive force, but for a well-designed air-induction system the difference, which depends on the difference in the mass-flow ratio for maximum pressure recovery and for minimum net drag, is usually small. The importance of this difference depends on the intended mission.

### FLOW UNIFORMITY AND STEADINESS<sup>6</sup>

Another problem of the engine-induction-system combination is the uniformity and steadiness of the flow that the air-induction system presents to the engine and the effects of irregularities on engine performance. Irregularities in pressure at the face of a compressor, particularly an axial-flow compressor, can reduce engine performance and cause vibration; pressure pulses or fluctuating flow angles can cause structural failure of compressor blades. Tolerances in flow uniformity have been suggested by Greatrex (ref. 27), but steadiness tolerances have not been established (see ref. 28). The indications are that these tolerances depend upon individual engine design. Conrad and Sobolewski (ref. 29) found that flow nonuniformity that was once thought to be unacceptable had no large effect on the engine which they tested; however, the tests of reference 30 with a different engine showed large reductions in performance. In the investigation of flow steadiness reported in reference 31, it was found that, although the induction system by itself produced unsteady flow, operation with a turbojet engine had a large attenuating effect.

Differences between engines in response to flow nonuniformity can often be explained by the fact that a compressor with a large pressure rise across the first stage has blades operating at high lift coefficients, and irregularities in the entering flow readily cause stall. A first stage with smaller loading can reach local stalled conditions only if the entering flow is more irregular. An induction system with flow nonuniformity sufficient to stall one or more blades leads to the phenomenon called "rotating stall" of the compressor with ensuing reduction in engine performance (thrust, allowable fuel consumption, and acceleration margin) and large vibratory stresses in the blades. (See, e.g., refs. 32, 33, 34, and 35.) Since the trend in the design of compressors for the engines of supersonic aircraft is toward larger flow rates and pressure ratios and toward lighter specific weight, blades are being made longer and thinner, with the result that the induction-system problems of flow

<sup>6</sup>In this report, a distinction is made between the problems of flow stability and steadiness which has often not been made in the past. By stability is meant the property of flow which enables it to return to an original steady condition after being disturbed; thus, a normal shock wave is unstable in a converging channel because it can exist in a steady condition only upstream of the inlet or downstream of the throat. By steadiness is meant the quality of the flow in regard to velocity or pressure fluctuations.

uniformity and steadiness are becoming more critical because of the greater likelihood of rotating stall and of structural failure. Even if a compressor is designed to avoid rotating stall, the effect of intake flow distortion is to move the compressor surge line to higher corrected weight flows, and thus toward the operating line, with an ensuing decrease in the operating range possible with the engine. Also, the results of reference 35 indicate that nonuniformity of the flow from the induction system can cause nonuniformity in the temperature distribution at the turbine entry with subsequent turbine failure. With ram-jet engines, adverse effects also result from irregular flow from the air-induction system. Reference 36 reports large losses in combustion efficiency on account of variations in velocity profile at a burner, and references 37 and 38 show that pressure pulsations must be avoided.

Flow uniformity is related to the problem of engine location. Such factors as the induced effects of other aircraft components and the length and path of ducts must be considered in preliminary design to produce an air-induction system with uniform flow at the engine face. Steadiness of the engine flow, particularly in supersonic flight, is affected by the operating mass-flow ratio of the induction system. In general, unsteady flow results from operation at low mass-flow ratios, and the associated pulsations can be violent. For safety, the flow must be steady from the operating speed to the windmilling speed of the engine, and a variable inlet area or an air bypass may be necessary to maintain high inlet mass-flow ratios. Considerations of these problems in relation to inlet design are discussed subsequently.

#### IV. DETAIL CONSIDERATIONS

##### INDUCTION

The purpose of this section is to discuss the pressure recovery, drag, flow uniformity, and flow steadiness of air-induction systems without describing in any detail considerations of other aircraft components. These latter factors are discussed later under the heading INTERFERENCE. The flow inside ducts can be treated independently of the flight Mach number, and this subject is presented first under the heading PRESSURE RECOVERY AND FLOW UNIFORMITY. In general, the problems of conducting air to an engine are described at subsonic and supersonic speeds to a Mach number of 2.

It should be mentioned at the outset that insufficient theoretical and experimental information is available to predict accurately the performance of practical air-induction systems through all the possible combinations and ranges of the many pertinent variables. For all but the simplest cases, refined design must depend upon test observations. The purpose here is to discuss what is known of basic design principles.

F

NACA RM A55F16

23

## PRESSURE RECOVERY AND FLOW UNIFORMITY

The design objective in regard to pressure recovery is to provide a passage by which the air required for best operation can flow to an engine with the least pumping power requirement at zero flight speed and by which the compression available from the kinetic energy of flight can be utilized to the maximum extent. The compression of more air per unit of engine intake area permits more fuel to be burned for the same limiting temperature with a resulting increase in the specific thrust for a smaller specific fuel consumption. In other words, as shown by equations (11) and (12), the total-pressure ratio must be high, for losses affect thrust in more than a 1:1 ratio. The problem of flow uniformity is discussed together with pressure recovery in this section because the two problems are closely allied.

## Ducts

There is no general method for designing the ducts of practical air-induction systems because the flow in the usual case is viscous, compressible, and three-dimensional. A summary of present knowledge of duct flow is presented here to develop empirical design rules. The two primary geometric factors which are of concern are the inlet-to-engine-face area ratio and the duct path. The area ratio is determined by the selected design conditions, and the duct path, or the length and offsets, is determined by the aircraft configuration and the necessity for avoiding pressure losses. The aerodynamic factors of concern are the initial flow distribution and the conditions which cause pressure losses and nonuniformity in the flow. The problem is to determine from consideration of these factors the shape of duct that produces the best operating conditions for the engine with the least cost in weight and complexity to the airframe.

Area ratio.- In regard to the area ratio between the inlet and the engine face, by assuming uniform, adiabatic flow of a perfect gas and using the continuity equation, it can be shown that (assuming  $A_2=A_2'$ )

$$\frac{A_2}{A_3} = \frac{p_{t3}/p_{t0}}{m_2/m_0} \frac{M_3}{M_0} \left( \frac{1 + \frac{\gamma-1}{2} M_0^2}{1 + \frac{\gamma-1}{2} M_3^2} \right)^{\frac{\gamma+1}{2(\gamma-1)}}$$

Thus, for a given area  $A_3$  at the engine face, the inlet area  $A_2$  increases as the total-pressure ratio and engine intake Mach number, but it decreases with increasing mass-flow ratio. Other factors being constant,  $A_2$  is a minimum at a flight Mach number of 1.0. For present-day turbojet engines in flight from sea level into the stratosphere at Mach numbers from 0 to 2.0,  $M_3$  is in the range from 0.4 to 0.6; thus the area ratio for an efficient air-induction system is between 0.7 and 0.9; and, for greater engine-intake Mach numbers which can be expected in the future, the ratio is more nearly 1. In other words, the change in area between inlet and engine face is relatively small and short ducts can be used without requiring large divergence of the flow. However, in the case of a ram-jet engine with the Mach number at the burner about 0.2, the area of the inlet must be about half of that for a turbojet engine, and the duct problem is more difficult.

Skin-friction losses.— In regard to the duct path, consider first a straight duct with no initial boundary layer. The boundary layer in the usual case is nearly all turbulent and the flow is subsonic; so, as long as the walls are relatively smooth and the length is short enough so that pipe flow does not develop (less than about 20 inlet diameters, see ref. 39), the skin friction can be estimated with sufficient accuracy from the formula

$$C_f = 0.074/\sqrt{R} \quad (21)$$

(see, e. g., refs. 40 and 41) where

$$C_f = \tau/qS$$

$\tau$       shearing force

$q$       dynamic pressure

$S$       wetted area

$R$       Reynolds number based on average flow properties in duct and on duct length  $l$

The decrease in skin-friction coefficient with Mach number (ref. 42) and with positive pressure gradient (ref. 43) need not be taken into account in most cases because the effect of the former is small and neglect of the latter produces a conservative estimate.

Beeton in reference 44 assumes one-dimensional compressible flow and no change in skin-friction coefficient with duct length in calculating the total-pressure ratios resulting from skin-friction losses in circular ducts with conical divergence. Two of the curves from this reference

are reproduced in figure 4;<sup>7</sup> similar curves can be calculated by the method of reference 45. Beeton shows that for the severe condition of  $A_3/A_2=1.2$ ,  $M_2=0.8$ , and  $(l/d_3 \times C_f/0.003)=10$  the total pressure ratio is 0.96. Since the loss in total pressure in this case is nearly proportional to the duct length, it is evident that here a shorter duct is desirable and that losses due to skin friction can be sizable. (Refs. 25 and 46 show that the incremental loss of turbojet-engine thrust  $\Delta F_n/F_n$  per unit decrease in total-pressure ratio is in the range of 1.2 to 1.5 for the flight conditions under discussion.) For long-range, subsonic aircraft, internal skin-friction losses must be minimized, and duct length requires careful consideration. If this duct were on a supersonic airplane with a very efficient method of external compression ( $M_2 \rightarrow 1.0$ ), the high inlet velocity and the resulting duct losses would counteract the nearly isentropic inlet flow, for the total-pressure ratio would be reduced to 0.95 by the greater internal skin friction. However, in the usual case of a supersonic design in which the duct is shorter and external compression occurs through shock waves, skin friction is a small portion of the total loss. The main concern in duct design is a shape that avoids separation and maintains uniform flow.<sup>8</sup>

Flow separation.— The problem of avoiding separation depends upon initial flow conditions and duct shape. For high-speed aircraft with efficient air-induction systems, the inlet Mach number is in the high subsonic range, for if the flow is uniform

$$M_2 = \frac{p_{t3}}{p_{t2}} \frac{A_3}{A_2} M_3 \left( \frac{1 + \frac{\gamma-1}{2} M_2^2}{1 + \frac{\gamma-1}{2} M_3^2} \right)^{\frac{\gamma+1}{2(\gamma-1)}} \quad (22)$$

and with  $\gamma=1.4$ ,  $p_{t3}/p_{t2} \approx 1.0$  and  $A_3/A_2=1.2$ ,  $M_2=1.0$  when  $M_3=0.6$ ; or

<sup>7</sup>Since the variation of total-pressure ratio with the parameter  $l/d_3 \times C_f/0.003$  is linear to the extent required by the accuracy of duct-design considerations from values of 2 to 10, the range of interest, only curves for values of 4 and 8 have been reproduced. Total-pressure ratios for other conditions can be obtained with sufficient accuracy by interpolation or extrapolation.

<sup>8</sup>Greatrex in reference 27 suggests that the ratio of the maximum-to-average engine intake velocity  $V_M/\bar{V}$  be used as a criterion for flow uniformity, and the examples presented indicate that this ratio should be less than about 1.2 for satisfactory engine operation. For fully developed pipe flow with a  $1/7$ -power velocity profile,  $V_M/\bar{V}=1.23$ . Since the ducts of the air-induction systems for aircraft are seldom, if ever, long enough for pipe flow to develop, it is evident that skin friction by itself is not sufficient, in the usual case, to cause serious nonuniformity.



$M_2=0.7$  when  $M_3=0.5$ . Such a high subsonic Mach number at the inlet makes the design of the upstream section of a duct critical because, assuming one-dimensional flow

$$\frac{dp}{dx} = - \left[ \frac{\gamma p_t M}{\left(1 + \frac{\gamma-1}{2} M^2\right)^{\frac{\gamma}{\gamma-1}}} \right] \frac{dM}{dx} \quad (23)$$

or assuming isentropic flow from the free stream to a local station in the duct entry,  $p_t=p_{t_0}$ , and

$$\frac{dp}{dx} = - \left[ \frac{\gamma p_0 \left(1 + \frac{\gamma-1}{2} M_0^2\right)^{\frac{\gamma}{\gamma-1}} M}{\left(1 + \frac{\gamma-1}{2} M^2\right)^{\frac{\gamma}{\gamma-1}}} \right] \frac{dM}{dx} \quad (24)$$

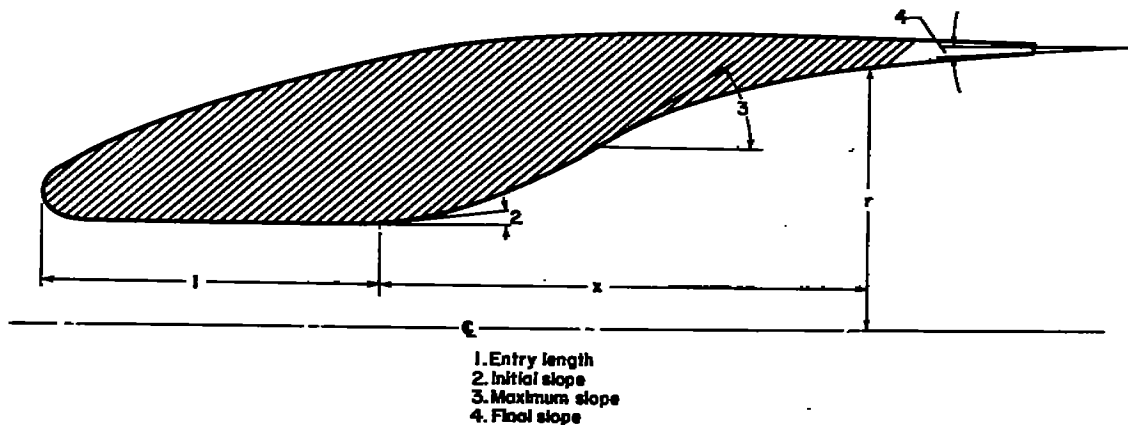
For a given local total pressure, or flight altitude and Mach number in the second case, the bracketed term of these equations has a maximum value at a local Mach number of 0.79 and changes little from  $M=0.6$  to 1.0. As a result, deceleration of flow in this range causes the most severe positive pressure gradients per unit of Mach number change, and the effect is aggravated by low-altitude flight at high Mach number. Since deceleration is produced by an expanding channel in subsonic flow, the initial portion of a duct must diverge slowly to avoid pressure gradients which separate the boundary layer.

With many induction systems, boundary layer from flow over surfaces upstream of the inlet enters the duct. In this case, the duct shape depends critically on the initial boundary-layer conditions because the pressure gradient that a boundary layer can withstand without separation decreases as the boundary-layer shape parameter  $H$  increases.<sup>9</sup> The shape parameter is increased when the boundary layer flows through adverse pressure gradients and over rough surfaces.

---

<sup>9</sup> $H=\delta^*/\theta$ =displacement thickness/momentum thickness. This ratio is a measure of the shape of the boundary-layer profile and is useful for indicating incipient separation. Reference 47 shows that separation does not occur in incompressible, two-dimensional flow if  $H<1.8$ , and reference 48 similarly shows that the criterion is valid for conical-diffuser flow.

Design.- Together with area ratio, length, initial Mach number, and initial boundary layer, the internal contours of ducts require careful consideration. The factors to be considered in axially symmetric straight ducts are shown in sketch (5). Many ducts also include some offset of the center line from entrance to exit, transitions in cross-section shape, and junctures between ducts. Since turbulent boundary-layer theory is not



Sketch (5)

yet sufficiently refined to provide, even for simple cases, a method by which an optimum diffuser can be determined (see refs. 43 and 49), the qualitative indications of many experiments must be utilized in design.

In regard to entry length, a section of nearly constant duct area is necessary to provide for reattachment of the flow for flight conditions in which separation occurs in the inlet. The data of Seddon (ref. 28) for zero flight speed indicate that for normal lip shapes, an entry length of possibly one inlet radius is desirable. For engine installations in supersonic aircraft, the data of references 50 and 51 show that entry lengths of six inlet radii provide a relatively wide range of mass-flow ratios in which engine flow is steady. Also, the studies of shock-wave stability of Kantrowitz (ref. 52) show that a constant-area section is desirable to prevent downstream pressure pulsations from forcing a terminal normal shock wave out of an inlet. (These considerations are further discussed in refs. 53 and 54.) Because of boundary-layer growth through the entry length, the duct walls must diverge slightly to provide a constant effective area. Study of duct data in which the boundary-layer displacement thickness was measured, such as references 48 and 55, indicates that an axially symmetric entry section should diverge at a half-angle of from  $0.5^\circ$  to  $1^\circ$ . (This range of incremental divergence angle also appears to be satisfactory for boundary-layer compensation in the initial, maximum, and exit slope regions when the boundary layer is not separated, i.e.,  $H < 1.8$ .)

In regard to initial slope, equation (23) indicates that to minimize adverse pressure gradients at high inlet Mach numbers the slope should be small and the change of curvature should be continuous. The need for such limitations is indicated by Naumann, reference 56 and is illustrated by the data of references 48, 55, and 57.<sup>10</sup> These data show that the abrupt expansion where a  $10^\circ$  or  $12^\circ$  conical diffuser is attached to a straight pipe causes nonuniformity, appreciable losses in pressure recovery, and some reduction in the maximum mass flow when the approach Mach number exceeds 0.7 to 0.8.

In regard to maximum slope, it determines the shortest duct which can be used without auxiliary methods of suppressing separation, such as those of references 58 and 59. As the local Mach number decreases from the throat along the length of a diffuser, the walls can diverge at an increasing rate without an increase in local pressure gradient. Thus, a maximum slope exists which depends upon the initial Mach number and the initial boundary-layer profile. The available experimental evidence, such as references 48, 55, 56, 57, and 60 through 62 for conical diffusers, indicates that the maximum included divergence angle is in the range from  $6^\circ$  to  $15^\circ$  with the largest angle being used only with thin initial boundary layers.

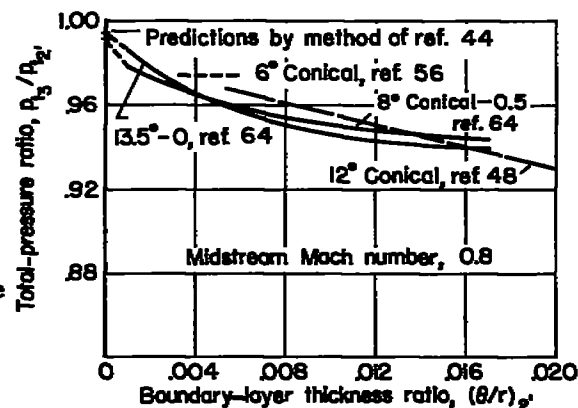
In regard to final slope, the theoretical studies of references 47 and 63 and the experiments of references 48, 55, and 57 show that for minimum-length diffusers having  $A_3/A_2' > 2.0$  this slope should be less than the maximum slope to avoid separation when the initial boundary layer is thin. All of these studies were made with conical diffusers; the fact that the final slope should have been less than the maximum slope is indicated by the measurements of the final profile which, at high values of  $M_2'$ , had  $H \gg 1.8$ . If the initial boundary layer is thick, the maximum slope cannot be large; in fact, the two slopes become equal. The data indicate that a  $3^\circ$  final divergence angle on a wall, or a  $6^\circ$  included angle, should be used with both thick and thin initial boundary layers.

These qualitative considerations indicate that for thick initial boundary layers and high initial Mach numbers, a diffusing straight duct should have a faired entry section and a conical diffuser of included angle no greater than  $8^\circ$  ( $6^\circ$  included angle plus a maximum of  $2^\circ$  for boundary-layer compensation). For other conditions, fair duct shapes which satisfy these considerations can be conveniently expressed as

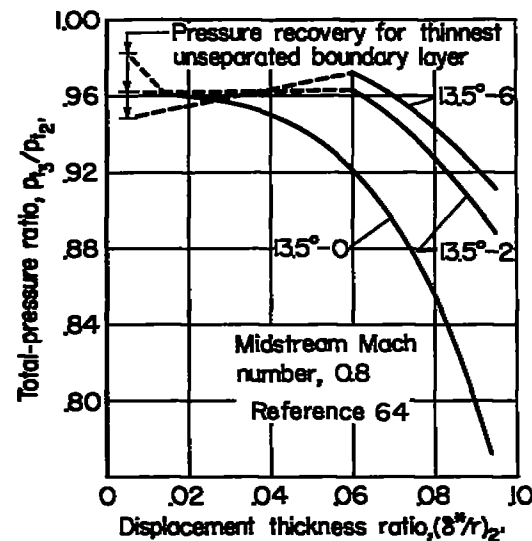
<sup>10</sup>The data on conical diffusers from these references were analyzed to determine desirable duct shapes by selecting longitudinal pressure distributions for which  $H \approx 1.8$ , and then calculating new duct shapes from one-dimensional relationships for this pressure distribution and values of  $M_2'$  approaching 1. The resulting calculated shapes all have small initial slopes because, as shown by equation (23), the Mach number gradient (i.e., the slope of the wall) must decrease to maintain a constant initial pressure gradient with increasing local Mach number.

exponential functions of the duct axial coordinate. Tests were made of a family of such diffusers with a ratio of throat area to exit area of 1 to 2 and a variation of the ratio of duct length to throat diameter of from 2 to 5. Tests were made with both separated and attached initial boundary layers at mass-flow ratios up to the maximum, and the results are reported in reference 64. Data from these and other tests are compared in sketch (6)<sup>11</sup> for the condition of an attached initial boundary layer. It is apparent that, for this comparison, the ratio of initial boundary-layer thickness to throat radius has a larger effect on pressure recovery than does diffuser shape. The measurements of reference 64 show that the important effect of duct shape is on flow uniformity and steadiness, for the uniformity ratio  $V_M/\bar{V}$  varied from 1.12 to 1.25 for ducts differing in total-pressure ratio by only 0.02 in tests with a thin initial boundary layer ( $(\theta/r)_2 = 0.0014$ ) and a high initial Mach number ( $M_2 \approx 0.85$ ).

Furthermore, two ducts having nearly equal uniformity and pressure recovery differed by a large amount in the quality of flow steadiness at high inlet Mach numbers. The comparison of pressure recovery predicted by the method of reference 44 with the experimental measurements of sketch (6) shows that the prediction is only accurate when the initial boundary-layer thickness is very small. If it is not small, the effective skin-friction coefficient is larger than that indicated by equation (21) and experiments are necessary for accurate loss predictions. (The data for sketch (6), and also (7), were calculated according to the mass-derived method; see Appendix B. The magnitude of the difference between experiment and theory depends upon which method of data reduction is used; the



Sketch (6)



Sketch (7)

<sup>11</sup>The ducts of reference 64 are designated by numbers which indicate the maximum slope in terms of included angle and the length of entry section in terms of inlet radius. Thus, 8° conical -0.5 indicates a conical divergence of 8° and an exponentially faired entry section of 0.5 inlet radius in length.

difference shown in sketch (6) would be smaller if the data had been reduced by the mass-flow weighting method.)

Sketch (7) shows the results of tests reported in reference 64 for three ducts with separated initial boundary layers. The data show that an extended entry section increases the skin-friction losses when the initial boundary layer is unseparated; therefore, if separation in the entering flow can be avoided, a long entry is undesirable. However, with initial separation which, as will be discussed later, can occur in low-speed flight at high mass-flow ratios or in high-speed flight at low mass-flow ratios, some entry length improves duct performance because it gives the boundary layer an opportunity to reattach. The fact that the pressure recovery can be higher for the long duct with the separated boundary layer than with the unseparated profile indicates that reattachment occurred after relatively extensive separation and that the small skin-friction force in the region of separation reduced the over-all losses. In regard to flow uniformity, the results of reference 64 show that for short ducts the flow is more uniform if the initial boundary layer is attached rather than separated. For a given initial profile of the separated type, the final uniformity is improved if the duct is made longer.

Reference 64 reports tests which were intended to investigate to some extent the manufacturing tolerances required in duct construction. Measurements were made with a duct having different degrees of surface roughness, waviness, and leakage. It was found that roughness caused by scratching the surfaces with coarse sandpaper or by putting discrete steps in the duct walls, as could occur with joints that are not flush, had no effect on the diffused flow. The maximum magnitude of the roughness was about 0.7 the momentum thickness of the boundary layer at the duct throat. The maximum waviness tested was similar to that which would occur because of pressure loads in high-speed flight; circumferential stiffeners were assumed to be  $0.6r_2$  apart, and the deflection was varied up to 19 times the momentum thickness, or 1.5 times the boundary-layer thickness, at the duct throat. For mass-flow ratios  $m_2'/m_2'^*$  below 0.85, even the maximum waviness tested had a negligible effect on the final flow. At greater mass-flow ratios, the maximum waviness reduced the pressure recovery, uniformity, and steadiness only slightly. Leakage, as might occur through joints in duct walls during high mass-flow operation in run-up on take-off, was found to have negligible effects when the leaks were in the low-velocity region of a duct. However, leakage near the duct inlet caused separation with ensuing sizable pressure losses and flow nonuniformity.

The internal-flow systems of most aircraft have some offset between the inlet and the exit, transitions in cross-section shape, and junctures with other ducts, all of which can cause losses in pressure recovery. The general problem in the design of these elements is the same as that of

a subsonic diffuser, that is, the prevention of local separation and reduction of skin friction.<sup>12</sup> One design feature that has always been beneficial is the use of generous fillets to avoid angled corners. (See refs. 67 and 68.) However, since the factors which cause pressure losses differ with each duct configuration, it is difficult to apply accurately general design information. The data of references 28, 60, 61, 69, and 70 indicate the trends to be expected. The magnitude of the total-pressure losses in s-bends is demonstrated by the tests of reference 71. Relatively short ducts ( $l/r_s = 4.0$ ) with several inlet cross-section shapes and a circular exit were tested at a Mach number of 1.9. The inlet had a wedge-shaped external-compression surface and the exit center line of the duct was offset 1.5 exit radii,  $r_s$ , from the inlet center line. The maximum total-pressure ratios measured with the ducts were of the order of 6 percent less than those measured with a straight duct. Reducing the mass-flow ratio decreased this difference to about 3 percent, a fact which indicates the dependence of duct losses on inlet Mach number. Although the total-pressure losses could be reduced by reducing mass-flow ratio, the exit velocity distributions show considerable nonuniformity for these conditions. Tests with offsets of one and two inlet radii reported in reference 64 indicate similar results. The center lines of these offsets were smooth curves similar to those of the duct-wall contours. At a mass-flow ratio of 0.9 with a thin initial boundary layer, the 1-radius offset reduced the total-pressure ratio 3 percent from that of a straight duct, and the 2-radius offset reduced it 6 percent. The steadiness and uniformity qualities of the flow decreased in a corresponding manner. For example, with the thin initial boundary layer, the maximum mass-flow ratio for steady flow was about 0.9 for the straight duct and 0.7 for the duct with the 2-radius offset. A fourfold increase in the initial boundary-layer thickness reduced the latter mass-flow ratio to 0.4. It is apparent that deviating from the optimum aerodynamic design of a duct can have serious consequences.

### Subsonic Flight

Since in subsonic flow, pressure losses and nonuniformity result from skin friction, separation, and entering flow that is asymmetric with respect to the inlet, the induction-system design problems in subsonic

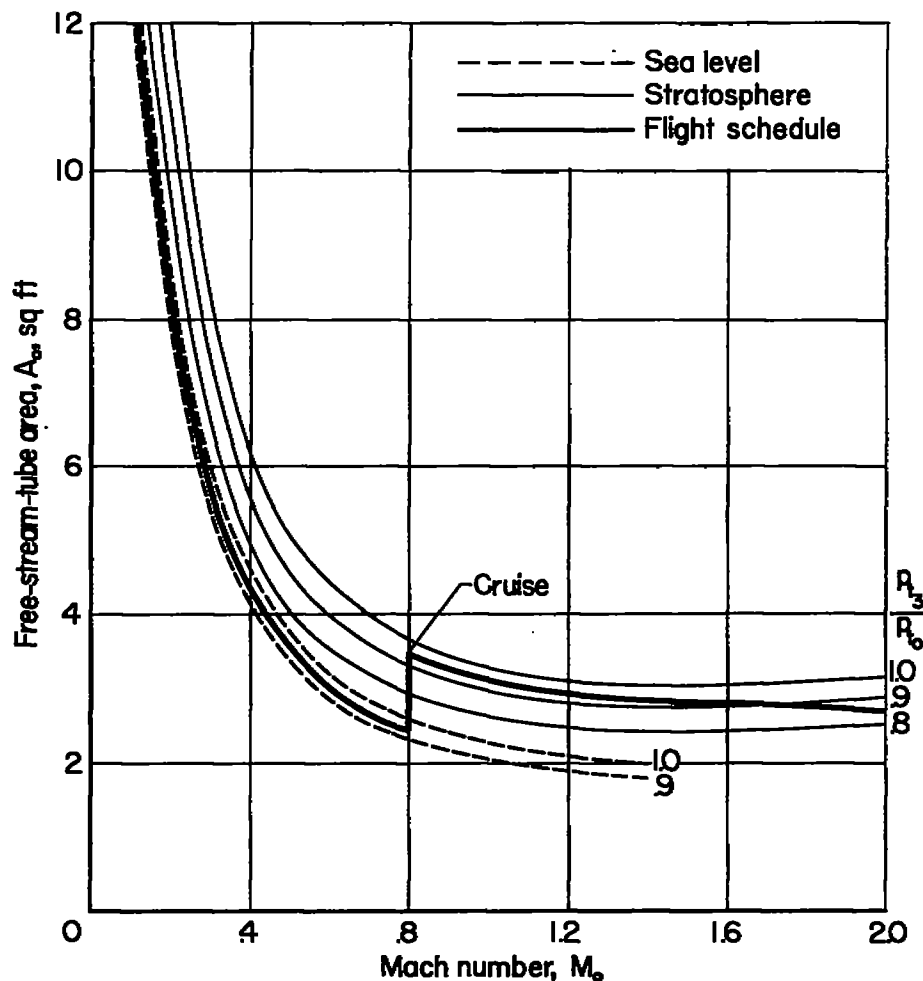
---

<sup>12</sup>The design principles for annular subsonic diffusers are like those of diffusers without center bodies, but the annular type, having more wetted area, has larger frictional pressure losses. Studies of annular diffusers are reported in references 65 and 66.

---

flight are to provide conditions that avoid or minimize these factors. Skin friction and internal separation are problems of duct design; the problems of separation in the inlet and symmetry are discussed in this section.

To illustrate the conditions which lead to the principal separation problem of inlet design in subsonic flight, sketch (8) shows a typical curve of the air requirements of a turbojet engine in terms of the free-stream area of the engine-air streamtube  $A_0$  as a function of flight



Sketch (8)

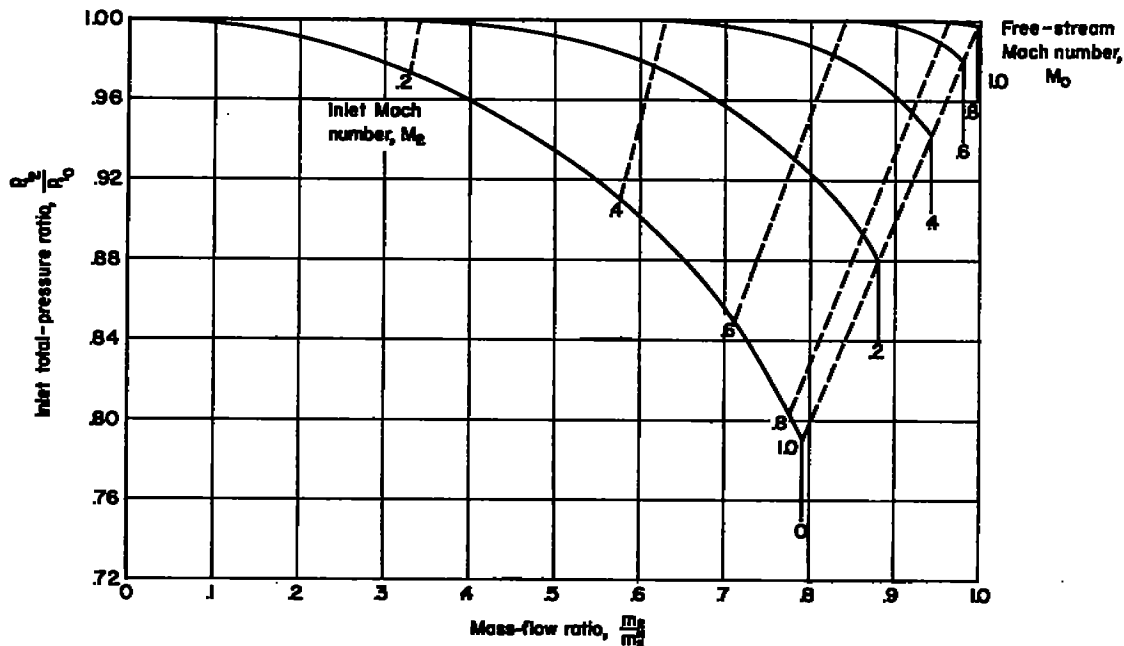
Mach number. It is here assumed that the airplane accelerates at sea level to a Mach number of 0.8, climbs at this Mach number to altitude,

and then accelerates from this cruise condition to a Mach number of 2. The air requirement is not only a function of  $M_0$ , but also of total-pressure ratio and altitude, as shown, and of engine design and power setting. Since cruising flight is usually an important design condition, the inlet area  $A_2$  must be selected to produce efficient cruise performance, and this, for high-speed aircraft, is generally at a relatively high mass-flow ratio, above about 0.8. The choice of this mass-flow ratio is a compromise between requirements for other flight conditions and the conflicting interests of the internal and external flows. A low mass-flow ratio ( $m_2/m_0 \equiv A_0/A_2 \ll 1$ ), that is, a diverging streamtube ahead of the inlet, is desirable to the internal flow because then most of the kinetic compression upstream of the engine, being in the external stream, is isentropic if there is no interference with a boundary layer; and, since the inlet velocity is low, internal skin-friction losses are minimized. On the other hand, a mass-flow ratio greater than 0.6, at least, is desirable to the external flow for two reasons: (1) External compression can thicken or separate the boundary layer on an upstream surface which is in the interference field of the engine flow; (2) a diverging streamtube subjects the inlet lips to large flow angles which can result in an increase in external drag because of wave drag due to local supersonic flow or because of skin friction due to immediate boundary-layer transition. In any event, the sketch shows that choice of an inlet area for the cruise condition produces an inlet much smaller than the area  $A_0$  of low flight speeds. Consequently, at low speeds the mass-flow ratio is high and the flow converges toward the inlet ( $A_0/A_2 \gg 1.0$ ) at large angles which can cause internal separation, low total-pressure ratios, and flow nonuniformity unless special precautions are taken. If the critical design condition is flight at a Mach number of 2 rather than subsonic cruise, the situation at low flight speeds is worse unless the inlet area can be varied with speed. The area that takes in the required air is even smaller at this high speed, and also little fairing of the lip profile is possible because it must be thin to minimize the wave drag of supersonic flight.

From this, it is evident that the principal problem of inlet design in subsonic flow is to select a lip shape and a variation of mass-flow ratio that avoids internal-flow separation at low speeds and detrimental disturbances in the external flow at high speeds. Of course, there is the limitation that the inlet area must not be chosen to be so small that it chokes at a low flight speed, for then the flow to the engine suffers large pressure losses and is nonuniform and unsteady. The conditions in which a Mach number of 1.0 can be reached in an inlet with a sharp lip in uniform flow are shown in figure 2.

Lip design.— The importance of lip shape to pressure recovery in subsonic flight can be seen from the analysis of Fradenburgh and Wyatt (ref. 14). The extreme case of a tube having very thin walls was studied by momentum methods, and the predicted variation of total-pressure ratio  $p_{t_2}/p_{t_0}$  with mass-flow ratio for various flight Mach numbers is reproduced





Sketch (9)

in sketch (9). (Losses in the duct behind the inlet can be added to these total-pressure ratios to determine the pressure at an engine face  $p_{t3}$ . At high mass-flow ratios when the lip is stalled the duct losses are small relative to those due to flow separation at the lip and are seldom known.) If the inlet area is selected for the altitude cruise condition and information similar to that of sketch (9) shows that the mass-flow ratio  $m_2/m_2^*$  is about 0.7 in take-off, the total-pressure ratio  $p_{t2}/p_{t0}$  at the inlet is then less than 0.9. Such pressure losses correspond to a 15- to 20-percent loss in engine thrust which, of course, represents a serious limitation on the acceleration characteristics of an airplane. The flow nonuniformity which accompanies the total-pressure losses can even further limit engine operation. If a smaller inlet area were chosen to suit more closely the requirements of supersonic or low-altitude high-speed flight, the losses would be even greater. On the other hand, the effects of increasing flight speed are rapidly alleviating.

These large pressure losses at low speeds that result from a sharp lip can be avoided by several methods. A curved internal lip profile which the flow can follow prevents separation and the attendant nonuniformity at high mass-flow ratios, or, for a given lip profile, the losses can be reduced by decreasing the mass-flow ratio either by increasing the inlet area or by taking air in through another inlet. Tests of lip profiles on circular nose inlets at low speeds are reported in references 72 to 75. Some of the results, in terms of  $p_{t3}/p_{t0}$ , are presented

in figure 5 and are compared with the prediction of  $p_{t2}/p_{t0}$  for the thin lip of sketch (9). Duct losses have not been subtracted from the theoretical prediction because a wide variety of duct designs are compared, and, in most cases, duct losses by themselves were not measured. For the cases in which smooth, nearly straight ducts were tested, the agreement between  $p_{t3}/p_{t0}$  and  $p_{t2}/p_{t0}$  is good at zero forward speed. However, the losses for the conical-shock inlet from reference 14 are considerably greater than the prediction, presumably because of the duct which was used in this particular test. The scatter of data at the maximum mass-flow ratio is considerable, and a large part of it is undoubtedly due to inaccuracies in total-pressure measurement. Blackaby and Watson (ref. 72) point out that near choking the flow through ducts is very unsteady, and, as mentioned in Appendix B, measurements of pressure recovery by normal methods under these conditions are not reliable. The data on the F-84F and F-100 airplanes are from full-scale tests. The fact that they correlate with the data from model tests indicate that the effects of scale are small. Also, since the predictions of the momentum analysis which have no relation to scale agree so well with experiment, negligible scale effects in regard to lip losses are to be expected.

The tests of reference 73 indicate that for a reasonable variation of shape external lip profile has practically no effect on internal flow. At zero flight speed, the data of reference 72 show that pressure recovery is not highly sensitive to internal profile, for there was little difference between elliptical and circular shapes. However, as shown in figure 5, internal lip profile is important at higher flight speeds, for the elliptical shapes are better than the circular ones. At the flight Mach number of this figure, 0.33, a sharp lip causes relatively large losses at high mass-flow ratios, as at zero forward speed; but, in this case, the prediction of  $p_{t2}/p_{t0}$  is greater than the measurement of  $p_{t3}/p_{t0}$  by 1 to 2 percent, whereas at zero forward speed there was no difference between theory and experiment for high mass-flow ratios. The desirability of the elliptical profile is further substantiated by the recommendations of Pendley, Milillo, and Fleming (ref. 76). An elliptical internal shape was selected for this investigation from previous experience, and it was found that the profile resulted in high total-pressure ratios for a nose inlet at zero angle of attack in the Mach number range from 0.6 to 1.1. At these flight speeds, the mass-flow ratio of an induction-system-engine combination rapidly decreases to values less than 1 (see sketch (8)), and the problem of internal separation from the lip disappears. In fact, even for a perfectly sharp lip, sketch (9) shows that internal pressure losses resulting from lip separation at the mass-flow ratios of interest (up to 0.9) are small at flight Mach numbers above about 0.5. Thus, at high subsonic speeds, skin friction is the major source of pressure loss in well-designed systems.

Some tests have been made of schemes for reducing the mass-flow ratio in low-speed flight to avoid lip separation. These methods consist

of increasing the area through which air can flow into the induction system. In reference 77 a sharp-lip nose inlet was tested with a secondary scoop having sharp lips that opened into the underside of the duct a short distance behind the inlet. At zero flight speed, it was found that the variation of  $P_{t3}/P_{t0}$  with  $m_t/m_t^*$  (where  $m_t$  is the mass-flow through the total area) was nearly identical no matter how much area (up to 68 percent of that of the main inlet) was provided in the auxiliary scoop. Thus, the improvement in pressure recovery that can be expected with this method is entirely the result of reducing the mass-flow ratio for a given engine operating condition. In reference 78 a supersonic conical-shock inlet with a sharp lip was tested with a translating cowl; that is, a short length of cowl including the sharp leading edge could be moved forward exposing a gap with a rounded lip and increasing the minimum throat area. Since the curve of total pressure ratio as a function of mass-flow ratio  $m_t/m_t^*$  ( $m_t$  is here based on the increased throat area) for the extended cowl lies above that with the cowl retracted, it is evident that this method not only increases the available inlet area, but it also improves the quality of the flow.

Angle of attack.— The flow approaching an inlet can be asymmetric with respect to the induction system axis because of the changing attitude of aircraft for various flight conditions, because of the induced flow field of the aircraft, or because the inlet is distorted by configuration requirements. The ultimate result of such asymmetry is internal separation. Data from tests of circular nose inlets at angle of attack and a flight Mach number of 0.24 (ref. 79) show that an inlet with blunt lips maintains high total-pressure ratios and uniform flow to greater angles of attack than one with sharp lips. For example, at an angle of attack of  $15^\circ$  and a mass-flow ratio of 2.0, the inlet with an elliptical blunt lip attained a total-pressure ratio of 0.97 whereas one with a sharp lip attained only 0.90. The corresponding deterioration in flow uniformity was a difference between maximum and minimum total-pressure ratios in the duct of 0.08 for the elliptical lip and 0.16 for the sharp lip.

At Mach numbers from 0.4 to 1.1, the results of references 23, 76, and 80 show that even with sharp lips pressure recovery is nearly insensitive to attitude to angle of attack of about  $8^\circ$  to mass-flow ratios as high as 0.9. At higher mass-flow ratios this range of insensitivity decreases. The sharp-lip inlet of reference 23 suffered greater losses at high angles and mass-flow ratios than did the blunter lips of the tests; at a Mach number of 0.9, an angle of attack of  $12^\circ$ , and a mass-flow ratio of 0.9 the total-pressure ratio was 0.92 whereas a blunter, but still relatively thin lip, had a total-pressure ratio of 0.94. For these flight conditions, the mass-flow ratio ( $m_2/m_0$ ) at which choking occurred with the sharp lip was 0.9 and that of the blunt lip was 0.95.

The sensitivity of an air-induction system to angle of attack is not only a function of lip profile, but it is also affected by the divergence

of the flow behind the inlet. In the tests of reference 76 it was found that an NACA 1-40-200 cowl was more sensitive to angle of attack and mass-flow ratio than a longer cowl, NACA 1-40-400, because the duct in the shorter cowl expanded more rapidly. Thus, some lip bluntness and slow divergence of the flow behind the inlet provides high pressure recovery over a sufficient angle-of-attack range for most purposes. For a still greater range of insensitivity, the lower lip can be drooped and staggered as suggested in reference 76 and tested in reference 81. In the latter investigation, a blunt, staggered-lip inlet was tested at a Mach number of 0.14, and it maintained high pressure recovery throughout the range of the tests from inlet velocity ratios of 0.6 to 2.2 and angles of attack from  $-5^{\circ}$  to  $12^{\circ}$ .

Inlet asymmetry.- An inlet that is distorted relative to the axis of an air-induction system can have larger pressure losses and greater flow nonuniformity than an axially symmetric inlet. For instance, Seddon and Trebble in reference 82 report tests of a wing-root inlet at zero forward speed. In comparing an inlet swept back  $52^{\circ}$  with an unswept inlet, it was found that the losses and flow nonuniformity were about twice those of the unswept inlet. The additional losses were due to separation in the outboard corner of the inlet which resulted from the fact that, for this operating condition, the flow must turn through a large angle to enter the duct, since it approaches nearly normal to the inlet plane. Guide vanes aligned with the duct axis in the outboard portion reduced the flow nonuniformity, but increased the pressure losses. Slots in the inlet lips similar to wing-leading-edge slots, but not swept, reduced both the losses and nonuniformity because they increased the inlet area and bled high-energy air into the region of potential separation.

An important effect of inlet frontal shape is shown by comparison of the flow-distribution measurements of references 83, 84, and 85 from tests of wing-root inlets at Mach numbers from 0.6 to 1.4. The results show that the uniformity of the flow in the portion of the inlet which was unaffected by the fuselage boundary layer - the outboard portion - was greatly improved as the shape was changed from the acute angle of a triangular inlet to a semielliptical or semicircular inlet.

### Supersonic Flight

The considerations of pressure recovery in supersonic flight are more complex than those at subsonic speeds because in supersonic compression of engine air the pressure losses and flow nonuniformity can be caused by two additional factors, shock waves and shock-wave-boundary-layer interaction. These factors become increasingly important as the local Mach number at which they occur increases above 1. Moreover, the necessary increase in thrust of air-consuming jet engines with speed depends upon the increase in total pressure

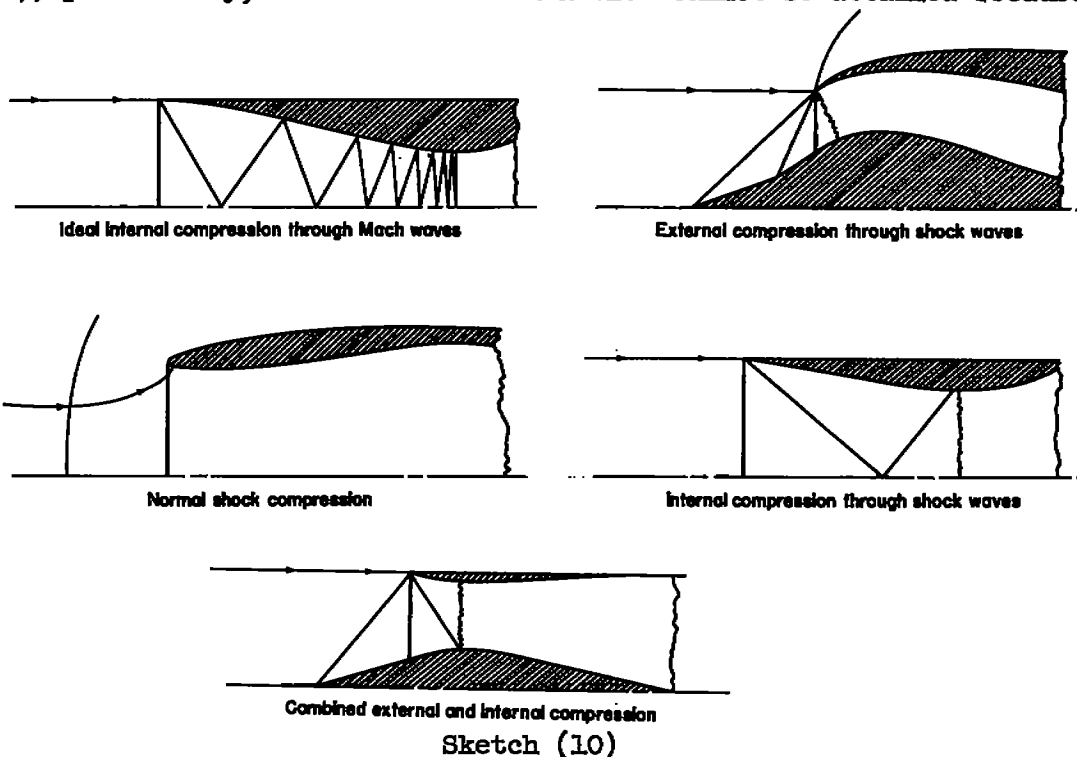
$$p_{t_0} = p_0(1 + 0.2M_0^2)^{3.5}$$

and density

$$\rho_{t_0} = \rho_0(1 + 0.2M_0^2)^{2.5}$$

Little of the available pressure and mass flow can be lost if an engine is to overcome the large drag forces of supersonic flight. In many cases, the margin of excess thrust at supersonic speeds is relatively small, and the thrust-available and thrust-required curves are slowly convergent. Then, small losses in total pressure cause large reductions in acceleration and maximum-speed performance.

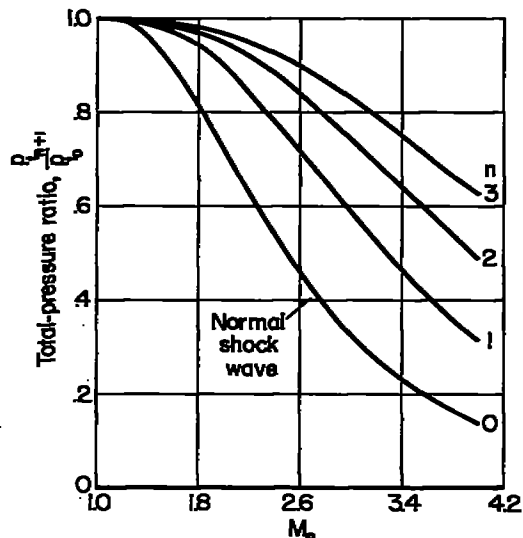
Supersonic compression<sup>13</sup>.— Since the local Mach number at the intake of present-day engines must be subsonic, the flow to the engine of a supersonic aircraft must be decelerated through a Mach number of 1. Ideally, this compression of the air can be accomplished isentropically through a reversed Laval nozzle with no external wave drag as indicated in sketch (10); practically, shock-free internal flow cannot be attained because



<sup>13</sup>Ferri in reference 86 and Lukasiewicz in references 53 and 87 discuss many of the principles involved in supersonic compression. In this report, these principles are mentioned only briefly, and the emphasis is on presenting information that is useful in design and in pointing out limitations for the flight conditions under consideration.

the flow through such a channel is in a state of neutral equilibrium. Any disturbance which causes a loss in total pressure between the entrance and the throat causes a decrease in mass flow through the throat because here the area and velocity are fixed. Air must then accumulate because more flows into the passage than can flow out, and a normal shock wave is formed which must move upstream, continually growing stronger, until it is expelled from the channel and spills the excess air. The shock wave cannot re-enter the channel unless the throat is opened sufficiently to pass the full mass flow at the stagnation pressure existing behind the normal shock wave in the free stream. (For detailed discussions of these phenomena see refs. 86 through 89.)

It is, of course, not necessary to attempt supersonic compression either in a closed channel or isentropically. The flow can be decelerated externally and through discrete shock waves as shown for several possible arrangements in sketch (10). The crudest method which entails the greatest losses is to accept a normal shock wave at the free-stream Mach number. Since these normal shock losses can be reduced by decreasing the Mach number at which they occur, higher total-pressure ratios can be attained by placing an inlet in a region of substream velocity on an aircraft, as will be discussed subsequently under INTERFERENCE, or by creating oblique shock waves to reduce the local Mach number but with less loss than that of a single normal shock wave. For a given local Mach number ahead of an air-induction system, the question arises as how best to utilize oblique shock waves. Oswatitsch (ref. 90) has shown that the maximum total-pressure ratio of a two-dimensional multishock system occurs when the total-pressure ratio across each oblique shock wave is the same. For such conditions, the variation of total-pressure ratio with Mach number for shock-wave compression ( $n$  oblique waves plus terminal normal shock wave) is shown in sketch (11). It is apparent that the losses through a single normal shock wave rapidly become intolerable above a Mach number of about 1.6 and that large improvements can be made by utilizing oblique shock waves.<sup>14</sup>



Sketch (11)

The variation of total-pressure ratio with deflection angle for various approach Mach numbers in two-dimensional flow is shown in figure 6 for a two-shock system (one oblique and a terminal normal shock wave) and in figure 7 for a three-shock system. Figure 8 presents these variations for a two-shock

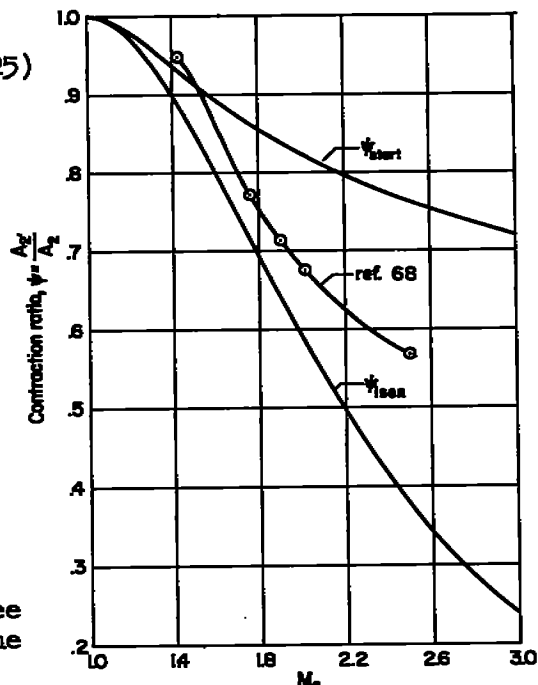
<sup>14</sup>Detailed information and design charts on shock waves can be obtained from such references as 91 and 92.

system in conical flow and is taken from reference 53 where it is assumed that the normal shock wave occurs at the average of the Mach number behind the conical shock wave and on the cone surface,  $(M_s + M_c)/2$ . This assumption is adequate for the Mach number and cone-angle range of interest in the flight conditions being considered in this report because the difference between  $M_s$  and  $M_c$  is small, less than 0.01. It is apparent from this fact that the maximum total-pressure ratio attainable in two-dimensional and conical flows is about the same. Lukasiewicz in reference 53 shows that this difference in total-pressure ratio at Mach numbers less than 2.0 is less than 0.015. The curves of figures 6, 7, and 8 show that total-pressure ratios near the maximum can be maintained for a relatively wide range of flow deflection angles, an important fact because an angle can be selected which produces nearly maximum recovery at the high-speed condition with little decrease from the maximum possible for a considerable range of lower Mach numbers. Also, the angle can be chosen so that a detached shock wave occurs only at a low supersonic speed where the entropy rise through a normal shock wave is small. For example, at an upstream Mach number of 1.8, the maximum total-pressure ratio with a two-shock system is 0.945, and the corresponding flow deflection angle is  $14^\circ$ , for which the detachment Mach number is 1.57. If a  $10^\circ$  deflection angle were selected, only 0.01 would be lost in total-pressure ratio at the design Mach number, but the shock-detachment Mach number would be reduced from 1.57 to 1.37 and, in this Mach number range, recovery would be improved several percent. The total-pressure ratios decrease beyond the maximums (the values plotted in sketch (11) for the two-dimensional cases) because the losses through the oblique waves exceed those through the normal wave until finally the oblique wave detaches from the deflecting surface and only the pressure recovery through a single normal shock wave is possible. The high level of total-pressure recovery that can be attained by conical-shock compression has been verified at Mach numbers to 2.1 in references 13, 93, and 94. In reference 94 a center body contoured for isentropic compression at a Mach number of 1.85 produced a total-pressure ratio of 0.967; with three oblique shock waves, the total-pressure ratio was 0.954; and with two, it was 0.945. In all cases, a uniform flow was measured after diffusion. These values are very close to those obtained by adding the predicted shock losses to the experimental duct losses described previously.

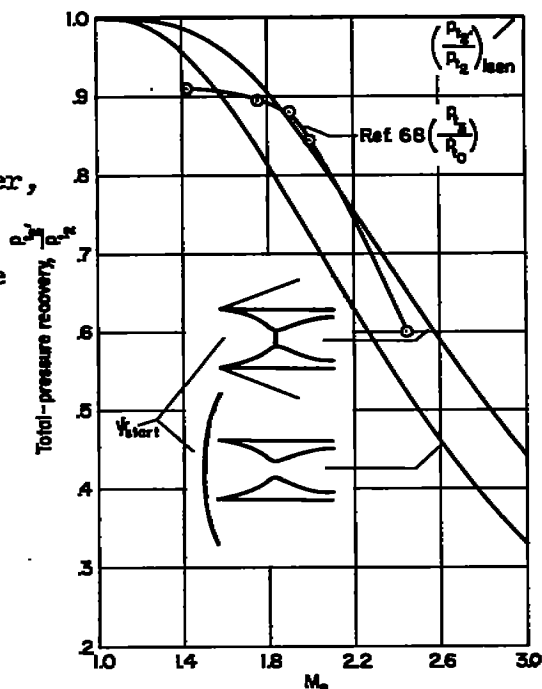
Limiting internal contraction.— For internal-compression systems through shock waves, the problem of flow stability exists as in the reversed Laval nozzle because of the two possible stable positions of the normal shock wave, ahead of the inlet or downstream of the throat. However, at the expense of complication, this disadvantage can be overcome, and this form of supersonic compression has the advantage over external compression of deflecting the flow toward the system axis rather than away from it. The frontal area, external drag, and amount of turning in the duct can thereby be reduced. Thus, the optimum arrangement for any specific case requires detailed evaluation. The relation between contraction ratio, total-pressure ratio, and Mach number is

$$\psi \equiv \frac{A_2'}{A_2} = \frac{M_2'}{M_2'} \left( \frac{1 + \frac{\gamma-1}{2} M_2'^2}{1 + \frac{\gamma-1}{2} M_2^2} \right)^{\frac{\gamma+1}{2(\gamma-1)}} \frac{p_{t_2}}{p_{t_2'}} \quad (25)$$

This relation is plotted in sketch (12a) for isentropic flow to a Mach number of 1 at the throat. Also shown is the contraction ratio which permits isentropic flow to a throat Mach number of 1 from the total pressure existing behind a normal shock wave. This is the contraction ratio at which supersonic flow can be established in a fixed internal-contraction inlet at a given flight Mach number and is designated  $\psi_{start}$ . Total-pressure-ratio curves for two positions of the normal shock wave for  $\psi_{start}$  are also shown for the cases where the normal shock wave is at the throat and in the free stream. It is, of course, possible for the normal shock wave to be downstream of the throat, in which case the pressure recovery decreases toward the lower curve in sketch (12b). It is apparent that the starting contraction ratio for a Mach number of 2.0, for instance, is less than that permissible at a lower Mach number. Thus, if an aircraft is to reach a Mach number of 2.0 and maintain the total-pressure ratios  $(p_{t_2}'/p_{t_0})_{\psi_{start}}$  or higher, the contraction ratio must decrease with increasing flight speed above a Mach number of 1. Also, it is apparent that above a Mach number of about 1.8, the total-pressure losses with  $\psi_{start}$  are unacceptably large, and it is desirable to decrease contraction ratio and increase supersonic compression toward the isentropic value. If the throat area is adjustable, this can be done as long as the flow at the throat is supersonic. For a given contraction ratio the Mach number at the throat can be calculated from equation (25), and the maximum total-pressure ratio possible is that of a normal shock wave occurring at Mach number  $M_2'$  with  $p_{t_2}'/p_{t_2}=1$ .



Sketch (12a)



Sketch (12b)



However, if the flow at the throat is subsonic due either to a contraction ratio that is too small or to the inlet being too large for the engine-air requirement, a normal shock wave ahead of the inlet reduces the total-pressure ratio to that of the lowest curve shown in sketch (12b). In fact, this type of air-induction system is sensitive to flow changes, and close control of both inlet-area and contraction ratio are necessary if it is to operate with an engine through a wide range of flight conditions. The pressure recovery can decrease abruptly from the maximum possible with small changes in either mass flow or angle of attack (see ref. 53).

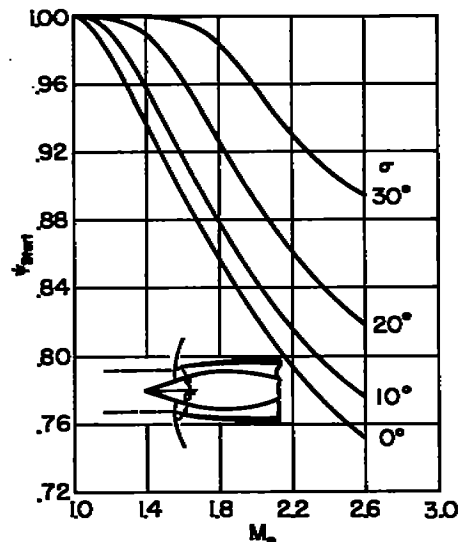
An induction system in which both inlet and throat areas were adjustable to match engine-air requirements and provide maximum total-pressure ratio with internal contraction through two oblique shock waves and a terminal normal wave has been reported by Scherrer and Gowen in reference 68. It was found, as shown by the data points in sketch (12), that in this particular test a contraction ratio well below  $V_{start}$  could be reached, but there were no significant improvements in corresponding total-pressure ratios. It was concluded that the increasing supersonic compression was counteracted by increasing losses in the duct and that greater refinement in duct design was required.

Other methods than adjustable passage walls have been investigated for avoiding the flow-stability problem of internal-contraction inlets. Evvard and Blakey (ref. 95) tested an open-nose inlet in which the contracting passage was perforated to permit the escape of excess flow between the inlet and the throat as the normal shock wave moved into the channel with increasing flight Mach number or mass-flow ratio. A high maximum total-pressure ratio, 0.93, was measured at a Mach number of 1.85, and the inlet was found to be relatively sensitive to mass flow but not to angle of attack. It was estimated that 5 percent of the total mass flow was lost through the perforations. Further tests on this method of flow stabilization are presented in references 96, 97, and 98. Although high pressure recovery is attained with this type of inlet, it is accompanied by high drag if the flow through the perforations is vented to the external stream. For example, the data of references 97 and 98 show that the drag of perforated inlets is as much as 25 percent greater than that of unperforated types. A similar method of providing flow stability when the terminal normal shock wave is at the throat has been reported by Neice, reference 99. Here, the channel walls are vented, immediately ahead of the throat to a chamber to permit the escape of excess mass flow when a disturbance tends to force the normal shock wave upstream into the converging passage.

Rectangular scoop inlets with side walls swept back toward the body as described in references 53, 100, and 101 are able to maintain supersonic flow to the throat of a contracting passage at reduced mass-flow ratios and flight Mach numbers because air can escape laterally as the normal shock wave moves down the channel. However, at low flight Mach numbers the first oblique shock wave from the compression surface is forward on the fuselage, and it interacts with the boundary layer causing both high drag and poor pressure recovery. These difficulties have been partially

circumvented by use of a leading-edge flap on the compression surface. (See ref. 101.) Deflection of this flap toward the body reduced the pressure rise across the oblique shock wave at a given Mach number, and delayed boundary-layer separation to lower Mach numbers.

For the conical-shock inlet, internal contraction can be used to produce additional supersonic compression, but at the expense of encountering the flow-stability problem and additional duct losses. Lukasiewicz derives in reference 53 the contraction ratio  $\psi_{\text{start}}$  that can be used with conical-shock inlets, based upon the assumption that the entrance Mach number is the average of that behind the shock wave and on the cone surface. This variation is presented in sketch (13). It is seen that for large cone angles the permissible contraction is small. Experiments at  $M_0 = 1.85$  (ref. 93) show that for an inlet with a straight lip (not cambered to meet the local flow), internal contraction reduces the optimum cone angle for maximum pressure recovery to about  $25^\circ$  as compared to  $30^\circ$  for an inlet with only conical-shock compression, (fig. 8). However, the difference in maximum possible recovery is small. Only for small cone angles where the oblique shock wave is not being fully utilized can internal contraction produce any great advantage. Tests have been made at a Mach number of 1.85 with conical-shock inlets having internal contraction and a perforated lip to provide flow stability. (See ref. 94.) The results indicate very high maximum total-pressure ratio, 0.95, for this arrangement. Both drag and pressure-recovery measurements were made for a conical-shock inlet with a  $20^\circ$  cone and a perforated cowl at Mach numbers of 1.59, 1.79, and 1.99 in reference 96. The results indicated that even though high pressure recovery was obtained at zero angle of attack a relatively large increase in external drag occurred relative to similar unperforated inlets. The pressure recovery was relatively insensitive to mass-flow change above the mass-flow ratio at which shock oscillation occurred. With increasing angle of attack both the range of mass flows for steady operation and the pressure recovery decreased at all Mach numbers, the latter being a more pronounced decrease than with similar unperforated inlets.



Sketch (13)

Limiting inlet Mach number.— For external-compression systems there is no problem of flow stability as there is with internal-compression systems. There is, however, a limitation on how nearly isentropic the compression can be, or, in other words, on the number of oblique shock

waves which it is practical to use. This limitation arises because the larger the number of shock waves, the higher the subsonic inlet Mach number and the greater the duct losses. Hence, optimum supersonic compression requires excellence in duct design. The following table shows the local Mach number and total-pressure ratio after the terminal normal shock wave in a pattern arranged with  $n$  oblique shock waves to produce the maximum supersonic compression at approach Mach numbers of 1.5 and 2.0. Subtracted from these total-pressure ratios are the duct losses corresponding to the inlet Mach number as measured with a duct with very small losses in reference 64. Thus, for these conditions, which are probably about the

Duct $13.5^\circ - 0$ , $(\theta/r)_2 = 0.00143$								
$M_0 = 1.5$					$M_0 = 2.0$			
$n$	$M_2$	$\frac{P_{t2}}{P_{t0}}$	$\frac{P_{t2}-P_{t3}}{P_{t0}}$	$\frac{P_{t3}}{P_{t0}}$	$M_2$	$\frac{P_{t2}}{P_{t0}}$	$\frac{P_{t2}-P_{t3}}{P_{t0}}$	$\frac{P_{t3}}{P_{t0}}$
0	0.70	0.93	0.02	0.91	0.58	0.72	0.01	0.71
1	.86	.98	.02	.96	.74	.90	.02	.88
2	.91	.99	.03	.96	.83	.95	.02	.93
3	.94	1.00	.04	.96	.90	.97	.03	.94

best that can be expected in the present state of practical design knowledge, little can be gained by using more than one oblique shock wave at a Mach number of 1.5 or two oblique waves at a Mach number of 2.0. If a poorer duct is used, say the duct with a thick initial boundary layer and a two-radius offset as described in reference 64, the following results are obtained when it is combined with shock-compression inlets:

Duct $13.5^\circ - 2$ (Offset = $2r_2$ ), $(\theta/r)_2 = 0.0156$								
$M_0 = 1.5$					$M_0 = 2.0$			
$n$	$M_2$	$\frac{P_{t2}}{P_{t0}}$	$\frac{P_{t2}-P_{t3}}{P_{t0}}$	$\frac{P_{t3}}{P_{t0}}$	$M_2$	$\frac{P_{t2}}{P_{t0}}$	$\frac{P_{t2}-P_{t3}}{P_{t0}}$	$\frac{P_{t3}}{P_{t0}}$
0	0.70	0.93	0.09	0.84	0.58	0.72	0.06	0.66
1	.86	.98	.14	.84	.74	.90	.10	.80
2	.91	.99	.16	.83	.83	.95	.13	.82
3	.94	1.00	.17	.83	.90	.97	.16	.82

Here, the advantages of high supersonic compression are further reduced. At a Mach number of 1.5, a normal shock wave might as well be used, and at a Mach number of 2.0, a single oblique shock wave very nearly produces maximum pressure recovery. Oswatitsch establishes this point in reference 90 by considering the arrangement of oblique shock waves which would produce the maximum static pressure behind the terminal normal shock wave. This would be the best initial condition for a poor duct installation.

It is shown that oblique shock waves produce no improvement to a Mach number of 1.6 and that a single oblique wave is sufficient to a Mach number of 2.0.

At flight Mach numbers greater than 2.0, another limit appears on the number of oblique shock waves that can be used beneficially. As pointed out by Lukasiewicz in reference 87 and Connors and Woollett in reference 102, supersonic flow can be turned and compressed by deflecting surfaces through such large angles that a normal shock wave must form at the streamline which turns through the maximum angle possible for attached flow. This normal shock wave occurs at Mach numbers above about 2.2 before essentially isentropic compression can be achieved; at lower Mach numbers, nearly isentropic compression is possible without the occurrence of a normal shock wave from this cause.

Boundary-layer shock-wave interaction.- Probably the most important limitation on supersonic compression is caused by the interaction of shock waves with boundary layers. For instance, Seddon in the note appended to reference 103 shows that for a side intake without boundary-layer removal and only a normal shock wave for supersonic compression, the total-pressure loss due to this interaction was greater than the sum of the losses from all other sources at Mach numbers between 1.0 and 1.4 and was about equal to that across a normal shock wave at 1.7, where, in general, normal-shock losses are unacceptably high. These interference losses were due to turbulent mixing in the flow after separation and to changes in skin friction and shock losses from their values in unseparated flow.

The boundary layer separates at relatively low local supersonic Mach numbers, about 1.25 and greater, when a normal shock wave interacts with a turbulent boundary layer; it separates at very low supersonic Mach numbers, locally about 1.1, when the interaction is with a laminar boundary layer. (See refs. 103 through 107.) Of course, if the profile of the boundary layer has developed an inflection ( $H \geq 1.8$  in incompressible flow) before the interaction, a less intense shock wave causes separation. The data of reference 106 show that for the range of flight conditions of interest in this report, the static pressure-rise ratio at separation is not a strong function of Reynolds number if the flow to the point of reattachment is turbulent. However, if transition occurs between separation and reattachment, there is a Reynolds number dependence. In air-induction-system design or testing in conditions in which a laminar boundary layer in the engine-flow streamtube could exist, provision should be made for causing transition upstream of shock waves. The reasons are that a shock wave of practically any strength can separate a laminar layer and that any saving in skin friction due to maintaining a laminar layer is negligible. Also, the Reynolds number dependence if the initial boundary layer were not turbulent could produce unreliable test measurements. Separation is to be avoided not only because of pressure losses but also because of flow unsteadiness and nonuniformity. However, small

~~CONFIDENTIAL~~

amounts of separation with subsequent reattachment are not necessarily serious, and information is required on the allowable tolerances for regions of separated flow.

With air-induction systems, the shock waves that interact with a boundary layer can originate from a change in surface slope, from neighboring surfaces, or from the normal shock wave which terminates supersonic compression. Bogdonoff and Kepler (ref. 105) indicate that for local Mach numbers through 2.0, a static-pressure-rise ratio of about 2 causes separation. Gadd, Holder, and Regan (ref. 106) show a value of 1.7; Nussdorfer (ref. 104) suggests a value of 1.89; Lukasiewicz (ref. 52), Seddon (ref. 103), and Dailey (ref. 108) suggest 1.8, the pressure ratio across a normal shock wave occurring at a Mach number of 1.3; and the criterion of Nitzberg and Grandall  $[(u_{sep}/u_{initial})^2 = 1/2]$  corresponds to a static-pressure-rise ratio of 1.7 (ref. 109). Such differences are due to the method used to determine separation and to test conditions. Nussdorfer's criterion of static-pressure-rise ratio of 1.9 was derived from a study of air-induction-system data which included both plane and conical compression surfaces. If this criterion is used as the one appropriate to present design methods for the case where a normal shock wave interacts with a turbulent boundary layer, the limitations on shock compression because of separation are those superimposed on the curves of total-pressure ratio as a function of flow deflection angle and Mach number presented in figures 6, 7, and 8. If it is assumed that the degree of separation at the boundary determined by Nussdorfer's criterion is sufficient to reduce induction-system performance, it is evident that in the Mach number range up to 2.0 inlets must be designed for nearly the optimum shock configuration. If a smaller deflection angle is used, the terminal normal shock wave is intense enough to cause separation. This interaction undoubtedly decreases performance in cases where the boundary layer just ahead of the normal shock wave is on the verge of separation and where the subsequent flow is not given an opportunity to reattach. For instance, the sketch in figure 7 shows a condition where the pressure rise in the vicinity of the oblique-shock reflection could be sufficient to cause local separation or at least disturb the boundary layer sufficiently so that the terminal normal shock wave would ensure separation. The limitations for avoiding separation in this case are more severe than indicated in this figure. Comparison of figures 6, 7, and 8 shows that a strict requirement of avoiding bow-shock wave detachment and separation due to the terminal normal shock wave through a range of flight Mach numbers makes systems in which the configuration can be varied necessary at Mach numbers above about 1.6 in two-dimensional flow and above about 2.0 in conical flow. (Other reasons for variable systems and information on those that have been tested will be discussed subsequently.)

Separation due to changes in surface slope and to impinging shock waves from other surfaces can be alleviated by reducing the pressure gradient by distributing the disturbance over some length. In other words, discrete shock waves are to be avoided. For instance, Chapman, Kuehn,

and Larson in some as yet unpublished results found that the turbulent boundary layer can withstand a large pressure rise on a curved surface where it has sufficient distance in which to re-energize itself. (See also refs. 43 and 110.)

If boundary-layer separation due to interaction with shock waves cannot be avoided in induction-system design, it can, of course, be prevented by removing or re-energizing the approaching boundary layer. Investigations of such methods are reported in references 111 through 115. The investigations of boundary-layer removal near the minimum-area station by both porous suction and slots show that some improvement in pressure recovery at low mass-flow ratios can be achieved. More important, however, is the improvement in flow uniformity and steadiness over a wide range of mass-flow ratios. Similar results are obtained with blowing methods of boundary-layer control in which the point of discharge is upstream of the minimum-area station. (See refs. 113 and 114.)

To summarize, separation can easily be caused by the interaction of shock waves with a boundary layer. To avoid separation, the boundary-layer profile approaching the region of supersonic compression should have no inflection; changes in surface slope and impinging disturbances should be distributed to reduce the pressure gradient; the proper arrangement of shock waves should be used to keep the interaction pressure ratio at the terminal normal shock wave below that which would produce separation; and the initial subsequent compression should be small. Thus, the mass-flow ratio should be high to minimize subsonic compression behind the terminal shock wave, and a nearly straight entry section should be used in the duct to minimize the pressure gradient and to permit reattachment if some separation does occur. The boundary layer can be removed or re-energized to avoid or reduce the interaction.

Lip design.— In supersonic flight, the problems of lip design are different from those of subsonic flight, for there is no possibility of external streamlines converging upon the inlet and causing separation of the internal flow. The problems are those of locating and shaping the lip properly to maintain high pressure recovery and low net drag without severely compromising these qualities in subsonic flight.

Tests of open-nose inlets to determine the effects of lip profile in supersonic flight are reported in references 23 and 116. It was found that curved internal surfaces that are satisfactory at subsonic speeds can be used at supersonic speeds at least to a Mach number of 1.7 without any sacrifice in total-pressure ratio. In fact, a lip described in reference 23 with  $(r/R)^2 = 1.15$  produces higher pressure recovery than a sharp lip at Mach numbers to 1.5, and, as shown in figure 5, this lip maintains high recovery to relatively large mass-flow ratios at subsonic speeds.

With internal-contraction inlets designed for the contraction ratio  $V_{start}$  (see p. 40), the profile of the contracting passage can as well be

a straight line as a theoretically more efficient contour because the permissible contraction is small to a flight Mach number of 2.0. For such inlets with an adjustable throat to increase the contraction while in flight to values less than  $V_{start}$ , a straight-line profile at the lip is also sufficiently refined in this Mach number range. The deflection angle at the lip leading edge should, of course, not exceed the angle for shock-wave detachment or for regular reflection (see refs. 53 and 92). However, as shown by the results in reference 54, and as discussed previously, it should be a sufficiently large angle to minimize the effects of interaction between the boundary layer and the terminal normal shock wave. (The results of Wyatt and Hunczak, ref. 54, further show that an extended entry section permits greater supersonic compression in this type of air-induction system, presumably because the separated boundary layer which follows a relatively strong normal shock wave has an opportunity to reattach.)

Lukasiewicz (ref. 53) in discussing conical-shock inlets with sharp lips shows that neither lip position nor lip incidence have, within reasonable design limits, great significance in affecting pressure recovery at Mach numbers less than about 2.0. Lip position is not important because the velocity gradients for reasonable positions in practical conical flow fields are small. Lip incidence has little importance because even if the shock wave from the lip is detached, it is of small intensity in a design having the relatively large cone angle necessary for maximum pressure recovery.

Although lip design has been found to be of secondary importance in regard to pressure recovery for external-compression inlets, it is of great importance in regard to drag, which will be discussed later.

Mass-flow variation.— Air-induction systems without an adjustable inlet area or a bypass must operate through a range of mass flow as flight conditions change. The previous discussion of supersonic compression has been concerned primarily with considerations of maximum total-pressure ratio at a single design condition, usually the "critical mass-flow ratio." This term denotes the internal flow when there is no subsonic spillage and the terminal normal shock wave occurs at the minimum-area section; that is, when the supersonic compression for the system is maximum. If the transition to subsonic flow occurs downstream of the minimum section, the mass-flow ratio is the same as at the critical condition because there is also no subsonic spillage, but the total-pressure ratio is less because the terminal shock wave occurs at a higher local Mach number. Such operation is termed "supercritical" and the total-pressure ratio is determined by the flight conditions and the requirements of flow continuity and of the flow schedule of the engine. From equation (16)

$$\frac{P_{t3}}{P_{t0}} = \frac{85.4 \left( \frac{m_2}{m_0} \right) M_0 A_2}{\frac{W_a \sqrt{\theta}}{8} \left( 1 + \frac{\gamma - 1}{2} M_0^2 \right)^{\frac{\gamma + 1}{2(\gamma - 1)}}} \quad (26)$$

Thus, for a specific mass-flow ratio, a reduction in inlet area produces a low pressure recovery for a given engine corrected air flow and flight Mach number; or, for a given inlet area and mass-flow ratio, corrected air flows or flight Mach numbers above the design value also reduce the total-pressure ratio. Systems are sometimes designed to operate at supercritical conditions in order to avoid flow unsteadiness which often occurs at mass-flow ratios just below critical, particularly at angle of attack with systems having a large amount of supersonic compression and no interference which alleviates angle-of-attack effects. (See, for instance, refs. 117 and 118.) When the transition to subsonic flow is upstream of the inlet, the subcritical condition, a normal shock wave occurs externally and flow is spilled behind it to reduce the mass-flow ratio from the maximum. The possible total-pressure ratio at these reduced mass flows can be calculated from the known shock pattern if the pressure rise through the shock waves is not so great as to cause separation losses or to distort a boundary layer enough to change the shock pattern.

Experimental investigations of isolated air-induction systems through the range of mass-flow ratios show, in general, that inlets which attain very high total-pressure ratios at the critical condition are very sensitive to changes in operating flow conditions. That is, total-pressure ratio is markedly reduced if operation is very far subcritical, and, as with any inlet, recovery decreases rapidly in the supercritical range. The data summarized by Lukasiewicz (ref. 53) illustrate this fact. Thus, an open-nose inlet which accepts supersonic compression through a normal shock wave does not, as shown in sketch (11), attain a high total-pressure ratio, but essentially the maximum total-pressure ratio with uniform flow at the compressor face is maintained throughout the subcritical range. The total-pressure ratio which has been measured in experiments is that calculated for the normal-shock wave minus the duct losses. An internal-contraction inlet suffers an abrupt total-pressure loss and operates as a normal-shock inlet as soon as the flow becomes subcritical. Conical-shock inlets designed with more than one oblique shock wave also have this disadvantage of an abrupt decrease in total-pressure ratio at subcritical mass-flow ratios, presumably because the boundary-layer profile approaches that for separation in passing through the large adverse pressure gradients of the supersonic compression. However, conical-shock inlets with one oblique shock wave designed for near-maximum-total-pressure ratio can maintain a high level of pressure recovery well into the subcritical range. Use of less than the optimum cone angle (included angles less than about  $50^\circ$ ) produces a terminal normal shock wave of too great intensity



which adversely affects subcritical operation. The most disturbing difficulties at reduced mass-flow ratios are flow nonuniformity and unsteadiness which are caused by separation that can arise from a number of sources. An extended subcritical range of mass-flow ratios in which the flow is steady can be obtained by choice of the proper shock pattern and duct design or by boundary-layer removal.

Since fixed-area intakes can be unsatisfactory at mass-flow ratios other than that chosen as the design point, systems must be considered in which a constant, or nearly constant, mass-flow ratio maintains a high level of over-all induction-system performance through a wide range of flight conditions. This can be accomplished by varying the inlet area; or, for a fixed inlet area, excess air can be bypassed to satisfy the engine air requirements while operating the induction system near its best design point. By these methods the reduction in propulsive-system performance from additive drag, reduced pressure recovery, or flow nonuniformity and unsteadiness can be avoided at the expense of weight and complication. For aircraft which must fly at widely different conditions of power, altitude, and speed, such complication is necessary. The best arrangement for any particular aircraft requires detailed evaluation.

Perhaps the simplest variable systems for matching the air requirements of an engine are an auxiliary scoop (ref. 74) and a bypass (ref. 119). With the former, the main inlet is matched in area for the high-speed flight condition and an auxiliary scoop is opened for flight at lower Mach numbers. With a bypass between the inlet and the engine, the inlet area is generally chosen for the altitude cruise condition and is large for flight at high speed or low altitude. The excess air is dumped overboard through the bypass. The analyses of references 74 and 119 show that these systems have various advantages and are superior to other systems for certain flight conditions. Experiments have demonstrated that at Mach numbers up to 2.0 the drag of the bypass can be small as long as the air is ejected nearly parallel to the local flow direction. (ref. 120).

Another variable system is a conical-shock inlet in which the center body can be moved fore and aft to regulate the mass-flow ratio. This is the translating-cone inlet (refs. 121, 122, and 123). When the oblique shock wave from the cone apex intersects the inlet lip, the mass-flow ratio is the maximum. When the cone is moved forward relative to the lip, the mass-flow ratio is reduced by supersonic spillage and the additive drag is not as large as if the spillage were behind a normal shock wave (see p. 64). Gorton shows in reference 122 that such inlets can be designed for high pressure recovery at Mach numbers from 1.5 to 2.0. The effects of various design compromises which must be made in the design of such translating-cone inlets are studied in reference 123. The performance of three inlets each in combination with three turbojet engines is compared. The choice of inlet was found to depend upon the engine air-flow schedule and the flight conditions selected as critical. In reference 31 tests with an operating turbojet engine of a translating-cone inlet and

of a bypass system at flight Mach numbers of 0, 0.6, 1.7, and 2.0 are described. Both systems eliminated flow spillage behind a normal shock wave, but the net propulsive forces were not determined. This investigation was extended in reference 124 to include automatic control of a system with a translating cone and a bypass combined. By sensing total pressure at the cone tip and cowl lip and static pressure just inside the inlet, the oblique shock wave could be maintained at the lip and the terminal shock wave could be positioned just inside the cowl. The total-pressure recovery varied from 0.92 to 0.88 as the Mach number was changed from 1.7 to 2.0 (see fig. 9).

Air-induction systems in which the deflection angle of the supersonic compression surfaces can be varied to provide for engine-inlet matching through a range of flight conditions have been tested in a wide variety of arrangements. In reference 125 a precompression ramp followed by a variable second ramp was used to improve the performance of a twin-scoop installation with fixed-area inlets. Precompression ramp angles of  $3^\circ$  and  $10^\circ$  were tested in combination with the variable second ramp; the larger angle produced the better pressure recovery. However, nonuniformity in the total-pressure distribution at the diffuser exit of more than 5 percent existed for all the configurations tested. An underslung scoop having a variable horizontal ramp or a variable vertical-wedge compression surface is described in reference 112. The total-pressure ratios attained in tests at Mach numbers from 1.4 to 1.8 are shown in figure 9. It is seen that these systems produce relatively high total-pressure ratios. Further tests reported in reference 112 of an underslung scoop with boundary-layer removal through porous suction over the compression surfaces show an increase in total-pressure ratio of as much as 5 percent with nearly the same gain in net propulsive force.

The problem of providing high values of net propulsive force for a self-accelerating ram-jet missile requires some form of variable inlet area, and the variation must be accomplished in a simple manner. A drop-able cowling to provide, in effect, two inlets is reported in reference 126. A cowling was added to a double-cone inlet designed for  $M_0 = 2.4$  so that the combination was a normal-shock inlet, and tests were made at Mach numbers of 0.64, 1.5, and 2.0. Substantial improvements in net propulsive force over that of the double-cone inlet were obtained at these Mach numbers.

Investigations of inlets having both variable inlet and throat areas are reported in references 68 and 127 and the pressure recovery characteristics are compared with those of other inlets in figure 9.

Angle of attack.- As in subsonic flight, the flow approaching an air-induction system at supersonic speeds can be at an angle to the system axis because of the attitude of the aircraft and because of induced effects. As in the case of mass-flow variations, inlets which attain very high total-pressure ratios are, in general, sensitive to angle of attack.

Lukasiewicz (ref. 53) shows that an open-nose inlet with normal-shock compression is not affected by angle of attack up to  $5^\circ$ ; but the other inlets, that is, the internal-contraction and conical-shock types, suffer losses in maximum total-pressure ratios of from 3 to 4 percent at angles of attack of  $5^\circ$ . (See refs. 53, 122, and 128.) At higher angles of attack separation from the lower lip of symmetric open-nose inlets reduces the pressure recovery until at angles of attack of the order of  $20^\circ$  at a Mach number of 1.42, the maximum total pressure ratio decreases from 0.95 to 0.85 (fig. 10). The reductions in pressure recovery are greater for conical-shock and internal-contraction inlets.

Several methods for maintaining the zero-angle-of-attack level of pressure recovery with changing angle of attack have been proposed. A summary of test results is presented in figure 10. Beheim suggested a pivoted cone in reference 129, and found that relative to a fixed-cone inlet, an increase in maximum pressure recovery, mass-flow ratio, and flow steadiness could be obtained at angle of attack. However, there was no improvement in flow uniformity, and maximum pressure recovery occurred at a reduced mass-flow ratio. A method is proposed in reference 130 in which an inlet with a vertical-wedge compression surface inside a conical cowl was modified by perforating the wedge center body and cutting back the lower half of the cowl lip. Total-pressure recovery obtained with this inlet, although lower than with comparable conical-shock inlets, was essentially constant with increasing angle of attack up to an angle of at least  $10^\circ$ , the limit of the tests. There was an increase in the subcritical mass-flow range for steady flow, and twin-duct instability was eliminated by cross-ventilation through the perforations. Other methods for maintaining the level of pressure recovery with changing angle of attack consist of either canting the inlet plane (refs. 131 and 132) or adding flow deflecting surfaces (refs. 26 and 133). Arrangements for utilizing interference from other aircraft components to keep the flow aligned with the system axis are discussed later under INTERFERENCE.

## DRAG

The design objective in regard to drag is to minimize disturbances in the external flow; that is, to maintain as much laminar flow as possible, to avoid separation, and to avoid shock waves or reduce their intensity. Since the forces of skin friction occur on all external surfaces and are not limited to those of air-induction systems, no detailed discussions of skin friction or of the allied problem of boundary-layer transition are presented in this report. References 41, 42, 134, 135, and 136 contain design information on these subjects.

In this section, only the drag of isolated air-induction systems is considered; that is, wing-root inlets and types which include interference drag forces are not discussed. In general, drag coefficients are based

on the maximum frontal area of the cowl or fuselage. As described previously, scoop incremental or additive drag should be computed to the stagnation point on the inlet lips; however, since the location of the stagnation point is seldom known, these quantities are here computed to the plane tangent to the leading edge of the lips. As discussed in reference 23, such an assumption is conservative. In order to have a reference for the relative importance of the drag components considered, the following table of representative aircraft dimensions and total drag coefficients has been compiled.

Aircraft	Inlet area, $A_2$ , sq ft	Maximum fuselage frontal area <sup>1</sup> , $A_M$ , sq ft	$\frac{A_2}{A_M}$	Wing area, $S$ , sq ft	$\frac{A_M}{S}$	Drag rise	$C_{Dmin} = D_{min}/qS$			References
							Subsonic	Transonic $M_0 = 1.10$	Supersonic $M_0 = 1.50$	
F-100	4.45	26.40	0.169	376.0	0.070	0.92	0.0120	0.0435	0.0430	137
XF-91	4.90	35.50	.138	320.0	.111	.85	.0175	.0630		137
F3B-1	3.72	26.50	.140	415.0	.064	.88	.015	.0515		137
F4D-1	4.28	25.00	.171	557.0	.045	.90	.0100	.0375	.0380	137
F-94C				232.8		.76	.0235			138
F-86D	2.45	24.14	.102	288.0	.084	.85	.0160			139
F-84F		19.41		343.5	.057	.77	.0140			140
XF-92A				425.0		.90	.0100			141
XF-85F	2.45			302.0		.80	.0140			142
F-102	4.20	33.60	.125	661.0	.051	.90	.0100	.0290	.0270	143
F-105		24.70		385.0	.064		.0250		.0340	144
FTU-1	3.20	23.26	.137	496.0	.047	.87	.0140	.0720		145

<sup>1</sup>This area is that of the maximum cross section of the fuselage.

Thus, an approximate figure for the ratio of maximum cowl or fuselage cross-section area to wing area for present-day aircraft is 0.1 and the supersonic drag coefficient at a Mach number of 1.5 is about 0.04. This figure corresponds to 0.400 based on maximum frontal area. Drag-coefficient reductions of 0.005 at supersonic speeds and 0.002 at subsonic speeds due to improvements in the air-induction system represent 1.25-percent reductions in airplane drag. Such increments in drag coefficient are probably the limit of preliminary design accuracy and are the least significant figures worthy of consideration in the following discussion.

### Subsonic Flight

In subsonic flight below the Mach number for drag divergence, the main drag problem of air-induction systems is to reduce skin friction by delaying boundary-layer transition and by minimizing wetted area. Drag due to separation is of little concern even for the relatively sharp lips of supersonic aircraft because, as shown by the discussion of sketch (8), mass-flow ratios are near or above 1 and the angularity of the external flow relative to the inlet lips is small. For subsonic aircraft in which it is desirable to minimize internal losses by having a large inlet area and low mass-flow ratios, external separation can be avoided by use of blunt lips. At the high angles of attack in landing and take-off operations, mass-flow ratios are greater than 1, so the engine-induced flow

counteracts the tendency toward external separation on upper inlet lips. Climb with jet-powered aircraft ordinarily occurs at relatively high speeds where the mass-flow ratio can be less than 1, but, because of the speed, the angle of attack of the airplane is not large. At high subsonic speeds, low mass-flow ratios must be avoided if divergence of the engine-air streamtube ahead of the inlet and shock stall on the inlet lips is to be prevented. Thus, since the external shape of an air-induction system can be considered independently of the duct shape (see ref. 2, p. 60), the design problem in regard to subsonic drag is to select an external contour that encloses the necessary induction system and maintains laminar, shock-free flow through the required range of mass flow and angle of attack.

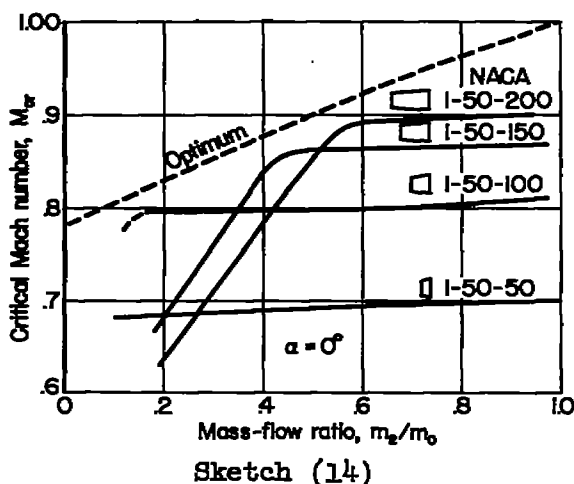
The net drag of an air-induction system is entirely due to skin friction as long as the flow is unseparated and irrotational outside of the boundary layer, for, as shown previously, the pressure force in the drag direction along the free surface of the engine-flow streamtube in equation (7) is offset by a pressure force on the cowl surface in the thrust direction. The experimental results of Blackaby and Watson (ref. 72) show that for a wedge-shaped lip profile ( $7-1/2^\circ$  wedge angle) there is no net pressure drag in low-speed flow at mass-flow ratios above 0.8; for blunter lips, lower mass-flow ratios (less than 0.6) were reached without external separation that caused any appreciable loss in lip suction force. Similarly, measurements to a Mach number of 1 show little change in net drag with mass-flow ratios as low as 0.8 for sharp lips and to less with blunt lips. (See refs. 76 and 146.) From these results, it is apparent that no net pressure drag need be experienced at subsonic speeds in the mass-flow-ratio range of interest. However, for the thin lips required for high-speed flight, a very localized lip suction force to counteract additive drag is not conducive to laminar flow, for a small region of very low pressure is followed by a rising pressure which causes transition to turbulent flow in the boundary layer. From the criterion of Kármán and Millikan (ref. 147) that laminar separation occurs in a positive pressure gradient when the local velocity is about 0.9 the maximum velocity and that laminar separation results in transition, it appears from the pressure-distribution data of reference 146 that at flight Mach numbers greater than 0.8 with a sharp lip, mass-flow ratios greater than 0.9 are necessary to prevent transition from occurring on the lip. For the NACA 1-series inlets of reference 76, mass-flow ratios as low as 0.8 with no serious adverse pressure gradient seem possible in flight to a Mach number of 1.0, although the scatter of the data prevents a definite conclusion. The pressure-distribution data on NACA 1-series inlets at a Mach number of 0.4 (ref. 80) indicate that for usual ratios of inlet to maximum diameter, no suction pressure peak with subsequent transition need occur to mass-flow ratios as low as about 0.4 at zero angle of attack. Similarly, the "class C" profiles of Küchemann and Weber (ref. 2) create no adverse pressure gradient until very low mass-flow ratios, less than 0.4, are reached. These shapes thus can produce low drag in subsonic flight; however, because of their blunt shape, they create high wave drag in supersonic flight (see, e.g., the data of ref. 148). For aircraft that

fly supersonically, thinner lips must be used together with a relatively high mass-flow ratio, greater than about 0.8, to have low external drag through the speed range.

The NACA 1-series profiles (ref. 80) and those described by Küchemann and Weber (ref. 2) were designed according to the criterion of maximizing the critical Mach number of lips, that is, the flight Mach number at which sonic velocity first occurs on the profile. It was thought that this Mach number would indicate the beginning of the transonic drag rise and thus should occur at as high a speed as possible. The drag rise is well predicted by critical Mach number for cowl shapes over which the pressure distribution is nearly uniform (see ref. 2); however, it is not predicted by the critical Mach number as applied to local high-velocity regions.<sup>15</sup> Since, from the skin-friction standpoint, shapes must be chosen that have a nearly uniform distribution of pressure, the critical Mach number is a good indication of the drag-rise Mach number for the shapes of interest. The NACA 1-series and the Küchemann and Weber class C series can thus be used with reliance placed on the predicted drag-rise Mach number. For high Mach numbers of drag divergence, the cowls must be slender as shown in sketch (14). The results of reference 148 show that at high mass-flow ratios, the details of lip shape for slender cowls have little effect on the magnitude of the external pressure drag to flight Mach numbers of 1. The important consideration is the axial distribution of cross-section area, particularly when in combination with other airplane components, as will be discussed later.

As shown by tests reported in references 150 and 151, the Mach number for drag divergence and the magnitude of the transonic drag rise for ducted bodies can be determined experimentally by tests of equivalent bodies. That is, the solid body equivalent to a ducted body from the external-wave-drag standpoint is the ducted body with the free-stream area of the engine streamtube subtracted from the longitudinal area distribution. At mass-flow ratios less than 1, an equivalent body thus has a blunt nose; nevertheless, the experiments indicate that the

<sup>15</sup>The unimportance of localized high-velocity regions on cowls is analogous to the observations of Nitzberg and Grandall regarding airfoils (see ref. 149). Here, it is shown that drag-rise Mach number can best be predicted by applying the Prandtl-Glauert rule to the pressure coefficient at the airfoil crest; in other words, supersonic flow must extend over a considerable portion of the surface for the drag rise to be predicted accurately by the critical Mach number.

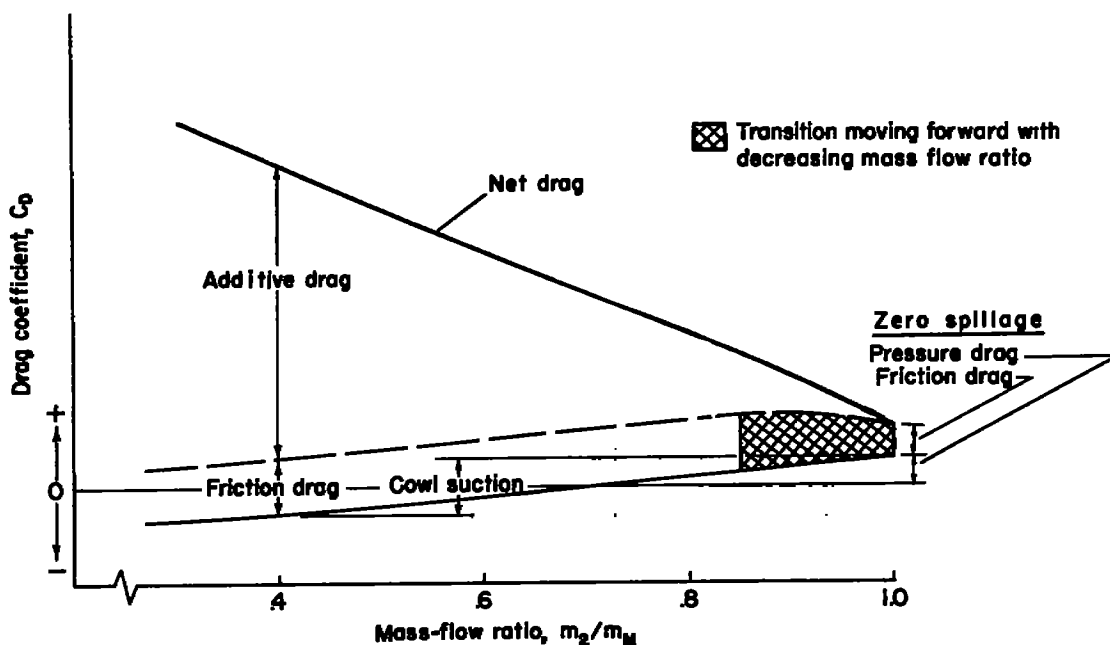


equivalent-body method is a reliable indication of ducted-body drag rise to mass-flow ratios as low as 0.7. The accuracy of this method is greatest for fair equivalent bodies having high fineness ratios.

The effect of angle of attack of air-induction systems on external drag is generally not a serious problem. At the lowest mass-flow ratio that would normally occur in high-speed flight, of the order of 0.6, the pressure-distribution data on the NACA 1-series inlets show that angles to  $4^\circ$  can be reached without a serious suction pressure peak for cowls that are not too slender. A slender cowl, the 1-50-200, for instance, develops a suction pressure peak at this angle whereas the 1-50-150 does not because of the thicker lip.

### Supersonic Flight

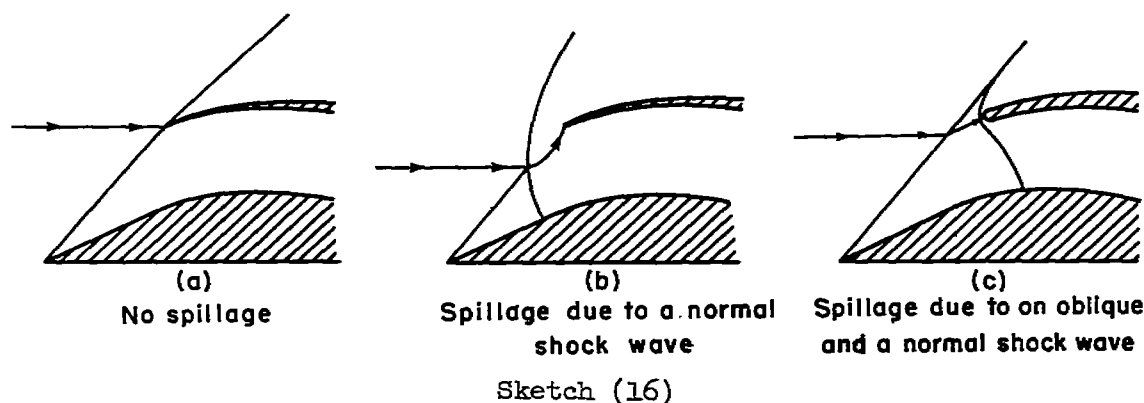
The following discussion of the drag of isolated air-induction systems at supersonic speeds is arranged according to the components which make up the net drag as shown in sketch (15). Here, typical variations of the components of the net drag coefficient with mass-flow ratio for a given flight



Sketch (15)

Mach number are presented. The net drag can be considered to consist of four parts:

1. The external wave (or pressure) drag when the system operates with no spillage, as in sketch (16a).
2. The pressure force on the deflected engine-flow streamtube, as in sketches (16b) and (16c). (This is additive drag.)
3. The change in external wave drag due to a reduction in mass-flow from the maximum, as in sketch (16b) or (16c). (This is called the cowl suction force.)
4. Skin friction (as mentioned on p. 52, this component of the drag is not discussed in this report).



External wave drag with no spillage.— Several methods have been developed for estimating the pressure distribution and wave drag of axially symmetric ducted bodies at zero angle of attack with an attached shock wave on the lip. These are listed with pertinent references as follows:

<u>Linearized methods</u>	<u>References</u>
Brown and Parker	86,152
Lighthill	153,154
Ward	155,156
Jack	157
Moore	158
Ferrari	159,160
Bolton-Shaw and Zienkiewicz	161
Parker	162

<u>Second-order method</u>	
Van Dyke	163,164,165



Higher-order methodReferences

Ferri

86,166

In general, the greater accuracy of the more complicated methods is obtained at the expense of greater labor in making calculations. Also, since the simpler methods utilize more assumptions, their range of applicability is less but is often sufficient for design purposes. In reference 157, the linearized method of characteristics is compared with the source-distribution method of reference 152. It was found that to produce the same accuracy the linearized method of characteristics requires much more computing time. In comparing with the characteristics method of reference 166, this latter procedure was found to require by far the greatest amount of effort, but the comparison showed that for large flow deflection angles at the lip ( $15.5^\circ$ ) the linearized methods underestimate the pressure on the lip and hence the drag, in this case ( $M_0 = 1.8$ ) by 36 percent. In terms of airplane drag, such an error would be equivalent to roughly 1 percent. Ferri compares calculations by the method of characteristics with those of the small-disturbance theory of reference 152 for a cowl with a  $3^\circ$  lip angle at a Mach number of 1.5 and finds that the approximate method underestimates only slightly the pressures along the cowl. In fact, rotation need be taken into account only when a strong curved external shock wave occurs and the variation of entropy along the shock wave is great. Similar comparisons at a flight Mach number of 2 have been made between the methods of references 152 and 164 for a conical and a curved cowl. The conical cowl had a  $3^\circ$  semiapex angle and the ratio of inlet-to-maximum area was 0.676. The curved cowling had a  $12.9^\circ$  initial deflection angle, an area ratio of 0.5, a length-to-diameter ratio  $l/d_M$  of 3.18 and a practical profile which is defined by the relation

$$x = 4.38(r - 1) + 15.51(r - 1)^2 + 77.07(r - 1)^3 + 1.73$$

The outer surface of this lip is parallel to the local flow direction when the shock wave from a  $50^\circ$  cone intersects the lip.<sup>16</sup> The results of this comparison are summarized in the following table:

---

<sup>16</sup>Lukasiewicz in reference 53 presents design information on the flow direction in conical flow fields and on the conditions for regular reflection and shock-wave detachment. It is shown that a lip incidence angle can be selected that is good for a wide range of Mach numbers. Also, a conical-shock inlet designed with a straight lip to provide internal contraction cannot have regular reflection at Mach numbers up to 2.0 if cone angles greater than  $25^\circ$  are used. In two-dimensional flow, attached flow on a straight lip is not possible at a Mach number of 2.0 if the flow deflection angle is greater than  $13^\circ$ .

---

Method	Pressure relationship	Drag coefficient, $\frac{D_{\text{wave}}}{qAM}$	
		Conical cowl	Curved cowl
2nd order	$C_p = \frac{2}{\gamma M^2} \left\{ \left[ 1 + \frac{\gamma - 1}{2} M^2 \left( 1 - \frac{U^2}{V_0^2} \right) \right]^{\frac{\gamma}{\gamma - 1}} - 1 \right\}$	0.0178	0.035
1st order	----- do -----	.0174	.030
Do-----	$C_p = -2 \frac{u}{V_0} - \frac{v^2}{V_0^2} + \frac{u^2}{V_0^2} \sqrt{M^2 - 1}$	.0174	.031
Do-----	$C_p = -2 \frac{u}{V_0} - \frac{v^2}{V_0^2}$	.0174	.029
Do-----	$C_p = -2 \frac{u}{V_0}$	.0187	.028

As in the previous comparisons, the first-order method underestimates the pressure on the lip and the drag; the difference is small if the deflection angle at the lip is small, but the error becomes sizable in terms of cowl drag for large angles<sup>17</sup> (in this case 14 percent when the complete pressure-coefficient relationship is used). In terms of airplane drag coefficient, even this error at large deflection angles is negligible. Van Dyke in reference 165 shows that for cones at Mach numbers less than 2 and cone angles to 30°, the second-order and exact theories give practically identical results. In this reference, it is also shown, as indicated in the table, that higher order terms should be retained in the pressure relationship for calculations involving three-dimensional flow. From these comparisons and knowledge of the shapes that are of practical interest, which will be discussed subsequently, it is concluded that since large lip angles create large drag forces that must be avoided by the designer, the linearized methods are of sufficient accuracy for most design purposes.

Comparison of the quasi-cylindrical theory of Lighthill (ref. 153) with experimental measurements of wave drag is made in references 146

<sup>17</sup>In applying the second-order theory to the curved cowling, it was found that considerably more computation time was required than expected. Reference 164 gives certain rules for selecting intervals for computation. Whereas about 6 intervals are sufficient for solid ogival bodies, the curved cowling required 11 intervals, which increased the labor of computation fourfold.

and 167. It was found that in spite of the fact that the models were not quasi-cylindrical (the ratios of inlet-to-maximum area were 0.25 and 0.50, and the corresponding initial lip angles were  $11.8^\circ$  and  $7.3^\circ$ ) the agreement was satisfactory, as indicated in the following table:

Model	$M_0$	External wave drag coefficient		Error prediction, percent
		Measured	Theoretical	
$A_2/A_M = 0.25$	1.41	0.119	0.136	14
	1.82	.099	.104	5
$A_2/A_M = 0.50$	1.41	.049	.055	12
	1.82	.040	.041	2.5

The theory overestimates the drag coefficient in spite of the fact that it underestimates the cowl pressures because too large a frontal area is assumed for the initial portion of the cowl in these cases. The experimental measurements also substantiate the following predictions:

1. The pressure at the cowl lip corresponds to that downstream of a two-dimensional oblique shock wave created by the lip deflection angle.
2. The pressures on the rear of the cowl approach asymptotically the value for a cone with the same slope. (This is true for all mass-flow ratios.)
3. An expansion about a discontinuity in surface slope is a Prandtl-Meyer expansion. At reduced mass-flow ratios, the Mach number ahead of the corner is determined by the local static pressure and the total pressure behind the normal shock wave.

At a Mach number of 1.33, the theory predicts the pressure on the cowl lip as well as it does at higher Mach numbers, but at  $M_0 = 1.17$  the experiments show that the pressure is overestimated. At lower supersonic Mach numbers this tendency increases. It is therefore concluded that the lower limit at which the linearized theory should be applied is a Mach number of about 1.2.

Warren and Gunn in reference 168 have extrapolated Ward's first-order theory for conical cowls to small values of the ratio of inlet-to-maximum area. The effect is to reduce the overestimation of wave drag shown in the previous table. Their method can be slightly improved at low values of  $A_2/A_M$  and  $M_0$  by using exact values for the drag of cones ( $A_2/A_M = 0$ ) and calculations from second-order theory to indicate more closely the proper trend of the extrapolation. Results from such a procedure are shown in figure 11. (Drag coefficient is based on maximum frontal area.)

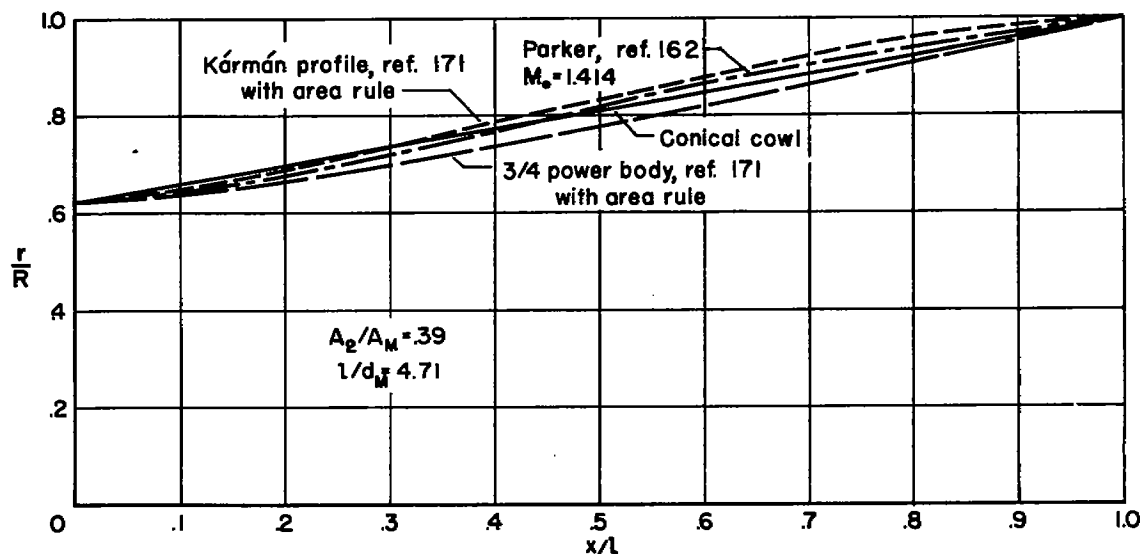
External profile.- From considerations of strictly supersonic flight with inlets having no spillage, the linearized theories have been used to determine the optimum profile of axially symmetric bodies from the stagnation point to the position of maximum diameter. Ward (ref. 169) concluded that the profile is very nearly a straight line, that is, a straight conical taper. Jack (ref. 157) calculated the drag of several profiles for a conical-shock inlet at a Mach number of 2.0 and found that less drag was produced by a conical taper than the curved profiles. Using more exact methods and imposing certain restrictive conditions, Ferrari (ref. 160) and Parker (ref. 162) have found that the optimum profile is curved. Similarly, Walters (ref. 150) and Howell (ref. 170) have applied the transonic-area-rule concept to the design of bodies with nose inlets and have found that the method suggests a curved profile and does produce low drag. The method is to add the longitudinal area distribution of a minimum-drag solid body and the area of the engine-air streamtube to obtain the area distribution of the minimum-drag ducted body. Not only did this method produce a lower drag at full flow than the other bodies which were tested, but also it is stated in reference 170 that more cowl suction force is obtained at reduced mass flow. However, the improvement in this regard is of small magnitude in terms of airplane drag coefficient.

In order to compare these proposed optimum shapes, calculations have been made for Mach numbers of 1.4 and 2.0 for practical nacelle shapes with ratios of inlet-to-maximum area of 0.16 and 0.36 and fineness ratios of 3 and 6. (As shown by the data of reference 76, fineness ratios less than 3 create large drag. Fineness ratios greater than 6 are so slender that small differences in profile have a negligible effect.)

Minimum-drag coefficients based on maximum cowl area for two optimum cowl shapes								
Shape	$M_0 = 1.4$				$M_0 = 2.0$			
	$A_2/A_M = 0.16$		$A_2/A_M = 0.36$		$A_2/A_M = 0.16$		$A_2/A_M = 0.36$	
	$l/d_M = 3$	$l/d_M = 6$	$l/d_M = 3$	$l/d_M = 6$	$l/d_M = 3$	$l/d_M = 6$	$l/d_M = 3$	$l/d_M = 6$
Conical	0.059	0.019	0.032	0.010	0.049	0.016	0.025	0.009
Parker (Ref. 162)	.056	.016	.031	.009	.048	.014	.025	.008

To indicate the differences in shapes, the radii of three minimum-drag cowls

are compared with the conical cowl in sketch (17). This comparison shows that both the differences in drag and radius distribution are small for these low-drag shapes, and it is concluded, as in the case of optimum



Sketch (17)

solid bodies (see refs. 171 and 172), that there is little difference no matter which shape near the optimum is selected. For most practical purposes the conical cowl is the optimum shape.

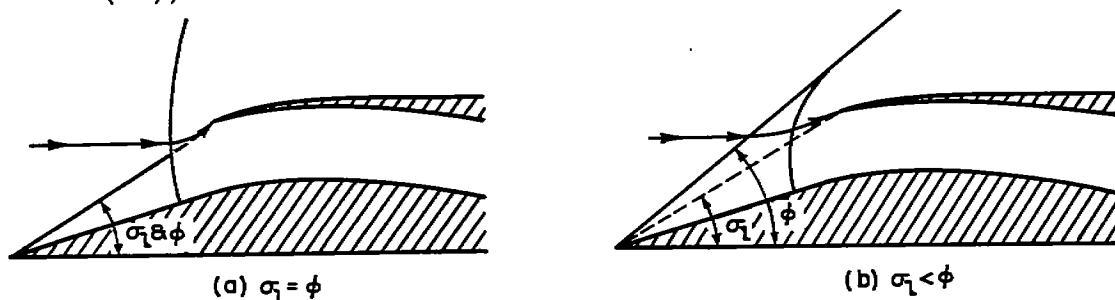
Warren and Gunn (ref. 168) have presented charts for the optimum angle of conical taper and the corresponding drag coefficient (including skin friction) as functions of Mach number, skin-friction coefficient, and area ratio. For a given area ratio, an optimum conical angle exists because the less the angle the smaller the wave drag but the greater the skin-friction drag. Charts resulting from the altered calculations mentioned on page 60 are shown in figure 12, and they show that for a given area ratio and skin-friction coefficient, an increase in Mach number increases the optimum angle and decreases the drag coefficient. However, the differences about the optimum are small.

For high-performance conical-shock inlets without internal supersonic compression, it is not possible to use a straight conical taper of near-optimum angle from the lip leading edge because insufficient lip thickness is available in which to enclose the required duct area and turn the flow back to the system center line. It is therefore necessary to camber the lip to meet the deflected streamline and have a curved external surface. The calculations of Ferri (ref. 13) indicate that it is better to expand and turn the flow in the immediate vicinity of the lip than to distribute the expansion along the length of the cowl. The position of the lip leading

edge is of little importance in regard to external drag; but, as discussed subsequently, it is of great importance in regard to net drag because to avoid the large force that can result from additive drag the lip should just intersect the oblique shock wave from the cone apex.

Additive drag.- As described in the section on definitions (p. 12), additive drag represents the momentum difference in the engine-flow streamtube between the inlet and the free stream when no aircraft components, other than those of the air-induction system, interfere with the streamtube. The simplest example of additive drag is that of an open-nose inlet at reduced mass-flow ratio; the additive drag is the pressure integral along the diverging streamtube between the external normal shock wave and the stagnation point on the inlet lip. This drag component can be calculated by the formula derived by Sibulkin (ref. 173) which is plotted in figure 13 for drag coefficient and mass-flow ratio based on capture area. Comparison with experimental measurements (see refs. 146 and 173) substantiates the reliability of these predictions. Since the table on page 53 shows that a rough value for the ratio of inlet-to-wing area is 0.01, the additive drag coefficient can, as an example, represent 0.0020 in airplane drag coefficient at a mass-flow ratio of 0.8 and a Mach number of 1.4. This force, particularly at lower mass-flow ratios and higher Mach numbers, therefore, can be an appreciable part of airplane drag, and, for efficient flight at supersonic speeds, the operating mass-flow ratio must be near 1.

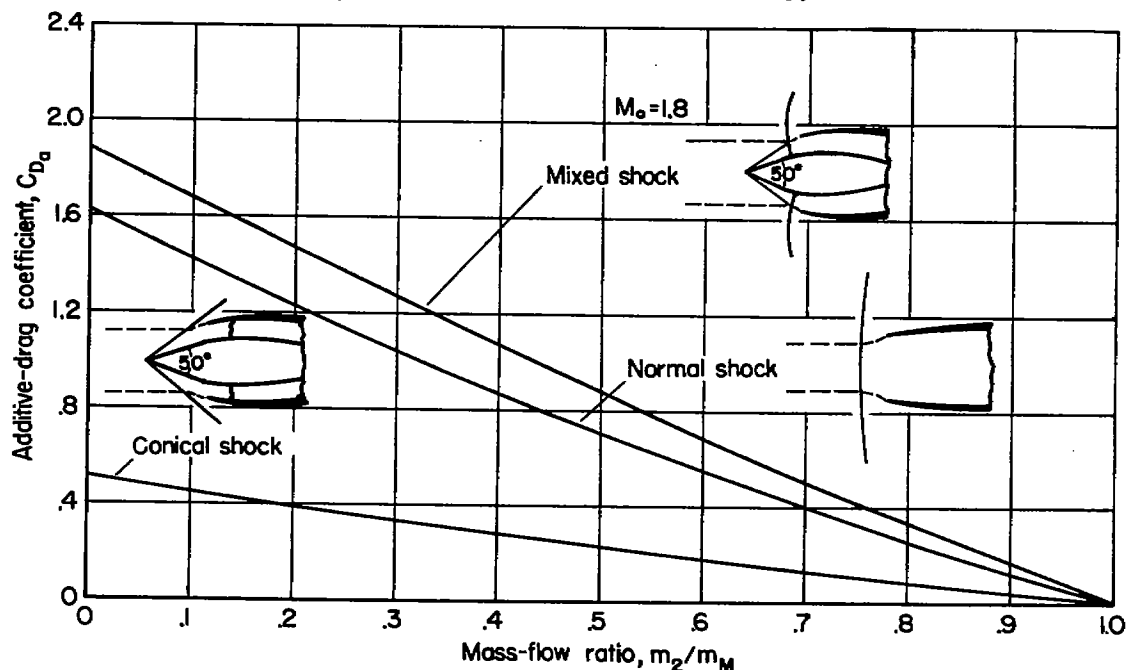
For a conical-shock inlet or one utilizing a wedge-type ramp, the pressures on a diverging streamtube ahead of the inlet (see sketches (16b) and (16c)) are, of course, affected by the shape of the precompression surface, and the problem of predicting additive drag is more complicated than for a simple open-nose inlet. Sibulkin (ref. 173) has studied the conical-shock inlet with supersonic inlet flow and presents the charts shown in figure 14 for the additive drag coefficient and mass-flow ratio based on capture area. The variation of cowl-position angle  $\sigma_1$  (see sketch (18)) with mass-flow ratio is also shown. The charts show that,



Sketch (18)

other factors being constant, the additive drag coefficient increases with cone angle, and, contrary to the normal-shock nose inlet, the additive drag coefficient decreases with increasing Mach number. For conical-shock inlets in which the flow at the inlet is not supersonic (sketch (18)), Sibulkin in the same reference has studied the effects of the center body

and of the assumed pressure recovery. The results show that the additive drag coefficient for these conditions at given values of cone angle, mass-flow ratio, and Mach number can be either greater or less than that of a normal-shock inlet, depending upon the location of the lip relative to the conical shock wave. If the lip is close to the oblique shock wave at maximum mass flow ( $\sigma_1 = \phi$ ) as shown in sketch (18a), the additive drag coefficient is high because the deflected streamtube is subjected to the pressure behind a normal shock wave occurring at stream Mach number. However, if the lip is far behind the conical shock wave (sketch (18b)), for a reduced mass-flow ratio the pressure on the streamtube is not as great as in the former case because of the weaker normal shock wave. In comparing predictions with experiment, Sibulkin has found good agreement for this form of spillage. Wyatt (ref. 12) has compared the additive drag coefficients resulting from reduced flow of the three possible types as shown in sketch (19). Thus, from the standpoint of drag, it is evident that air



Sketch (19)

should not be spilled from behind a normal shock wave, and, as Sibulkin points out, for flight Mach numbers below the design value ( $\sigma_1 = \phi$ ), it is desirable to increase the center body projection (translating-cone-inlet, p. 50) to maintain supersonic flow at the inlet. For a two-dimensional inlet with a precompression ramp the additive drag can be calculated from momentum relationships as has been done for conical-shock inlets.

Change in external wave drag.— When mass-flow ratio is reduced below the maximum value, the pressures on cowls change because the inclination of the flow with respect to the lip leading edge changes. Because of the

greater inclination of the local streamlines, the cowl pressures decrease, thereby creating an incremental suction force that is in the thrust direction. As shown, for instance, by Fradenburgh and Wyatt (ref. 14), at subsonic speeds this lip suction force counterbalances the additive drag if the flow remains irrotational. However, at supersonic speeds, the presence of shock waves causes rotational flow and this balance of forces cannot be accomplished. Several investigators have presented analyses of the change in cowl pressure forces with decreasing mass-flow ratio. Fraenkel (ref. 174) has studied the problem as applied to normal-shock inlets using momentum methods, but experiment shows that the predictions underestimate the cowl suction force at mass-flow ratios above about 0.6 even though the cowls tested had sharp lips. (See refs. 146 and 167.) The analysis of Graham (ref. 175), which includes an allowance for lip thickness, agrees with that of Fraenkel for mass-flow ratios greater than 0.8. Griggs and Goldsmith (ref. 146) use the analysis of Moeckel (ref. 176) to predict some portion of the lip suction force, but since the whole cowl is not considered, this method also underestimates measured suction forces. Figure 15 presents a compilation of experimental data and a comparison with the prediction of Fraenkel. (Drag coefficient is based on inlet area, and the increment of mass-flow ratio  $\Delta(m/m_M)$  is 0.3 corresponding to a change in mass-flow ratio from 1.0 to 0.7. It is assumed that the variation of drag coefficient is essentially linear over this range.) The data of references 146 and 167 represent pressure-distribution measurements and, for the more slender cowl ( $A_M/A_2 = 2.0$ ), the predicted decrease in available cowl suction force with flight Mach number is fairly well substantiated. For the larger cowl angle ( $A_M/A_2 = 4.1$ ), however, much more total suction force is recovered; the pressure measurements show that the suction pressures are less in magnitude than those on the thinner lip but they act on a greater frontal area. This increased suction force at low mass-flow ratios is at the expense of greater drag at a mass-flow ratio of 1. The remaining data represent the results of force-test measurements, and they show considerable scatter, as would be expected since the accuracy in determining this relatively small force component is not so good as with pressure measurements. These results tend to substantiate the conclusion that blunt lips can recover more suction force than sharp lips.

Lip bluntness.— Much of the previous discussion on drag at supersonic speeds has been concerned with thin, sharp lips on which shock waves would be attached at maximum mass flow. However, since such lip shapes cause large total-pressure losses at the high mass-flow ratios encountered in low-speed flight, the penalty in drag at supersonic speeds resulting from bluntness must be known in order to resolve the necessary compromise. As pointed out by Graham (ref. 175), it is to be expected that the maximum cowl suction force attainable is limited by lip bluntness; that is, for a given ratio of inlet-to-maximum-cowl area, above some degree of bluntness, high pressures on the large frontal area at the leading edge more than counterbalance the incremental suction force caused by expansion of the flow over the relatively small frontal area between the lip and the maximum cowl diameter.



Fraenkel has studied the problem of lip bluntness when <sup>18</sup> $(m_2/m_0)_M=1.0$  (ref. 167) by assuming that the drag of the profile is that of an isolated lip plus a small component due to the expansion behind the lip acting on the downstream profile. These assumptions tend to limit the analysis to relatively blunt lips. By evaluating a factor empirically, a design chart was obtained. Comparison of these results with other experiments produces no reliable correlation. The experiments of reference 23 show that with an inlet of  $A_2/A_M = 0.185$  and a lip of  $(r/R)^2 = 1.17$  there is no more net drag than with a sharp lip at mass-flow ratios above 0.8 at supersonic speeds. At the high-mass-flow ratios of low-speed flight, this lip causes about half as much loss in total-pressure ratio as does a sharp lip (fig. 5). The tests also show that the net drag changes little to angles of attack of  $5^\circ$ .

From the discussion of lip shape in regard to pressure recovery and drag, it appears that a reasonable lip profile for supersonic aircraft (flight to a Mach number of 2.0) is elliptical on the internal surface with  $(r/R)^2 \approx 1.15$  and  $a/b \approx 3.6$  (see fig. 5) to provide acceptable pressure recovery in low-speed flight. The profile is straight on the external surface with the angle between the surface and the approaching flow direction about  $3^\circ$  for the least wave drag in supersonic flight. For inlet areas of 2 to 5 square feet, the thickness behind the leading edge of such a lip would be from 1 to 1-1/2 inches.

Net wave drag<sup>19</sup>.— The previous discussion of drag has been largely concerned with relatively idealized configurations. For air-induction systems which are complicated by the necessity of many design compromises, accurate predictions of net drag can be made only for quite restricted conditions.

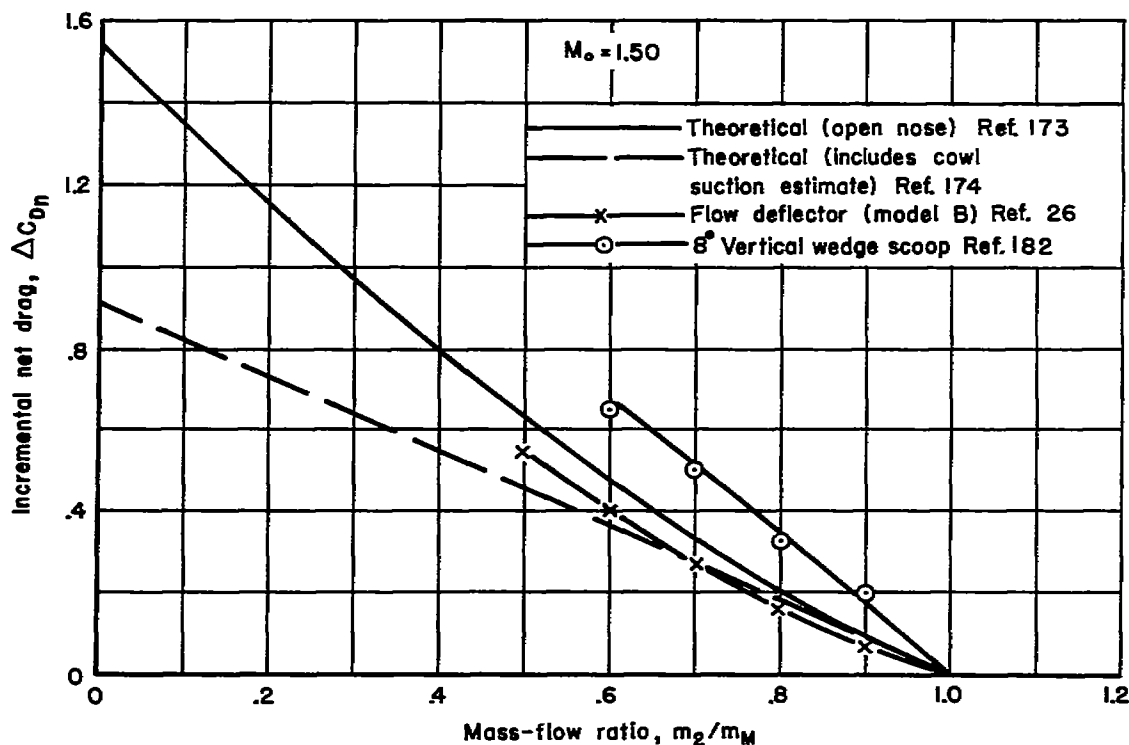
---

<sup>18</sup>Because of the contraction between the lip leading edge and station 2', it would be expected from one-dimensional considerations that  $(m_2'/m_0)_M$  would be greater than 1. The experimental evidence of Fraenkel for relatively blunt lips indicates that compression due to contraction is hardly realized and the maximum mass-flow ratio is very nearly 1. Mossman and Anderson (ref. 23) found that for less blunt lips nearly the full effect of the contraction is attained. This result is confirmed by recent work of Trimpf and Cohen (NACA RM L55C16).

<sup>19</sup>The experimental determination of net wave drag by means of direct force measurements and total-pressure surveys is a difficult procedure because several very accurate measurements must be made to obtain reliable values. It is possible to determine this force in supersonic flow from schlieren or shadowgraph photographs by calculation of the entropy rise or momentum change through the external bow shock wave. However, accurate evaluations by this method also require considerable care. Descriptions and studies of the method are presented in references 178 through 181.

---

For instance, as shown in sketch (20), the rises in net drag with decreasing mass-flow ratio for the vertical-wedge inlet of reference 182 and the inlet with a flow deflector of reference 26 are considerably different.



Sketch (20)

These inlets are similar in that both had a wedge-type precompression surface; the flow-deflection angle for the vertical-wedge inlet was  $8^\circ$  and that of the flow-deflector inlet was  $6.5^\circ$ . However, the inlets were otherwise entirely different. At mass-flow ratios above 0.7, the drag rise of the two differ by a factor of about 2. The estimations of Sibulkin (ref. 173) and of Fraenkel (ref. 174), which take no account of the precompression surfaces or of skin friction, apparently predict the drag of the flow-deflector inlet very well. However, account must be taken of the precompression surface to predict the drag of the vertical-wedge inlet. Obviously, the theories cannot be relied upon to predict the drag at low mass-flow ratios of such distorted inlet shapes. However, in normal operation, supersonic aircraft must avoid low mass-flow ratios because of the large additive drag force (or, at least, air should not be spilled from behind a normal shock wave). For mass-flow ratios of about 0.9 and greater the incremental drag due to a reduced mass flow is not a large force, and the significance of the error in estimating it is correspondingly reduced. Therefore, the following simple formula of Fraenkel (ref. 174) for the net wave drag of open-nose bodies at zero angle of attack is

possibly useful for estimating the drag of slender complicated configurations at high mass-flow ratios.

$$C_{D_{nW}} = C_{D_{exW}} + \frac{(p_1 - p_0)(A_2 - A_0)}{q_0 A_M} = C_{D_{exW}} + \frac{A_2}{A_M} \left( \frac{p_1 - p_0}{q_0} \right) \left( 1 - \frac{m_2}{m_0} \right) \quad (27)$$

and

$$\frac{\partial C_{D_{nW}}}{\partial (m_2/m_0)} = - \frac{p_0}{q_0} \left( \frac{p_1}{p_0} - 1 \right) \quad (28)$$

(Here  $p_1$  is the static pressure behind a normal shock wave.) Thus, according to this estimation, net wave drag is the sum of the external wave drag of the cowl with no spillage and the product of the relative static pressure behind a normal shock wave ( $p_1 - p_0$ ) and the annular frontal area of the diverging streamtube ( $A_2 - A_0$ ). The expression is a linear function of mass-flow ratio. Since there is little difference in the slopes of curves of additive and net wave drag coefficients with mass-flow ratio at mass-flow ratios above 0.8 according to Fraenkel, cowl suction force is of no consequence in this range for slender cowls. However, as indicated in figure 15, a sizable portion of the additive drag can be counteracted with blunt cowls and, if the high drag of these cowls with no spillage is acceptable, cowl suction force should, in this case, be taken into account.

## FLOW STEADINESS

In the operation of air-induction systems, unsteady flows limit propulsion-system performance for several reasons - duct rumble, that is, noise and vibration from the system which disturb the pilot, fluctuations which cause structural fatigue, or fluctuations which affect engine operation. In the following section, flow steadiness is discussed as a basic property of air-induction systems as was pressure recovery, flow uniformity, and drag previously. In this discussion, however, some consideration is given to interference from other aircraft components because unsteadiness in the engine flow often arises on account of the boundary layer from other surfaces.

## Subsonic Flight

Choked flow.- In low-speed flight with a fixed-area inlet designed for high-speed flight at altitude, the mass-flow ratio can be large

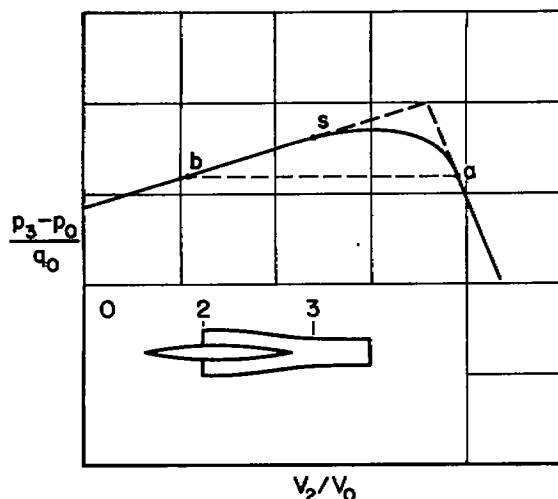
enough to choke the inlet. Aside from the low total-pressure ratio and nonuniformity associated with this condition, it must be avoided because of flow unsteadiness. The results of Blackaby and Watson (ref. 72) show that at zero forward speed with a sharp-lip inlet, fluctuations as large as 8 percent of the ambient pressure occur at frequencies up to about 200 cycles per second at mass-flow ratios  $m_2/m_2^*$  above about 0.6. Such unsteadiness was reduced both by increasing either the flight Mach number or the radius of the inlet lip. The results of Milillo (ref. 73) in tests at zero forward speed indicate large nonuniformity in the diffused flow, differences in local total-pressure ratio of as much as 0.10, for inlets with rounded lips just prior to choking. Thus, both flow unsteadiness and nonuniformity are to be expected in operation near choked conditions.

Duct rumble.— Several aircraft in flight at high subsonic speeds have encountered duct rumble. So far as is known, operation has been affected only by the noise and vibration which are sufficient to disturb the pilot so that the conditions under which they occur are consciously avoided. The phenomenon has been reported only with air-induction systems having side inlets and is apparently the result of interference with the approaching boundary layer. The tests of Mathews (ref. 183) on an under-slung scoop for the cooling air of the engine of a propeller-driven airplane indicate that duct rumble was due to flow separation ahead of the scoop. The separation was apparently caused by external compression resulting from a low inlet-velocity ratio. The rumble was eliminated by increasing the inlet-velocity ratio through a reduction of the inlet area and by relieving the flow through the boundary-layer gutter by increasing its depth. An air bypass which increased the inlet-velocity ratio was also a successful means of avoiding the rumble. Similarly, reference 184 reports duct rumble at inlet-velocity ratios less than 0.4 at flight Mach numbers from 0.65 to 0.92. Twin-duct instability is suggested as the cause of the rumble; upstream separation at the low inlet-velocity ratios was probably the cause of the unsteady nature of the instability. Other instances of duct rumble have been encountered, but descriptions of them have not been published.

Since available evidence indicates that duct rumble is generally caused by boundary-layer interference, it can be avoided by removing the boundary layer from the influence of the compression field or by reducing the compression field through an increase in mass-flow ratio. (Methods of boundary-layer removal are discussed later under INTERFERENCE.) Duct rumble is to be expected when the static-pressure gradient in the external compression field is sufficient to separate a turbulent boundary layer. In two-dimensional subsonic flow a rough design criterion regarding turbulent separation is that it can occur in positive pressure gradients when the local velocity is less than two-thirds of the initial velocity. However, larger pressure rises have been observed with air-induction-system installations possibly because the flow was three-dimensional or because the gradient was small. The boundary-layer surveys immediately ahead of the inlets described in references 185 and 186 show that without

boundary-layer removal an approaching boundary layer thickens rapidly and separates at inlet-velocity ratios less than about 0.6. With some boundary-layer removal this rapid thickening occurs at inlet-velocity ratios less than about 0.4. These figures can be used as rough indications of when duct rumble might be expected.

Twin-duct instability.— Martin and Holzhauser (ref. 187) have studied the stability problem of the flow through ducts from symmetrical twin intakes emptying at a juncture into a common chamber as shown in sketch (21).



Sketch (21)

From the assumption that the static pressure just downstream of the juncture (which is here called station 3) is uniform across the common duct, it is demonstrated that for a variation of recovered static pressures as shown in the sketch the flow is unstable at inlet-velocity ratios of the system less than that for maximum static-pressure recovery. That is, if the two ducts initially operate at the joint inlet-velocity ratio corresponding to point s, a small disturbance which causes an increase in inlet-velocity ratio in one duct causes the flow in that duct to increase to point a and that in the other duct to decrease to point b. From the continuity relationship in incompressible flow, it is evident that

$$(V_2/V_0)_s = \frac{(V_2/V_0)_a + (V_2/V_0)_b}{2} \quad (29)$$

Thus, as a result of the continuity requirement and the assumption of uniform static pressure at station 3, it is apparent from simple geometry that operation below the inlet-velocity ratio for maximum recovery is possible either at s or at a and b. However, if s is above the maximum, operation is possible only at the joint inlet-velocity ratio. For these events to occur it is necessary that the shape of the curve be similar to that of the sketch; that is, the negative slope at high inlet-velocity ratios must be greater in absolute magnitude than the positive slope at low inlet-velocity ratios. The assumption of uniform static pressure has been found from experiments to be realistic, and the shape of the curve has also been found to be typical of those of twin-scoops into which boundary layer flows. If two nose inlets or scoops with complete boundary-layer removal were used, the slope of the curve would not reverse; it would decrease from an inlet-velocity ratio of zero. Unstable flow could then not occur. From the sketch it can be seen that if the

joint inlet-velocity ratio is sufficiently small, the point *b* would be at an inlet-velocity ratio of zero. A disturbance in duct *a* that then reduced the static pressure at 3 would cause a reversal of the flow through duct *a* - a phenomenon that has been observed.

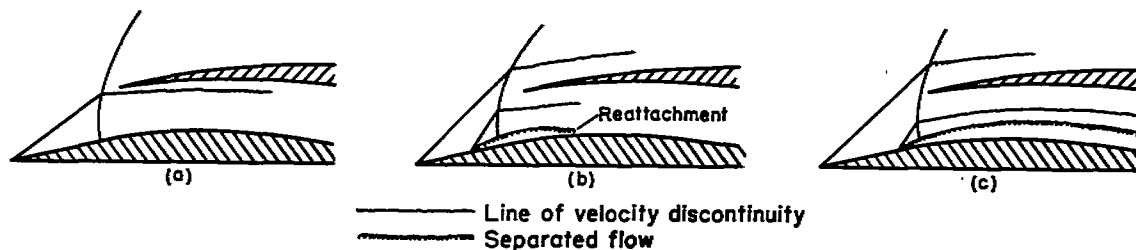
Since the static-pressure-recovery curve does not have a sharp peak in actual flow, unsteadiness can be expected if the point *s* is in the region of zero slope because disturbances in either duct could cause one and then the other to operate at the high and then the low inlet-velocity-ratio conditions. The magnitudes of the disturbances and the slopes determine how close to the peak *s* would have to be for such unsteadiness to occur. If *s* were below some limit, the operation would be stable at *a* and *b*.

Since all the conditions which lead to twin-duct instability and unsteadiness in subsonic flight can exist at supersonic speeds, these difficulties can also occur as demonstrated in reference 188, and systems should be designed to avoid them. A method of reducing twin-duct interaction in an air-induction system for supersonic aircraft is reported in reference 130. The wall between two ducts upstream of the junction was perforated to equalize the static pressure and enable crossflow to provide viscous damping.

### Supersonic Flight

Causes of unsteadiness.- Unsteady flow in air-induction systems occurs more readily in supersonic than in subsonic flight essentially because larger positive pressure gradients are encountered which separate the flow. Unsteadiness occurs either at subcritical mass-flow ratios or at the very low total-pressure ratios of operation far in the supercritical regime. The design problem is to maintain steady flow through a range of mass-flow ratios sufficient to satisfy all engine operating conditions.

Unsteadiness has been observed to occur in a variety of situations some of which are illustrated in sketch (22). The first two examples are



Sketch (22)

those described by Ferri and Nucci in reference 50. Here, the velocity discontinuity downstream of the intersection of an oblique shock wave and the terminal normal shock wave enters the inlet as a result of the normal shock wave moving forward due to a reduction in mass-flow ratio. Since the total pressure and velocity are less in the streamtube on the outside of the line of discontinuity, subsonic compression tends to bring this air to rest sooner than it does the high-velocity streamtube next to the center body. When the local Mach number behind the oblique bow shock wave is near 1.0, as it should be to avoid significant shock-wave boundary-layer interaction, the velocity difference across the discontinuity is large, and the velocity of the outside streamtube approaches zero in the duct while that of the inside streamtube is still high. Unsteady flow results when the line of discontinuity just crosses the lip because a large percentage growth in streamtube area of the low velocity stream occurs while a uniform static pressure is maintained across the discontinuity. Even though the contraction of the high-velocity stream is small, it is sufficient to choke the major portion of the flow because of the high local velocity, and air must be spilled. Once this happens, the pressure recovery decreases, which tends to draw the flow back to its original position, choking again occurs, and the cycle repeats. This explanation is obviously oversimplified because the effects of viscosity are ignored; neither turbulent mixing across the line of discontinuity nor the presence of a boundary layer is considered. The experiments which were reported with this explanation show that an entry section which is sufficiently long to permit mixing to reduce the velocity discontinuity provides an increased range of steady subcritical mass-flow ratios. When separation occurred on the central body as shown in sketch (22b) in these tests, it was found that unsteadiness occurred as the mass-flow ratio was reduced when the velocity discontinuity from behind the lambda shock approached the lip from the inside. When separation was prevented by boundary-layer removal, unsteadiness resulted only from the prior explanation. It was concluded from this study that unsteadiness can be avoided by positioning the external compression surface so that the line of velocity discontinuity cannot move across the lip for the range of flight conditions of interest so long as extensive separation on the compression surface is also avoided.

The results of references 51 and 189 show the importance of separation, as illustrated in sketch (22c), as a source of unsteadiness and indicate that factors other than lines of velocity discontinuity must be considered. It is shown in reference 51 that a conical-shock diffuser with a  $25^\circ$  semicone angle and a  $6^\circ$  equivalent conical subsonic diffuser has a very small range of steady subcritical flow even though the relation of the lip to the oblique bow shock wave is changed. The same inlet, however, with a length of duct-entry section of 3.5 hydraulic diameters always had a much wider steady range. Since there was separation on the cone surface throughout the subcritical mass-flow range in these tests, it is apparent that this and the duct shape can be dominant causes of unsteadiness. When the duct did not have an entry length of small pressure

gradient sufficient to permit the boundary layer to reattach and recover a profile that could withstand subsequent compression ( $H < 1.8$ ), unsteadiness resulted. This conclusion is substantiated by the results of references 111 and 190 in which unsteadiness was eliminated by forcing a separated boundary layer to reattach by suction. Also, the results of reference 128 show that relatively small irregularities in area distribution in the entry section of a duct in which the pressure gradient is positive can have serious consequences in reducing the range of steady flow.<sup>20</sup> Additional data, on the flow unsteadiness in one scoop-type air-induction system, are reported in reference 191.

Character of unsteadiness.- The wind-tunnel tests of reference 192 for an air-induction system without an engine showed flow unsteadiness after diffusion with a frequency of about 20 cycles per second and amplitudes as great as 30 percent of the local static pressure. The quantities are, of course, dependent upon the particular design and also upon engine operating conditions. Reference 193, for instance, shows that for a ram-jet engine the effects of approaching flow unsteadiness are attenuated by an increase in the pressure drop across the flame holder and that an increase in engine total-temperature ratio can amplify the pressure fluctuations. With a turbojet engine controlling the flow through a conical-shock inlet, Nettles and Leissler, reference 31, found that the engine steadied the flow through the inlet. Both the range of steady operation and the intensity of fluctuations were less with the engine operating than with the flow controlled by a choked exit plug. In fact, in the latter case the fluctuations built up to a violent level in certain ranges of unsteadiness; whereas with the engine controlling the flow, the inlet could be operated through the same range of mass-flow ratios without difficulty. Since, in general, flow unsteadiness from the air-induction system causes reduced performance with the degree of permissible unsteadiness dependent upon the refinement of the engine, the requirement in air-induction-system design is to provide steady flow to engines over the needed range of flow conditions. Thus, the detailed nature of flow unsteadiness is of interest only insofar as it shows when serious unsteadiness is to be expected or what parameters are effective in alleviating adverse effects.

Several investigations of unsteady internal flows have been reported. (See refs. 38, 194, 195, and 196.) The theoretical and experimental study of Trimpi, which analyzes the problem by considering traveling plane waves, indicates that the frequency of the flow oscillation decreases as the duct length increases. The frequency is also affected by mass-flow ratio, increasing somewhat with decreasing mass flow. Probably the most important

---

<sup>20</sup>In the tests reported in reference 123, the models used had small irregularities in area distribution near the duct entry, but the range of steady mass-flow ratios was large. The cause of this difference was that in this latter case the pressure gradient through the duct entry was slightly negative or zero.

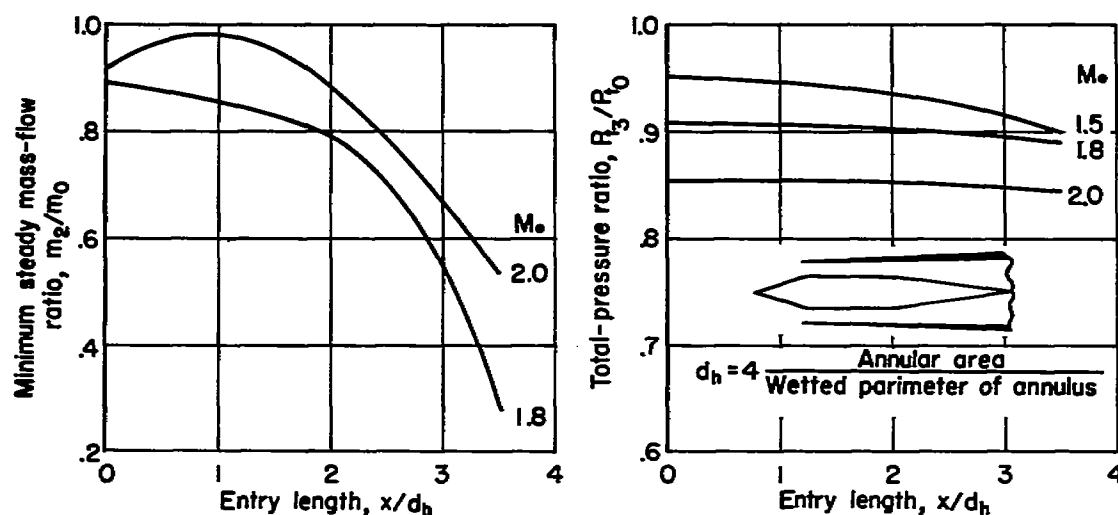
---



conclusions are those related to the origin of the unsteadiness. It was found that the relation between the time rates of change of entering mass flow, of boundary-layer growth at the inlet station, and of the instantaneous value of entropy averaged across the inlet was the critical factor causing unsteadiness. Further, it was shown that, although waves caused by changes in engine thrust can move the shock pattern to a position at which unsteadiness might arise, the disturbance which initiates unsteadiness originates near the entrance and need not be sufficient to choke the flow. The experiments of references 194 and 195 indicate that the magnitude of unsteadiness as caused by a line of velocity discontinuity crossing a lip (sketch (22a)) is less than that caused by separation of center-body boundary layer (sketch (22c)). Since numerous inlet configurations were investigated in references 194 and 195, it is possible that this result could have some generality.

Prevention of unsteadiness.- The obvious method of avoiding flow unsteadiness is to operate a propulsive system only at mass-flow ratios near or slightly above the critical with an inlet designed so that a line of velocity discontinuity does not cross the lip and so that serious boundary-layer shock-wave interaction is avoided. The fact that this can be accomplished with a fixed-area inlet for a relatively wide range of Mach number variations has been demonstrated in reference 50. However, for operation through a wide range of Mach numbers, altitudes, and power settings, one of the variable systems described previously would be required to maintain nearly a constant mass-flow ratio. Since this remedy is accompanied by the addition of weight and complication, other methods of avoiding unsteadiness can be more desirable. From the discussion of the causes of flow unsteadiness, it is apparent that the difficulty can be delayed by reducing severe velocity discontinuities and adverse pressure gradients in the entering flow. However, if these must occur, the effects can be minimized by giving the flow an opportunity to re-establish a more uniform high-energy profile that can withstand additional compression. As shown by references 51, 111, 190, and 197, this can be accomplished by removing boundary-layer air or by providing sufficient distance for turbulent mixing to re-energize the flow. The latter method has been investigated by providing a long entry section of very nearly constant cross-section area. The increase in the range of steady subcritical mass-flow ratios that can be accomplished by this method is shown in sketch (23) which is reproduced from the data of reference 51. For the models tested, the flow was steady through the mass-flow range at a Mach number of 1.5. However, there was an appreciable loss in maximum pressure recovery at this Mach number as entry length was increased because of the high local Mach number at the inlet and the associated increase in friction losses.

The previous discussion of steadiness has been concerned only with conditions at zero angle of attack. It is, of course, necessary to maintain steady flow for satisfactory engine operation during maneuvers. In the tests of conical-shock inlets of reference 50, the steady range of mass-flow ratios was small at zero angle of attack, and it was slightly



Sketch (23)

greater at angles of attack up to  $9^\circ$ . A similar result was found in the tests of reference 51 for conical-shock inlets which had small steady ranges at zero angle. However, when a long entry passage was added to provide a wide range of steady operation at zero angle of attack, there was an abrupt reduction in the steady range at angles of attack from  $3^\circ$  to  $5^\circ$ . At higher angles there was little difference between the inlets with the long and short entry sections. A tilting cone on a conical-shock inlet to provide improved steadiness at large angles of attack is reported in reference 129. At an angle of attack of  $10^\circ$ , with the cone at  $0^\circ$  angle of attack, steady flow was maintained to a mass-flow ratio of 0.4; with the cone and cowl at  $10^\circ$  angle of attack, the minimum steady mass-flow ratio was 0.9. In reference 198 tests of conical-shock inlets with booms protruding from the center bodies are described. An increase in angle of attack to  $10^\circ$  reduced the range of steady mass-flow ratios by 25 percent. Interaction between shock waves and the boundary layer on the booms was the cause of this large decrease.

Other investigations have demonstrated methods of improving flow steadiness to some extent. References 197 and 199 show small increases in the steady mass-flow ratio range (0.06 in ref. 197) as a result of the internal contraction with a blunt lip. References 197 and 200 show that removal of the boundary layer from the center body of a conical-shock inlet reduces unsteadiness, with the greater effectiveness occurring when removal is upstream of the terminal normal shock wave. In fact, at an angle of attack of  $0^\circ$  an improvement of 0.16 in the range of steady mass-flow ratio was attained (ref. 197), but it decreased with increasing angle of attack. Although these and most of the previous references are concerned with conical-shock inlets, the principles of design for providing

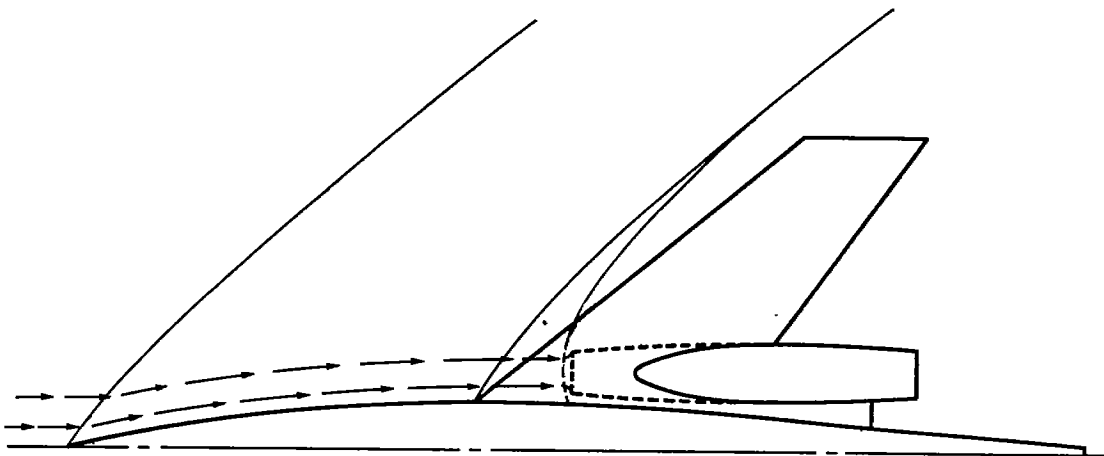
steady flow are the same for other types. (See, e.g., refs. 188, 190, 191, 199 through 202.)

### INTERFERENCE

The purpose of this section is to discuss the aerodynamic factors other than those of the induction system itself which affect design; it is entitled "INTERFERENCE" because the changes in the forces due to combining an air-induction system and other aircraft components are considered. The section is divided into two principal parts:

1. The interference of aircraft flow fields with those of induction systems - the induced effects of body shape, angle of attack, and the viscous effects of forebody boundary layer.
2. The interference of air-induction-system flow fields with other aircraft components - the effects of induction systems on aircraft drag, lift, and pitching moment.

The type of factors involved are illustrated in sketch (24). Here, the



Sketch (24)

the performance of an under-wing nacelle is affected by

1. Bow shock wave of the fuselage
2. Velocity increment at inlet due to fuselage pressure field
3. Shock wave from wing leading edge

4. Velocity increment at inlet due to wing pressure field
5. Uniformity of the flow velocity at the inlet

The performance of the other aircraft components is affected by

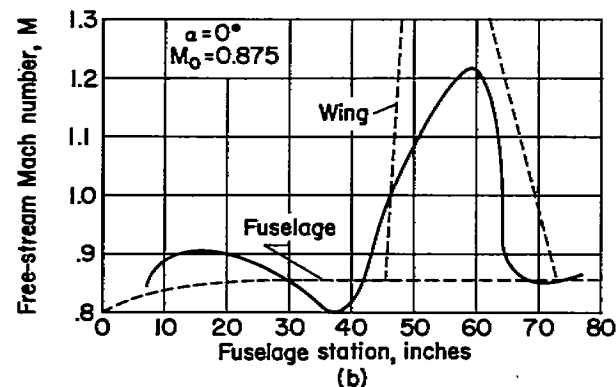
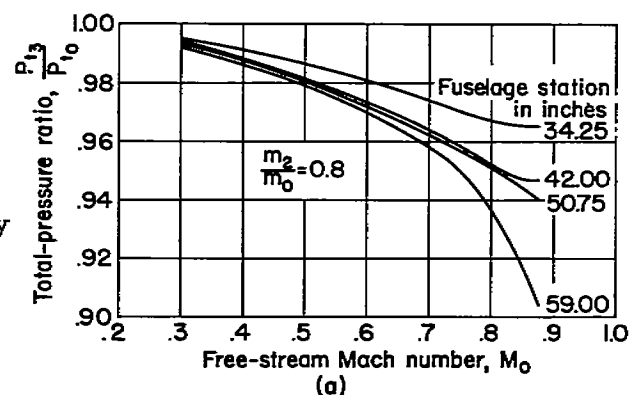
1. Interference of pressure field of engine streamtube with the wing and fuselage boundary layers and pressure fields
2. Interference of pressure field of engine fairing with the wing and fuselage boundary layers and pressure fields

Obviously, the problems of interference are complicated, and quantitative evaluation requires experimental studies of specific configurations. However, an induction system that must be placed in the flow field of another object can either benefit or suffer from the resulting interference, and careful consideration must be given to the conditions of shape and position in order to produce favorable effects. (See, e.g., ref. 203.)

## AIRCRAFT-INDUCTION SYSTEM

### Effects of Inlet Location

Subsonic flight.— From the standpoint of pressure recovery at the inlet, the best longitudinal position of an inlet is in the stagnation region near the nose of a body because the local Mach number is low and any external compression resulting from a mass-flow ratio less than 1 is essentially isentropic. As an inlet is moved aft along the body, the amount of boundary layer flowing through it increases with a resulting reduction in total-pressure ratio. This direct effect of low-energy boundary-layer air is normally not large in subsonic flight, but secondary effects, flow nonuniformity and unsteadiness, can be very important at mass-flow ratios of the order of 0.5. The effects on total-pressure ratio of moving an NACA submerged inlet operating at a mass-flow ratio of 0.8 aft along the fuselage of a wing-fuselage combination is shown in sketch (25) together with the local



Sketch (25)

Mach number distribution along the fuselage. These results were taken from the data of references 204 and 205. At flight Mach numbers less than 0.3, there is essentially no effect of moving the inlet aft. The greater boundary-layer thickness at the rearward stations becomes important at a Mach number of about 0.5, and at Mach numbers above about 0.7, it becomes of great importance at the most rearward station. Here, the total-pressure ratio decreases rapidly at high subsonic Mach numbers because of both the high local Mach number illustrated in sketch (25b) and the thick boundary layer. The most rearward location is in the pressure field of the wing, and at a flight Mach number of 0.9, the local Mach number at the inlet is supersonic ( $M = 1.22$ ). Thus, pressure fields with large induced velocities should be avoided.

A method for estimating the velocities in two-dimensional combined subsonic velocity fields is discussed in reference 206. Superposition is assumed to be valid and the resulting relationship is

$$\frac{V_{\text{local}}}{V_0} = 1 + \left( \frac{\Delta V_{\text{local}}}{V_0} \right)_1 + \left( \frac{\Delta V_{\text{local}}}{V_0} \right)_2 + \dots \quad (30)$$

where  $\Delta V_{\text{local}}$  denotes the induced velocity increment in incompressible flow. This method of predicting maximum induced velocity has been compared with experiment for a wing-nacelle combination in reference 207. Here, the method predicted maximum velocity ratios about 3 percent less than those measured. To predict the effects of compressibility, the Prandtl-Glauert rule can be used for two-dimensional flow.

$$\left( \frac{V_{\text{local}}}{V_0} \right)_{\text{compressible}} = \frac{1}{\sqrt{1 - M_0^2}} \left( \frac{V_{\text{local}}}{V_0} \right)_{\text{incompressible}} \quad (31)$$

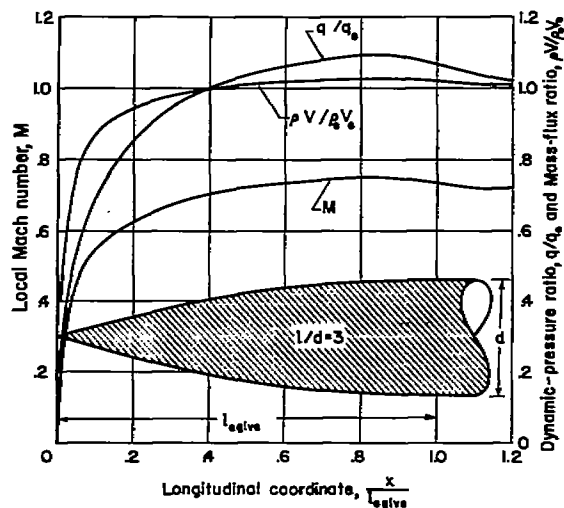
and in the three-dimensional case, the methods of Herriot (ref. 208) should be used. In terms of pressure coefficient in three-dimensional flow,

$$\frac{C_{P_{\text{compressible}}}}{C_{P_{\text{incompressible}}}} = 1 + \frac{\ln(1 - M^2)}{\ln\left(\frac{t}{l}\right)^2 + 0.6138}$$

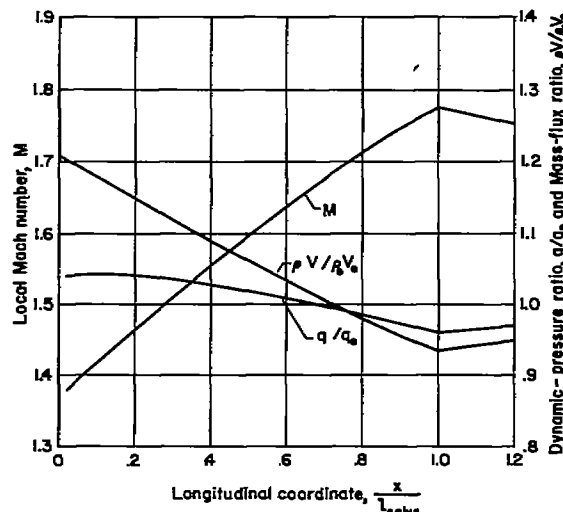
where  $t/l$  is one-half the body fineness ratio. Herriot points out that in junctures, such as those between a wing and nacelle, the flow is more

nearly two-dimensional than three-dimensional, and thus the Prandtl-Glauert rule is a better approximation for this case.

Supersonic flight.— Sketch (26) shows a comparison of flow properties over a typical body at a subsonic and a supersonic Mach number. If in the subsonic case the boundary layer is neglected, the total-pressure



(a) Free stream Mach number,  $M_0 = 0.70$



(b) Free stream Mach number,  $M_0 = 1.70$

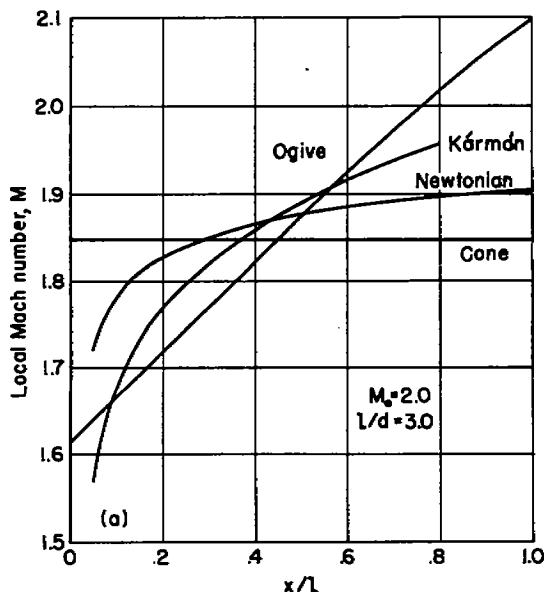
### Sketch (26)

ratio of any streamtube about the body is 1, and the mass flow per unit area and the local dynamic pressure change little downstream from a short distance behind the nose. Thus, from these standpoints, longitudinal position of an inlet makes little difference. In the supersonic case, however, there is an initial loss in total-pressure ratio due to the bow shock wave, in this case 1 percent, and there are subsequent changes in local flow properties which have important consequences in regard to air-induction-systems performance. As an example, consider the flow conditions at  $x/l = 0.05$  and at  $x/l = 0.9$  where the local Mach numbers are 1.38 and 1.75, respectively. If no significant radial change in Mach number through an engine streamtube is assumed, a normal shock wave occurring at the forward location would create a 4-percent loss in total-pressure ratio and the loss through the optimum oblique-normal-shock-wave combination would be 1 percent (see fig. 6). However, at the rearward station, the normal-shock loss would be 17 percent and the two-shock loss would be 5 percent. If there were no body, that is, if the supersonic compression occurred at the free-stream Mach number, the normal-shock loss would be 14 percent and the two-shock loss, 4 percent. Similarly, from the standpoint of flow rate per unit area, or inlet size, location in a compression field is advantageous. From the standpoint of drag per unit area, a

compression field is detrimental because of the high dynamic pressure. However, for the conditions illustrated in sketch (22), the greater flow rate is the dominant factor, and the forward position of the inlet can be shown to have 7-percent-less external wave drag than the rearward position due to its smaller size. Thus, location can have important effects on net propulsive force, and it can be beneficial to place an inlet in the compression field of other aircraft components.

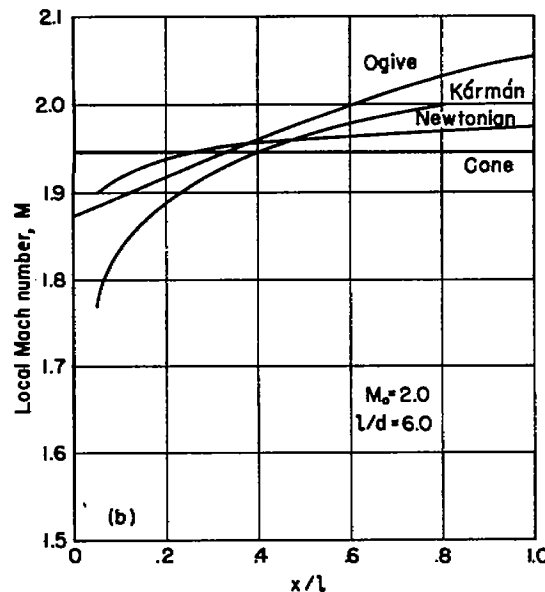
In regard to the effects of the radial velocity field into which an inlet is placed, Hasel in reference 209 has investigated the problem experimentally at a Mach number of 2.0. Half-conical-shock inlets were tested on a flat plate and on bodies of revolution having forebody fineness ratios of 4.0, 6.5, and 7.5; the total-pressure ratio of an inlet on the bodies was always less than that of the inlet on a flat plate. When all of the forebody boundary layer was removed, the maximum total-pressure ratio attained with an inlet on a body of fineness ratio 4 was 0.08 less than that with the inlet on a flat plate; this difference was 0.04 with the fineness ratio 7.5 forebody. About half of these differences could be attributed to the bow-shock waves and the local Mach numbers at the inlet stations; the remainder was thought to be due to the differences in the radial velocity field. Thus, appreciable losses are to be expected from this cause with forebodies of low fineness ratio.

Since the local Mach number at an inlet determines the magnitude of the pressure losses through the shock waves used for supersonic compression, the forebody shape should be selected to minimize this Mach number without, of course, creating any additional drag. Considerations which are important are indicated in sketch (27). (See refs. 172 and 210.)



(a)

Sketch (27)



(b)

For forebodies of low fineness ratio, a considerable reduction in local Mach number can be achieved by using conical, or minimum-drag shapes rather than an ogive if the inlet must be located upstream of  $x/l = 1.0$ . For forebodies of high fineness ratio, the differences are smaller. The data of reference 172 show that for a fineness ratio of 3.0, the Karman and hypersonic optimum (Newtonian) shapes have at least 20-percent less forebody drag than the cone and ogive at zero angle of attack at supersonic Mach numbers up to 2.0. However, these minimum-drag nose shapes have blunt tips, and, depending upon the size of the engine streamtube, the loss in total pressure through the locally intense bow shock wave counteracts the drag difference. Reference 211, for instance, reports that a relatively small amount of tip bluntness that had a negligible effect on minimum drag caused 1-percent losses in total-pressure ratio and maximum mass-flow ratio as compared to a pointed tip. Thus, any specific design requires study and evaluation of these factors. Because an air inlet at positions other than the nose intercepts but a small part of the air compressed by the body, the major consideration in choice of body shape is drag. The design problem is to find the optimum inlet location on a low-drag body.

Tests of very blunt noses, in which the nose-radius to body-radius ratio was near 1.0, are reported in references 211 and 212. It was found that a 4-percent loss in total-pressure ratio was suffered at a flight Mach number of 1.4 and a 6-percent loss at a Mach number of 1.7 due to nose bluntness and to the large radial velocity gradients. The minimum-drag coefficients, as compared to those of bodies with more slender shapes, were more than doubled. Because of the reduced total pressure and the overexpansion of the flow behind the juncture of the hemisphere and the subsequent body, there were also considerable losses in maximum mass-flow ratio in both investigations.

In the general case, forebodies are not axially symmetric as has been assumed in this discussion. The theoretical study of reference 213 indicates that small reductions in drag can be produced by axial asymmetry, and a similar conclusion has been reached as a result of the tests reported in reference 214. It is possible that circumferential pressure gradients and reduced local Mach numbers can be produced by asymmetric bodies that are beneficial to air-induction-system performance. To date, no studies of this kind have been made.

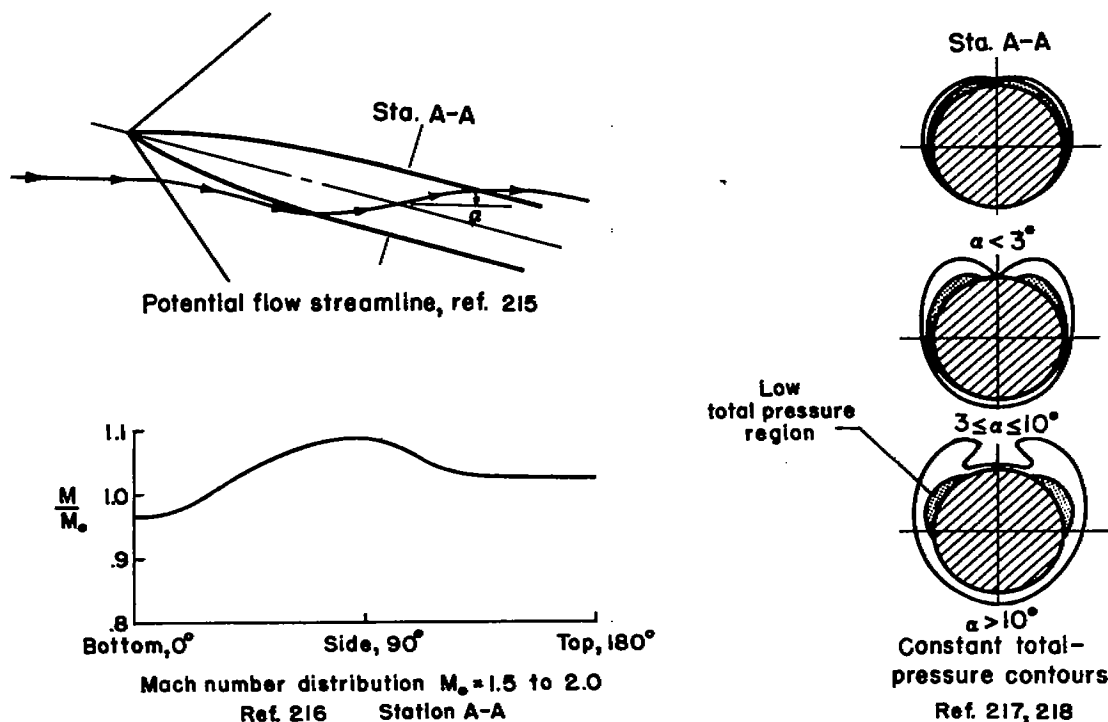
#### Induced Effects of Angle of Attack

Bodies.— In selecting the circumferential position of an inlet on a body, the induced effects of angle of attack are of primary concern. The

~~CONFIDENTIAL~~



flow phenomena that must be considered are illustrated in sketch (28).

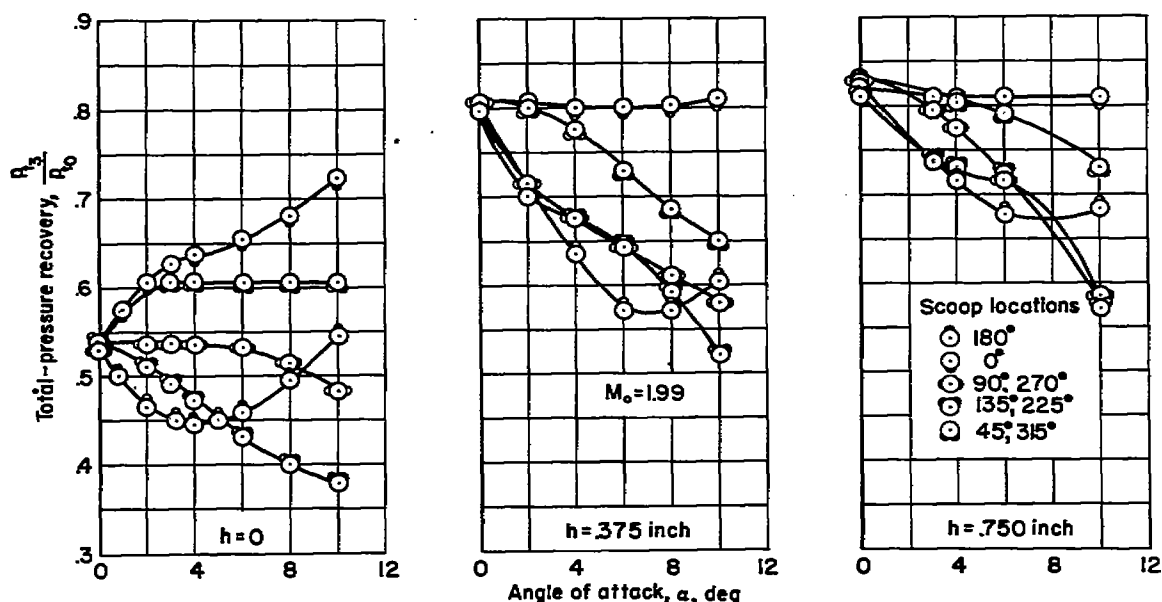


Sketch (28)

It is seen that along the top and bottom of a body in potential flow, the flow direction is nearly parallel to the body center line (i.e., at the angle of attack  $\alpha$  with respect to the flight direction); whereas along the body sides the flow inclination is greater, being  $2\alpha$  on a right circular cylinder. Similarly, the local Mach number is greatest on the body sides and is least in the forward bottom location. On the leeward side of the body, the flow is affected by viscosity so that the boundary layer accumulates in lobes and, at sufficiently high angles of attack, this low-energy air leaves the surface of the body as a vortex wake. These general characteristics of the flow occur at subsonic as well as supersonic speeds.

Several investigations of air-induction systems in the flow fields of inclined bodies have been made. (See refs. 199, 209, 218, 219, and 220.)

Typical results are shown in sketch (29) in which the maximum total-pressure ratios attained are plotted as functions of angle of attack.



Sketch (29)

Half-conical shock inlets were mounted on a slender, low-drag body at about the maximum-diameter station, and the height of the boundary-layer diverter  $h$  was varied. The 0.375-inch diverter height  $h$  was about equal to the undisturbed boundary-layer thickness at the inlet station at zero angle of attack. These results confirm the desirability of the bottom location in regard to pressure recovery. This would be expected from the reduced viscous effects and flow angularity relative to this inlet which was aligned with the body axis. The angle-of-attack performance of inlets in the side location can be improved by use of the flow-deflector principle (see ref. 26) or by aligning the inlet axis with the mean flow directions. (See ref. 221.)

Kremzier and Campbell in reference 220 compare the net propulsive force of a body-propulsion-unit combination with the inlet on the top or bottom of the body. Because of a lower drag of the inlet in the top position, the net propulsive force was slightly greater at a given angle of attack. However, at the same lift coefficient, the bottom location was superior because of a negative shift in the angle for zero lift and an increase in lift-curve slope for this position. In reference 222 tests are described of the top inlet of reference 220 with two large triangular fences extending ahead of the inlet to shield it from the leeward boundary layer. The net propulsive force of this arrangement at moderate angles

of attack was greater than that of the bottom inlet. A final evaluation would, of course, require study of the effects of such large vertical surfaces on aircraft directional stability and other related factors.

Since the upwash about a body decreases as the square of the distance from the body center line (refs. 215 and 223), the adverse effect of angle of attack on pressure recovery of side inlets can be alleviated by moving the air-intake outboard. Thus, a comparison of the data of references 218 and 224 shows that if a nacelle with a conical-shock inlet were used rather than a half-conical shock scoop on the body sides, the same maximum total-pressure ratio could be maintained by the nacelle at twice the angle of attack of the scoop-body combination when the nacelle was over about 1-1/2 nacelle diameters from the body center line.

Wings.- When the Mach number normal to the leading edge of wings is subsonic, the circulation accompanying lift creates an upwash field ahead of wings which increases the effective angle of attack of inlets in or near the leading edge. At low mass-flow ratios this upwash is aggravated by the diverging engine streamtube. Fortunately, turbojet-powered supersonic aircraft, which are quite subject to lip stall because of thin lips, seldom encounter the condition of high lift coefficient and low mass-flow ratio. High-speed maneuvers are made with full power and normal landings are made with some power at mass-flow ratios greater than 1. For subsonic aircraft designed with a relatively large inlet area, internal lip stall in landing would be more likely if it were not for the thicker lips that can be used.

An investigation of leading-edge inlets in a straight wing at subsonic speeds is reported in reference 225 in which it is shown that the induced upwash from the wing causes an abrupt decrease in total-pressure ratio for an inlet not designed to account for the additional flow inclination. For example, an inlet with relatively thick lips maintained a total-pressure ratio of 0.99 to an angle of attack of  $6^\circ$ , at which angle the pressure recovery rapidly decreased to 0.92 at an angle of  $8.5^\circ$ . This decrease in total-pressure ratio was caused by internal-flow separation from the lower lip. It was found that the separation could be delayed by canting the duct axis just behind the lips downward and also staggering the inlet plane. Tests of a similar leading-edge inlet at subsonic speeds in a swept wing are reported in reference 226. Here, it was found that a serious spanwise flow occurs in the inlet at low mass-flow ratios when the wing carries lift. At mass-flow ratios greater than 0.4 and angles of attack less than about  $4^\circ$ , the performance of the inlet in the swept wing was nearly equal to that in the unswept wing. At greater angles, however, the pressure recovery decreased rapidly due to separation of the internal flow. It is probable that this separation could have been delayed somewhat by canting the lower inlet lip downward as was done with the inlet in the unswept wing. At angles of attack greater than  $6^\circ$  to  $8^\circ$  and at mass-flow ratios less than 0.8, separation occurred downstream of the

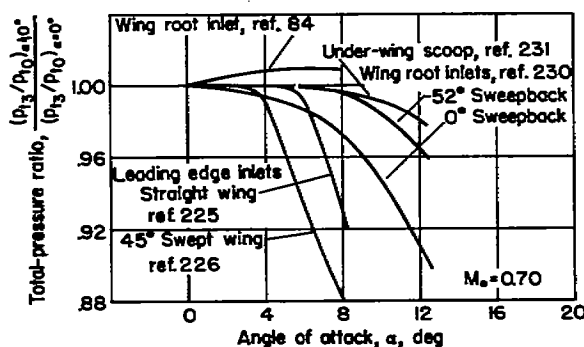
outboard edge of the inlet on the external surface of this swept wing and resulted in an increase in drag and a loss in lift.

Inlets located in the wing leading edge for supersonic aircraft have received little attention because of the transitions and bends needed to duct air through a thin wing to a turbojet engine. Investigations of wing leading-edge inlets for application to split-wing ramjets at Mach numbers above 2.0 are reported in references 127, 128, 227, 228, and 229. Probably the most important factor in the interference of the aircraft on this type of inlet at supersonic speeds is that for unswept leading edges there is no upwash induced ahead of the inlet by the wing. Body upwash, however, can be present at supersonic as well as subsonic speeds.

From tests of wing-root inlets, in which both the induced effects of wing and body increase the local flow angles, it has been found that a high level of pressure recovery can be maintained to angles of attack of at least  $8^\circ$  at subsonic speeds by employing relatively thick lips with stagger and negative incidence. (See refs. 186, 230, and 84.) The investigation of wing-root inlets of reference 84 included pressure-recovery measurements at Mach numbers up to 1.3. A total-pressure ratio of 0.89 was attained at a Mach number of 1.25, and this pressure ratio was maintained from  $-2^\circ$  to  $8^\circ$  angle of attack.

The results of reference 231 show that good angle-of-attack performance can be attained by placing the inlet of an underwing scoop downstream of a wing leading edge so that the local flow direction is along the induction-system axis. A compilation of all these results from tests at subsonic

speeds is shown in sketch (30) as the change in total-pressure ratio as the angle of attack increases from zero. The mass-flow ratios of the data are those for maximum pressure recovery. In this sketch, the wing-root inlet of reference 84 shows improvement in pressure recovery with increasing angle of attack because at zero angle the recovery is relatively low (0.96). Angle of attack increases the pressure recovery because the inlets are canted and because part of the approaching boundary layer is swept past them by body crossflow. In terms of absolute total-pressure ratio at angle of attack, the wing root inlets are inferior to isolated inlets or those with upstream flow-deflecting surfaces. Although most of these tests were performed at Mach numbers less than 0.7, the low-speed results have been transformed to conditions at a Mach number of 0.7 to obtain a consistent correlation. As mentioned previously, this transformation can be reliably accomplished if it is assumed that the measured

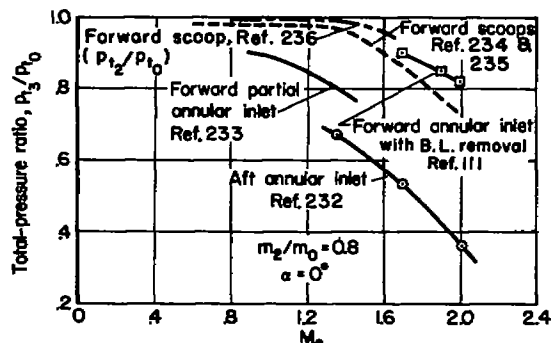


Sketch (30)

ram-recovery ratio is independent of subsonic flight Mach number and this measurement is converted to total-pressure ratio by equation (13).

### Effects of Forebody Boundary Layer

As previous discussion has often indicated, forebody boundary layer flowing into an air-induction system can reduce engine performance because of losses in total pressure, unsteadiness, and nonuniformity. A comparison of the maximum total-pressure ratios as a function of flight Mach number attained with a variety of arrangements in which entering boundary layer was not removed is shown in sketch (31). The boundary-layer effects



Sketch (31)

are particularly large with annular intakes which encircle bodies where the local Mach number is high. Such inlets receive all the boundary layer from the flow over the forebody (the ratio of retarded to free air is large), and this layer is either thickened or separated by compression from the high local Mach number. The results of the tests of reference 232 show that total-pressure ratios of annular inlets mounted on an ogival body are about 0.3 less than those of a normal shock wave occurring at flight

Mach numbers from 1.4 to 2.0. Similarly, the results at transonic speeds of the nearly annular intake of references 237 and 233 indicate a relatively low total-pressure ratio when compared to nose or scoop inlets. A conical-shock inlet with a small cone angle suffers from these same difficulties, and, as shown in reference 111, boundary-layer removal is necessary to provide steady operation. However, by using a scoop which encompasses only a small portion of the forebody and thus receives a small proportion of boundary-layer air, high total-pressure ratios can be more readily attained. Thus, the results of references 234, 235, and 236 show that scoops mounted just under the body nose where the boundary layer is thin and the local Mach number is low attain high pressure recovery. However, with scoops located downstream of the body nose where the approaching boundary layer is thick and the local Mach number is nearly equal to or greater than that of flight, large total-pressure losses occur unless the boundary layer is removed.

Seddon, in reference 28, has correlated wind tunnel and flight data to show the decrease in pressure recovery resulting from taking forebody boundary layer into air-induction systems. Seddon (see also ref. 2) correlates data by means of the relationship

$$\frac{P_{t3} - P_{t0}}{q_2} = C_f \left[ 1 + J(V_0/V_2)^3 \right]$$

where

$$J = k_\xi (1 - \eta_b) \frac{S}{A_2}$$

$C_f I$  represents the internal skin-friction losses in terms of  $\Delta p_t/q_2$  and  $J$  accounts for pre-entry effects. Thus,  $k$  is an empirical constant which includes the effects of inlet-velocity ratio  $V_0/V_2$ , and  $\xi$  is a correction to the skin-friction coefficient due to the previous history of the boundary layer before it reaches the inlet ( $\xi = C_{f\text{forebody}}/C_{f\text{duct}}$ );

$\eta_b$  is an efficiency factor to account for the amount of boundary-layer removal; and  $S/A_2$  is the ratio of forebody surface wetted by the flow to the inlet divided by the inlet area. At reduced inlet-velocity ratios and high speeds without complete boundary-layer removal, the boundary-layer thickness ahead of the entry increases rapidly and, as a result,  $k$ ,  $\xi$ , and  $\eta_b$  become functions of  $V_0/V_2$  and Mach number which must be evaluated experimentally if accurate results are to be obtained.

#### Boundary-Layer Removal

The design problem with a boundary-layer removal system is to avoid incurring any appreciable drag penalty while removing sufficient retarded air to minimize pressure losses, unsteadiness, and nonuniformity in the engine streamtube. The boundary layer can be removed by providing suction across a slot or a porous surface or by raising the inlet from the forebody surface so that the boundary layer flows beneath the inlet and is diverted around the external surfaces of the duct fairing.<sup>21</sup> In doing this, it is necessary to minimize any additional total-pressure losses and interference with other parts of the flow field. The following discussion on removal systems is divided according to the method by which forebody boundary layer is prevented from entering the air-induction system - by suction or by diversion. These methods are similar in some respects, but a suction method is one in which a pressure difference is provided across some length of closed duct to draw off the boundary layer, and a diversion method is one in which the flow is unrestrained in a lateral direction. Under certain conditions, the effects of boundary layer can be minimized by providing large-scale mixing with the engine flow, as is the case with the NACA submerged inlet. This method is also discussed.

<sup>21</sup> Some tests have been made of diffusers in which energy is added to the boundary layer by blowing air from a high-pressure source along the forebody wall; the results are reported in references 113, 114, and 238. However, extensive development of this method as applied to air-induction systems has not yet been performed.

Suction.-- An evaluation of a suction-removal system on the basis of aircraft range has been reported by Fradenburgh and Kremzier in reference 19. Tests were made with half-conical shock inlets with semicone angles of  $25^\circ$  and  $30^\circ$  with various heights of boundary-layer removal slot at Mach numbers of 1.5, 1.8, and 2.0. Because of the large drag force contributed by this specific boundary-layer removal system as noted in both references 19 and 239, boundary-layer removal produced essentially no increase in maximum range in spite of the substantial improvement in pressure recovery. Thus, careful consideration must be given to the detail design of removal systems to prevent energy losses and to achieve the potential improvement in performance.

The data of reference 185 show that in subsonic flight, operation of an air-induction system at inlet-velocity ratios less than 0.6 causes rapid thickening of the forebody boundary layer flowing into an inlet. The tests of a boundary-layer removal system that were included in this investigation show that the inlet-velocity ratio of the removal system must be greater than about 0.5 to maintain a net drag force less than that for the configuration without boundary-layer removal. The boundary-layer scoop in this study was in the plane of the main inlet and was produced by indenting the forebody. It was found that an indentation approach angle of  $7^\circ$  caused unsteady flow. An approach angle of  $3^\circ$  resulted in satisfactory operation; however, as discussed later in regard to submerged inlets, such approach angles would cause unacceptable losses in pressure recovery at supersonic flight speeds.

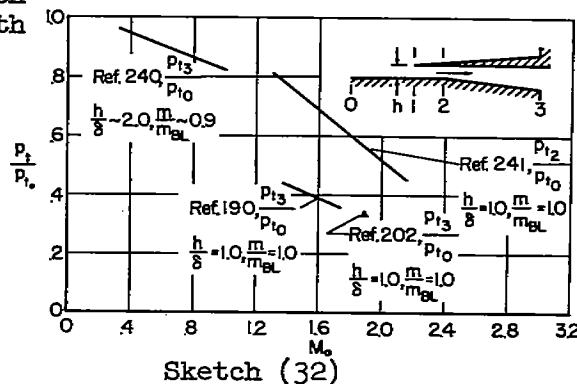
In the tests reported in reference 240, a removal slot of depth equal to about twice the local boundary-layer thickness was located ahead of a semicircular main inlet a distance of about 85 percent of the inlet radius. Tests were made at low speed at inlet-velocity ratios greater than 0.6; hence, the effects of removal on total-pressure ratio were not large. In these tests it was found that the boundary layer on the surface between the boundary-layer scoop and the main inlet grows rapidly at low inlet-velocity ratios. Thus, this length should be minimized.

A study of boundary-layer removal at a Mach number of 1.88 for a half-conical-shock inlet mounted on a flat plate is reported in reference 202. Here, it was shown that the maximum total-pressure ratio attainable in the main duct decreased appreciably as the amount of boundary layer removed was decreased. As the parameter  $h/\delta$  was reduced from 1.0 to 0 ( $h$  is the boundary-layer-scoop height and  $\delta$  is the local undisturbed boundary-layer thickness) the maximum total-pressure ratio decreased from 0.86 to 0.72. In this case, the mass-flow ratio of the removal scoop was the maximum possible; at any value of  $h/\delta$  below 1.0, reductions in scoop mass-flow ratio caused additional total-pressure losses. Also, with this air-induction system the flow became unsteady when the engine mass-flow ratio was reduced below that for maximum total-pressure ratio.

Tests at Mach numbers from 1.3 to 1.8 of a suction-removal system for a normal-shock inlet are described by Frazer and Anderson in reference 190. It was found that boundary-layer removal produced an improvement in total-pressure ratio of from 0.06 to 0.08 through the Mach number range of the tests. The fact that this improvement was considerably less than that attained with the half-conical shock inlet of reference 202 is probably due to the difference in the methods of external compression and of duct design. The air-induction system of reference 202 was more refined in regard to supersonic compression but less refined in the duct. Thus, with nearly complete boundary-layer removal, higher total-pressure ratios were possible but with no boundary-layer removal greater duct losses would be expected. Frazer and Anderson show that pressure recovery could be fairly well predicted by integrating the local pressure recovery of a normal shock wave occurring at the local Mach number of each element of the flow approaching the inlet and adding an allowance for the skin-friction loss in the duct. This method of prediction is also recommended in reference 241. The tests showed that, if  $h/\delta \cong 1.0$  and no additional method of boundary-layer removal is used, the leading edge of the suction scoop must be upstream of the main inlet and the normal shock wave must occur on the intervening surface - not ahead of the boundary-layer scoop - if flow unsteadiness is to be avoided. For mass-flow ratios greater than 0.9 at Mach numbers from 1.3 to 1.8, it was found in this test that the suction scoop must be at least a distance of 0.4 of the inlet radius upstream of the main inlet. (The cross section of the main inlet was a semicircle.) The mass-flow ratio of the suction scoop was maintained at the maximum value in this investigation, and by measuring the total pressure in both the main and the boundary-layer ducts the net propulsive force possible with the system was evaluated. It was found that the maximum net propulsive force occurred when the suction-scoop height was 0.7 of the undisturbed boundary-layer thickness and that the system could produce net propulsive forces from 96 to 100 percent of those produced by a normal-shock inlet not in the presence of forebody boundary layer.

In suction-removal systems, the performance penalty for removing the boundary layer appears as the pressure loss in the removal duct. This, together with the mass flow in the scoop, allows calculation of an effective drag of the boundary-layer removal system. A summary of available data for the pressure recovery of suction-removal ducts shows a large decrease with flight Mach number as indicated in sketch (32). (See also ref. 242.)

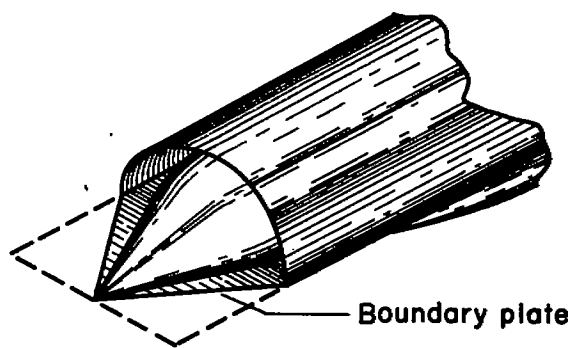
Diversion. - To minimize the drag of a boundary-layer diversion system, the depth of the boundary-layer passage should be no greater than that required to maintain satisfactory engine flow, and the speed and direction of the diverted flow should change as little as possible.





Thus, the main inlet and duct should be designed to be insensitive to at least small amounts of retarded air from a forebody; wetted area and deflection angles in the diverter must be small; and the passage height must diverge both longitudinally and laterally to minimize flow resistance.

The boundary-layer suction scoop of reference 202, which was tested with a half-conical shock inlet on a flat plate, was converted to a diverter system by removing the scoop side walls to a point about one inlet radius aft of the cowl lip and taking no flow through the boundary-layer duct. It was found that maximum total-pressure ratios from 0.02 to 0.03 less than those of the suction system could be attained by sweeping back the leading edge of the plate forming the upper surface of the diverter, that is, the boundary plate, as shown in sketch (33). This



Sketch (33)

plate was swept back along a line joining the apex of the cone with the main inlet lip rather than the leading edge of the plate being normal to the stream direction at the cone apex. It was concluded from these tests that sensitivity to removal-system mass-flow ratio can be reduced by sweeping the leading edges of the boundary plate so that the intensity of the disturbance created by the shock wave from the edges and the extent of the upstream influence through the boundary layer are reduced. Swept edges also create a lateral pressure gradient

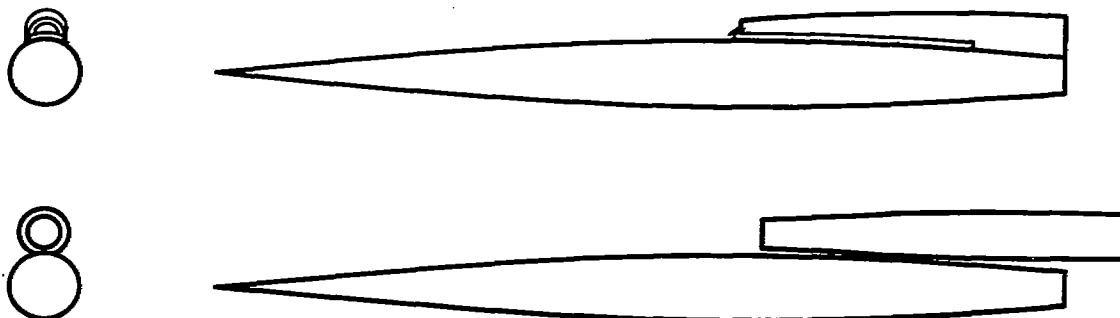
which tends to divert the boundary layer. It was found that extending the boundary-layer passage downstream beyond the plane of the main inlet reduced the angle through which the boundary layer was diverted and prevented the boundary layer from being drawn into the engine streamtube. (See also ref. 243.) Tests of other inlets which utilize these design principles are described in references 182, 244, 245, and 246.

The results of tests of a wedge diverter of about  $60^\circ$  included angle beneath a half-conical shock inlet mounted on a flat plate are presented in reference 243. As would be expected from the results of Goelzer and Cortright (ref. 202), this large wedge angle turned the boundary layer so abruptly that it spilled over the swept leading edges of the boundary plate and flowed into the main inlet. In order to attain the total-pressure ratios possible with a suction scoop, it was necessary to have a diverter passage height 1.4 times the local undisturbed boundary thickness; thus, a high drag would be expected. In reference 247, a series of wedges were tested in an arrangement simulating a diverter passage. It was found that the included wedge angle must be less than  $28^\circ$  if the pressure drag is to be small and that the apex of the wedge must be about one passage height downstream of the apex of the leading edges of a swept boundary plate in order to eliminate the upstream influence of

the wedge on the engine flow. The photographs of the boundary-layer flow of Piercy and Johnson (ref. 247), which were obtained by use of a liquid-film technique, emphasize the importance of minimizing the disturbances imposed upon the boundary layer in the region of an air-induction-system inlet. The necessity of a small wedge angle, a swept and thin boundary plate, and a wedge apex downstream of the splitter-plate apex are all graphically illustrated.

The drag forces on wedge diverters in various types of installations have been measured and are reported in references 218 and 248. With a  $16^\circ$  included-angle diverter, the pressure drag was negligible, but the viscous component of the drag was large. In fact, even though the frontal area of the diverter was only 3 percent of the total frontal area of the model of reference 248, to a flight Mach number of 2.0 and  $h/\delta = 1.0$ , the drag of the diverter was 23 percent of the total model drag, or, in other words, the diverter-plus-interference drag coefficient based on the diverter frontal area was high, 0.95. Improvements can be expected through reduction of the viscous drag due to shock-boundary-layer interaction and turbulent mixing in the vortex from sharp side edges. Not only should wetted area and velocity changes be minimized, but also a high lateral velocity component over nearly square side edges should be avoided because a vortex develops under such conditions and dissipates energy as drag. (A vortex from this cause is used to advantage with NACA submerged inlets at subsonic flight speeds.)

The fact that a low-drag passage between an air-induction system and a body can be attained is illustrated by the investigation of Kremzier and Dryer (ref. 249) in which a circular nacelle was tested in contact with a circular fuselage. This configuration is shown together with a body scoop diverter in sketch (34). By comparing the drag coefficients of the configurations less the body drag on the basis of equal area, it was found that the drag coefficient of the scoop-diverter combination was about twice that of the nacelle. Some of this difference is due to the fact that the



Sketch (34)

models were not strictly comparable; however, the difference is so large that the superiority of the nacelle installation is apparent. Similar results were obtained by comparing a ramp-type scoop inlet and diverter (ref. 248) with the nacelle. These comparisons and present knowledge of diverter design indicate that a low-drag diverter should be designed according to the following principles:

1. To reduce the upstream influence of the diverter, the leading edges of the boundary plate should be swept back, when this is consistent with the inlet-shock configuration, and the diverter apex should be at least one diverter height back of the boundary-plate apex.
2. To reduce pressure and friction drag and to minimize the lateral velocity component, the included angle of the diverter wedge should be about  $20^\circ$ .
3. To prevent the formation of a strong vortex, the boundary-layer passage side edges should have large-radius fairings rather than sharp corners.

As discussed previously, the distribution of boundary layer about a body at angle of attack is not uniform and it accumulates on the leeward side (sketch (28)). If an inlet is located in this position, the design of the boundary-layer removal system must account for the local growth of the boundary layer in angle-of-attack operation. (See, e.g., refs. 220 and 244.) If a large boundary-layer diverter is necessary to maintain engine performance at high angles of attack, a drag penalty results at low angles. As shown by the data of reference 199, this difficulty is avoided at positive angles of attack by a bottom location of a side inlet.

Tests have been made of combined suction and diverter systems; that is, a portion of the approaching boundary layer is drawn into a closed duct, usually for cooling purposes, and the remaining boundary layer is diverted. (See refs. 116 and 250.) With the suction scoop at the apex of the diverter wedge, the upstream influence of the diverter is reduced by increasing the local flow rate and reducing the local deflection angles; in other words, it allows lower diverter wedge angles. If the auxiliary system requires low-energy air, the best point at which to locate an auxiliary inlet in a diverter passage might not always be at the wedge leading edge. It is apparent that the lowest energy air can best be obtained at the exit of the diverter passage. It is possible that such an installation would have less drag than one with a forward auxiliary air intake because the dynamic pressure of the local flow is smaller.

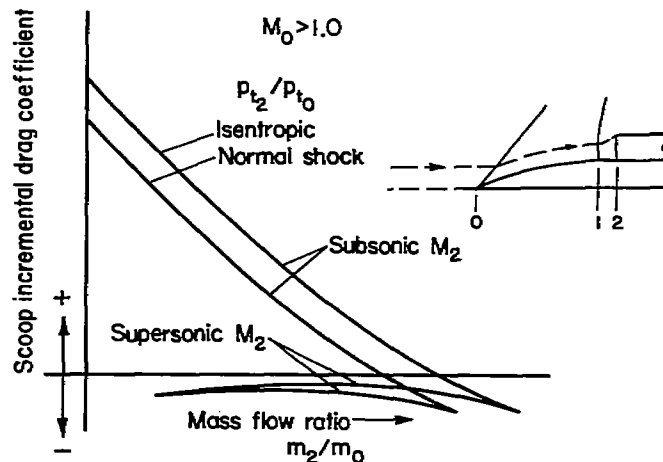
Submerged inlets.- Inlets which are submerged in the surfaces of bodies and wings have all the boundary-layer-removal problems of scoops. A number of variations of inlets of this type have been investigated and, as with scoops, high pressure recovery can be attained at subsonic speeds

when the adverse effects of the approaching boundary layer are removed. Investigations of submerged inlets having curved or steep-angle approach ramps with parallel sides are reported in references 251, 252, and 253. In general, the total-pressure ratios attained were less than those of similarly placed scoops. A submerged inlet having a relatively small ramp angle (about  $7^\circ$ ) and diverging ramp side walls has been found to be comparable to scoops in regard to pressure recovery. (See refs. 254, 255, and 256.) The experimental investigation of reference 257 and the theoretical study of reference 258 provide an explanation of the relatively high pressure recovery of this arrangement. Flow over the square corner of the ramp side walls creates a vortex which thins the boundary layer on the ramp and sweeps the retarded air into the vortex core. When the vortex flows into the inlet at high mass-flow ratios, it represents a loss in total-pressure ratio, but less of a loss than if the boundary layer were permitted to grow normally; at low mass-flow ratios, the vortex is discharged externally and represents an increase in drag. Tests at low subsonic speeds, reference 28, have indicated that the drag of submerged inlets can be greater than that of scoops. However, flight tests comparing a submerged and a scoop installation (ref. 256) have shown that the former has equal or slightly better performance. Apparently, the merits of the two depend upon the installation, and they can be equal in subsonic flight. However, investigation at supersonic speeds, reference 259, has shown that the expansion of the flow over the ramp leads to a high inlet Mach number and large pressure losses at flight Mach numbers greater than about 1.2. Thus, the submerged inlet is limited in application to subsonic airplanes as either a main or an auxiliary air intake. (For the latter application, see refs. 251 and 260.)

#### Combined Effects

Scoop incremental drag.— As discussed previously, scoop incremental drag represents the difference in the total flight momentum of the air in the engine streamtube and the momentum at the initial station of an air-induction system. It is, therefore, an interference force resulting from both the pressure and skin-friction drag forces on surfaces upstream of an induction system when no provision is made for removing

forebody boundary layer from the engine streamtube. Klein (ref. 7) has calculated scoop incremental drag coefficient  $C_{Dg} = D_g/q_0 A_2$  as a function mass-flow ratio, flight Mach number, and total-pressure ratio between free stream and inlet. An example of the variation is shown in sketch (35).



Sketch (35)

Thus, when the average inlet Mach number is subsonic in supersonic flight, the scoop incremental drag force is large at low mass-flow ratios, particularly if the forebody wave and skin-friction drag forces are small, because then the local pressure rise ahead of the inlet is large. (The symbol  $p_{t_2}$  is the average total pressure at the inlet, and it includes the total-pressure loss of any entering boundary-layer air which eventually flows to the engine.) With supersonic flow into the inlet, the scoop incremental drag coefficient is negative because the spillage drag<sup>22</sup> is small (zero at maximum mass flow) and the forebody drag term  $F_B$  of equation (7) is dominant.

For air-induction systems having this interference force, the net drag consists of the sum of the external wave drag when the inlet operates with no spillage, the scoop incremental wave drag, the change in external wave drag due to a reduction in mass flow from the maximum, and skin friction. Thus, the scoop incremental drag replaces the additive drag of systems having no forebody interference.

Wakes.— The pressure recovery of an air-induction system that takes in air from the wake of an upstream body is, of course, reduced. The tests at a Mach number of 2.0 of reference 224 in which a nacelle was placed behind the tip of a canard control surface illustrate the magnitude of this effect. With the control surface deflected  $10^\circ$ , the maximum total-pressure ratio attainable was 0.10 less than when the nacelle was moved outboard away from the influence of the tip vortex.

#### INDUCTION-SYSTEM AIRCRAFT

The interference between an air-induction system and other aircraft components can affect any of the forces and moments which determine performance. For instance, drag can be increased if a nacelle is placed so that a positive pressure gradient from it causes boundary-layer transition or separation on a neighboring surface; the lift of a wing with a leading-edge inlet can be a function of mass-flow ratio; tail loads can be affected by a change in circulation distribution resulting from changing the wing plan form to extend the duct of a wing-root inlet; side force and yawing moment can result from shock or expansion interference from an outboard nacelle with a vertical tail surface, and this interference could be changed by power setting. It is the purpose of this section to discuss these problems and principles regarding them which have resulted from theoretical and experimental studies.

---

<sup>22</sup>Spillage drag is the pressure force on the external streamlines which are affected by the inlet mass-flow ratio. In this case, it is the local additive drag.

---

## Drag

Skin friction and separation.- In reference 207 a series of wing-nacelles were tested to demonstrate a method for maintaining long runs of laminar flow over the combinations. By making the leading edges coincident and matching the pressure distributions so as to maintain a negative gradient to the position of maximum thickness of the wing, the minimum drag coefficient was reduced to less than two-thirds that of conventional wing-nacelle combinations when the inlet-velocity ratio was greater than 0.5.

The tuft studies of reference 185 show that an inlet-velocity ratio less than 0.6 with a scoop in the presence of forebody boundary layer not only causes separation of the internal flow, but also causes the separated region to spread around the inlet and to affect the external flow. Although interference drag was not measured, it is undoubtedly increased by the turbulent mixing. The flight tests reported in reference 256 show the possible effect of such separation. Drag measurements were made with a boundary-layer bypass sealed, and with it discharging normal to the external flow, it was found that at a flight Mach number of 0.8, discharge of the boundary-layer normal to the air stream increased the airplane drag coefficient 0.0015, or 7 percent.

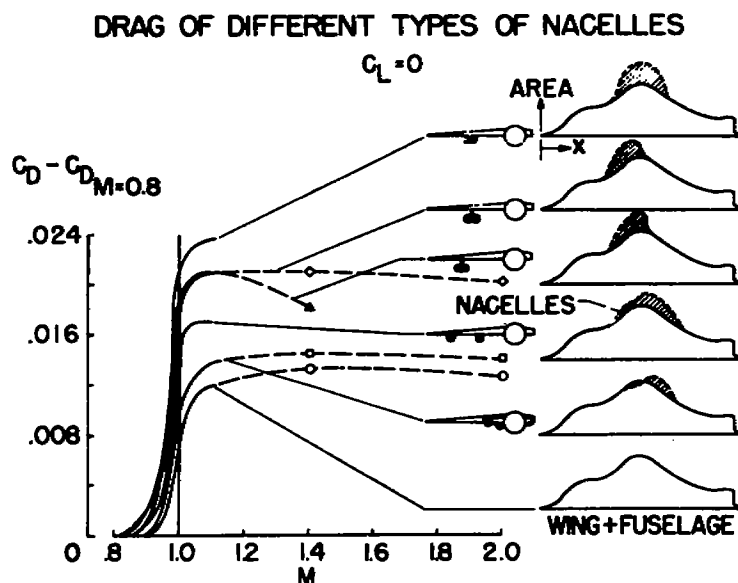
At supersonic speeds the boundary layer on other aircraft components can be affected by shock waves or the pressure field from propulsive systems, and, the local pressure gradients caused by shaping a surface so as to minimize wave drag can be sufficient to separate a turbulent boundary layer. Therefore, this form of interaction also requires careful attention. Shock-wave boundary-layer interaction has been discussed previously, but the studies of Morokovin, Migotsky, Bailey, and Phinney (ref. 261) are particularly pertinent here. This investigation of the interaction of a plane oblique shock wave intersecting a circular cylinder across the axis shows that if the incident shock wave is weak, the pressure rise across the reflection is that predicted for two-dimensional flow. However, if the shock wave is relatively strong (flow deflection angle of  $11.2^\circ$  in this case) the over-all pressure rise is but half that predicted for a flat plate. This difference is presumably the result of three-dimensional relief and the resulting lateral pressure gradient. Because of the decreased surface pressure rise for a given shock wave, it appears that more intense shock waves can be withstood without encountering separation of turbulent boundary layers in three-dimensional rather than two-dimensional flow.

Transonic drag rise.- In general, the addition of an air-induction system to the pressure field of another body alters the pressure distribution and thus the transonic drag rise. The investigations of references 225, 84, 85, 230, 231, and 262 show, however, that wing root or wing leading-edge inlets and nacelles operating at mass-flow ratios near 1

can be designed so that they do not decrease appreciably the drag-rise Mach number of a wing-body combination. (Methods of predicting the drag-rise Mach number have been discussed previously and are presented in references 149 and 208.)

For supersonic aircraft, the drag-rise Mach number is an important cruise consideration; the magnitude of the rise and methods for minimizing it are of essential importance in determining acceleration performance and fuel consumption. The "transonic area rule" presented in references 263 and 264 states that for slender configurations, the transonic rise in wave drag is a function of the longitudinal distribution of cross-section area and is independent of cross-section shape. Thus, an aircraft with the least drag rise has the same distribution of cross-section area as a minimum-drag body of revolution. Conversely, the magnitude of the increase in wave drag at transonic speeds for complicated configurations can be predicted for flight at zero angle of attack from information on bodies of revolution with the same cross-sectional-area distribution. It follows from this rule that for low drag rise the equivalent body of revolution must be fair and slender, and these design requirements also result in high drag-rise Mach number.

In regard to interference of the air-induction system on the aircraft, the transonic area rule is a design criterion for placing and shaping induction systems. For instance, the data presented in reference 265 show that the drag rise is the least and the drag-rise Mach number is the greatest when the addition of an air-induction system to a wing-body combination causes no abrupt or large changes in the distribution of cross-section area. This result is illustrated by sketch (36) which was reproduced from refer-



ence 265. References 170, 266, and 267 present more experimental information concerning the interference of air-induction systems with aircraft at transonic flight speeds.

Wave-drag.—The transonic area rule has been extended for application at supersonic speeds by R. T. Jones in reference 268, and the limitations of this extension have been examined by Lomax in reference 269. It is shown that, for slender aircraft, cross-section areas can be taken in planes through a point on the body axis inclined at the flight Mach

Sketch (36)

angle to obtain an equivalent area distribution. A sufficient number of planes must be chosen so that an accurate average oblique section area can be computed. Then, from this equivalent area distribution, the wave drag can be calculated by slender-body theory. For configurations in which the area distribution is chosen so as to minimize the drag, the design is near optimum only for a small range of flight Mach numbers about the design point. The experiments of reference 268 substantiate the use of this method as a design criterion. Analysis of drag data for a wide variety of configurations indicates that predictions of drag are in error by a maximum of about 20 percent with a mean error of about 7 percent. As pointed out by Jones, these area rules are basically methods of wave cancellation - the pressure drag of one component is canceled by proper use of the pressure field from another component.

More detailed theoretical investigations of wing-body combinations in supersonic flow indicate how components can best be shaped and arranged to provide wave cancellation. Baldwin and Dickey in reference 270 demonstrate the importance of the moments of the area distribution at Mach numbers above 1. Both experiment and theory show that the Mach number for drag rise is high and the subsequent drag rise is low if the longitudinal distribution of the moments of area is smooth and gradual. (At low supersonic speeds moments greater than the second are of negligible importance.) Nacelles can be used to improve the moment distribution of wing-body combinations, and the data of reference 270 show that the high-speed drag characteristics of a wing-body-nacelle combination can be less than those of the corresponding wing-body combination. The studies of references 271 and 272 indicate that rotational asymmetry of body cross sections in the region of a wing juncture provides greater wave cancellation than a symmetric indentation. Nielsen (ref. 272) employs linearized theory to determine the change in shape of a circular cylinder required to cancel the wave drag of wings. The method can be extended to the interference problems of nacelle-fuselage or to nacelle-wing-fuselage combinations as long as the flow is quasi-cylindrical.

In reference 273, Friedman and Cohen consider the minimum wave drag of two- and three-body combinations. It is shown by linearized theory that the least drag is produced in supersonic flight when the bodies are close together and staggered so that the pressure fields interact to produce a buoyant force in the flight direction. The general trends of this analysis have been substantiated by the experiments of reference 249. Here, the forces on both single and twin nacelles with normal-shock inlets operating supercritically were measured in the presence of a body of revolution having a parabolic-arc radius distribution. The nacelles were moved both axially and radially, and it was found that the theoretical predictions were fairly accurate for forward locations, but for rearward inboard locations there was considerable deviation from experiment. The favorable interference effects at the rear inboard locations were equal to or greater than those indicated by theory. In reference 274 a nacelle with a conical-shock inlet operating subcritically at a flight Mach number



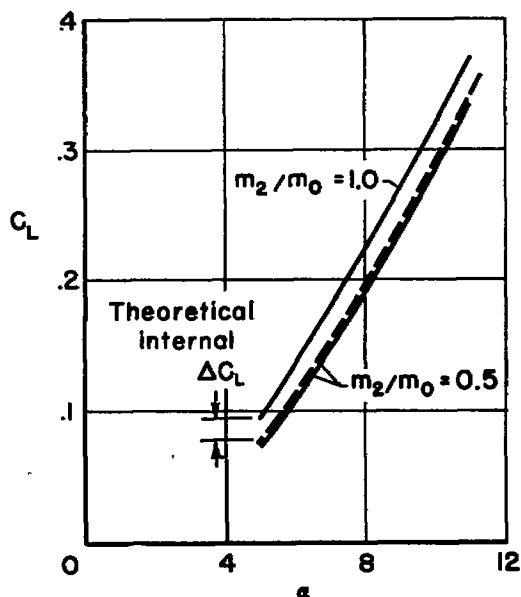
of 2.0 was located at two positions in the pressure field of a complete aircraft configuration. A 10-percent increase in drag coefficient resulted at zero angle of attack when the nacelle was moved from a forward to a rearward location. This large increase in drag, which is opposite to the trend indicated in reference 249, was attributed to the strong shock wave from the inlet.

### Lift and Pitching Moment

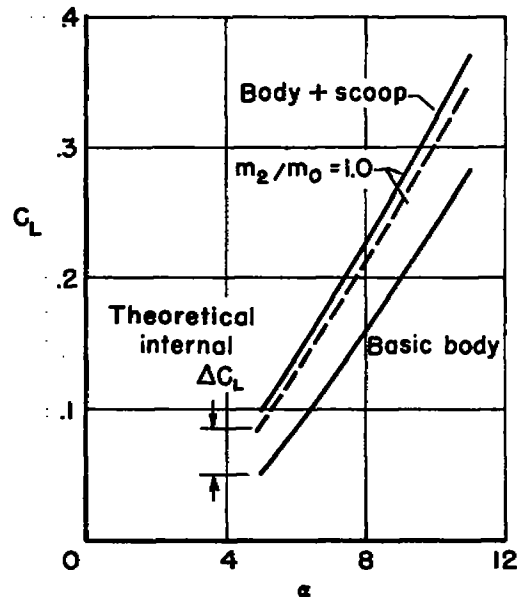
The lift force of an air-induction system consists of the lift component of the pressure forces on the external surfaces and of the reaction from the force required to turn the engine streamtube from the flight direction to that of the induction-system axis. This force from turning the internal flow is carried on the lips, see reference 275; and, as shown in reference 152, in terms of the incremental lift coefficient based on maximum body frontal area for a slender body, it is

$$\Delta C_L = 2\alpha \frac{A_2}{A_{\text{body}}} \frac{m_2}{m_0} \quad (\alpha \text{ in radians}) \quad (33)$$

the corresponding incremental pitching-moment coefficient is, of course, the product of this lift coefficient and the distance from the inlet to the moment reference point divided by the moment reference length. Pierpont and Braden in reference 234 compare this prediction with data taken at subsonic speeds on a body having an underslung scoop just behind the nose. The results for a flight Mach number of 0.8 are shown in sketch (37). The effect of mass-flow ratio on the lift of the body-scoop



(a) Effect of mass-flow ratio



(b) Effect of basic body

Sketch (37)

combination is closely predicted (sketch (37a)), but there is some error in predicting the lift resulting from addition of the scoop with a mass-flow ratio of 1.0 to the basic body (sketch (37b)). This difference is probably due to the fact that interference with the pressure field of the basic body resulting from addition of the scoop was not taken into account. The incremental pitching moment of this configuration was not well predicted apparently because the drag component of the moment contributed by the asymmetric scoop changed with mass flow and angle of attack and counteracted the moment due to the incremental lift. A comparison of experimental and theoretical lift coefficients at supersonic speed for a slender, open-nosed body of revolution is presented in reference 152. Here it was found that up to an angle of attack of  $4^\circ$  the prediction agreed with experiment within 7 percent and there was comparable accuracy in the pitching-moment comparison. The contribution of these effects to the lift and pitching moment of a complete airplane is, in general, relatively small; for instance, the incremental lift-curve slope due to turning the engine flow at a mass-flow ratio of 1 is only about 1 percent of that of a normal airplane. Thus, in most cases great accuracy in predicting mass-flow effects on lift and its moments is not necessary.

In the following discussion, the interference of various air-induction systems on lift and pitching moment are presented. Forces and moments in other planes are not discussed because, in general, they result from the same phenomena.

Wing leading-edge inlets.- Tests of wing leading-edge inlets in both straight and swept wings with NACA 63-012 airfoil sections are described in references 225 and 226. For the straight wing, the effect of internal flow on both the lift- and pitching-moment-curve slopes was negligible. There was a large effect of inlet-velocity ratio on maximum lift coefficient at very low flow rates, but for the range of usual interest, inlet-velocity ratios above 0.8, the maximum lift coefficient of the basic wing was maintained. With the swept wing, there was a large change in the flow at the downstream corner of the inlet at lift coefficients above 0.6. The maximum section lift coefficient at 0.8 inlet-velocity ratio was 1.10 at the upstream corner but, at the other corner, it was 0.72. Reducing the inlet-velocity ratio to 0 or increasing it to 1.6 changed these section lift coefficients by 0.10 at most. It is thus apparent that with a swept wing, flow through a leading-edge inlet can seriously interfere with the lifting force and its distribution.

Wing-root inlets.- A wing-root inlet of triangular frontal shape was tested on a  $45^\circ$  sweptback wing-body combination as described in reference 186. The inlet lips were parallel to the wing leading edge, and the lip profiles were refined by changing inclination and stagger so that for mass-flow ratios from 0 to 1.5 internal flow had no effect on lift-curve slope or maximum lift coefficient. Tests reported in reference 84 at higher speeds showed no effects at mass-flow ratios from 0.4 to 0.7 up to a flight Mach number of 1.2. In reference 85, the results of tests

of a similar configuration differing only in inlet frontal shape (semi-elliptical rather than triangular) are presented. The effects of internal flow on lift were again negligible, but here pitching moment was measured. It was found that at Mach numbers above 0.9, the presence of the inlet with mass-flow ratios of 0.4 or 0.8 increased the static longitudinal stability of the wing-body combination tested by 25 percent. In this test, the inlet had no effect on the lift coefficient at which the slope of the moment curve reversed.

Tests of a wing-root inlet mounted on a swept wing with the inlet plane normal to the flight direction are described in reference 276. The inlet plane was ahead of the leading edge of the root chord of the wing alone, and thus the installation of the air-induction system modified the wing plan form. Flight tests revealed a strong pitch-up above an angle of attack of  $8^\circ$ , and wind-tunnel tests showed this to be caused by an abrupt change in downwash at the tail, due to a change in circulation about the wing as the angle of attack was increased. The pitch-up was eliminated by changing the section contour of the outboard portion of the wing leading edge and by adding fences both at the inlet and outboard on the wing. An inlet with the outboard radius about half the scoop depth, and an inlet width-to-height ratio near 1.0 also eliminated the pitch-up. It was concluded that the wing plan form and sharp side edge resulting from the addition of the extended wing-root inlet was the cause of the unexpected downwash variation. Tests of a somewhat similar configuration for a supersonic airplane are reported in reference 144. In this case there was no longitudinal instability for the condition of no flap deflection, probably because of the low position of the horizontal-tail surfaces and the rounded side edges of the inlet.

Scoops.— The effects of scoops on the lift of a complete airplane are generally not large, just as the body lift is not a large percentage of the total lift unless the body diameter and wing span are nearly equal. Thus, top and bottom scoop locations would be expected to have small effects on lift and moment, and the effect of side scoops would depend on the width of the body-scoop combination relative to the body diameter or wing span. These trends are illustrated for subsonic speeds by the data of references 234 and 277. The effect of body plan-form changes due to the addition of scoops on the lift increment due to viscous crossflow effects can be estimated by the method of reference 216.

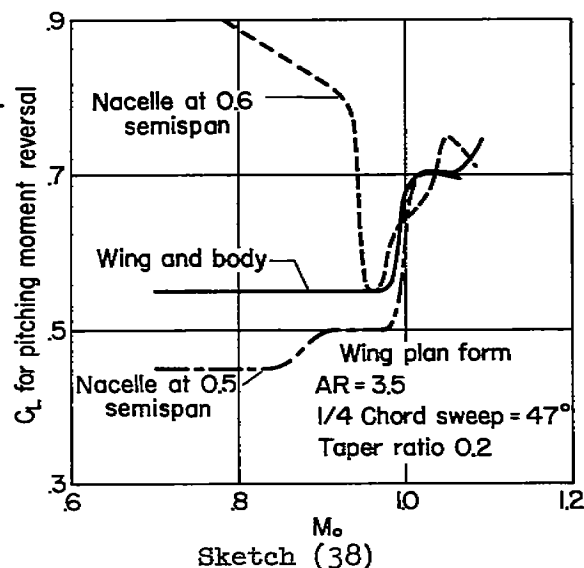
The lift and moment effects of scoops mounted on bodies in tests at Mach numbers of 1.5, 1.8, and 2.0 are described in references 220 and 239. In the former investigation, scoop locations on the top and bottom of a body were compared. The scoop had a ramp-type compression surface and was operated supercritically. At zero angle of attack, the bottom location included a small positive lift force, and the top location induced an equal negative force; the shift in the angle for zero lift from that of the body alone was plus and minus  $2^\circ$ , respectively. This difference was maintained to an angle of attack of  $8^\circ$ ; at greater angles, the bottom

location caused an increasing lift-curve slope, whereas the slope remained nearly constant for the top location. Through the angle-of-attack range of  $10^\circ$ , the slope of the pitching-moment curve for the bottom location was constant whereas that for the top location increased. This means that the center of pressure moved rearward for the bottom scoop and forward for the top scoop. The results of reference 239 for an underslung scoop confirm these trends. A reduction in mass-flow ratio in these latter tests from 1.0 to 0.7 had no appreciable effect on lift or moment.

Nacelles.— The investigation of references 207, 231, 278, and 279 were of wing-nacelle combinations in which the nacelle inlet was at the leading edge of both straight and swept wings and the nacelles extended behind the trailing edges. As would be expected from such plan forms, the lift-curve slope and the stability of the combinations (based on wing dimensions) were greater than those of the wing alone. The effects of internal flow on lift-curve slope and maximum lift coefficient were small in the tests in which lift was measured, (refs. 207 and 231).

For nacelles that extend ahead of a wing, the lift on the projecting body is destabilizing. The magnitude of this effect for some nacelles in subsonic flow is reported in reference 81. Some of the nacelles of this reference were located just below the wing; this position resulted in an increase in the angle for zero lift above that for the wing alone because of the high induced velocities on the lower wing surface in the region of the wing-nacelle juncture. This effect also changed the span loading of the wing. The nacelles described in this reference did not change the maximum lift coefficient attainable with the wing alone, but the lift-curve slope was increased as much as 10 percent. This large increase was due to the nacelles being tested only on a short wing panel; on a complete wing the increase in lift-curve slope would be of the order of 4 percent.

In reference 278 it is shown that the destabilizing effect of forward nacelle locations can be counterbalanced by mounting the nacelle from a vertical strut and moving it downward. The results of reference 279 show that the spanwise position of such a strut-mounted nacelle can be selected so as to increase the lift coefficient at which the slope of the pitching-moment curve of a sweptback wing reverses. Here, moving the nacelle from 0.5 to 0.6 of the wing semispan changed the flow over the wing to such an extent that loss of lift at the tips was delayed. As shown in sketch (38), at flight Mach numbers below about 0.9 this effect was large.



The nacelles tested at subsonic speeds as reported in reference 278 and 279 were also tested at Mach numbers of 1.6 and 2.0 as described in references 280 and 281. These nacelles were mounted in several positions on and below the chord plane of the sweptback wing at various spanwise locations. The aerodynamic characteristics were similar to those at subsonic speeds; that is, all the nacelles increased the lift-curve slope, the nacelles in the wing root increased stability but those mounted outboard decreased it. The magnitudes of the effects depend upon the specific configuration, but they seldom exceeded 10 percent of the lift or moment of the wing alone.

A theoretical study of the lift of bodies and combinations of bodies is presented in reference 282. Slender-body theory was used to predict the interference of a fuselage on an open-nose nacelle downstream of the intersection of the nacelle with the fuselage bow-shock wave. In the region of this intersection, slender-body theory is not applicable, but account was made of this by assuming that the reflection is that of two-dimensional flow, and the results of reference 261 substantiate this assumption for weak shock waves. The predictions of this method were compared with experiment as described in reference 249. Here, tests were performed at Mach numbers of 1.8 and 2.0 with a slender fuselage having open-nose nacelles mounted above and below in the pitch plane. Normal force was measured with the nacelles in several axial and vertical positions. With the nacelles almost in contact with the fuselage, the sum of the normal forces of the component bodies was as much as 25 percent greater than the total measured normal force at an angle of attack of  $4^\circ$ . At higher angle of attack, the normal force decreased to half the sum of the component forces. This lift interference is, of course, due to the bodies being in crossflow wakes. The theory proposed does not include all of the factors involved in crossflow and, depending upon relative location, predicted normal-force interference with errors from 0 to 25 percent of the measured values. With the nacelle axis over 2 fuselage diameters from the fuselage axis there was no normal-force interference within the limits of angle of attack ( $8^\circ$ ) and axial spacing investigated.


The lift- and pitching-moment characteristics at Mach numbers of 1.5, 1.8, and 2.0 of a canard configuration having one of the nacelle arrangements of reference 249 are described by Obery and Krasnow (ref. 283). The nacelle axes were located one fuselage diameter from the fuselage axis and the nacelle inlets were at 70 percent of the fuselage length behind the nose. Since the nacelles were nearly half as long as the fuselage, they extended a considerable distance downstream and contributed a stabilizing moment to the fuselage. Because of lift interference due to crossflow, the lift of the combination could not be accurately predicted by the theory of reference 282. This model was also tested with the nacelles in the horizontal rather than the vertical plane (ref. 284). They were placed 1-1/2 fuselage diameters from the center line and the inlets were at about the mid-length station of the fuselage. The increase in lift-curve slope due to adding the nacelles (15 percent) was about twice

as great as when they were added in the vertical plane, and the effect on stability was not as great. The addition of nacelles to the basic aircraft configuration of references 266 and 267, however, resulted in large percentage changes in pitching moment.

The range performances of the various combinations investigated in references 239, 283, and 284 are compared in reference 19. It was found that the configuration with scoops which had the least minimum drag had slightly greater range than the configuration with nacelles in the horizontal plane which had the least drag due to lift. This evaluation depends, of course, on the specific conditions assumed in the study.

The interference of a nacelle having a conical-shock inlet operating subcritically at a flight Mach number of 2.0 with an aircraft configuration is described in reference 274. A comparison with the nacelle in a forward and an aft location shows a decrease in lift-curve slope from 0.026 to 0.021 per degree and an increase in angle for zero lift from  $0.5^{\circ}$  to  $1.9^{\circ}$  due to moving the nacelle from a location forward below the body to one rearward and over the wing. There was a corresponding forward shift of the aerodynamic center.

Ames Aeronautical Laboratory  
National Advisory Committee for Aeronautics  
Moffett Field, Calif., June 16, 1955



## APPENDIX A

## SYMBOLS

A	area
$A_c$	capture area
$C_D$	drag coefficient
$C_f$	skin-friction coefficient based on wetted area
$C_L$	lift coefficient
$C_p$	pressure coefficient
D	drag
$D_n$	net drag
d	diameter
$F_n$	engine net thrust
$F_{np}$	net propulsive force
$\Delta F_n$	difference between ideal and actual net thrust, $F_{ni} - F_{na}$
g	gravitational constant
H	ratio of boundary-layer-displacement thickness to momentum thickness, $\frac{\delta^*}{\theta}$
h	altitude
h	height of boundary-layer diverter
l	length
$M_I$	total momentum of the engine streamtube in the inlet plane
M	Mach number
m	mass flow
$m_M$	maximum mass flow, $m_M = \rho_0 V_0 A_c$

n	engine rotational speed
n	number of oblique shock waves
p	pressure <sup>1</sup>
Q	fuel consumption
q	dynamic pressure
R	Reynolds number
R	gas constant
r	local radius
S	wing area or wetted area
T	temperature <sup>1</sup>
U	local velocity of flow, $U^2 = (V+u)^2 + v^2 + w^2$
u,v,w	local velocity components in the x,y, and z directions, respectively
V	stream velocity
$W_a$	weight flow of air
$W_{ac}$	corrected weight flow of air
$W_f$	weight flow of fuel
x,y,z	Cartesian coordinates with x positive in the stream direction
$\alpha$	angle of attack
$\beta$	angle of sideslip
$\gamma$	ratio of specific heats
$\delta$	relative absolute pressure, $\frac{p_{t3}}{p_{s1}}$
$\delta$	boundary-layer thickness
$\delta^*$	boundary-layer displacement thickness

---

<sup>1</sup>When used without the subscript t, the symbols, p,  $\rho$ , and T denote static pressure, static density, and static temperature, respectively.

---



$\epsilon$	angle of flow deflection
$\theta$	relative absolute temperature, $\frac{T_{ts}}{T_{SL}}$
$\theta$	boundary-layer momentum thickness
$\lambda$	cowl angle, the angle between the free-stream direction and a line connecting the inlet and cowl maximum diameters
$\xi_1, \xi_2, \xi_3$	functions defined by equations (B5), (B7), and (B8), respectively
$\rho$	mass density <sup>2</sup>
$\sigma$	cone semiapex angle
$\sigma_L$	cowl-position angle, the angle between the apex of a pre-compression surface and the cowl lip (see sketch (18))
$\tau$	local shear stress
$\varphi$	shock-wave angle
$\psi$	area ratio, $\frac{A_2'}{A_2}$

## Subscripts

$0, 1, 2, 2', 3, \dots \infty$	denote stations in the flow as shown in sketch (1)
a	actual or additive
B	forebody
b	body
c	cone surface
ex	external
f	friction
h	hydraulic diameter

---

<sup>2</sup>See footnote 1, page 105.

I	refers to the plane enclosed by the stagnation points on the inlet lips
in	internal
i	ideal
j	jet
l	lip
M	maximum
n	net
r	ramp
s	shock wave
s	scoop
t	total
V	viscous
W	wave
cr	critical
isen	denotes isentropic flow
SL	denotes standard sea-level conditions

## Superscripts

( )*	denotes conditions where $M = 1.0$
$\overline{(\quad)}$	average or effective value

## APPENDIX B

MEASUREMENTS AND INTERPRETATION

In tests of air-induction systems accurate measurements must be made of effective total pressure, mass-flow rate, and drag. Not only must each measurement be made accurately, but also the method of data interpretation must be one which best suits design purposes. Some of the considerations involved are discussed in this appendix.

## MEASUREMENT ACCURACY

The accuracy of determining effective total pressure  $\bar{p}_{t3}$  from measurements with a rake of total-pressure tubes depends upon the precision of each measurement of  $p_{t3}$ . Pitot tubes alined with a subsonic stream indicate true total pressure at the tube center line only when the flow is uniform and steady. The information of reference 285 shows that there is little error in measurement if the tube is alined within  $10^\circ$  of the flow direction if the bore of a tube with a hemispherical head is greater than about 0.3 the external diameter. The study of reference 286 shows that when a tube is in a transverse total-pressure gradient, the effective center of total pressure is displaced towards the region of higher velocity by a small amount. This correction is negligible in the testing of well-designed air-induction systems because sizable transverse pressure gradients do not exist in large portions of the flow and the pitot tubes are normally small relative to the duct area. Since duct flow can often be unsteady, measurements under these conditions are not at all reliable. In reference 287 it is shown that in incompressible flow the reading of a total-pressure tube alined with the mean stream velocity  $V$  is

$$p + \rho \frac{V^2}{2} + \frac{\rho}{2} (\overline{u^2} + \overline{v^2} + \overline{w^2}) \quad (B1)$$

where  $u$ ,  $v$ , and  $w$  are the components of the turbulent fluctuations. Thus, in unsteady flow the readings of pitot tubes are always greater than the true value, and calculations of effective total pressure, internal drag, or mass flow based on the indication can be considerably in error. (See also refs. 288 and 289.) The importance of this source of error is indicated by the tests of reference 290 in which measurements were made in the turbulent flow behind orifice plates. It was found that the measurement of mean total pressure decreased with distance behind the plate, a trend to be expected from the decay of turbulence. Errors in the measurement of flow quantity of 10 to 15 percent resulted from readings

with pitot tubes in this turbulent flow. It is therefore necessary that some method of indicating unsteady flow be used with pitot-tube measurements in air-induction systems.

In making measurements with a rake of pitot tubes, the number of tubes which can be conveniently used is occasionally limited. Under such circumstances the spacing of the tubes to give the most accurate average can be chosen according to the method of Gauss, references 291 and 292. Integration must be performed according to the Gaussian formula, which requires more computation than do the normal methods.

A rake of pitot and static tubes is used in induction-system testing when area- or mass-flow-averaged total pressures and flow uniformity are to be measured. Because of the errors which can arise and because of the importance of the mass-flow measurement in determining accurately net drag and optimum-performance conditions, it is advisable to calibrate rake installations with a standard orifice meter. As a result of these complications, total pressure and mass flow are often determined simply from measurements of static pressure at two stations of different area in the duct. If steady, one-dimensional, isentropic flow of a perfect gas is assumed between the measurement stations

$$\frac{p_2}{p_{t2}} = \left[ \frac{(p_1/p_2)^{10/7} (A_1/A_2)^2 - 1}{(p_1/p_2)^{12/7} (A_1/A_2)^2 - 1} \right]^{7/2} \quad (B2)$$

where the subscript 2 refers to the throat or minimum section. Hence, the total pressure  $p_{t2}$  can be determined from measurements of static pressure and area at local stations 1 and 2. From knowledge of the total temperature and pressure, the static pressure, and the cross-section area at a station, mass flow can be calculated from the formula

$$m_2 = p_{t2} A_2 \left( \frac{0.00408}{T_{t2}} \right)^{1/2} \left( \frac{p_2}{p_{t2}} \right)^{5/7} \left[ 1 - \left( \frac{p_2}{p_{t2}} \right)^{2/7} \right]^{1/2} \quad (B3)$$

These formulas involve assumptions which often are not met in tests of air-induction systems, and again check calibrations and careful consideration of sources of error are necessary. (See, e.g., refs. 285, 288, and 293.) The uncertainty (see ref. 293) in mass-flow measurement is given by the relationship

$$\frac{\Delta m}{m} \equiv \left\{ \left( \frac{\Delta p}{p} \right)^2 + \left( \frac{\Delta A}{A} \right)^2 + \frac{1}{4} \left( \frac{\Delta T_t}{A} \right)^2 + \xi_1 \left[ \left( \frac{\Delta p}{p} \right)^2 + \left( \frac{\Delta p_t}{p_t} \right)^2 \right] \right\}^{1/2} \quad (B4)$$

and is a function of Mach number at the measurement station because

$$\xi_1 = \frac{1}{49} \left[ \frac{(p/p_t)^{2/7} - 2}{1 - (p/p_t)^{2/7}} \right]^2 \quad (B5)$$

Plotting  $\xi_1$  as a function of Mach number shows that large errors in mass-flow determination result from errors in measurement of static and total pressure if the throat Mach number is less than about 0.7. Similarly, the uncertainty in total pressure is

$$\frac{\Delta p_t}{p_t} \equiv \left\{ \xi_2 \left[ \left( \frac{\Delta A_1}{A_1} \right)^2 + \left( \frac{\Delta A_2}{A_2} \right)^2 \right] + \xi_3 \left[ \left( \frac{\Delta p_1}{p_1} \right)^2 + \left( \frac{\Delta p_2}{p_2} \right)^2 \right] + \left( \frac{\Delta p_2}{p_2} \right)^2 \right\}^{1/2} \quad (B6)$$

where

$$\xi_2 = \left\{ \frac{7(A_1/A_2)^2(p_1/p_2)^{10/7} [1 - (p_1/p_2)^{2/7}]}{[(A_1/A_2)^2(p_1/p_2)^{10/7} - 1][(p_1/p_2)^{12/7}(A_1/A_2)^2 - 1]} \right\}^2 \quad (B7)$$

and

$$\xi_3 = \left\{ \frac{(A_1/A_2)^2(p_1/p_2)^{10/7} [(A_1/A_2)^2(p_1/p_2)^{12/7} - 6(p_1/p_2)^{2/7} + 5]}{[(A_1/A_2)^2(p_1/p_2)^{10/7} - 1][(A_1/A_2)^2(p_1/p_2)^{12/7} - 1]} \right\} \quad (B8)$$

Thus, the error in total pressure is a function of the ratios  $A_1/A_2$ ,  $p_1/p_2$ , and the component uncertainties in the area and pressure measurements. The variation of  $\Delta p_t/p_t$  and  $\Delta m/m$  as a function of throat Mach

5F

NACA RM A55F16

111

number  $M_2$  is illustrated in sketch (39) for an assumed error in static-pressure and area-ratio measurements of 1/2 percent. The uncertainties are directly proportional to the errors in these ratios, and uncertainties for other values of the assumed error can be determined by simply multiplying by the proper factor. It is evident that a contraction in area of about 0.7 with a near sonic value of  $M_2$  produces relatively great accuracy. In order to maintain accuracy through a wide range of mass flow, it is necessary to employ a variable throat.

### EFFECTIVE TOTAL PRESSURE

Three methods of determining effective total pressure at diffuser exits are in common use. None are exact. They are described by the following equations for incompressible, two-dimensional flow with uniform static pressure:

Method of equation (B2) (the "Mass-Derived Method" of reference 294)

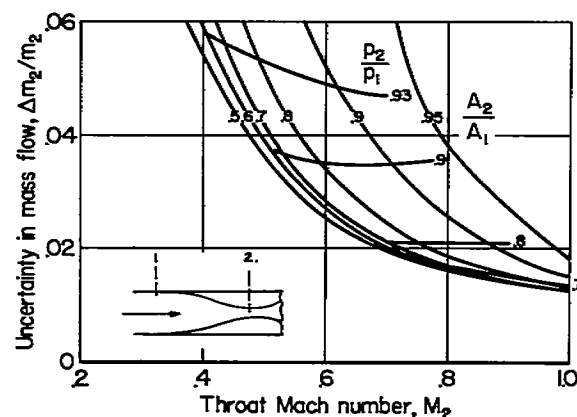
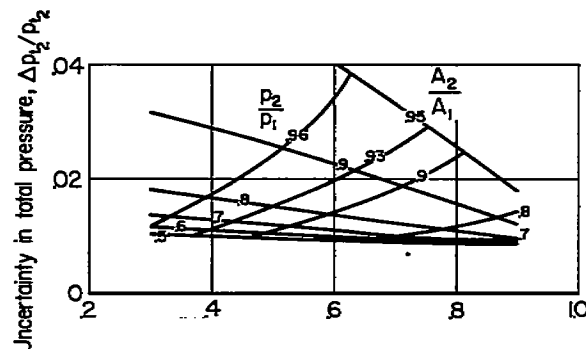
$$\left. \begin{aligned} \overline{p_t} &= p + \frac{\rho}{2} \left( \frac{1}{A} \int U dA \right)^2 \\ \text{or} \quad \overline{p_t} &= p + f(\overline{U})^2 \end{aligned} \right\} \quad (B9)$$

Area-weighting method

$$\left. \begin{aligned} \overline{p_t} &= p + \frac{\rho}{2A} \int U^2 dA \\ \text{or} \quad \overline{p_t} &= p + f(\overline{U^2}) \end{aligned} \right\} \quad (B10)$$

Mass-flow weighting method

$$\left. \begin{aligned} \overline{p_t} &= p + \frac{\rho}{2AU} \int U^3 dA \\ \text{or} \quad \overline{p_t} &= p + f(\overline{U^3}) \end{aligned} \right\} \quad (B11)$$



Sketch (39)

Security Classification of This Report Has Been Cancelled

Since none of these can be substantiated by rigorous proofs as giving the true effective total pressure, the question of accuracy must be settled by comparison with a more exact estimate. Such a comparison is presented by Wyatt in reference 295 where the more exact estimate is made by determining an effective total pressure which satisfies the momentum and continuity relationships which are involved in calculating engine thrust. For uniform flow, all methods agree, but for nonuniform flow, such as those which occur because of separation, the methods do not agree. The method of equation (B2) is, in general, the least accurate; but it requires the simplest instrumentation, for the other methods require a pitot-tube survey. Data reduction by the mass-flow weighting method requires the most effort. The area-weighting method is usually as accurate as the mass-flow method, and it produces a conservative value of total-pressure ratio which the mass-flow weighting method does not. However, in the calculation of the internal thrust of a wind-tunnel model, a conservative value of total pressure produces too low an indication of net drag. Under conditions which are normally encountered in well-designed air-induction systems, that is, relatively uniform steady flow, one method is as accurate as another, and selection can be made on the basis of convenience. However, for nonuniform flow such as exists in ducts with bends, care must be exercised in evaluating data.

## REFERENCES

1. Sulkin, M. A.: Aerodynamic Considerations for the Design of Submerged Turbojet Power Plant Installations. IAS Symposium on Flight Propulsion, Cleveland, Ohio, Mar. 16, 1951. Pub. by Central Air Documents Office, Wright-Patterson Air Force Base, Dayton, Ohio, May 1951.
2. Kuechemann, D., and Weber, J.: Aerodynamics of Propulsion. McGraw-Hill Book Co., 1953.
3. Anon.: Bibliography of NACA and Other Reports on Air Inlets and Internal Flows. NACA RM 8J05, 1948.
4. Cushing, W. R.: An Analysis of Thrust Estimation. Aircraft Eng., vol. XXVII, no. 311, Jan. 1955, pp. 9-13.
- ✓ 5. Quick, A. W.: Turbojet Intake Configurations. Interavia, Nov. 1949, pp. 679-684.
- ✓ 6. Jacobsson, Bengt: Definition and Measurement of Jet Engine Thrust. Jour. Roy. Aero. Soc., Apr. 1951, pp. 226-243.
7. Klein, Harold: The Calculation of the Scoop Drag for a General Configuration in a Supersonic Stream. Rep. No. SM-13744, Douglas Aircraft Co., Santa Monica, Apr. 1950.
8. Brajnikoff, George B.: Method and Graphs for the Evaluation of Air-Induction Systems. NACA TN 2697, 1952. (NACA Rep. 1141, 1953)
9. Sanders, Newell D., and Palasics, John: Analysis of Effects of Inlet Pressure Losses on Performance of Axial-Flow Type Turbojet Engine. NACA RM E8J25b, 1948.
10. Hansen, Frederick H., Jr., and Mossman, Emmet A.: Effect of Pressure Recovery on the Performance of a Jet-Propelled Airplane. NACA TN 1695, 1948.
- ✓ 11. Palme, H. O.: Approximate Methods to Transform Air Inlet Losses Measured in Low-Speed Wind Tunnel to Varying Flight Conditions. SAAB TN 2, SAAB Aircraft Company, 1951.
- ✓ 12. Wyatt, DeMarquis D.: Aerodynamic Forces Associated With Inlets of Turbojet Installations. Aero. Eng. Rev., Oct. 1951, pp. 20-23, 31.
13. Ferri, Antonio, and Nucci, Louis M.: Preliminary Investigation of a New Type of Supersonic Inlet. NACA TN 2286, 1951. (Formerly NACA RM L6J31)



14. Fradenburgh, Evan A., and Wyatt, DeMarquis D.: Theoretical Performance Characteristics of Sharp-Lip Inlets at Subsonic Speeds. NACA TN 3004, 1953.
15. Optimization of Power Plant and Airplane Performance. A Symposium. Aero. Eng. Rev., June 1954, pp. 42-61.
16. Klein, Harold: Small-Scale Tests on Jet Engine Pebble Aspiration. Rep. No. SM-14885, Douglas Aircraft Co., Santa Monica, 1953.
17. Rodert, Lewis A., and Garrett, Floyd B.: Ingestion of Foreign Objects into Turbine Engines by Vortices. NACA TN 3330, 1955.
18. Lindell, Keith: Foreign Object Damage Tests - J35 Turbo Jet Engines. AF Tech. Note WCLP-52-83, Wright Air Development Center, Ohio, 1952.
19. Fradenburgh, Evan A., and Kremzier, Emil J.: Performance Comparison of Three Canard-Type Ram-Jet Missile Configurations at Mach Numbers from 1.5 to 2.0. NACA RM E53F11, 1953.
20. Woodworth, L. R., and Kelber, C. C.: The Generalized Approach to the Selection of Propulsion Systems for Aircraft. IAS Preprint No. 345, 1951.
21. Meyer, C. A., and Faught, H. F.: A Method of Presenting the Performance of Turbojet Engines. IAS Preprint No. 293, 1950.
22. Wyatt, DeMarquis D.: An Analysis of Turbojet-Engine-Inlet Matching. NACA TN 3012, 1953.
23. Mossman, Emmet A., and Anderson, Warren E.: The Effect of Lip Shape on a Nose-Inlet Installation at Mach Numbers from 0 to 1.5 and a Method for Optimizing Engine-Inlet Combinations. NACA RM A54B08, 1954.
24. Kremzier, Emil J.: A Method for Evaluating the Effects of Drag and Inlet Pressure Recovery on Propulsion-System Performance. NACA TN 3261. 1954.
25. Schueller, Carl F., and Esenwein, Fred T.: Analytical and Experimental Investigation of Inlet-Engine Matching for Turbojet-Powered Aircraft at Mach Numbers up to 2.0. NACA RM E51K20, 1952.
26. Anderson, Warren E., and Scherrer, Richard: Investigation of a Flow Deflector and an Auxiliary Scoop for Improving Off-Design Performance of Nose Inlets. NACA RM A54E06, 1954.
27. Greatrex, F. B.: Air Intake Efficiency. Jour. Roy. Aero. Soc., vol. 58, no. 525, Sept. 1954, pp. 639-648.

28. Seddon, J.: Air Intakes for Aircraft Gas Turbines. Jour. Roy. Aero. Soc., Oct. 1952, pp. 747-781.
29. Conrad, E. William, and Sobolewski, Adam E.: Investigation of Effects of Inlet-Air Velocity Distortion on Performance of Turbojet Engine. NACA RM E50G11, 1950.
30. Walker, Lewis E., Conrad, E. William, and Prince, William R.: Effect of Uneven Air-Flow Distribution to the Twin Inlets of an Axial-Flow Turbojet Engine. NACA RM E52K06, 1953.
31. Nettles, J. C., and Leissler, L. A.: Investigation of Adjustable Supersonic Inlet in Combination With J-34 Engine Up to Mach Number 2.0. NACA RM E54H11, 1954.
32. Huppert, Merle C.: Preliminary Investigation of Flow Fluctuations During Surge and Blade Row Stall in Axial-Flow Compressors. NACA RM E52E28, 1952.
33. Graham, Robert W., and Prian, Vasily D.: Experimental and Theoretical Investigation of Rotating-Stall Characteristics of Single-Stage Axial-Flow Compressor With Hub-Tip Ratio of 0.76. NACA RM E53I09, 1953.
34. Huppert, Merle C., Johnson, Donald F., and Castilow, Eleanor C.: Preliminary Investigation of Compressor Blade Vibration Excited by Rotating Stall. NACA RM E52J15, 1952.
35. Walker, Curtis L., Silvo, Joseph N., and Jansen, Emmert T.: Effect of Unequal Air-Flow Distribution from Twin Inlet Ducts on Performance of an Axial-Flow Turbojet Engine. NACA RM E54E13, 1954.
36. Conrad, E. William, Schulze, Frederick W., and Usow, Karl H.: Effect of Diffuser Design, Diffuser-Exit Velocity Profile and Fuel Distribution on Altitude Performance of Several Afterburner Configurations. NACA RM E53A30, 1953.
37. Connors, James F.: Effect of Ram-Jet Pressure Pulsations on Supersonic Diffuser Performance. NACA RM E50H22, 1950.
38. Sterbenz, William H., and Evvard, John C.: Criteria for Prediction and Control of Ram-Jet Flow Pulsations. NACA RM E51C27, 1951.
39. Shapiro, Ascher H., and Smith, R. Douglas.: Friction Coefficients in the Inlet Length of Smooth Round Tubes. NACA TN 1785, 1948.
40. Dodge, Russell A., and Thompson, Milton J.: Fluid Mechanics. McGraw-Hill Book Co., Inc., 1937.

41. Monaghan, R. J.: Some Remarks on the Choice and Presentation of Formulae for Turbulent Skin Friction in Compressible Flow. R.A.E. TN No. Aero. 2246, British A.R.C., May 1953.
42. Chapman, Dean R., and Kester, Robert H.: Turbulent Boundary-Layer and Skin-Friction Measurements in Axial Flow Along Cylinders at Mach Numbers Between 0.5 and 3.6. NACA TN 3097, 1954.
43. Clauser, Francis H.: Turbulent Boundary Layers in Adverse Pressure Gradients. Jour. Aero. Sci., Feb. 1954, pp. 91-108.
44. Beeton, A. B. P.: Curves for the Theoretical Skin Friction Loss in Air Intake Ducts. R.A.E. TN No. Aero. 2035, British A.R.C., Feb. 1950.
45. Shapiro, A. H., Hawthorne, W. R., and Edelman, G. M.: The Mechanics and Thermodynamics of Steady One-Dimensional Gas Flow With Tables for Numerical Solutions. M.I.T. Meteor Rep. 14, Dec. 1, 1947.
46. Luskin, H., and Klein, H.: High Speed Aerodynamic Problems of Turbo-jet Installations. (Contributed by the Aviation and Gas Turbine Power Divisions for presentation at the Annual Meeting of the A.S.M.E., New York, N. Y., Nov. 26-Dec. 1, 1950, A.S.M.E. Paper 50-A-102, 1950. (Also available as Rep. No. SM-13830, Douglas Aircraft Co., Santa Monica, Sept. 1, 1950)
47. Von Doenhoff, Albert E., and Tetervin, Neal: Determination of General Relations for the Behavior of Turbulent Boundary Layers. NACA Rep. 772, 1943. (Formerly NACA ACR 3G13 and WR L-382)
48. Little, B. H., Jr., and Wilbur, Stafford W.: High-Subsonic Performance Characteristics and Boundary-Layer Investigations of a  $12^\circ$  10-Inch-Inlet-Diameter Conical Diffuser. NACA RM L50C02a, 1950.
49. Fage, A., and Raymer, W. G.: Note on Empirical Relations for a Turbulent Boundary Layer. R. & M. No. 2255, British A.R.C., 1948.
50. Ferri, Antonio, and Nucci, Louis M.: The Origin of Aerodynamic Instability of Supersonic Inlets at Subcritical Conditions. NACA RM L50K30, 1951.
51. Nettles, J. C.: The Effect of Initial Rate of Subsonic Diffusion on the Stable Subcritical Mass-Flow Range of a Conical-Shock Diffuser. NACA RM E53E26, 1953.
52. Kantrowitz, Arthur: The Formation and Stability of Normal Shock Waves in Channel Flow. NACA TN 1225, 1947.

53. Lukasiewicz, J.: Diffusers for Small Supersonic Mach Numbers; Design Data. R.A.E. TN No. Aero. 1973, (SD 84), British A.R.C., 1948.
54. Wyatt, DeMarquis D., and Hunczak, Henry R.: An Investigation of Convergent-Divergent Diffusers at Mach Number 1.85. NACA RM E50K07, 1951. (Formerly NACA RM E6K21)
55. Copp, Martin R., and Klevatt, Paul L.: Investigation of High-Subsonic Performance Characteristics of a  $12^\circ$  21-Inch Conical Diffuser, Including the Effects of Change in Inlet-Boundary-Layer Thickness. NACA RM L9H10, 1950.
56. Naumann: Wirkungsgrad von Diffusoren bei hohen Unterschallgeschwindigkeiten. FB Nr 1705, Luftfahrtforschung (Berlin-Adlershof), 1942.
57. Copp, Martin R.: Effects of Inlet Wall Contour on the Pressure Recovery of a  $10^\circ$  10-Inch-Inlet-Diameter Conical Diffuser. NACA RM L51E11a, 1951.
58. Manoni, L. R.: Wide Angle Diffusers Employing Boundary Layer Control. Rep. R-94560-12, Contract AF-33(038)-21506, Res. Dept., United Aircraft Corp., Mar. 19, 1952.
59. Taylor, H. D.: Summary Report on Vortex Generators. Rep. 05280-9, United Aircraft Corp., 1950.
60. Patterson, G. N.: Modern Diffuser Design. Aircraft Eng., vol X, no. 115, Sept. 1938, pp. 267-273.
61. Henry, John R.: Design of Power-Plant Installations. Pressure-Loss Characteristics of Duct Components. NACA WR L-208, June 1944. (Formerly NACA ARR L4F26)
62. Squire, H. B.: Experiments on Conical Diffusers. R & M No. 2751, British A.R.C., Nov. 1950. (Formerly RAE TN No. Aero. 2216)
63. Garner, H. C.: Development of Turbulent Boundary Layers. R. & M. No. 2133, British A.R.C., June 1944.
64. Scherrer, Richard, and Anderson, Warren E.: Preliminary Investigation of a Family of Diffusers Designed for Near-Sonic Inlet Velocities. NACA TN 3668, 1956.
65. Nelson, William J., and Popp, Eileen G.: Performance Characteristics of Two  $6^\circ$  and  $12^\circ$  Diffusers at High Flow Rates. NACA RM L9H09, 1949.
66. Johnston, I. H.: The Effect of Inlet Conditions on the Flow in Annular Diffusers. Memo No. M.167, Nat. Gas Turbine Estab., Jan. 1953. (Also available as MOS C.P. No. 178, British A.R.C.)

67. Valerino, Alfred S.: Effects of Internal Corner Fillets on Pressure Recovery - Mass Flow Characteristics of Scoop-Type Conical Supersonic Inlets. NACA RM E52J10, 1952.
68. Scherrer, Richard, and Gowen, Forrest E.: Preliminary Experimental Investigation of a Variable-Area, Variable Internal-Contraction Inlet at Mach Numbers Between 1.42 and 2.44. NACA RM A55F23, 1955.
69. Weske, John R.: Experimental Investigation of Velocity Distributions Downstream of a Single Duct Bend. NACA TN 1471, 1948.
70. Rogallo, F. M.: Internal-Flow Systems for Aircraft. NACA Rep. 713, 1941. (Formerly NACA TN 777.)
71. Piercy, Thomas G., and Weinstein, Maynard I.: Preliminary Investigation at Mach Number 1.9 of Simulated Wing Root Inlets. NACA RM E54I24, 1955.
72. Blackaby, James R., and Watson, Earl C.: An Experimental Investigation at Low Speeds of the Effects of Lip Shape on the Drag and Pressure Recovery of a Nose Inlet in a Body of Revolution. NACA TN 3170, 1954.
73. Milillo, Joseph R.: Some Internal Flow Characteristics of Supersonic Inlets at Zero Flight Speed. NACA RM L54E19, 1954.
74. Scherrer, Richard, Stroud, John F., and Swift, John T.: Preliminary Investigation of a Variable-Area Auxiliary Air-Intake System at Mach Numbers From 0 to 1.3. NACA RM A53A13, 1953.
75. Bryan, Carroll R., and Fleming, Frank F.: Some Internal-Flow Characteristics of Several Axisymmetrical NACA 1-Series Nose Air Inlets At Zero Flight Speed. NACA RM L54E19a, 1954.
76. Pendley, Robert E., Milillo, Joseph R., and Fleming, Frank F.: An Investigation of Three NACA 1-Series Nose Inlets at Subsonic and Transonic Speeds. NACA RM L52J23, 1953.
77. Brajnikoff, George B., and Stroud, John F.: Experimental Investigation of the Effect of Entrance Width-to-Height Ratio on the Performance of an Auxiliary Scoop-Type Inlet at Mach Numbers From 0 to 1.3. NACA RM A53E28, 1953.
78. Cortright, Edgar M., Jr.: Preliminary Investigation of a Translating Cowl Technique for Improving Take-Off Performance of a Sharp-Lip Supersonic Diffuser. NACA RM E51I24, 1951.

3F

NACA RM A55F16

119

79. Blackaby, James R.: Low-Speed Investigation of the Effects of Angle of Attack on the Pressure Recovery of a Circular Nose Inlet With Several Lip Shapes. NACA TN 3394, 1955.
80. Baals, Donald D., Smith, Norman F., and Wright, John B.: The Development and Application of High-Critical-Speed Nose Inlets. NACA Rep. 920, 1948. (Formerly NACA ACR L5F30a)
81. Dannenberg, Robert E.: The Development of Jet-Engine Nacelles for a High-Speed Bomber Design. NACA RM A7D10, 1947.
82. Seddon, J., and Trebble, W. J. G.: Experiments on the Flow Into a Swept Leading-Edge Intake at Zero Forward Speed With Notes on the Wider Uses of a Slotted Intake. R. & M. No. 2909, British A.R.C., 1954.
83. Trescot, Charles D., Jr., and Keith, Arvid L., Jr.: Investigation at Transonic Speeds of the Aerodynamic Characteristics of a Semi-Circular Air Inlet in the Root of a  $45^\circ$  Sweptback Wing. NACA RM L55A05a, 1955.
84. Howell, Robert R., and Keith, Arvid L. Jr.: An Investigation at Transonic Speeds of the Aerodynamic Characteristics of an Air Inlet Installed in the Root of a  $45^\circ$  Sweptback Wing. NACA RM L52H08a, 1952.
85. Howell, Robert R., and Trescot, Charles D., Jr.: Investigation at Transonic Speeds of Aerodynamic Characteristics of a Semielliptical Air Inlet in the Root of a  $45^\circ$  Sweptback Wing. NACA RM L53J22a, 1953.
86. Ferri, Antonio: Elements of Aerodynamics in Supersonic Flows. The MacMillan Co., New York, 1949.
87. Lukasiewicz, J.: Supersonic Diffusers. R. & M. No. 2501, British A.R.C., 1946. (Originally R.A.E. GAS 8, June 1946)
88. Kantrowitz, A., and Donaldson, C. du P.: Preliminary Investigation of Supersonic Diffusers. NACA WR L-713, 1945. (Formerly NACA ACR L5D20)
89. Clauser, F. H.: Ramjet Diffusers at Supersonic Speeds, Jour. Amer. Rocket Soc., vol. 24, no. 2, Mar.-Apr., 1954, pp. 79-84, 94, and 112.
90. Oswatitsch, K.: Pressure Recovery for Missiles with Reaction Propulsion at High Supersonic Speeds (The Efficiency of Shock Diffusers). NACA TM 1140, 1947.

120.

NACA RM A55F16

91. Moeckel, W. E., and Connors, J. F.: Charts for the Determination of Supersonic Air Flow Against Inclined Planes and Axially Symmetric Cones. NACA TN 1373, 1947.
92. Staff of Ames Aeronautical Laboratory: Equations, Tables, and Charts for Compressible Flow. NACA Rep. 1135, 1953.
93. Moeckel, W. E., Connors, J. F., and Schroeder, A. H.: Investigation of Shock Diffusers at Mach Number 1.85. I. Projecting Single-Shock Cones. NACA RM E6K27, 1947.
94. Moeckel, W. E., and Connors, J. F.: Investigation of Shock Diffusers at Mach Number 1.85. III. Multiple-Shock and Curved-Contour Projecting Cones. NACA RM E7F13, 1947.
95. Evvard, John C., and Blakey, John W.: The Use of Perforated Inlets for Efficient Supersonic Diffusion. NACA RM E51B10, 1951. (Formerly NACA RM E7C26.)
96. Madden, Robert T., and Kremzier, Emil J.: Force and Pressure Characteristics for a Series of Nose Inlets at Mach Numbers from 1.59 to 1.99. IV. Conical-Spike External-Internal Compression Inlet Utilizing Perforated Cowl. NACA RM E51B05, 1951.
97. McLafferty, George: Development of the Multi-Unit Perforated Diffuser for Operation at Mach Number 2.0. Rep. R-5348430, Res. Dept., United Aircraft Corp., Sept. 1952.
98. Oblinger, Fred G.: Report of Lift, Drag, and Pitching-Moment Tests on the 8.14 Percent Scale Grumman XSSm-N-6a Rigel Tactical Missile Model TM-8 at Mach Number 2.05. Rep. 24-1-9, Eng. CTR., Univ. of Southern Calif., Sept. 8, 1953.
99. Neice, Stanford E.: A Method for Stabilizing Shock Waves in Channel Flow by Means of a Surge Chamber. NACA TN 2694, 1953.
100. Comenzo, Raymond J., and Mackley, Ernest A.: Preliminary Investigation of a Rectangular Supersonic Scoop Inlet with Swept Sides Designed for Low Drag at a Mach Number of 2.7. NACA RM L52J02, 1952.
101. Ferri, Antonio: Some Recent Advances in the Design of Supersonic Diffusers. Supersonic Inlet Symposium, Jan. 23, 1953. Rep. No. 1692, Wright Aero. Div., Wood-Ridge, N. J., pp. F-1 - F-18.
102. Connors, J. F., and Woollett, R. R.: Characteristics of Flow About Axially-Symmetric Isentropic Spikes for Nose Inlets at Mach Number 3.85. NACA RM E54F08, 1951.

103. Holder, D. W., Pearcey, H. H., and Gadd, G. E.: The Interaction Between Shock waves and Boundary Layers, With a Note on the Effects of the Interaction on the Performance of Supersonic Intakes By J. Seddon. No. 16,526 (Perf. 1199; FM 2017), Performance Sub-Committee, British A.R.C., Feb 2, 1954.
104. Nussdorfer, T. J.: Some Observations of Shock-Induced Turbulent Separation on Supersonic Diffusers. NACA RM E51L26, 1954.
105. Bogdonoff, S. M., and Kepler, C. E.: Separation of a Supersonic Turbulent Boundary Layer. Rep. 249, Dept. of Aero. Eng., Princeton Univ., Jan. 1954.
106. Gadd, G. E., Holder, D. W., and Regan, J. D.: The Experimental Investigation of the Interaction Between Shock Waves and Boundary Layers. Proc. of the Roy. Soc., Ser. A., vol. 226, Nov. 1954, pp. 227-253.
107. Gadd, G. E., and Holder, D. W.: Further Remarks on Interactions Between Wholly Laminar or Wholly Turbulent Boundary Layers and Shock Waves Strong Enough to Cause Separation. Jour. Aero. Sci., vol. 21, no. 8, Aug. 1954, pp. 571-572.
108. Dailey, C. L.: Diffuser Instability in Subcritical Operation. Univ. of Southern Calif., Sept. 26, 1950.
109. Nitzberg, Gerald E., and Crandall, Stewart: Some Fundamental Similarities Between Boundary-Layer Flow at Transonic and Low Speeds. NACA TN 1623, 1948.
110. Drougge, Georg: An Experimental Investigation of the Influence of Strong Adverse Pressure Gradients on Turbulent Boundary Layers at Supersonic Speeds. Flygtekniska Forsoksanstalten, Stockholm. Meddelande 46, 1952.
111. Obery, Leonard J., Englert, Gerald W., and Nussdorfer, Theodore J.: Pressure Recovery, Drag, and Subcritical Stability Characteristics of Conical Supersonic Diffusers With Boundary-Layer Removal. NACA RM E51H29, 1952.
112. Campbell, Robert C.: Performance of a Supersonic Ramp Inlet With Internal Boundary-Layer Scoop. NACA RM E54IO1, 1954.
113. Piercy, Thomas G.: Preliminary Investigation of Some Internal Boundary-Layer Control Systems on a Side Inlet at Mach Number 2.96. NACA RM E54K01, 1955.



114. Davis, Wallace F., and Brajnikoff, George B.: Pressure Recovery at Supersonic Speeds Through Annular Duct Inlets Situated in a Region of Appreciable Boundary Layer. I - Addition of Energy to the Boundary Layer. NACA RM A8A13, 1948.
115. Obery, L. S., and Cubbison, R. W.: Effectiveness of Boundary Layer Removal Near the Throat of Ramp-Type Side Inlets at Free-Stream Mach Number 2.0. NACA RM E54I14, 1954.
116. Davids, Joseph, and Wise, George A.: Investigation at Mach Numbers 1.5 and 1.7 of Twin-Duct Side Intake System with Two-Dimensional 60° Compression Ramps Mounted on a Supersonic Airplane. NACA RM E53H19, 1953.
117. Clark, D. B., and McCrea, J. W.: The Development of an Inlet from Drawing Board to Flight. Supersonic Inlet Symposium, Jan. 23, 1953. Rep. No. 1692, Wright Aero. Div., Wood-Ridge, N. J. pp. A-1 - A-18.
118. Clark, D. B., and Carlson, P. G.: Inlet Aerodynamics as Related to Ram Jet Control. Supersonic Inlet Symposium, Jan. 23, 1953. Rep. No. 1692, Wright Aero. Div., Wood-Ridge, N. J., pp. B-1 - B-8.
119. Allen, J. L., and Beke, Andrew: Performance Comparison at Supersonic Speeds of Inlets Spilling Excess Flow by Means of Bow Shock, Conical Shock or Bypass. NACA RM E53H11, 1953.
120. Allen J. L., and Beke, Andrew: Force and Pressure Recovery Characteristics at Supersonic Speeds of a Conical Spike Inlet with Bypasses Discharging in an Axial Direction. NACA RM E52K14, 1953.
121. Gorton, Gerald C.: Investigation of Translating-Spike Supersonic Inlet as Means of Mass-Flow Control at Mach Numbers of 1.5, 1.8, and 2.0. NACA RM E53G10, 1953.
122. Gorton, Gerald C.: Investigation at Supersonic Speeds of a Translating Spike Inlet Employing a Steep-Lip Cowl. NACA RM E54G29, 1954.
123. Gorton, Gerald C., and Dryer, Murry: Comparison at Supersonic Speeds of Translating-Spike Inlets Having Blunt- and Sharp-Lip Cows. NACA RM E54J07, 1955.
124. Leissler, L. Abbott, and Nettles, J. Cary: Investigation to Mach Number 2.0 of Shock-Positioning Controls for Variable-Geometry Inlet in Combination With a J34 Turbojet Engine. NACA RM E54I27, 1954.
125. Stitt, Leonard E., and Wise, George A.: Investigation of Several Double-Ramp Side Inlets. NACA RM E54D20, 1954.

126. Pennington, Donald, Rabb, Leonard, and Simpkinson, Scott H.: Performance of a Double-Cone Inlet With and Without Shroud at Below-Design Mach Numbers. NACA RM E54L27, 1955.
127. Comenzo, Raymond J.: A Preliminary Investigation of the Pressure Recovery of Several Two-Dimensional Supersonic Inlets at a Mach Number of 2.01. NACA RM L54D14, 1954.
128. Leissler, L. Abbott, and Sterbentz, William H.: Investigation of a Translating-Cone Inlet at Mach Numbers From 1.5 to 2.0. NACA RM E54B23, 1954.
129. Beheim, Milton A.: A Preliminary Investigation at Mach Number 1.91 of a Diffuser Employing a Pivoted Cone to Improve Operation at Angle of Attack. NACA RM E53I30, 1953.
130. Leissler, L. Abbott, and Hearth, Donald P.: Preliminary Investigation of Effect of Angle of Attack on Pressure Recovery and Stability Characteristics for a Vertical-Wedge-Nose Inlet at Mach Number of 1.90. NACA RM E52E14, 1952.
131. Carter, Howard S., and Merlet, Charles F.: Preliminary Investigation of the Total-Pressure-Recovery Characteristics of a Symmetric and an Asymmetric Nose Inlet Over a Wide Range of Angle of Attack at Supersonic Mach Numbers. NACA RM L53J30, 1953.
132. Connors, James F., and Woollett, Richard R.: Preliminary Investigation of an Asymmetric Swept Nose Inlet of Circular Projection at a Mach Number of 3.85. NACA RM E54G26, 1954.
133. Beheim, Milton A.: A Preliminary Investigation at Mach Number 1.91 of an Inlet Configuration Designed for Insensitivity to Positive Angle-of-Attack Operation. NACA RM E53E20, 1953.
134. Young, A. B.: The Calculation of the Profile Drag of Aerofoils and Bodies of Revolution at Supersonic Speeds. Rep. No. 73, College of Aeronautics, Cranfield, England, Apr. 1953.
135. Czarnecki, K. R., and Sinclair, A. R.: Factors Affecting Transition at Supersonic Speeds. NACA RM L53I18a, 1953.
136. Hilton, John H., Jr., and Czarnecki, K. R.: An Exploratory Investigation of Skin Friction and Transition on Three Bodies of Revolution at a Mach Number of 1.61. NACA TN 3193, 1954.
137. Purser, Paul E.: Comparison of Wind-Tunnel Rocket, and Flight Drag Measurements of Eight Airplane Configurations at Mach Numbers Between 0.7 and 1.6. NACA RM L54F18, 1954.

138. Owens, Billy F., and Curtis, Thomas H.: Phase II Flight Tests of the Lockheed F-94C Airplane, USAF No. 50-596. Tech. Rep. 52-14, Edwards Air Force Base, Aug., 1952.
139. Redd, Joseph W., Jr., and Stephens, Robert L.: Phase IV Performance Flight Tests of the F-86D Aircraft USAF S/N 50-459. Tech Rep. 53-26, Edwards Air Force Base, (1953)
140. Phillips, Alfred D., and Stephens, R. L.: Phase II Performance and Stability Tests of YRF-84F Airplane USAF No. 51-1828. Tech. Rep. 52-32, Edwards Air Force Base, Jan. 16, 1953.
141. Redd, Joseph W., Yeager, Charles E., and Everest, Frank K.: Performance Flight Tests of the XF-92A Airplane, USAF S/N 46-682 with a J33-A-29 Power Plant. Tech. Rep. 53-11, Edwards Air Force Base, Mar. 1953.
142. Yancey, Marion H., Jr., and Carson, James S.: Phase IV Performance Flight Tests of the F-86F Airplane USAF No. 52-4349. Tech. Rep. 54-10, Edwards Air Force Base, May 1954.
143. Wesesky, John L., and Stephens, Robert L.: Phase II Flight Tests of the YF-102 Airplane S/N USAF No. 52-7995. Tech. Rep. 54-14, Edwards Air Force Base, July 1954.
144. Fertel, P. F-105: Areas, Dimensions, and Data on 1/22 Scale Model. Rep. EAR-311, Republic Aviation Corp., Farmingdale, N. Y., Feb. 3, 1954.
145. Green, M., and Carter, Wayne: Model XF7U-1, F7U-1 Airplanes, Summary of High Mach Number Characteristics. Rep. 8198 Engr. Dept., Chance Vought Aircraft, Dallas, Aug. 24, 1950.
146. Griggs, C. F., and Goldsmith, E. L.: Measurements of Spillage Drag on a Pitot Type Intake at Supersonic Speeds. R.A.E. TN No. Aero. 2256, (British), 1953.
147. von Karman, Th., and Millikan, C. B.: On the Theory of Laminar Boundary Layers Involving Separation. NACA Rep. 504, 1934.
148. Sears, R. I., Merlet, C. F., and Putland, L. W.: Flight Determination of Drag of Normal-Shock Nose Inlets With Various Cowling Profiles at Mach Numbers from 0.9 to 1.5. NACA RM L53I25a, 1953.
149. Nitzberg, Gerald E., and Crandall, Stewart: A Study of Flow Changes Associated With Airfoil Section Drag Rise at Supercritical Speeds. NACA TN 1813, 1949.

150. Walters, Richard E.: Application of Transonic Area Rule to a Sharp-Lipped Ducted Nacelle. NACA RM L53J09b, 1954.
151. Hall, James R.: Comparison of Free-Flight Measurements of the Zero-Lift Drag Rise of Six Airplane Configurations and Their Equivalent Bodies of Revolution at Transonic Speeds. NACA RM L53J21a, 1954.
152. Brown, Clinton E., and Parker, Herman H.: A Method for the Calculation of External Lift, Moment, and Pressure Drag of Slender Open-Nose Bodies on Revolution at Supersonic Speeds. NACA Rep. 808, 1945. (Formerly NACA ACR L5L29)
153. Lighthill, M. J.: Supersonic Flow Past Bodies of Revolution. R. & M. No. 2003, British A.R.C., 1945.
154. Lighthill, M. J.: Supersonic Flow Past Slender Bodies of Revolution the Slope of Whose Meridian Section is Discontinuous. Quart. Jour. Mech. and Appl. Math., vol. I, pt. 1, Mar. 1948, pp. 90-102.
155. Ward, G. N.: The Approximate Exterior and Interior Flow Past a Quasi-Cylindrical Tube Moving at Supersonic Speeds. Quart. Jour. Mech. and Appl. Math., vol. I, pt 2, June 1948, pp. 225-245.
156. Ward, G. N.: Supersonic Flow Past Slender Pointed Bodies. Quart. Jour. Mech. and Appl. Math., vol. II, pt. 1, Mar. 1949, pp. 75-97.
157. Jack, John R.: Theoretical Wave Drags and Pressure Distributions for Axially Symmetric Open-Nose Bodies. NACA TN 2115, 1950.
158. Moore, Franklin: Linearized Supersonic Axially Symmetric Flow About Open-Nosed Bodies Obtained by Use of Stream Function. NACA TN 2116, 1950.
159. Ferrari, Carlo: Determination of the Exterior Contour of a Body of Revolution With a Central Duct so as to Give Minimum Drag in Supersonic Flow, With Various Perimetral Conditions Imposed Upon the Missile Geometry. Rep. No. AF-814-A1 (Contract No. N6 ori-119) Cornell Aero, Lab., Inc., Buffalo, Mar. 1953.
160. Ferrari, Carlo: Determination of the External Contour of a Body of Revolution with a Central Duct So As to Give Minimum Drag in Supersonic Flow, with Various Perimetral Conditions Imposed Upon the Missile Geometry. Part III - Numerical Applications. Rep. AF-814-A-2, Cornell Aeronautical Lab., Inc., Buffalo, Nov. 1953.
161. Bolton-Shaw, B. W., and Zienkiewicz, H. K.: The Rapid, Accurate Prediction of Pressure on Non-Lifting Ogival Heads of Arbitrary Shape at Supersonic Speeds. British ARC CP 154, 1954.

162. Parker, Hermon H.: Minimum-Drag Ducted and Pointed Bodies of Revolution Based on Linearized Supersonic Theory. NACA TN 3189, 1954.
163. Van Dyke, Milton D.: First- and Second-Order Theory of Supersonic Flow Past Bodies of Revolution. Jour. Aero. Sci., vol. 18, no. 3, Mar. 1951, pp. 161-179.
164. Van Dyke, Milton D.: Practical Calculation of Second-Order Supersonic Flow Past Nonlifting Bodies of Revolution. NACA TN 2744, 1952.
165. Van Dyke, Milton D.: A Study of Second-Order Supersonic-Flow Theory. NACA Rep. 1081, 1952. (Formerly NACA TN 2200)
166. Ferri, Antonio: Application of the Method of Characteristics to Supersonic Rotational Flow. NACA Rep. 841, 1946.
167. Fraenkel, L. E.: The Exterior Drag of Some Pitot-Type Intakes at Supersonic Speeds, Part II. British R.A.E. Rep. No. Aero. 2422, 1951.
168. Warren, C. H. E., and Gunn, R. E. W.: Estimation of Exterior Drag of an Axially Symmetric Conical Nose Entry for Jet Engines at Supersonic Speeds. R.A.E. TN No. Aero. 1934, S. D. 66, Jan. 1948.
169. Ward, G. N.: The Wave Lift and Drag Forces on a Propulsive Duct (Athodyd) Moving at Supersonic Speeds. Quart. Jour. Mech. and Appl. Math., vol. 1, no. 2, 1948.
170. Howell, Robert R.: A Method for Designing Low Drag Nose Inlet Bodies for Operation at Moderate Supersonic Speeds. NACA RM L54I01a, 1954.
171. Jorgensen, Leland H.: Nose Shapes for Minimum Pressure Drag at Supersonic Mach Numbers. Jour. Aero. Sci., Apr. 1954, pp. 276-279.
172. Perkins, Edward W., and Jorgensen, Leland H.: Investigation of the Drag of Various Axially Symmetric Nose Shapes of Fineness Ratio 3 for Mach Numbers From 1.24 to 3.67. NACA RM A52H28, 1952.
173. Sibulkin, Merwin: Theoretical and Experimental Investigation of Additive Drag. NACA RM E51B13, 1951.
174. Fraenkel, L. E.: The Exterior Drag of Some Pitot-Type Intakes at Supersonic Speeds, Part I. R.A.E. Rep. No. Aero. 2380, June 1950.
175. Graham, E. W.: Notes on the Drag of Scoops and Blunt Bodies. Rep. SM-13747, Douglas Aircraft Co., Inc., Santa Monica, 1950.

176. Moeckel, W. E.: Approximate Method for Predicting Form and Location of Detached Shock Waves Ahead of Plane or Axially Symmetric Bodies. NACA TN 1921, 1949.
177. Sears, Richard I., and Merlet, C. F.: Flight Determination of Drag and Pressure Recovery of a Nose Inlet of Parabolic Profile at Mach Numbers From 0.8 to 1.7. NACA RM L51E02, 1951.
178. Ferri, Antonio: Method for Evaluating from Shadow or Schlieren Photographs the Pressure Drag in Two-Dimensional or Axially-Symmetrical Flow Phenomena With Detached Shock. NACA TN 1808, 1949.
179. Nucci, Louis M.: The External-Shock Drag of Supersonic Inlets Having Subsonic Entrance Flow. NACA RM L50G14a, 1950.
180. Öhman, Lars: An Experimental Method of Determining the Drag of a Shock Wave with Application to a Ducted Body. The Flygtekniska Försöksanstalten, Stockholm Meddelande 51, Jan. 1954.
181. Brajnikoff, George B., and Rogers, Arthur W.: Characteristics of Four Nose Inlets as Measured at Mach Numbers Between 1.4 and 2.0. NACA RM A51C12, 1951.
182. Esenwein, Fred T.: Performance Characteristics at Mach Numbers to 2.00 of Various Types of Side Inlets Mounted on Fuselage of Proposed Supersonic Airplane. III - Normal-Wedge Inlet with Semicircular Cowling. NACA RM E52H20, 1952.
183. Matthews, Howard F.: Elimination of Rumble from the Cooling Ducts of a Single-Engine Pursuit Airplane. NACA WR A-70, 1943.
184. Richter, A.: Flight Test Investigation of Engine Inlet Duct Rumble on the Model XF4D-1 for a Mach Number Range of 0.7 to 0.92. Rep. No. DEV-1338, Douglas Aircraft Co., Inc., Santa Monica, June 29, 1953.
185. Smith, Norman F., and Beals, Donald B.: Wind-Tunnel Investigation of a High-Critical-Speed Fuselage Scoop Including the Effects of Boundary Layer. NACA WR L-733, 1945; (Formerly NACA ACR L5B01a)
186. Keith, Arvid L., Jr., and Schiff, Jack: Low-Speed Wind Tunnel Investigation of a Triangular Swept Back Air Inlet in the Root of a 45° Sweptback Wing. NACA RM L50I01, 1950.
187. Martin, Norman J., and Holzhauser, Curt A.: Analysis of Factors Influencing the Stability Characteristics of Symmetrical Twin-Intake-Air-Induction Systems. NACA TN 2049, 1950.

188. Mossman, Emmet A., Pfyl, Frank A., and Lazzeroni, Frank A.:  
Experimental Investigation at Mach Numbers From 0 to 1.9 of  
Trapezoidal and Circular Side-Inlets for a Fighter-Type Airplane.  
NACA RM A55D27, 1955.
189. Nussdorfer, Theodore J., Obery, Leonard J., and Englert, Gerald W.:  
Pressure Recovery, Drag, and Subcritical Stability Characteristics  
of Three Conical Supersonic Diffusers at Stream Mach Numbers from  
1.7 to 2.0. NACA RM E51H27, 1952.
190. Frazer, Alson C., and Anderson, Warren E.: Performance of a Normal-  
Shock Scoop Inlet With Boundary-Layer Control. NACA RM A53D29,  
1953.
191. Obery, Leonard J., Cubbison, Robert W., and Mercer, T. G.: Stabiliza-  
tion Techniques for Ramp Type Side Inlets at Supersonic Speeds.  
NACA RM E55A26, 1955.
192. Perchonok, E., Wilcox, Fred, and Pennington, Donald: Effect of Angle  
of Attack and Exit Nozzle Design on the Performance of a 16-Inch  
Ram Jet at Mach Numbers from 1.5 to 2.0. NACA RM E51G26, 1951.
193. Dangle, E. E., Cervenka, A. J., and Perchonok, Eugene: Effect of  
Mechanically Induced Sinusoidal Air-Flow Oscillations on Operation  
of a Ram-Jet Engine. NACA RM E54D01, 1954.
194. Trimpi, Robert L.: A Theory for Stability and Buzz Pulsation Ampli-  
tude in Ram Jets and an Experimental Investigation Including Scale  
Effects. NACA RM L53G28, 1953.
195. Griggs, C. F., and Goldsmith, E. L.: Shock Oscillations Ahead of  
Centre-Body Intakes at Supersonic Speeds. R.A.E. Rep. No. Aero.  
2477, Sept. 1952.
196. Dailey, C. L.: Development of Supersonic Ramjet Diffusers, Summary  
Report. Rep. 8-1, Univ. of Southern Calif., Jan. 10, 1951.
197. Trimpi, Robert L., and Cohen, Nathaniel B.: Effect of Several  
Modifications to Center Body and Cowling on Subcritical Performance  
of a Supersonic Inlet at Mach Number of 2.02. NACA RM L55C16, 1955.
198. Englert, Gerald W., and Obery, Leonard J.: Evaluation of Five Conical  
Center-Body Supersonic Diffusers at Several Angles of Attack.  
NACA RM E51L04, 1952.
199. Hasel, Lowell E., Lankford, John L., and Robins, A. W.: Investigation  
of a Half-Conical Scoop Inlet Mounted at Five Alternate Circumferen-  
tial Locations Around a Circular Fuselage. Pressure-Recovery  
Results at a Mach Number of 2.01. NACA RM L53D30b, 1953.

200. Piercy, Thomas G.: Preliminary Investigation of Some Internal Boundary-Layer-Control Systems on a Side Inlet at Mach Number 2.96. NACA RM E54K01, 1955.
201. Mossman, Emmet A., Lazzeroni, Frank A., and Pfyl, Frank A.: An Experimental Investigation of the Air-Flow Stability of a Scoop-Type Normal-Shock Inlet. NACA RM A55A13, 1955.
202. Goelzer, H. Fred, and Cortright, Edgar M., Jr.: Investigation at Mach Number 1.88 of a Conical Spike Diffuser Mounted as a Side Inlet With Boundary Layer Control. NACA RM E51G06, 1951.
203. Ferri, Antonio, and Clarke, Joseph H.: On the Use of Interference Effects for Shock Drag Reduction at Supersonic Speeds. PIBAL Rep. 258, Polytechnic Inst. of Brooklyn, Dept. of Aero. Eng. and Appl. Mech., July 1954.
204. Hall, Charles F., and Frank, Joseph L.: Ram-Recovery Characteristics of NACA Submerged Inlets at High Subsonic Speeds. NACA RM A8I29, 1948.
205. Hall, Charles F., and Barclay, F. Dorn: An Experimental Investigation of NACA Submerged Inlets at High Subsonic Speeds. I - Inlets Forward of the Wing Leading Edge. NACA RM A8B16, 1948.
206. Robinson, Russell G., and Wright Ray H.: Estimation of Critical Speeds of Airfoils and Streamlined Bodies. NACA WR L-781, 1940. (Formerly NACA ACR L781)
207. Allen, H. Julian, Frick, Charles W., and Erickson, Myles D.: An Experimental Investigation of Several Low-Drag Wing-Nacelle Combinations With Internal Flow. NACA ACR 5A15, 1945.
208. Herriot, John G.: The Linear Perturbation Theory of Axially Symmetric Compressible Flow With Application to the Effect of Compressibility on the Pressure Coefficient at the Surface of a Body of Revolution. NACA RM A6H19, 1947.
209. Hasel, Lowell E.: The Performance of Conical Supersonic Scoop Inlets on Circular Fuselages. NACA RM L53I14a, 1953.
210. Jorgensen, Leland H.: Correlation by the Hypersonic Similarity Rule of Pressure Distributions and Wave Drags for Minimum-Drag Nose Shapes at Zero Angle of Attack. NACA RM A53F12, 1953.
211. Stroud, John F.: Experimental Investigation of the Effect of Forebody Bluntness on the Pressure Recovery and Drag of a Twin-Scoop Inlet-Body Combination at Mach Numbers of 1.4 and 1.7. NACA RM A51K14, 1952.



212. Merlet, Charles F., and Carter, Howard S.: Total-Pressure Recovery of a Circular Underslung Inlet With Three Different Nose Shapes at a Mach Number of 1.42. NACA RM L51K05, 1952.
213. Ferri, Antonio, Ness, N., and Kaplita, T.: Supersonic Flow Over Conical Bodies Without Axial Symmetry. Jour. Aero. Sci., Aug. 1953, pp. 563-571.
214. Stoney, William E., Jr., and Putland, Leonard W.: Some Effects of Body Cross-Sectional Shape, Including a Sunken-Canopy Design, on Drag as Shown by Rocket-Powered-Model Tests at Mach Numbers from 0.8 to 1.5. NACA RM L52D07, 1952.
215. Beskin, L.: Determination of Upwash Around a Body of Revolution at Supersonic Velocities. Rep. CM-251, Applied Physics Lab., Johns Hopkins Univ., May 27, 1946.
216. Allen, H. Julian, and Perkins, Edward W.: Characteristics of Flow Over Inclined Bodies of Revolution. NACA RM A50L07, 1951.
217. Luidens, Roger W., and Simon, Paul C.: Aerodynamic Characteristics of NACA RM-10 Missile in 8- by 6-Foot Supersonic Wind Tunnel at Mach Numbers of 1.49 to 1.98. I - Presentation and Analysis of Pressure Measurements (Stabilizing Fins Removed). NACA RM E50D10, 1950.
218. Valerino, Alfred S., Pennington, Donald B., and Vargo, Donald J.: Effect of Circumferential Location on Angle of Attack Performance of Twin Half-Conical Scoop-Type Inlets Mounted Symmetrically on the RM-10 Body of Revolution. NACA RM E53G09, 1953.
219. Weinstein, M. I.: Performance of Supersonic Scoop Inlets. NACA RM E52A22, 1952.
220. Kremzier, Emil J., and Campbell, Robert C.: Angle-of-Attack Supersonic Performance of a Configuration Consisting of a Ramp-Type Scoop Inlet Located Either on Top or Bottom of a Body of Revolution. NACA RM E54C09, 1954.
221. Schaefer, Raymond F.: Some Design Considerations of Half-Round Side Inlets. Supersonic Inlet Symposium Paper in Wright Aeronautical Rep. No. 1692, Wright Aero. Div., Curtiss-Wright Corp., Wood-Ridge, N. J., Sec. D, Jan. 23, 1953, pp. 29-39.
222. Kremzier, Emil J., and Campbell, Robert C.: Effect of Fuselage Fences on the Angle-of-Attack Supersonic Performance of a Top-Inlet-Fuselage Configuration. NACA RM E54J04, 1955.

223. Spahr, J. Richard, and Dickey, Robert R.: Wind-Tunnel Investigation of the Vortex Wake and Downwash Field Behind Triangular Wings and Wing-Body Combinations at Supersonic Speeds. NACA RM A53D10, 1953.
224. Obery, Leonard J., and Krasnow, H. S.: Influence of a Canard-Type Control Surface on the Internal and External Performance Characteristics of Nacelle-Mounted Supersonic Diffusers (Conical Centerbody) at a Rearward Body Station for a Mach Number of 2.0. NACA RM E52F16, 1952.
225. Dannenberg, Robert E.: A Design Study of Leading-Edge Inlets for Unswept Wings. NACA TN 3126, 1954.
226. Dannenberg, Robert E.: Low-Speed Characteristics of a  $45^\circ$  Swept Wing With Leading-Edge Inlets. NACA RM A51E29, 1951.
227. Connors, James F., and Woollett, Richard R.: Experimental Investigation of a Two-Dimensional Split-Wing Ram-Jet Inlet at Mach Number of 3.85. NACA RM E52F04, 1952.
228. Douglass, Wm. M.: Wing-Ram Jet Development USCAL Report 3-9, Univ. of So. Calif. Aero. Lab. Navy Research Project. June 15, 1948.
229. Anon.: Evaluation of Supersonic Split Wing Ram Jets. Convair Rep. No. ZM-9136-001, Consolidated Vultee Aircraft Corp., May 1949.
230. Seddon, J., and Kettle, D. J.: Low Speed Wind Tunnel Tests on the Characteristics of Leading Edge Air Intakes in Swept Wings. R.A.E. Rep. Aero. 2402, Nov. 1950.
231. Dannenberg, Robert E., and Blackaby, James R.: An Experimental Investigation of a Jet-Engine Nacelle in Several Positions on a  $37.25^\circ$  Sweptback Wing. NACA RM A50A13, 1950.
232. Davis, Wallace F., Brajnikoff, George B., Goldstein, David L., and Spiegel, Joseph M.: An Experimental Investigation at Supersonic Speeds of Annular Duct Inlets Situated in a Region of Appreciable Boundary Layer. NACA RM A7G15, 1947.
233. Carter, Howard S., and Merlet, Charles F.: Flight Determination of the Pressure Recovery and Drag Characteristics of a Twin Side-Inlet Model at Transonic Speeds. NACA RM L53E05, 1953.
234. Pierpont, P. Kenneth, and Braden, John A.: Investigation at Transonic Speeds of a Forward-Located Underslung Air Inlet on a Body of Revolution. NACA RM L52K17, 1953.

235. Boswinkle, Robert W., Jr., and Mitchell, Meade H., Jr.: Experimental Investigation of the Internal-Flow Characteristics of Forward Underslung Fuselage Scoops With Unswept and Sweptback Entrances at Mach Numbers of 1.41 to 1.96. NACA RM L52A24, 1952.
236. Merlet, Charles F.: Pressure Recovery and Drag Characteristics of a Forward Located Circular Scoop Inlet as Determined From Flight Tests for Mach Numbers From 0.8 to 1.6. NACA RM L54B23, 1954.
237. Nichols, Mark R., and Goral, Edwin B.: A Low Speed Investigation of a Fuselage-Side Air Inlet for Use at Transonic Flight Speeds. NACA TN 2684, 1952.
238. Spiegel, Joseph M., Hofstetter, Robert U., and Kuehn, Donald M.: Applications of Auxiliary Air Injectors to Supersonic Wind Tunnels. NACA RM A53I01, 1953.
239. Fradenburgh, Evan A., and Campbell, Robert C.: Characteristics of a Canard-Type Missile Configuration With an Underslung Scoop Inlet at Mach Numbers From 1.5 to 2.0. NACA RM E52J22, 1953.
240. Watson, Earl C.: Some Low-Speed Characteristics of an Air-Induction System Having Scoop-Type Inlets With Provisions for Boundary-Layer Control. NACA RM A51F15, 1951.
241. McLafferty, George: Theoretical Pressure Recovery Through a Normal Shock in a Duct With Initial Boundary Layer. Jour. Aero. Sci., vol. 20, no. 3, Mar. 1953, pp. 169-174.
242. Simon, Paul C.: Internal Performance of a Series of Circular Auxiliary-Air Inlets Immersed in a Turbulent Boundary Layer Mach Number Range: 1.5 to 2.0. NACA RM E54L03, 1955.
243. Piercy, Thomas G., and Johnson, Harry W.: A Comparison of Several Systems of Boundary-Layer Removal Ahead of a Typical Conical External-Compression Side Inlet at Mach Numbers of 1.88 and 2.93. NACA RM E53F16, 1953.
244. Valerino, Alfred S.: Performance Characteristics at Mach Numbers to 2.0 of Various Types of Side Inlets Mounted on Fuselage of Proposed Supersonic Airplane. I - Two-Dimensional Compression-Ramp Inlets With Semicircular Cowls. NACA RM E52E02, 1952.
245. Allen, J. L., and Simon, P. C.: Performance Characteristics at Mach Numbers to 2.0 of Various Types of Side Inlets Mounted on Fuselage of Proposed Supersonic Airplane. II - Inlets Utilizing Half of a Conical Spike. NACA RM E52G08, 1952.

246. Simon, Paul C.: Performance Characteristics at Mach Numbers to 2.0 of Various Types of Side Inlets Mounted on Fuselage of Proposed Supersonic Airplane. IV - Rectangular-Cowl Inlets With Two-Dimensional Compression Ramps. NACA RM E52H29, 1952.
247. Piercy, Thomas G., and Johnson, Harry W.: Experimental Investigation at Mach Numbers 1.88, 3.16, and 3.83 of Pressure Drag of Wedge Diverters Simulating Boundary-Layer-Removal Systems for Side Inlets. NACA RM E53L14b, 1954.
248. Campbell, Robert C., and Kremzier, Emil J.: Performance of Wedge-Type Boundary Layer Diverters for Side Inlets at Supersonic Speeds. NACA RM E54C23, 1954.
249. Kremzier, Emil J., and Dryer, Murray: Aerodynamic Interference Effects on Normal and Axial Force Coefficients of Several Engine-Strut-Body Configurations at Mach Numbers of 1.8 and 2.0. NACA RM E52B21, 1952.
250. Obery, Leonard J., and Stitt, Leonard E.: Investigation at Mach Numbers of 1.5 and 1.7 of Twin-Duct Side Air-Intake System with 90° Compression Ramp Including Modifications to Boundary-Layer-Removal Wedges and Effects of a Bypass System. NACA RM E53H04, 1953.
251. Roberts, Howard E., and Langtry, B. D.: The Influence of Design Parameters on the Performance of Subsonic Air Inlets. IAS Preprint No. 260, Jan. 25, 1950.
252. Nichols, Mark R., and Pierpont, P. Kenneth: Preliminary Investigation of a Submerged Air Scoop Utilizing Boundary-Layer Suction to Obtain Increased Pressure Recovery. NACA RM L50A13, 1950.
253. Pierpont, P. Kenneth, and Howell, Robert R.: Low-Speed Investigation of a Semisubmerged Air Scoop With and Without Boundary-Layer Suction. NACA RM L50H15, 1951.
254. Braden, John A., and Pierpont, P. Kenneth: Pressure and Force Characteristics at Transonic Speeds of a Submerged Divergent-Walled Air Inlet on a Body of Revolution. NACA RM L53C13, 1953.
255. Frank, Joseph L., and Taylor, Robert A.: Comparison of Drag, Pressure Recovery and Surface Pressure of a Scoop-Type Inlet and an NACA Submerged Inlet at Transonic Speeds. NACA RM A51H20a, 1951.
256. Rolls, L. Stewart: A Flight Comparison of a Submerged Inlet and a Scoop Inlet at Transonic Speeds. NACA RM A53A06, 1953.

257. Frick, Charles W., Davis, Wallace F., Randall, Lauros M., and Mossman, Emmet A.: An Experimental Investigation of NACA Submerged-Duct Entrances. NACA ACR A5I20, 1945.
258. Sacks, Alvin H., and Spreiter, John R.: Theoretical Investigation of Submerged Inlets at Low Speeds. NACA TN 2323, 1951.
259. Anderson, Warren E., and Frazer, Alson C.: Investigation of an NACA Submerged Inlet at Mach Numbers From 1.17 to 1.99. NACA RM A52F17, 1952.
260. Pennington, Donald B., and Simon, Paul C.: Internal Performance at Mach Numbers to 2.0 of Two Auxiliary Inlets Immersed in Fuselage Boundary Layer. NACA RM E53L28b, 1954.
261. Morkovin, M. V., Migotsky, E., Bailey, H. E., and Phinney, R. E.: Experiments on Interaction of Shock Waves and Cylindrical Bodies at Supersonic Speeds. Jour. Aero. Sci., vol. 19, no. 4, Apr. 1952, pp. 237-248.
262. Keith, Arvid L., Jr.: Transonic Wind-Tunnel Investigation of the Effects of Body Indentation on the Aerodynamic Characteristics of a Semielliptical Sweptback Wing-Root Inlet Configuration. NACA RM L54A29, 1954.
263. Whitcomb, Richard T.: A Study of the Zero-Lift Drag-Rise Characteristics of Wing-Body Combinations Near the Speed of Sound. NACA RM L52H08, 1952.
264. Hayes, Wallace D.: Linearized Supersonic Flow. Rep. AL-222, North American Aviation, Inc., Los Angeles, Calif., June 18, 1947.
265. Smith, Norman F., Bielat, Ralph P., and Guy, Lawrence D.: Drag of External Stores and Nacelles at Transonic and Supersonic Speeds. NACA RM L53I23b, 1953.
266. Conrad, O.: 2.4-Transitions Between Wing and Power Unit. K<sub>3</sub> - The Installation of Jet Propulsion Units, D. Kuchemann, ed., AVA Monographs, A. Betz, ed., VG 238, British Ministry of Aircraft Production, Volkenrode, Oct. 15, 1947.
267. Hoffman, Sherwood, and Wolff, Austin L.: Transonic Flight Tests to Determine Zero-Lift Drag and Pressure Recovery of Nacelles Located at the Wing Root on a 45° Sweptback Wing and Body Configuration. NACA RM L53H20, 1953.
268. Jones, Robert T.: Theory of Wing-Body Drag at Supersonic Speeds. NACA RM A53H18a, 1953.

269. Lomax, Harvard: The Wave Drag of Arbitrary Configurations in Linearized Flow as Determined by Areas and Forces in Oblique Planes. NACA RM A55A18, 1955.
270. Baldwin, Barrett S., Jr., and Dickey, Robert R.: Application of Wing-Body Theory to Drag Reduction at Low Supersonic Speeds. NACA RM A54J19, 1955.
271. Lomax, Harvard, and Heaslet, Max. A.: A Special Method for Finding Body Distortions That Reduce the Wave Drag of Wing and Body Combinations at Supersonic Speeds. NACA RM A55B16, 1955.
272. Nielsen, Jack N.: General Theory of Wave Drag Reduction for Combinations Employing Quasi-Cylindrical Bodies With an Application to Swept Wing and Body Combinations. NACA RM A55B07, 1955.
273. Friedman, Morris D., and Cohen, Doris.: Arrangement of Fusiform-Bodies to Reduce the Wave Drag at Supersonic Speeds. NACA TN 3345, 1954.
274. Spahr, J. Richard, and Robinson, Robert A.: Wind-Tunnel Investigation at Mach Numbers of 2.0 and 2.9 of Several Configurations of a Supersonic Ram-Jet Test Vehicle. NACA RM A50C20, 1950.
275. Luskin, Harold, and Klein, Harold: The Influence of Turbo-Jet Airflow on the Aerodynamic Design of Airplanes. Douglas Aircraft Co., Rep. SM-19111, June 3, 1955.
276. Bollech, Thomas V., and Kelley, H. Neale: Low-Speed Longitudinal Stability and Lateral Control Characteristics of a 0.3-Scale Model of a 40° Swept Wing Fighter Type Airplane. NACA RM L54B17, 1954.
277. Scherer, A.: 2.3-Fillet Between Fuselage and Power Unit. K<sub>3</sub> - The Installation of Jet Propulsion Units, D. Küchemann, ed., AVA Monographs, A. Betz, ed., VG 239, British Ministry of Aircraft Production, Volkenrode, Oct. 15, 1947.
278. Bielat, Ralph P., and Harrison, Daniel E.: A Transonic Wind-Tunnel Investigation of the Effects of Nacelle Shape and Position on the Aerodynamic Characteristics of Two 47° Sweptback Wing-Body Combinations. NACA RM L52G02, 1952.
279. Carmel, Melvin M., and Fischetti, Thomas L.: A Transonic Wind-Tunnel Investigation of the Effects of Nacelles on the Aerodynamic Characteristics of a Complete Model Configuration. NACA RM L53F22a, 1953.

280. Hasel, Lowell E., and Sevier, John R., Jr.: Aerodynamic Characteristics at Supersonic Speeds of a Series of Wing-Body Combinations Having Cambered Wings With an Aspect Ratio of 3.5 and a Taper Ratio of 0.2. Effect at  $M = 1.60$  of Nacelle Shape and Position on the Aerodynamic Characteristics in Pitch of Two Wing-Body Combinations with  $47^\circ$  Sweptback Wings. NACA RM L51K14a, 1952.
281. Driver, Cornelius: Aerodynamic Characteristics at Supersonic Speeds of a Series of Wing-Body Combinations Having Cambered Wings With an Aspect Ratio of 3.5 and a Taper Ratio of 0.2. Effect at  $M = 2.01$  of Nacelle Shape and Position on the Aerodynamic Characteristics in Pitch of Two Wing-Body Combinations With  $47^\circ$  Sweptback Wings. NACA RM L52F03, 1952.
282. Moskowitz, Barry: Approximate Theory for Calculation of Lift of Bodies, Afterbodies, and Combinations of Bodies. NACA TN 2669, 1952.
283. Obery, Leonard J., and Krasnow, Howard S.: Performance Characteristics of Canard-Type Missile With Vertically Mounted Nacelle Engines at Mach Numbers 1.5 to 2.0. NACA RM E52H08, 1952.
284. Kremzier, Emil J., and Davids, Joseph: Performance Characteristics of Canard-Type Missile With Wing-Mounted Nacelle Engines at Mach Numbers 1.5 to 2.0. NACA RM E52J08, 1952.
285. Pankhurst, R. C., and Holder, D. W.: Wind Tunnel Technique. Pitman Pub. Co., London, 1952.
286. Young, A. D., and Maas, J. H.: The Behavior of a Pitot Tube in a Transverse Total-Pressure Gradient. R. & M. 1770, British A.R.C., 1936.
287. Goldstein, S.: A Note on the Measurement of Total Head and Static Pressure in a Turbulent Stream. Proc. of the Roy. Soc., ser. A, vol. 155, no. A-886, 1936, pp. 570-575.
288. Fage, A.: On the Static Pressure in Fully-Developed Turbulent Flow. Proc. of the Roy. Soc., ser. A, vol. 155, July 1, 1936, pp. 576-596.
289. Persh, Jerome, and Bailey, Bruce M.: A Method for Estimating the Effect of Turbulent Velocity Fluctuations in the Boundary Layer on Diffuser Total-Pressure-Loss Measurements. NACA TN 3124, 1954.
290. Nielsen, Jack N.: Effect of Turbulence on Air-Flow Measurements Behind Orifice Plates. NACA WR L-274, 1943. (Formerly NACA ARR 3G30)

291. Kroll, A. Edgar: Gauss's Formula in Chemical Engineering Calculations. Chemical Engineering, vol 53, no. 9, Sept. 1946, pp. 102-105.
292. Scarbrough, James B.: Numerical Mathematical Analysis. The Johns Hopkins Press, 1930.
293. Dean, Robert. Jr., ed.: Aerodynamic Measurements. Gas Turbine Laboratory, M.I.T., 1953.
294. Wyatt, DeMarquis D.: Analysis of Errors Introduced by Several Methods of Weighing Nonuniform Duct Flows. NACA TN 3400, 1955.



## BIBLIOGRAPHY

The following bibliography has been arranged chronologically under the headings of the table of contents. The numbers of the references that are pertinent to each subject are also listed. The majority of the reports included in this bibliography were published after June 1947, because the NACA Bibliography of reference 3 lists previous reports.

## II. DEFINITIONS

See references 2 and 5 through 13.

Rudnick, Philip: Momentum Relations in Propulsive Ducts. Jour. Aero. Sci., vol. 14, no. 9, Sept. 1947, pp. 540-544.

## III. PRELIMINARY CONSIDERATIONS

AIRCRAFT REQUIREMENTS

See references 15, 16, 20, and 25.

Cleveland Laboratory Staff: Performance and Ranges of Application of Various Types of Aircraft-Propulsion System. NACA TN 1349, 1947.

Brewster, J. H.: The Determination of the Optimum Airplane-Powerplant Combination. SAE Preprint No. 89, Dec. 1947.

Lubarsky, Bernard: Performance and Load-Range Characteristics of Turbojet Engine in Transonic Speed Range. NACA TN 2088, 1950.

Sturdevant, C. R., and Woodworth, L. R.: A Generalized Turbojet Weight, Size, and Performance Study. Rep. R-166, Rand Corp., Santa Monica, Dec. 15, 1949.

Krebs, Richard P., and Wilcox, E. Clinton: Analysis of the Turbojet Engine for Propulsion of Supersonic Bombers. NACA RM E54A21, 1954.

Koutz, Stanley L., and Hensley, Reece V.: Loitering and Range Performance of Turbojet-Powered Aircraft Determined by Off-Design Engine Cycle Analysis. NACA RM E51K29, 1952.

Gabriel, David S., Krebs, Richard P., Wilcox, E. Clinton, and Koutz, Stanley L.: Analysis of the Turbojet Engine for Propulsion of Supersonic Fighter Airplanes. NACA RM E52F17, 1953.

AIRFRAME-INDUCTION-SYSTEM COMBINATION

See references 1, 2, 5, 10, and 15 to 18.

Blatz, William J.: Air Inlets and Nacelles. IAS Preprint 142, Mar. 19, 1948.

ENGINE-INDUCTION-SYSTEM COMBINATIONS

## MATCHING

See references 6, 8 to 10, 12, and 21 to 24.

Sanders, Newell D., and Behun, Michael: Generalization of Turbojet-Engine Performance in Terms of Pumping Characteristics. NACA TN 1927, 1949.

## OPTIMIZATION

See references 8, 19, and 24.

Blackaby, James R.: An Analytical Study of the Comparative Performance of Four Air-Induction Systems for Turbojet-Powered Airplanes Designed to Operate at Mach Numbers up to 1.5. NACA RM A52C14, 1952.

Watson, Earl C.: An Analytical Study of the Comparative Performance of Six Air-Induction Systems for Turbojet-Powered Airplanes Designed to Operate at Mach Numbers up to 2.0. NACA RM A53H03, 1953.

McLafferty, George: Simplified Methods for Comparing the Performance of Supersonic Ramjet Diffusers. Rep. R-23596-1, Res. Dept., United Aircraft Corp., Mar. 25, 1953.

Allen, J. L., and Beke, Andrew: Performance Comparison at Supersonic Speeds of Inlets Spilling Excess Flow by Means of Bow Shock, Conical Shock, or Bypass. NACA RM E53H11, 1953.

## FLOW UNIFORMITY AND STEADINESS

See references 27 to 38.

Pearce, R. B.: Causes and Control of Powerplant Surge. Aviation Week, vol. 52, no. 3, Jan. 16, 1950, pp. 21-25.

Mark, Herman, and Zettle, Eugene V.: Effect of Air Distribution on Radial Temperature Distribution in One-Sixth Sector of Annular Turbo-jet Combustor. NACA RM E9I22, 1950.

#### IV. DETAIL CONSIDERATIONS

##### INDUCTION

##### PRESSURE RECOVERY AND FLOW UNIFORMITY

##### Ducts

##### Skin friction and separation

See references 39 to 44, 63, 109, 135, and 136.

Griffith, A. A.: Reducing Surface Friction Between a Solid and a Fluid. Patent 578,763 (Br.), Aug. 25, 1942, no. 11973.

Regenscheit, B.: Drag Reduction by Suction of the Boundary Layer Separated Behind Shock-Wave Formation at High Mach Numbers. NACA TM 1168, 1947.

Pierpont, P. Kenneth: Investigation of Suction-Slot Shapes for Controlling a Turbulent Boundary Layer. NACA TN 1292, 1947.

Dryden, Hugh L.: Recent Advances in the Mechanics of Boundary Layer Flow. Vol. I, Advances in Applied Mechanics, sec. 1, von Mises, Richard, and von Kármán, Theodore, eds., Academic Press, Inc., N. Y., 1948, pp. 2-40.

Oswatitsch, K., and Wieghardt, K.: Theoretical Analysis of Stationary Potential Flows and Boundary Layers at High Speed. NACA TM 1189, 1948.

Lagerstrom, Paco, Cole, Julian M., and Trilling, Leon: On Viscous Effects in Compressible Flow. Paper presented at meeting of Institute for Fluid Mechanics and Heat Transfer, Pasadena, Cal., June 23, 1948.

Kay, J. M.: Experimental Investigation of Boundary Layer Flow Along a Flat Plate with Uniform Suction. Aero. Com. no. 11,476, British A.R.C., 1948.

Dickinson, H. B.: Flight and Tunnel Test Research on Boundary-Layer Control. Jour. Aero. Sci., vol. 16, no. 4, Apr. 1949, pp. 243-251.

- Schlichting, H.: Lecture Series, "Boundary Layer Theory." Pt. I - Laminar Flows. NACA TM 1217, 1949. Pt. II - Turbulent Flows. NACA TM 1218, 1949.
- Van Driest, E. R.: Turbulent Boundary Layer for Compressible Fluids on an Insulated Flat Plate. Rep. AL-958, North American Aviation, Inc., Sept. 15, 1949.
- Kay, J. M.: Turbulent Boundary Layer Flow with Uniform Suction. Fluid Motion. Sub-Com. British A.R.C. 12,193, 1949.
- von Doenhoff, A. E., and Loftin, L. K., Jr.: Present Status of Research on Boundary-Layer Control. Jour. Aero. Sci., vol. 16, no. 12, Dec. 1949, pp. 729-740, 760.
- Van Driest, E. R.: Turbulent Boundary Layer for Compressible Fluids on a Flat Plate with Heat Transfer. Rep. AL-997, North American Aviation, Inc., Jan. 27, 1950.
- Ferrari, Carlo: Study of the Boundary Layer at Supersonic Speeds in Turbulent Flow: Case of Flow Along a Flat Plate. Quart. Appl. Math., vol. VIII, no. 1, pp. 33-57, Apr. 1950.
- Davis, Don D., Jr., and Woods, George P.: Preliminary Investigation of Reflections of Oblique Waves from a Porous Wall. NACA RM L50G19a, 1950.
- Anderson, K. G.: Preliminary Investigation of Boundary Layer Control at High Subsonic Speeds. Tech. Rep. No. 6186, U. S. Air Force, Wright-Patterson Air Force Base, 1950.
- Tucker, Maurice: Approximate Turbulent Boundary-Layer Development in Plane Compressible Flow along Thermally Insulated Surfaces with Application to Supersonic-Tunnel Contour Correction. NACA TN 2045, 1950.
- Young, A. D.: The Equations of Motion and Energy and the Velocity Profile of a Turbulent Boundary Layer in a Compressible Fluid. College of Aeronautics, Cranfield, England, Rep. 42, Jan. 1951.
- Van Driest, E. R.: Turbulent Boundary Layer in Compressible Fluids. Jour. Aero. Sci., vol. 18, no. 3, Mar. 1951, pp. 145-160, 216.
- Young, A. D.: Boundary Layers and Skin Friction in High-Speed Flow. Jour. R. Ae. Soc., May, 1951, pp. 285-302.
- Rubesin, Morris W., Maydew, Randall C., and Varga, Steven A.: An Analytical and Experimental Investigation of the Skin Friction of the Turbulent Boundary Layer on a Flat Plate at Supersonic Speeds. NACA TN 2305, 1951.

Tucker, Maurice: Approximate Calculation of Turbulent Boundary-Layer Development in Compressible Flow. NACA TN 2337, 1951.

Klebanoff, P. S., and Diehl, Z. W.: Some Features of Artificially Thickened Fully Developed Turbulent Boundary Layers With Zero Pressure Gradient. NACA TN 2475, 1951.

Rubert, Kennedy F., and Persh, Jerome: A Procedure for Calculating the Development of Turbulent Boundary Layers Under the Influence of Adverse Pressure Gradients. NACA TN 2478, 1951.

Schubauer, G. B., and Klebanoff, P. S.: Investigation of Separation of the Turbulent Boundary Layer. NACA Rep. 1030, 1951. (Supersedes NACA TN 2133)

Tetervin, Neal, and Lin, Chia Chiao: A General Integral Form of the Boundary-Layer Equation for Incompressible Flow With an Application to the Calculation of the Separation Point of Turbulent Boundary Layers. NACA Rep. 1046, 1951. (Supersedes NACA TN 2158)

McCullough, George B., and Gambucci, Bruno J.: Boundary-Layer Measurements on Several Porous Materials with Suction Applied. NACA RM A52D01b, 1952.

Anderson, Oiva R.: Investigation of Perforation Exhaust Flow and Its Effect on External Skin Friction. Rep. R-53484-31, Research Dept., United Aircraft Corp., Sept. 1952.

Lee, J. D.: The Influence of High Adverse Pressure Gradients on Boundary Layers in Supersonic Flow. Rep. 21, Institute of Aerophysics, University of Toronto, Oct. 1952.

Anderson, K. G.: Investigation of Boundary-Layer Control at High Subsonic Speeds. Tech. Rep. 6344, pt. 1, U. S. Air Force, WADC, Jan. 1951.

### Design

See references 29, 44, 45, 48, 55 to 65, 69 to 71, 92, and 118.

Gray, S.: A Survey of Existing Information on the Flow in Bent Channels and the Losses Involved. Power Jets Rep. R. 1104, Power Jets (Res. and Dev.), Ltd, June 1945.

Seddon, J., and Spence, A.: Wind Tunnel Measurements of Internal Loss on a Full-Scale Model of a Wing Root Intake Duct for a Proposed Jet Propelled Fighter. British, R.A.E. TN No. Aero. 1737, Dec. 1945.

- Cohen, Herbert N.: Investigation of Intake Ducts for a High-Speed Subsonic Jet-Propelled Airplane. NACA RM L7C24a, 1947.
- Turner, L. Richard, Addie, Albert N., and Zimmerman, Richard H.: Charts for the Analysis of One-Dimensional Steady Compressible Flow. NACA TN 1419, 1948.
- Shapiro, Ascher H., and Hawthorne, W. R.: The Mechanics and Thermodynamics of Steady One-Dimensional Gas Flow. Jour. Appl. Mech., vol. 14, no. 4, Dec. 1947, pp. A317-A336.
- Burcher, Marie A.: Compressible Flow Tables for Air. NACA TN 1592, 1948.
- Gratzer, L. B., and Smith, R. H.: Boundary Layer Control for Wide Angle Diffusers. Rep. 300 (ONR Contract N6ori-217, Task Order I, Project No. NR-061-004), Univ. Washington Aero. Lab., Nov. 22, 1948.
- Palme, Hans Olof: An Investigation of the Effect of Boundary Layer Suction on the Air Resistance in Channel Elbows. KTH-Aero TN 2, Roy. Inst. of Tech., Flygtekniska Institutionen, Stockholm, Sweden, 1948.
- Taylor, H. D.: Application of Vortex Generator Mixing Principle to Diffusers. Concluding report, Air Force contract W33-038 ac-21825. Research Dept. R-15064-5, United Aircraft Corp., East Hartford, Conn., Dec. 31, 1948.
- Schwartz, Ira R.: Investigations of an Annular Diffuser-Fan Combination Handling Rotating Flow. NACA RM L9B28, 1949.
- Nelson, William J., and Popp, Eileen G.: Performance Characteristics of Two 6° and Two 12° Diffusers at High Flow Rates. NACA RM L9H09, 1949.
- Hawthorne, William R.: Secondary Circulation in Fluid Flow. Gas Turbine Lab., M.I.T., May 1950.
- Neumann, Ernest P., and Lustwerk, F.: High-Efficiency Supersonic Diffusers. M.I.T. Meteor Rep. 56, June 1950.
- Persh, Jerome: The Effect of the Inlet Mach Number and Inlet-Boundary-Layer Thickness on the Performance of a 23° Conical-Diffuser - Tail-Pipe Combination. NACA RM L9K10, 1950.
- Squire, H. B., and Carter, P.: Further Experiments on Conical Diffusers. Rep. No. 13,499, British A.R.C., Nov. 6, 1950.
- Sibulkin, Merwin, and Koffel, William K.: Chart for Simplifying Calculations of Pressure Drop of a High-Speed Compressible Fluid under Simultaneous Action of Friction and Heat Transfer - Application to Combustion Chamber Cooling Passages. NACA TN 2067, 1950.

- Squire, H. B., and Winter, K. G.: The Secondary Flow in a Cascade of Airfoils in a Nonuniform Stream. Jour. Aero. Sci., vol. 18, no. 4, Apr. 1951, pp. 271-277.
- Kronauer, Richard E.: Secondary flow in fluid dynamics. Proc. National Congress of Appl. Mech., pp. 747-756, 1951.
- Warren, C. H. E., Dudley, R. E., and Herbert, P. J.: A Theoretical and Experimental Investigation of the Flow in a Duct of Varying Cross Section, with Particular Application to the Design of Ducts for Free-Flight Ground-Launched Model Tests. British A.R.C. Tech. Rep. 13726, C.P. No. 60, 1951.
- Wood, Charles C.: Preliminary Investigation of the Effects of Rectangular Vortex Generators on the Performance of a Short 1.9:1 Straight-Wall Annular Diffuser. NACA RM L51G09, 1951.
- Persh, Jerome: The Effect of Surface Roughness on the Performance of a 23° Conical Diffuser at Subsonic Mach Numbers. NACA RM L51K09, 1951.
- Valentine, E. Floyd, and Carroll, Raymond B.: Effects of Several Arrangements of Rectangular Vortex Generators on the Static-Pressure Rise Through a Short 2:1 Diffuser. NACA RM L50L04, 1951.
- Valentine, E. Floyd, and Carroll, Raymond B.: Effects of Some Primary Variables of Rectangular Vortex Generators on the Static-Pressure Rise Through a Short Diffuser. NACA RM L52B13, 1952.
- Stanitz, John D.: Design of Two-Dimensional Channels with Prescribed Velocity Distributions Along the Channel Walls. I - Relaxation Solutions. NACA TN 2593, 1952.
- Kramer, James J., and Stanitz, John D.: Two-Dimensional Shear Flow in a 90° Elbow. NACA TN 2736, 1952.
- Wood, Charles C., and Higginbotham, James T.: Flow Diffusion in a Constant-Diameter Duct Downstream of an Abruptly Terminated Center Body. NACA RM L53D23, 1953.
- Valentine, E. Floyd, and Copp, Martin R.: Investigation to Determine Effects of Rectangular Vortex Generators on the Static-Pressure Drop Through a 90° Circular Elbow. NACA RM L53G08, 1953.
- Wood, Charles C., and Higginbotham, James T.: Performance Characteristics of a 24° Straight-Outer-Wall Annular-Diffuser-Tailpipe Combination Utilizing Rectangular Vortex Generators for Flow Control. NACA RM L53H17a, 1953.

Wood, Charles C., and Higginbotham, James T.: The Influence of Vortex Generators on the Performance of a Short 1.9:1 Straight-Wall Annular Diffuser With a Whirling Inlet Flow. NACA RM L52L01a, 1953.

Reid, Elliott G.: Performance Characteristics of Plane-Wall Two-Dimensional Diffusers. NACA TN 2888, 1953.

Persh, Jerome, and Bailey, Bruce M.: Effect of Surface Roughness Over the Downstream Region of a  $23^\circ$  Conical Diffuser. NACA TN 3066, 1954.

Farley, John M., and Welna, Henry J.: Investigation of Conical Subsonic Diffusers for Ram-Jet Engines. NACA RM E53L15, 1954.

Mallett, William E., and Harp, James L., Jr.: Performance Characteristics of Several Short Annular Diffusers for Turbojet Engine Afterburners. NACA RM E54B09, 1954.

Henry, John R.: Aspects of Internal-Flow-System Design for Helicopter Propulsive Units. NACA RM L54F29, 1954.

Wood, Charles C., and Higginbotham, James T.: Effects of Diffuser and Center-Body Length on Performance of Annular Diffusers with Constant-Diameter Outer Walls and with Vortex-Generator Flow Controls. NACA RM L54G21, 1954.

Henry, John R., and Wilbur, Stafford W.: Preliminary Investigation of the Flow in an Annular-Diffuser-Tailpipe Combination with an Abrupt Area Expansion and Suction, Injection, and Vortex-Generator Flow Controls. NACA RM L53K30, 1954.

Persh, Jerome, and Bailey, Bruce M.: Effect of Various Arrangements of Triangular Ledges on the Performance of a  $23^\circ$  Conical Diffuser at Subsonic Mach Numbers. NACA TN 3123, 1954.

#### Subsonic Flight

See references 14, 28, 73, 78, 82, and 185.

Dennard, John S.: An Investigation of the Low-Speed Characteristics of Two Sharp-Edge Supersonic Inlets Designed for Essentially External Supersonic Compression. NACA RM L7D03, 1947.

Baals, Donald D., Smith, Norman F., and Wright, John B.: The Development and Application of High-Critical-Speed Nose Inlets. NACA Rep. 920, 1948.



- Connor, F., and Widlund, J.: Flight Tests of F84E Induction System Pressure Recovery. EFTMR No. 1193, Republic Aviation Corp., Mar. 20, 1951.
- Becker, John Vernon: Wind-Tunnel Investigation of Air Inlet and Outlet Openings on a Streamline Body. NACA Rep. 1038, 1951. (Supersedes NACA ACR, Nov. 1940)
- Brajnikoff, George B., and Stroud, John F.: Experimental Investigation of the Effect of Entrance Width-to-Height Ratio on the Performance of an Auxiliary Scoop-Type Inlet at Mach Numbers From 0 to 1.3. NACA RM A53E28, 1953.
- Bryan, Carroll R., and Fleming, Frank F.: Some Internal-Flow Characteristics of Several Axisymmetric NACA 1-Series Nose Air Inlets at Zero Flight Speed. NACA RM L54E19a, 1954.

### Supersonic Flight

#### Supersonic compression

- See references 13, 53, 54, 87 to 97, 100, 102, 111, 116, 125, 127, 177, 181, 182, 189, 190, and 219.
- Moeckel, W. E., Connors, J. F., and Schroeder, A. H.: Investigation of Shock Diffusers at Mach Number 1.85. II - Projecting Double-Shock Cones. NACA RM E6L13, 1947.
- Staff of the Computing Section, Center of Analysis, Under Direction of Zdeněk Kopal: Tables of Supersonic Flow Around Cones. Tech. Rep. 1, M.I.T., 1947.
- LaVallee, Stanley, and Billman, Louis S.: Pressure Recovery in a Ram-Jet Diffuser with a Conical Nose and an Annular Inlet. Meteor Rep. UAC-20, United Aircraft Corp., Apr. 1948.
- Schroeder, Albert H., and Connors, James F.: Preliminary Investigation of Effects of Combustion in Ram Jet on Performance of Supersonic Diffusers. II - Perforated Supersonic Inlet. NACA RM E8G16, 1948.
- Burcher, Marie A.: Compressible Flow Tables for Air. NACA TN 1592, 1948.
- Neice, Mary M.: Tables and Charts of Flow Parameters Across Oblique Shocks. NACA TN 1673, 1948.

- McLafferty, G. H.: An Estimation of the Momentum Recovery of Flow Lost in Perforated Diffusers with Shrouds. Rep. M-12133-8, Research Dept., United Aircraft Corp., East Hartford, Conn., Nov. 1949.
- McLafferty, George H.: A Stepwise Method for Designing Perforated Supersonic Diffusers. Rep. R-12133-5, Research Dept., United Aircraft Corp., East Hartford, Conn., Nov. 17, 1949.
- Fraenkel, L. E., and Goldsmith, E. L.: A Preliminary Investigation of the Performance of Conical Supersonic Diffusers. R.A.E. TN Aero. 2000, British, 1949.
- Schweiger, Marvin: Internal Flow Characteristics of the MUV-2 Diffuser at Supersonic Velocities. Meteor Rep. UAC-33, Research Dept., United Aircraft Corp., East Hartford, Conn., Apr. 1949.
- Robertson, J. M., and Ross, D.: Water Tunnel Diffuser Flow Studies; Part II - Experimental Research. Penn. State College, School of Engr., Ordnance Research Lab., 1949.
- Hunczak, Henry R., and Kremzier, Emil J.: Characteristics of Perforated Diffusers at Free-Stream Mach Number 1.90. NACA RM E50B02, 1950.
- McLafferty, George H.: Tests of Perforated Convergent-Divergent Diffusers for Multi-Unit Ramjet Application. Rep. R-53133, Research Dept., United Aircraft Corp., East Hartford, Conn., June 1950.
- Nicks, O. W., and Pearce, R. B.: Supersonic Diffuser Research. North American Aviation, Inc., Los Angeles, CM616 (AL-1057) June 21, 1950.
- Pearce, R. B.: Comparison of Supersonic-Inlet Diffuser Tests at  $M_0 = 2.8$ . (Project MX-770) North American Aviation, Inc., Los Angeles, AL-1027, July 18, 1950.
- Weinstein, Maynard I.: Investigation of Perforated Convergent-Divergent Diffusers with Initial Boundary Layer. NACA RM E50F12, 1950.
- Pearce, R. B.: Tests of Multishock Diffusers. (Project MX-770) Rep. AL-1117, North American Aviation, Inc., Sept. 21, 1950.
- McLafferty, George, and Schweiger, Marvin: Low-Loss, Perforated, Convergent-Divergent Diffusers for Multi-Unit Application. (For presentation at symposium on aerodynamics of ramjet supersonic inlets, Wright-Patterson Air Force Base, Oct. 3-4, 1950) United Aircraft Corp., East Hartford, Conn., Research Dept.
- McLafferty, George: Tests of Unit and Multi-Unit Perforated Diffusers at Mach Numbers up to 3.0. Rep. R-53372-8, Res. Dept., United Aircraft Corp., East Hartford, Conn., Dec., 1950.

McLafferty, George: A Study of Perforation Configurations for Supersonic Diffusers. Rep. R-53372-7, Research Dept., United Aircraft Corp., East Hartford, Conn., Dec. 1950.

Rae, Randolph S.: Some Recent Results Obtained with the Streamlined Cowling Diffuser. Applied Physics Lab., Johns Hopkins Univ., 1950.

Ruden, P.: Two-Dimensional Symmetrical Inlets With External Compression. NACA TM 1279, 1950.

Goldsmith, E. L., Fraenkel, L. E., and Griggs, C. F.: The Performance of Some Centre Body Diffusers at Supersonic Speeds. R.A.E. Rep. No. Aero. 2372, June 1950.

Esenwein, Fred T., and Valerino, Alfred S.: Force and Pressure Characteristics for a Series of Nose Inlets at Mach Numbers from 1.59 to 1.99. I - Conical Spike All-External Compression Inlet with Subsonic Cowl Lip. NACA RM E50J26, 1951.

Obery, L. J., and Englert, G. W.: Force and Pressure Characteristics for a Series of Nose Inlets at Mach Numbers from 1.59 to 1.99. II - Isentropic-Spike All-External Compression Inlet. NACA RM E50J26a, 1951.

Weinstein, Maynard I., and Davids, Joseph: Force and Pressure Characteristics for a Series of Nose Inlets at Mach Numbers from 1.59 to 1.99. III - Conical-Spike All-External-Compression Inlet with Supersonic Cowl Lip. NACA RM E50J30, 1951.

Baughman, L. Eugene, and Gould, Lawrence I.: Investigation of Three Types of Supersonic Diffusers Over a Range of Mach Numbers From 1.75 to 2.74. NACA RM E50L08, 1951.

Sears, Richard I., and Merlet, C. F.: Flight Determination of the Drag and Pressure Recovery of an NACA 1-40-250 Nose Inlet at Mach Numbers from 0.9 to 1.8. NACA RM L50L18, 1951.

Fox, Jerome L.: Supersonic Tunnel Investigation by Means of Inclined-Plate Technique to Determine Performance of Several Nose Inlets Over Mach Number Range of 1.72 to 2.18. NACA RM E50K14, 1951.

Perchonok, Eugene, and Farley, John M.: Internal Flow and Burning Characteristics of 16-Inch Ram Jet Operating in a Free Jet at Mach Numbers of 1.35 and 1.73. NACA RM E51C16, 1951.

Moeckel, W. E.: Flow Separation Ahead of Blunt Bodies at Supersonic Speeds. NACA TN 2418, 1951.

McLafferty, George: Tests of Perforated Diffusers for Multi-Unit Ramjet Application-Phase IV. Rep. R-53416-11, Research Dept., United Aircraft Corp., Hartford, Conn., Sept. 1951.

Moeckel, W. E., and Evans, P. J., Jr.: Preliminary Investigation of Use of Conical Flow Separation for Efficient Supersonic Diffusion. NACA RM E51J08, 1951.

Fraenkel, L. E.: Some Curves for Use in Calculations of the Performance of Conical Centrebody Intakes at Supersonic Speeds and at Full Mass Flow. R.A.E. TN No. Aero. 2135, British, Dec. 1951.

Beastall, D., and Turner, J.: The Effect of a Spike Protruding in Front of a Bluff Body at Supersonic Speeds. R.A.E. TN No. Aero. 2137, British, Jan. 1952.

Jones, Jim J.: Flow Separation from Rods Ahead of Blunt Noses at Mach Number 2.72. NACA RM L52E05a, 1952.

Cortright, Edgar M., Jr., and Connors, James F.: Survey of Some Preliminary Investigations of Supersonic Diffusers at High Mach Numbers. NACA RM E52E20, 1952.

Mair, W. A.: Experiments on Separation of Boundary Layers on Probes in Front of Blunt-Nosed Bodies in a Supersonic Air Stream. Phil. Mag., ser. 7, vol. 43, no. 342, July 1952, pp. 695-716.

Connors, James F., and Woollett, Richard R.: Performance Characteristics of Several Types of Axially Symmetric Nose Inlets at Mach Number 3.85. NACA RM E52I15, 1952.

Beke, Andrew, and Allen, J. L.: Force and Pressure-Recovery Characteristics of a Conical-Type Nose Inlet Operating at Mach Numbers of 1.6 to 2.0 and at Angles of Attack of  $9^\circ$ . NACA RM E52I30, 1952.

Selna, James, Bright, Loren G., and Schlaff, Bernard A.: Investigation of Drag and Pressure Recovery of a Scoop Inlet in the Transonic Speed Range. NACA RM A52F27, 1952.

Evvard, John C., and Maslen, Stephen H.: Three-Dimensional Supersonic Nozzles and Inlets of Arbitrary Exit Cross Section. NACA TN 2688, 1952.

Bernstein, Harry, and Haefeli, Rudolph C.: Investigation of Pressure Recovery of a Single-Conical-Shock Nose Inlet at Mach Number 5.4. NACA RM E53A12, 1953.

Haefeli, Rudolph C., and Bernstein, Harry: Performance of Separation Nose Inlets at Mach Number 5.5. NACA RM E53I23, 1953.

~~CONFIDENTIAL~~

- Sears, Richard I.: Some Considerations Concerning Inlets and Ducted Bodies at Mach Numbers from 0.8 to 2.0. NACA RM L53I25b, 1953.
- Hearth, Donald P., and Gorton, Gerald C.: Investigation at Supersonic Speeds of an Inlet Employing Conical Flow Separation from a Probe Ahead of a Blunt Body. NACA RM E52K18, 1953.
- Lukasiewicz, J.: Supersonic Ramjet Performance. Aircraft Engineering, vol. XXV, no. 296, Oct. 1953, pp. 298-306.
- Wallace, Donald A.: Report of Tests on .05 Scale Scoop Duct Model. Chance Vought Research and Development Program at Mach Numbers 1.6, 1.8, 2.0 and Transonic. Rep. USCEC 24-1-8, Engr. Center, Univ. of Southern California, Dec. 24, 1953.
- Bernstein, Harry, and Haefeli, Rudolph C.: Performance of Isentropic Nose Inlets at Mach Number of 5.6. NACA RM E54B24, 1954.
- Hunczak, Henry R.: Pressure Recovery and Mass-Flow Performance of Four Annular Nose Inlets Operating in Mach Number Region of 3.1 and Reynolds Number Range of Approximately  $0.45 \times 10^6$  to  $2.20 \times 10^6$ . NACA RM E54A07, 1954.
- Connors, James F., and Woollett, Richard R.: Force, Moment, and Pressure Characteristics of Several Annular Nose Inlets at Mach Number 3.85. NACA RM E53J09, 1954.
- Marsh, B. W., and Sears, G. A.: Introduction to the Analysis of Supersonic Ramjet Power Plants. Jet Propulsion, vol. 24, no. 3, May-June 1954, pp. 155-161.
- Offenbartz, Edward: An Experimental Investigation of Two-Dimensional, Supersonic Cascade-Type Inlets at a Mach Number of 3.11. NACA RM L54E17, 1954.
- Lean, G. H.: Report on the Flow Phenomena at Supersonic Speed in the Neighbourhood of the Entry of a Propulsive Duct. R. and M. 2827, British A.R.C., 1954. (Also issued as: A.R.C. Engine Aerodynamics and Propellers, Sub-Comm. 11,868, 1945)

Limiting internal contraction and limiting inlet Mach number

See reference 113.

JF

NACA RM A55F16

151

Connors, J. F., and Schroeder, A. H.: Preliminary Investigation of Effects of Combustion in Ram Jet on Performance of Supersonic Diffusers. I - Shock Diffuser With Triple-Shock Projecting Cone. NACA RM E8F15, 1948.

Schroeder, Albert H., and Connors, James F.: Preliminary Investigation of Effects of Combustion in Ram Jet on Performance of Supersonic Diffusers. III - Normal-Shock Diffuser. NACA RM E8J18, 1948.

Neumann, E. P., and Lustwerk, F.: Supersonic Diffusers for Wind Tunnels. Jour. Appl. Mech., vol. 16, no. 2, June 1949, pp. 195-202.

Stoolman, Leo, and Francis, Donald L.: Supersonic Diffuser Performance With and Without Combustion. JPL Preprint, Jet Prop. Lab., C.I.T., Sept. 18, 1950.

Connors, James F., and Woollett, Richard R.: Some Observations of Flow at the Throat of a Two-Dimensional Diffuser at a Mach Number of 3.85. NACA RM E52I04, 1952.

Himka, Theodore: Methods of Starting Scoop-Type Inlets. Wright Aero. Rep. No. 1692, sec. G, Supersonic Inlet Symposium, Curtiss-Wright Corp., Wright Aero. Div., Wood-Ridge, New Jersey, Jan. 23, 1953, pp. 67-80.

#### Boundary-layer shock-wave interaction

See references 103 to 107.

Fage, A., and Sargent, R. F.: Shock-Wave and Boundary-Layer Phenomena Near a Flat Surface. Proc. Roy. Soc. (London), ser. A., vol. 190, no. 1020, June 17, 1947, pp. 1-20.

Lees, L.: Remarks on the Interaction Between Shock Waves and Boundary Layer in Transonic and Supersonic Flow. Rep. 120, Aero. Engr. Dept., Princeton Univ., Nov. 1, 1947.

Pearce, R. B.: Shock Waves on Surfaces with Thick Boundary Layers. Rep. AL-399, North American Aviation, Inc., Los Angeles, Calif., Dec. 30, 1947.

Ackeret, J., Feldmann, F., Rott, N.: Investigations of Compression Shocks and Boundary Layers in Gases Moving at High Speed. NACA TM 1113, 1947.

Weise, A.: On the Separation of Flow Due to Compressibility Shock. NACA TM 1152, 1947.

Zalovcik, John A., and Luke, Ernest P.: Some Flight Measurements of Pressure-Distribution and Boundary-Layer Characteristics in the Presence of Shock. NACA RM L8C22, 1948.

Lukasiewicz, J.: Conical Flow as a Result of Shock and Boundary Layer Interaction on a Probe. R. and M. 2669, British A.R.C. 12,023, Sept. 1948.

Outman, Vernon, and Lambert, Arthur: Transonic Separation. Jour. Aero. Sci., vol. 15, 1948, pp. 671-674.

Howarth, L.: The Propagation of Steady Disturbances in a Supersonic Stream Bounded on One Side by a Parallel Subsonic Stream. Proc. Cambridge Phil. Soc., vol. 44, pt. 3, 1947, pp. 380-390.

Lees, Lester: Interaction Between the Laminar Boundary Layer Over a Plane Surface and an Incident Oblique Shock Wave. Rep. 143, Aero. Engr. Lab., Princeton Univ., Jan. 24, 1949.

Neuman, B. G.: The Re-Attachment of a Turbulent Boundary-Layer Behind a Spoiler. Rep. A 64, Dept. of Supply and Development, Aero. Research Lab., Melbourne, Australia, Oct. 1949.

Tsien, H. S., and Finston, M.: Interaction Between Parallel Streams of Subsonic and Supersonic Velocities. Jour. Aero. Sci., vol. 16, no. 9, Sept. 1949, pp. 515-528.

Barry, F. W., Shapiro, A. H., and Neumann, E. P.: The Interaction of Shock Waves with Boundary Layers on a Flat Surface. Meteor Rep. 52, M.I.T., Mar. 1950.

Robinson, A.: Wave Reflection Near a Wall. Rep. 37, College of Aeronautics, Cranfield, England, May 1950.

Bardsley, O., and Mair, W. A.: The Interaction Between an Oblique Shock Wave and a Turbulent Boundary Layer. Phil. Mag., ser. 7, vol. 42, Jan. 1951, pp. 29-36.

Barry, F. W., Shapiro, A. H., and Neumann, E. P.: The Interaction of Shock Waves With Boundary Layers on a Flat Surface. Jour. Aero. Sci., vol. 18, no. 4, Apr. 1951, pp. 229-238.

Stewartson, K.: On the Interaction Between Shock Waves and Boundary Layers. Proc. Cambridge Phil. Soc., vol. 47, pt. 3, July 1951, pp. 545-553.

Cooper, George E., and Bray, Richard S.: Schlieren Investigation of the Wing Shock-Wave Boundary-Layer Interaction in Flight. NACA RM A51G09, 1951.

Bogdonoff, S. M., and Solarski, A. H.: A Preliminary Investigation of a Shock Wave-Turbulent Boundary Layer Interaction. Rep. 184, Princeton Univ., Aero. Engr. Lab., Nov. 30, 1951.

Crocco, L., and Lees, L.: A Mixing Theory for the Interaction Between Dissipative Flows and Nearly-Isentropic Streams. Rep. 187, Princeton Univ., Aero. Engr. Dept., Jan. 15, 1952.

Johannesen, N. H.: Experiments on Two-Dimensional Supersonic Flow in Corners and Over Concave Surfaces. British A.R.C. Fluid Motion Sub-Comm., 14,607 - F.M. 1669, Jan. 29, 1952.

Gadd, G. E., and Holder, D. W.: The Interaction of an Oblique Shock Wave with the Boundary Layer on a Flat Plate. Part I - Results for  $M = 2$ . British A.R.C. Fluid Motion Sub-Comm., 14,848 - F.M. 1714, Apr. 24, 1952.

Gadd, G. E.: On the Interaction with a Completely Laminar Boundary Layer of a Shock Wave Generated in the Mainstream. British A.R.C. Fluid Motion Sub-Comm., 15,100 - F.M. 1770, Aug. 1, 1952.

Barry, F. W.: A Review of Experimental Results on Boundary Layer - Shock Wave Interaction. (Project MX 770) Rep. AL-1599, North American Aviation, Inc., Downey, Calif., Dec. 15, 1952.

Cope, W. F.: The Measurement of Skin Friction in a Turbulent Boundary Layer at a Mach Number of 2.5, Including the Effect of a Shock Wave. Proc. Roy. Soc., ser. A, vol. 215, 1952, pp. 84-99.

Liepmann, H. W., Roshko, A., and Dhawan, S.: On Reflection of Shock Waves from Boundary Layers. NACA Rep. 1100, 1952. (Supersedes NACA TN 2334)

Harrin, E. N.: A Flight Investigation on the Effect of Shape and Thickness of the Boundary Layer on the Pressure Distribution in the Presence of Shock. NACA TN 2765, 1952.

Gadd, G. E.: A Semi-Empirical Theory for Interactions Between Turbulent Boundary Layers and Shock Waves Strong Enough to Cause Separation. British A.R.C. Fluid Motion Sub-Comm., 15,543 - F.M. 1849, Jan 10, 1953.

Gadd, G. E., Holder, D. W., and Regan, J. D.: The Interaction of an Oblique Shock Wave with the Boundary Layer on a Flat Plate. Part II - Interim Note on the Results for  $M = 1.5, 2, 3$  and  $4$ . British A.R.C. Fluid Motion Sub-Comm., 15,591 - F.M. 1855, Jan. 30, 1953.

Bogdonoff, S. M., Kepler, C. E., and Sanlorenzo, E.: A Study of Shock Wave Turbulent Boundary Layer Interaction at  $M = 3$ . Rep. 222, Princeton Univ., Aero. Engr. Dept., July 1953.



Kepler, C. E., and Bogdonoff, S. M.: Interaction of a Turbulent Boundary Layer with a Step at  $M = 3$ . Rep. 238, Princeton Univ., Forrestal Research Center, Sept. 1, 1953.

Gadd, G. E.: Interactions Between Wholly Laminar or Wholly Turbulent Boundary Layers and Shock Waves Strong Enough to Cause Separation. Jour. Aero. Sci., vol. 20, no. 11, Nov. 1953, pp. 729-750.

Harrin, E. N.: A Flight Investigation of Laminar and Turbulent Boundary Layers Passing Through Shock Waves at Full-Scale Reynolds Numbers. NACA TN 3056, 1953.

Lighthill, M. J.: On Boundary Layers and Upstream Influence; Part I - A Comparison Between Subsonic and Supersonic Flows. Proc. Roy. Soc., vol. 217, 1953, pp. 344-357.

Lighthill, M. J.: On Boundary Layers and Upstream Influence, Part II, Supersonic Flows with Separation. Proc. Roy. Soc., vol. 217, 1953, pp. 478-507.

Drougge, Georg: An Experimental Investigation of the Influence of Strong Adverse Pressure Gradients on Turbulent Boundary Layers at Supersonic Speeds. Flygtekniska Forsöksanstalten, Stockholm.

Lange, Roy H.: Present Status of Information Relative to the Prediction of Shock-Induced Boundary-Layer Separation. NACA TN 3065, 1954.

#### Lip design

See references 23, 132, 197, and 209.

Nichols, Mark R., and Pendley, Robert E.: Performance of Air Inlets at Transonic and Low Supersonic Speeds. NACA RM L52A07, 1952.

Holzhauser, Curt A.: The Effect of Entrance Mach Number and Lip Shape on the Subsonic Characteristics of a Scoop-Type-Air-Induction System for a Supersonic Airplane. NACA RM A51J19a, 1952.

Dennard, John S., and Nelson, William J.: Preliminary Investigation of the Effect of Inlet Asymmetry on the Performance of Converging-Diverging Diffusers at Transonic Speeds. NACA RM L52J20, 1952.

#### Mass-flow variation

See references 74, 77, 112, 117, 119 to 124, 126, and 128.

Hayes, Clyde: Preliminary Investigation of a Variable Mass-Flow Supersonic Nose Inlet. NACA RM L9J11, 1949.

Allen, J. L., and Beke, Andrew: Force and Pressure Recovery Characteristics at Supersonic Speeds of a Conical Spike Inlet with a Bypass Discharging from the Top or Bottom of the Diffuser in an Axial Direction. NACA RM E53A29, 1953.

Hinners, Arthur H., Jr., and Lee, John B.: Preliminary Investigation of the Total-Pressure-Recovery Characteristics of a  $15^\circ$  Semiangle Movable-Cone Variable-Geometry Ram-Jet Inlet at Free-Jet Mach Numbers of 1.62, 2.00, 2.53, and 3.05. NACA RM L52K10, 1953.

Beke, Andrew, and Allen, J. L.: Force and Pressure-Recovery Characteristics at Supersonic Speeds of a Conical Nose Inlet with Bypasses Discharging Outward from the Body Axis. NACA RM E52L18a, 1953.

#### Angle of attack

See references 26, 129, 130, 131, 133, and 198.

Beke, Andrew, and Allen, J. L.: Force and Pressure-Recovery Characteristics of a Conical-Type Nose Inlet Operating at Mach Numbers of 1.6 to 2.0 and at Angles of Attack to  $9^\circ$ . NACA RM E52I30, 1952.

Comenzo, Raymond J., and Mackley, Ernest A.: Effect of Yaw and Angle of Attack on Pressure Recovery and Mass Flow Characteristics of a Rectangular Supersonic Scoop Inlet at a Mach Number of 2.71. NACA RM L54G22, 1954.

#### DRAG

#### Subsonic Flight

See references 72, 76, and 80.

Küchemann, D., and Weber, J., eds.: J<sub>2</sub> Power-Unit Ducts. Ministry of Aircraft Production, Volkenrode, VG 287 (Rep. and Trans. 987), June 1, 1948, AVA Monographs, A. Betz, gen. ed.

Nichols, Mark R., and Keith, Arvid L., Jr.: Investigation of a Systematic Group of NACA 1-Series Cowlings With and Without Spinners. NACA Rep. 950, 1949. (Supersedes NACA RM L8A15)

Pendley, Robert E., and Robinson, Harold L.: An Investigation of Several NACA 1-Series Nose Inlets With and Without Protruding Central Bodies at High-Subsonic Mach Numbers and at a Mach Number of 1.2. NACA RM L9L23a, 1950.

Becker, John Vernon: Wind-Tunnel Investigation of Air Inlet and Outlet Openings on a Streamline Body. NACA Rep. 1038, 1951.

Selna, James, Bright, Loren G., and Schlaaff, Bernard A.: Investigation of Drag and Pressure Recovery of a Scoop Inlet in the Transonic Speed Range. NACA RM A52F27, 1952.

Cole, Richard I.: Pressure Distributions on Bodies of Revolution at Subsonic and Transonic Speeds. NACA RM L52D30, 1952.

Pendley, Robert E., Milillo, Joseph R., Fleming, Frank F., and Bryan, Carroll R.: An Experimental Study of Five Annular Air Inlet Configurations at Subsonic and Transonic Speeds. NACA RM L53F18a, 1953.

### Supersonic Flight

#### External wave drag with no spillage

See references 134, 150 to 171, 179, 180, and 213.

Lighthill, M. J.: Supersonic Flow Past Slender Pointed Bodies of Revolution at Yaw. Quart. Jour. Mech. and Appl. Math., vol. I, pt. 1, Mar. 1948, pp. 76-89.

Stone, A. H.: On Supersonic Flow past a Slightly Yawing Cone. Jour. Math. and Phys., vol. XXVII, no. 1, Apr. 1948, pp. 67-81.

Lighthill, M. J.: Supersonic Flow Past Bodies of Revolution. R. and M. 2003, British A.R.C., Jan. 3, 1945.

Munk, Max M., and Crown, J. Conrad: The Head Shock Wave. Proc. 7th Int. Congr. Appl. Math., vol. 2, pt. 2, Sept. 1948, pp. 470-484.

Broderick, J. B.: Supersonic Flow Round Pointed Bodies of Revolution. Quart. Jour. Mech. and Appl. Math., vol. II, pt. 1, Mar. 1949, pp. 98-120.

Graham, Ernest W.: The Pressure on a Slender Body of Non-Uniform Cross-Sectional Shape in Axial Supersonic Flow. Rep. SM-13346A, Douglas Aircraft Co., Inc., Santa Monica, July 20, 1949.

Moeckel, W. E.: Use of Characteristic Surfaces for Unsymmetrical Supersonic Flow Problems. NACA TN 1849, 1949.

Busemann, Adolf: A Review of Analytical Methods for the Treatment of Flow with Detached Shocks. NACA TN 1858, 1949.

Nucci, Louis M.: The External-Shock Drag of Supersonic Inlets Having Subsonic Entrance Flow. NACA RM L50G14a, 1950.

Stoney, William E., Jr.: Pressure Distributions at Mach Numbers From 0.6 to 1.9 Measured in Free Flight on a Parabolic Body of Revolution With Sharply Convergent Afterbody. NACA RM L51L03, 1952.

Rossow, Vernon J.: Applicability of the Hypersonic Similarity Rule to Pressure Distributions Which Include the Effects of Rotation for Bodies of Revolution at Zero Angle of Attack. NACA TN 2399, 1951.

Fraenkel, L. E.: The Theoretical Wave Drag of Some Bodies of Revolution. R.A.E. Rep. Aero. 2420, May 1951.

Ringleb, F. O.: Theory and Application of the Flow Over a Cusp. Rep. 192, Princeton Univ., Dept. of Aero. Engr., Mar. 1952.

Ferrari, Carlo: The Determination of the Projectile of Minimum Wave-Resistance. RTP Trans. 1180, British Ministry of Aircraft Production, Sept., 1939.

Fraenkel, L. E.: Supersonic Flow Past Slender Bodies of Elliptic Cross-Section. R.A.E. Rep. Aero. 2466, British, May 1952.

#### Additive drag

See references 12, 146, 173, and 174.

#### Change in external wave drag

See references 23, 146, 153, 162, 167, 173 to 176, and 178.

Lighthill, M. J.: The Position of the Shock-Wave in Certain Aerodynamic Problems. Quart. Jour. Mech. and Appl. Math., vol. I, pt. 3, Sept. 1948, pp. 309-318.

Moeckel, W. E.: Experimental Investigation of Supersonic Flow With Detached Shock Waves for Mach Numbers Between 1.8 and 2.9. NACA RM E50D05, 1950.

Heberle, Juergen W., Wood, George P., and Gooderum, Paul B.: Data on Shape and Location of Detached Shock Waves on Cones and Spheres. NACA TN 2000, 1950.

Moeckel, W. E.: Flow Separation Ahead of a Blunt Axially Symmetric Body at Mach numbers 1.76 to 2.10. NACA RM E51I25, 1951.

#### Lip bluntness

See references 23, 167, and 175.

Net wave drag

See references 23, 98, 100, 116, 120, 148, 174, and 176 to 182.

Kinghorn, George F., and Disher, John H.: Free-Flight Investigation of 16-Inch-Diameter Supersonic Ram-Jet Unit. NACA RM E8A26, 1948.

Ferri, Antonio, and Nucci, Louis M.: Theoretical and Experimental Analysis of Low-Drag Supersonic Inlets Having a Circular Cross Section and a Central Body at Mach Numbers of 3.30, 2.75, and 2.45. NACA RM L8H13, 1948.

Pendley, Robert E., and Smith, Norman F.: An Investigation of the Characteristics of Three NACA 1-Series Nose Inlets at Subcritical and Supercritical Mach Numbers. NACA RM L8L06, 1949.

Esenwein, Fred T., and Valerino, Alfred S.: Force and Pressure Characteristics for a Series of Nose Inlets at Mach Numbers from 1.59 to 1.99. I - Conical-Spike All-External Compression Inlet with a Subsonic Cowl Lip. NACA RM E50J26, 1951.

Messing, Wesley E., and Acker, Loren W.: Transonic Free-Flight Drag Results of Full-Scale Models of 16-Inch-Diameter Ram-Jet Engines. NACA RM E52B19, 1952.

Messing, Wesley E., and Rabb, Leonard: Transonic Free-Flight Investigation of the Total Drag and of the Component Drags (Cowl Pressure, Additive, Base, Friction, and Internal) Encountered by a 16-Inch-Diameter Ram-Jet Engine for Mach Numbers from 0.80 to 1.43. NACA RM E52F02, 1952.

Allen, J. L., and Beke, Andrew: Force and Pressure-Recovery Characteristics of a Conical-Type Nose Inlet Operating at Mach Numbers of 1.6 to 2.0 and at Angles of Attack of  $9^\circ$ . NACA RM E52I30, 1952.

Allen J. L., and Beke, Andrew: Force and Pressure Recovery Characteristics at Supersonic Speeds of a Conical Spike Inlet with a Bypass Discharging from the Top or Bottom of the Diffuser in an Axial Direction. NACA RM E53A29, 1953.

Connors, James F., and Woollett, Richard R.: Force, Moment, and Pressure Characteristics of Several Annular Nose Inlets at Mach Number 3.85. NACA RM E53J09, 1954.

Obery, Leonard J., Stitt, Leonard E., and Wise, George A.: Evaluation at Supersonic Speeds of Twin-Duct Side-Intake System with Two-Dimensional Double-Shock Inlets. NACA RM E54C08, 1954.

Merchant, D. G.: A Collection of Drag Data for Wings and Bodies at Supersonic Speeds. Tech. Note HSA TN6, Aero. Res. Labs., Dept. of Supply, Australia, Aug. 1954.

Merlet, Charles F., and Putland, Leonard W.: Flight Determination of the Drag of Conical-Shock Nose Inlets with Various Cowling Shapes and Axial Positions of the Center Body at Mach Numbers from 0.8 to 2.0. NACA RM L54G21a, 1954.

#### FLOW STEADINESS

##### Subsonic Flight

###### Choked flow

See references 72 and 73.

###### Duct rumble

See references 183 to 186.

###### Twin-duct instability

See references 130 and 187.

##### Supersonic Flight

###### Causes of unsteadiness

See references 50, 51, 111, 189 to 191, and 199.

###### Character of unsteadiness

See references 37, 38, 52, 99, 108, 130, and 191 to 196.

Dailey, C. L.: Comments on the Subcritical Buzz Phenomenon Encountered with Supersonic Ram Jet Diffusers. USCAL 5-1-16, Aero. Lab., Univ. of Southern California, June 1, 1948. (Navy Contract NOa(s)9242.)

~~CONFIDENTIAL~~

Connors, James F., and Schroeder, Albert H.: Experimental Investigation of Pressure Fluctuations in 3.6-Inch Ram Jet at Mach Number 1.92. NACA RM E9H12, 1949.

Orlin, W. J., and Dunsworth, L. C.: A Criterion for Flow Instability in Supersonic Diffuser Inlets. (Model X3SM-N-6 and XR-43-MA-1) Rep. 5144 (Contracts NOa(s)9403 and AF 33(038)-11231) Marquardt Aircraft Co., Van Nuys, Calif., Apr. 2, 1951.

Orlin W. James: The Flow Instability Problem in Supersonic Ramjet Engines. Rep. 5202, Marquardt Aircraft Co., Van Nuys, Calif., Nov. 20, 1951.

Trimpi, Robert L.: An Analysis of Buzzing in Supersonic Ram Jets by a Modified One-Dimensional Nonstationary Wave Theory. NACA RM L52A18, 1952.

Sterbentz, William H., and Davids, Joseph: Amplitude of Supersonic Diffuser Flow Pulsations. NACA RM E52I24, 1952.

Dailey, C. L.: Supersonic Diffuser Instability. Ph.D. Thesis, C.I.T., 1954.

#### Prevention of unsteadiness

See references 50, 51, 111, 123, 129, 189, and 199.

Fisher, R. E.: Controlling the Subcritical Stability of Conical Shock Inlets. Marquardt Aircraft Co., Van Nuys, Calif. (Presented at the symposium on the Aerodynamics of Ramjet Supersonic Inlets, Wright-Patterson Air Force Base, Ohio), Oct. 3 and 4, 1950.

Fox, Jerome L.: Preliminary Investigation of Helmholtz Resonators for Damping Pressure Fluctuations in 3.6-Inch Ram Jet at Mach Number 1.90. NACA RM E51C05, 1951.

#### INTERFERENCE

##### AIRCRAFT-INDUCTION SYSTEM

##### Effects of Inlet Location

##### Subsonic flight

See references 204 to 208.

Pendley, Robert E., Robinson, Harold L., and Williams, Claude V.: An Investigation of Three Transonic Fuselage Air Inlets at Mach Numbers from 0.4 to 0.94 and at a Mach Number of 1.19. NACA RM L50H24, 1950.

Thompson, Jim Rogers: Measurements of the Drag and Pressure Distribution on a Body of Revolution Throughout Transition From Subsonic to Supersonic Speeds. NACA RM L9J27, 1950.

Holzhauser, Curt A.: An Experimental Investigation at Subsonic Speeds of a Scoop-Type Air-Induction System for a Supersonic Airplane. NACA RM A51E24, 1951.

Nichols, Mark R., and Rinkoski, Donald W.: A Low-Speed Investigation of an Annular Transonic Air Inlet. NACA TN 2685, 1952. (Supersedes NACA RM L6J04)

### Supersonic flight

See references 172, 209 to 214, and 259.

### Induced Effects of Angle of Attack

#### Bodies

See references 85, 199, 209, 213, 215, 216, 218 to 220, 224, 232, 233, and 237.

Allen, H. Julian: Estimation of the Forces and Moments Acting on Inclined Bodies of Revolution of High Fineness Ratio. NACA RM A9I26, 1949.

Allen, H. Julian: Pressure Distribution and Some Effects of Viscosity on Slender Inclined Bodies of Revolution. NACA TN 2044, 1950.

Anon.: Design and Analysis of Three Supersonic Side Inlet Diffuser Models. Rep. 1755, Wright Aero. Div., Wood-Ridge, N. J., Sept. 22, 1953.

#### Wings

See references 127, 186, and 225 to 231.



## Effects of Forebody Boundary Layer

See references 28, 114, and 232 to 238.

Davis, Wallace F., and Goldstein, David L.: Experimental Investigation at Supersonic Speeds of Twin-Scoop Duct Inlets of Equal Area. I - An Inlet Enclosing 61.5 Percent of the Maximum Circumference of the Forebody. NACA RM A7J27, 1948.

Davis, Wallace F., and Goldstein, David L.: Experimental Investigation at Supersonic Speeds of Twin-Scoop Duct Inlets of Equal Area. II - Effects of Slots upon an Inlet Enclosing 61.5 Percent of the Maximum Circumference of the Forebody. NACA RM A8C11, 1948.

Davis, Wallace F., and Edwards, Sherman S.: Experimental Investigation at Supersonic Speeds of Twin-Scoop Duct Inlets of Equal Area. III - Inlet Enclosing 37.2 Percent of the Maximum Circumference of the Forebody. NACA RM A8E04, 1948.

Brajnikoff, George B.: Pressure Recovery at Supersonic Speeds Through Annular Duct Inlets Situated in a Region of Appreciable Boundary Layer. II - Effect of an Oblique Shock Wave Immediately Ahead of the Inlet. NACA RM A8F08, 1948.

Davis, Wallace F., Edwards, Sherman S., and Brajnikoff, George B.: Experimental Investigation at Supersonic Speeds of Twin-Scoop Duct Inlets of Equal Area. IV - Some Effects of Internal Duct Shape Upon an Inlet Enclosing 37.2 Percent of the Forebody Circumference. NACA RM A9A31, 1949.

Wittliff, Charles E., and Byrne, Robert W.: Preliminary Investigation of a Supersonic Scoop Inlet Derived from a Conical-Spike Nose Inlet. NACA RM L51G11, 1951.

## Boundary-Layer Removal

Suction

See references 19, 123, 185, 202, and 240 to 242.

Edwards, Sherman S.: Experimental Investigation at Supersonic Speeds of Side Scoops Employing Boundary-Layer Suction. NACA RM A9I29, 1949.

Piercy, Thomas G., and Johnson, Harry W.: Investigation at Mach Number 2.93 of Half of a Conical-Spike Diffuser Mounted as a Side Inlet with Boundary-Layer Control. NACA RM E52G23, 1952.

Flax, A. H., Treanor, C. E., and Curtis, J. T.: Stability of Flow in Air-Induction Systems for Boundary-Layer Suction. Tech. Rep. 53-189, Wright Air Development Corp., May 1953.

#### Diversion

See references 116, 182, 202, 218, and 243 to 250.

Kochendorfer, Fred D.: Investigation at a Mach Number of 1.90 of a Diverter-Type Boundary-Layer Removal System for a Scoop Inlet. NACA RM E53D07, 1953.

Johnson, Harry W., and Piercy, Thomas G.: Effect of Wedge-Type Boundary-Layer Diverters on Performance of Half-Conical Side Inlets at Mach Number 2.96. NACA RM E54E20, 1954.

#### Submerged inlets

See references 204, 205, and 251 to 260.

Mossman, Emmet A., and Randall, Lauros M.: An Experimental Investigation of the Design Variables for NACA Submerged Duct Entrances. NACA RM A7I30, 1948.

Delany, Noel K.: An Investigation of Submerged Air Inlets on a 1/4-Scale Model of a Typical Fighter-Type Airplane. NACA RM A8A20, 1948.

Axelsson, John A., and Taylor, Robert A.: Preliminary Investigation of the Transonic Characteristics of an NACA Submerged Inlet. NACA RM A50C13, 1950.

Holzhauser, Curt A.: An Experimental Investigation at Large Scale of an NACA Submerged Intake and Deflector Installation on the Rearward Portion of a Fuselage. NACA RM A50F13, 1950.

Selna, James: Preliminary Investigation of a Submerged Inlet and a Nose Inlet in the Transonic Flight Range With Free-Fall Models. NACA RM A51B14, 1951.

Seddon, J., and Raney, D. J.: Low Speed Wind Tunnel Model Tests of Submerged Air Intakes on the Undersurface of a Delta Wing. R.A.E. Rep. Aero. 2428, British, July 1951.

Taylor, Robert A.: Some Effects of Side-Wall Modifications on the Drag and Pressure Recovery of an NACA Submerged Inlet at Transonic Speeds. NACA RM A51L03a, 1952.

#### Combined Effects

##### Scoop incremental drag

See reference 7.

##### Wakes

See reference 224.

Wise, George A., and Dryer, Murray: Influence of a Canard-Type Control Surface on Flow Field in Vicinity of Symmetrical Fuselage at Mach Numbers 1.8 and 2.0. NACA RM E52E13, 1952.

Dryer, Murray, and Beke, Andrew: Performance Characteristics of a Normal-Shock Side Inlet Located Downstream of a Canard Control Surface at Mach Numbers of 1.5 and 1.8. NACA RM E52F09, 1952.

Fradenburgh, Evan A., Obery, Leonard J., and Mello, John F.: Influence of Fuselage and Canard-Type Control Surface on the Flow Field Adjacent to a Rearward Fuselage Station at a Mach Number of 2.0 - Data Presentation. NACA RM E51K05, 1952.

#### INDUCTION-SYSTEM AIRCRAFT

##### Drag

##### Skin friction and separation

See references 185, 256, and 267.

Seddon, J.: Fuselage and Air Intake Drag Measurements at Low Mach Number on a Model of a Single-Engined Jet Aircraft With Exit at the Tail. R.A.E. TN Aero. 2051, British, May 1950.

Brodel, Walter: Theory of Plane, Symmetrical Intake Diffusers. NACA TM 1267, 1950.

Transonic drag rise

See references 262 to 267.

Küchemann, D., ed.: The Installation of Jet-Propulsion Units. Ministry of Aircraft Production, VG 237 (Rep. and Trans. 937), Oct. 1, 1947, and VG 240 (Rep. and Trans. 940), Oct. 15, 1947, AVA Monographs, A. Betz, gen. ed.

Pepper, William B., Jr., and Hoffman, Sherwood: Transonic Flight Tests to Compare the Zero-Lift Drag of Underslung and Symmetrical Nacelles Varied Chordwise at 40 Percent Semispan of a  $45^\circ$  Sweptback, Tapered Wing. NACA RM L50G17a, 1950.

Pepper, William B., Jr., and Hoffman, Sherwood: Comparison of Zero-Lift Drags Determined by Flight Tests at Transonic Speeds of Symmetrically Mounted Nacelles in Various Spanwise Positions on a  $45^\circ$  Sweptback Wing and Body Combination. NACA RM L51D06, 1951.

Hoffman, Sherwood: Comparison of Zero-Lift Drag Determined by Flight Tests at Transonic Speeds of Pylon, Underslung, and Symmetrically Mounted Nacelles at 40 Percent Semispan of a  $45^\circ$  Sweptback Wing and Body Combination. NACA RM L51D26, 1951.

Pepper, William B., Jr., and Hoffman, Sherwood: Comparison of Zero-Lift Drags Determined by Flight Tests at Transonic Speeds of Symmetrically Mounted Nacelles in Various Chordwise Positions at the Wing Tip of a  $45^\circ$  Sweptback Wing and Body Combination. NACA RM L51F13, 1951.

Hoffman, Sherwood: Transonic Flight Tests to Compare the Zero-Lift Drags of Underslung Nacelles Varied Spanwise on a  $45^\circ$  Sweptback Wing and Body Combination. NACA RM L52D04a, 1952.

Hoffman, Sherwood, and Pepper, William B., Jr.: Transonic Flight Tests to Determine Zero-Lift Drag and Pressure Recovery of Nacelles Located at the Wing Tips on a  $45^\circ$  Sweptback Wing and Body Combination. NACA RM L51K02, 1952.

Hoffman, Sherwood, and Mapp, Richard C., Jr.: Transonic Flight Tests to Compare the Zero-Lift Drags of  $45^\circ$  Sweptback Wings of Aspect Ratio 3.55 and 6.0 With and Without Nacelles at the Wing Tips. NACA RM L51L27, 1952.

Hoffman, Sherwood, and Pepper, William B., Jr.: The Effect of Nacelle Combinations and Size on the Zero-Lift Drag of a  $45^\circ$  Sweptback Wing and Body Configuration as Determined by Free-Flight Tests at Mach Numbers Between 0.8 and 1.3. NACA RM L53E25, 1953.

Hopko, Russell N., Piland, Robert O., and Hall, James R.: Drag Measurements at Low Lift of a Four-Nacelle Airplane Configuration Having a Longitudinal Distribution of Cross-Sectional Area Conducive to Low Transonic Drag Rise. NACA RM L53E29, 1953.

Holdaway, George H.: Comparison of Theoretical and Experimental Zero-Lift Drag-Rise Characteristics of Wing-Body-Tail Combinations Near the Speed of Sound. NACA RM A53E17, 1953.

Whitcomb, Richard T.: Recent Results Pertaining to the Application of the "Area Rule." NACA RM L53E15a, 1953.

Hall, James Rudyard: Comparison of Free-Flight Measurements of the Zero-Lift Drag Rise of Six Airplane Configurations and Their Equivalent Bodies of Revolution at Transonic Speeds. NACA RM L53J21a, 1954.

Donlan, Charles J.: An Assessment of the Airplane Drag Problem at Transonic and Supersonic Speeds. NACA RM L54F16, 1954.

#### Wave drag

See references 261 and 267 to 272.

Leiss, Abraham: Flight Measurements at Mach Numbers 1.1 to 1.9 of the Zero-Lift Drag of a Twin-Engine Supersonic Ram-Jet Configuration. NACA RM L52D24, 1952.

Whitcomb, Richard T., and Fischetti, Thomas L.: Development of a Supersonic Area Rule and an Application to the Design of a Wing-Body Combination Having High Lift-to-Drag Ratios. NACA RM L53H31a, 1953.

#### Lift and Pitching Moment

##### Wing leading-edge inlets

See references 225 to 230.

Ruden, P.: Two-Dimensional Symmetrical Inlets with External Compression. NACA TM 1279, 1950.

Brödel, Walter: Theory of Plane, Symmetrical Inlet Diffusers. NACA TM 1267, 1950.

Smith, Norman F.: High-Speed Investigation of Low-Drag Wing Inlets. NACA WR L-732, 1944. (Supersedes NACA ACR L4I18)

Von Doenhoff, Albert E., and Horton, Elmer A.: Preliminary Investigation in the NACA Low-Turbulence Tunnel of Low-Drag Airfoil Sections Suitable for Admitting Air at the Leading Edge. NACA WR L-694, 1942.

Racisz, Stanley F.: Development of Wing Inlets. NACA WR L-727, 1946.  
(Supersedes NACA ACR L6B18)

Bartlett, Walter A., Jr., and Goral, Edwin B.: Wind-Tunnel Investigation of Wing Inlets for a Four-Engine Airplane. NACA RM L6L11, 1947.

Perl, W., and Moses, H. E.: Velocity Distributions on Two-Dimensional Wing-Duct Inlets by Conformal Mapping. NACA Rep. 893, 1948.

Douglass, William M.: Wing-Ramjet Development. USCAL Rep. 3-9, Univ. of Southern California, Aero. Lab., Navy Research Proj., June 15, 1948.

#### Wing root inlets

See references 84, 85, 186, 230, 274, and 275.

#### Scoops

See references 220, 234, and 276.

#### Nacelles

See references 81, 207, 211, 249, 272, 273, and 277 to 284.

Hansen, Frederick H., Jr., and Dannenberg, Robert E.: Effect of a Nacelle on the Low-Speed Aerodynamic Characteristics of a Swept-Back Wing. NACA RM A8E12, 1948.

Welsh, Clement J., and Morrow, John D.: Effect of Wing-Tank Location on the Drag and Trim of a Swept-Wing Model As Measured in Flight at Transonic Speeds. NACA RM L50A19, 1950.

Silvers, H. Norman, King, Thomas, J., Jr., and Pasteur, Thomas B., Jr.: Investigation of the Effect of a Nacelle at Various Chordwise and Vertical Positions on the Aerodynamic Characteristics at High Subsonic Speeds of a  $45^\circ$  Wing With and Without a Fuselage. NACA RM L51H16, 1951.

~~CONFIDENTIAL~~

- Bielat, Ralph P., Harrison, Daniel E., and Coppolino, Domenic A.: An Investigation at Transonic Speeds of the Effects of Thickness Ratio and of Thickened Root Sections on the Aerodynamic Characteristics of Wings with  $47^\circ$  Sweepback, Aspect Ratio 3.5, and Taper Ratio 0.2 in the Slotted Test Section of the Langley 8-Foot High-Speed Tunnel. NACA RM L51I04a, 1951.
- Spreemann, Kenneth P., and Alford, William J., Jr.: Investigation of the Effects of Geometric Changes in an Underwing Pylon-Suspended External-Store Installation on the Aerodynamic Characteristics of a  $45^\circ$  Sweptback Wing at High Subsonic Speeds. NACA RM L50L12, 1951.
- Jacobsen, Carl R.: Effects of Systematically Varying the Spanwise and Vertical Location of an External Store on the Aerodynamic Characteristics of an Unswept Wing of Aspect Ratio 4 at Mach Numbers of 1.41, 1.62, and 1.96. NACA RM L52F13, 1952.
- Kolesar, Charles E.: Transonic and Supersonic Nacelle Investigation. Rep. D-13085, Boeing Aircraft Co., Apr. 24, 1952.
- Jacobsen, Carl R.: Effects of the Spanwise, Chordwise, and Vertical Location of an External Store on the Aerodynamic Characteristics of a  $60^\circ$  Delta Wing at Mach Numbers of 1.41, 1.62, and 1.96. NACA RM L52H29, 1952.
- Silvers, H. Norman, and King, Thomas J., Jr.: A Small-Scale Investigation of the Effect of Spanwise and Chordwise Positioning of an Ogive-Cylinder Underwing Nacelle on the High-Speed Aerodynamic Characteristics of a  $45^\circ$  Sweptback Tapered-in-Thickness Wing of Aspect Ratio 6. NACA RM L52J22, 1952.
- Jacobsen, Carl R.: Effects of the Spanwise, Chordwise, and Vertical Location of an External Store on the Aerodynamic Characteristics of a  $45^\circ$  Sweptback Tapered Wing of Aspect Ratio 4 at Mach Numbers of 1.41, 1.62, and 1.96. NACA RM L52J27, 1953.
- Carmel, Melvin M.: Transonic Wind-Tunnel Investigation of the Effects of Aspect Ratio, Spanwise Variations in Section Thickness Ratio, and a Body Indentation on the Aerodynamic Characteristics of a  $45^\circ$  Sweptback Wing-Body Combination. NACA RM L52L26b, 1953.

## APPENDIX B

## MEASUREMENTS AND INSTRUMENTATION

See references 285 to 294.

Smith, Norman F.: Numerical Evaluation of Mass-Flow Coefficient and Associated Parameters from Wake Survey Equations. NACA TN 1381, 1947.

Holder, D. W., North, R. J., and Chinneck, A.: Experiments with Static Tubes in a Supersonic Airstream. Parts I and II. R. & M. 2782, British A.R.C., 1953.

Luidens, Roger W., and Madden, Robert T.: Interpretation of Boundary-Layer Pressure-Rake Data in Flow with a Detached Shock. NACA RM E50I29a, 1950.

Kraushaar, Robert J.: Manometers in Pulsating Systems. Tech. Memo. NYU-14, New York Univ., Project SQUID, Aug. 22, 1951.



170

[REDACTED]

NACA RM A55F16

[REDACTED]

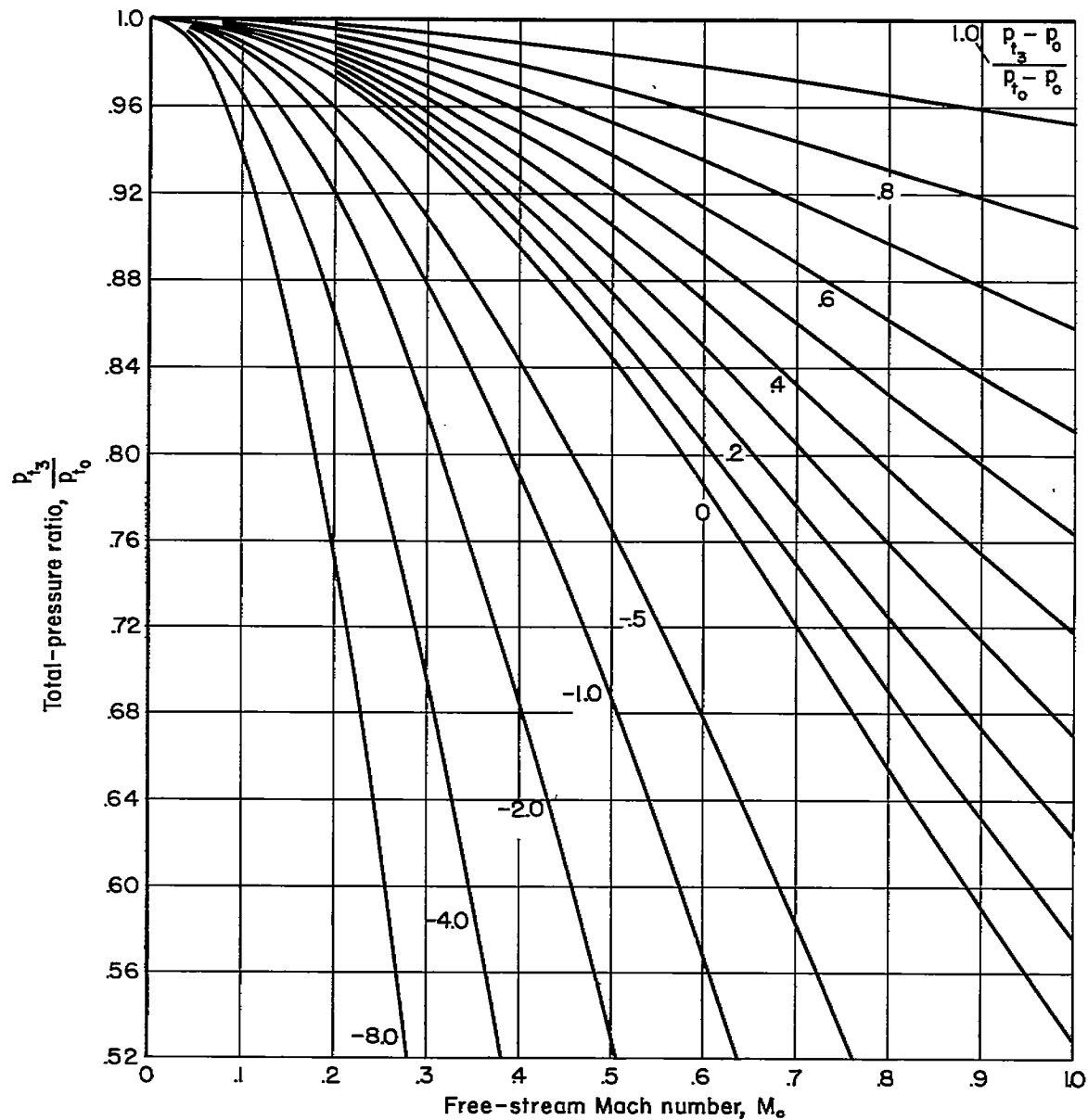


Figure 1.- Variation of total-pressure ratio with flight Mach number for various ram-recovery ratios.

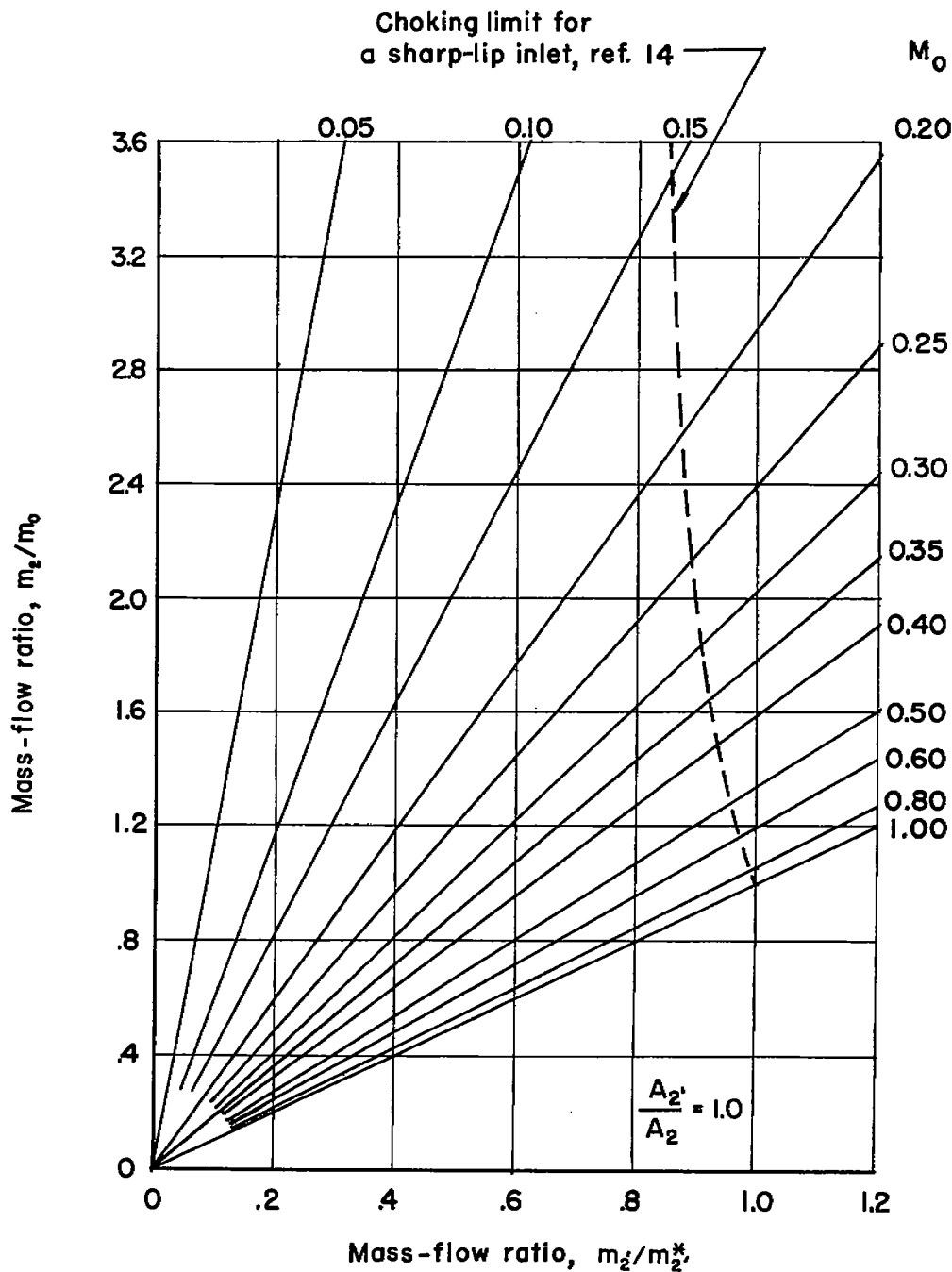


Figure 2.- Variation of mass-flow ratio based on free-stream properties with mass-flow ratio based on choked inlet properties.

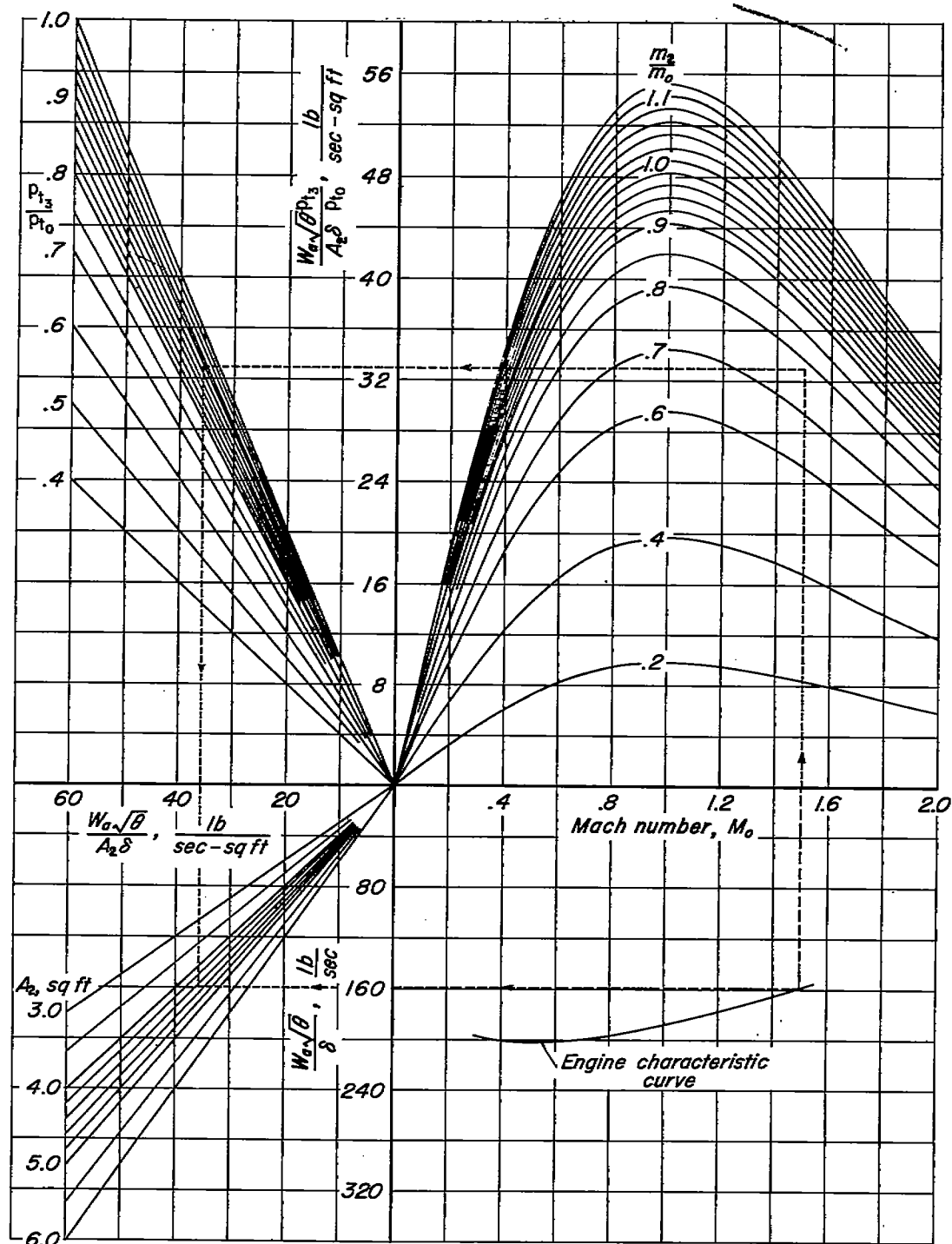
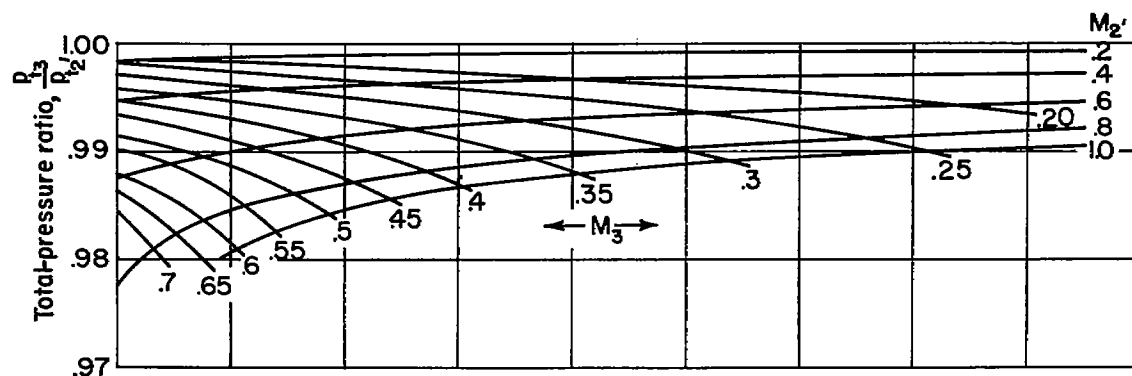
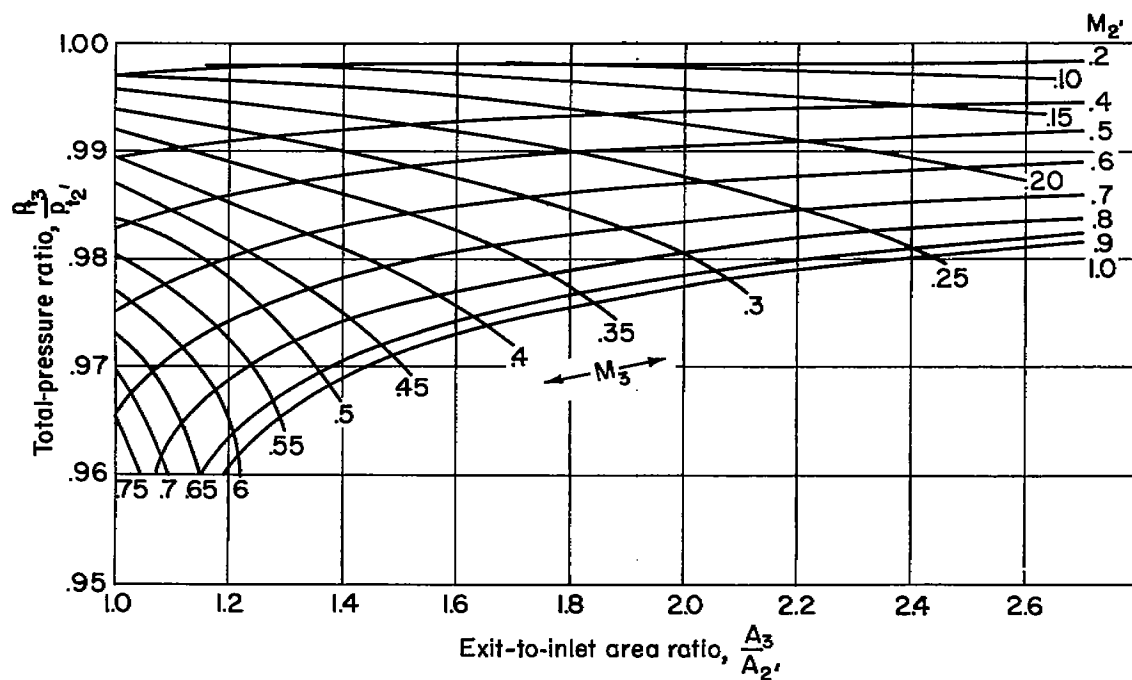


Figure 3.- Chart for matching an inlet with an engine.



$$(a) \frac{l}{d_3} \times \frac{C_f}{0.003} = 4$$



$$(b) \frac{l}{d_3} \times \frac{C_f}{0.003} = 8$$

Figure 4.- Variation of total-pressure ratio with area ratio for various flow conditions in circular conical diffusers.

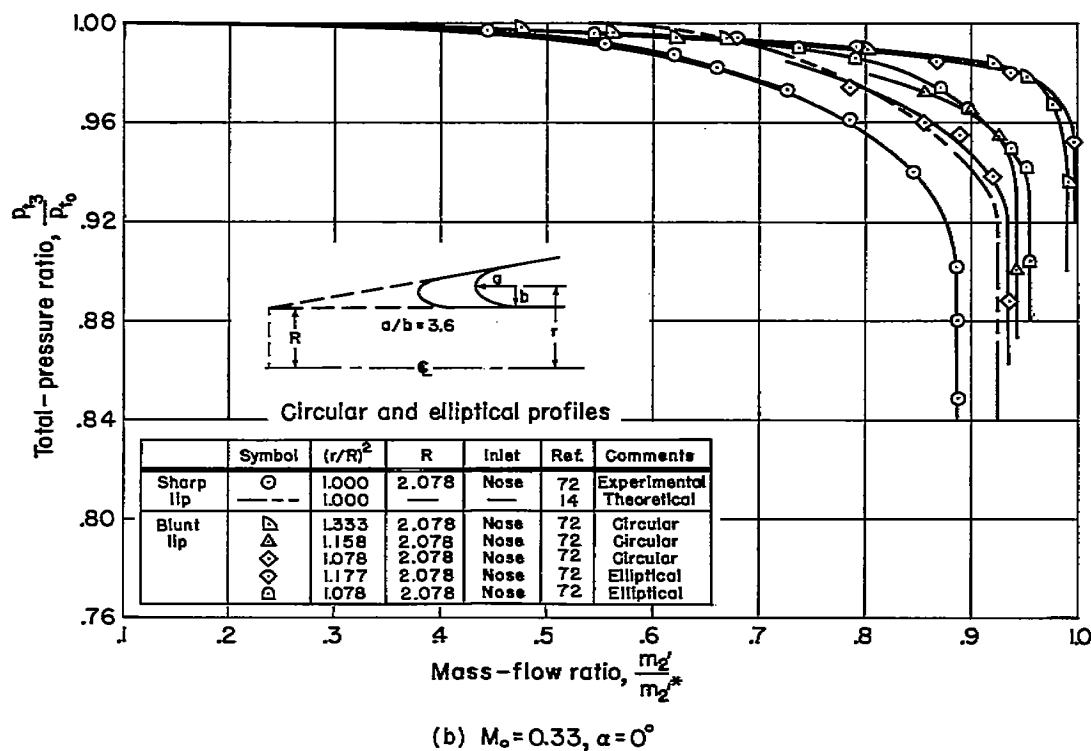
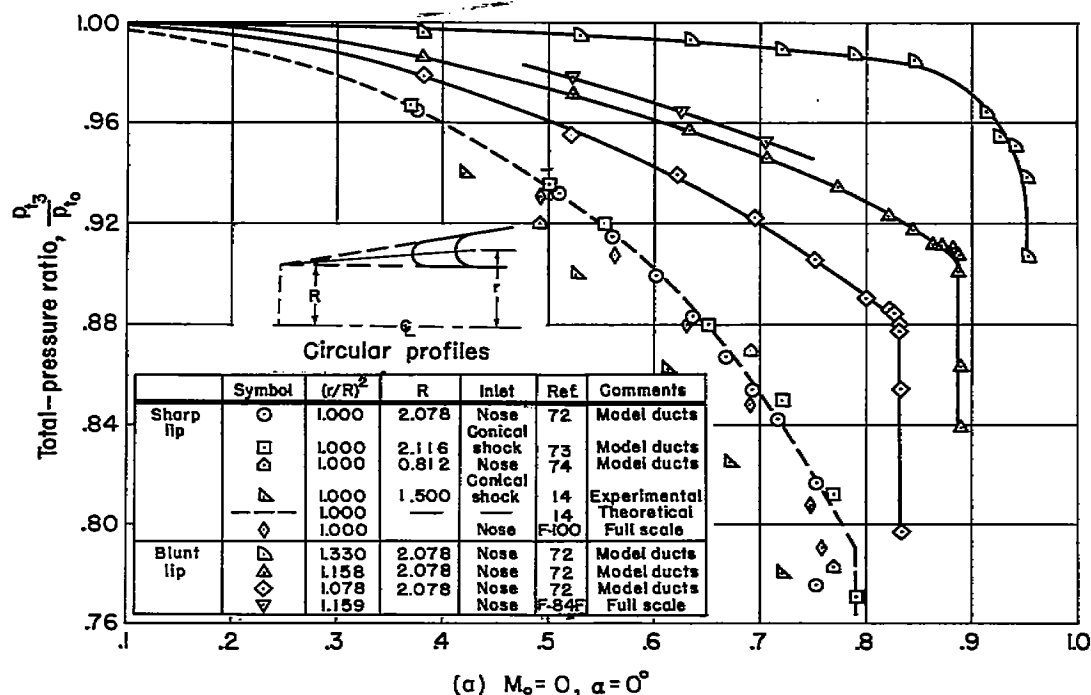


Figure 5.- Total-pressure-ratio variation of inlets differing in lip shape.

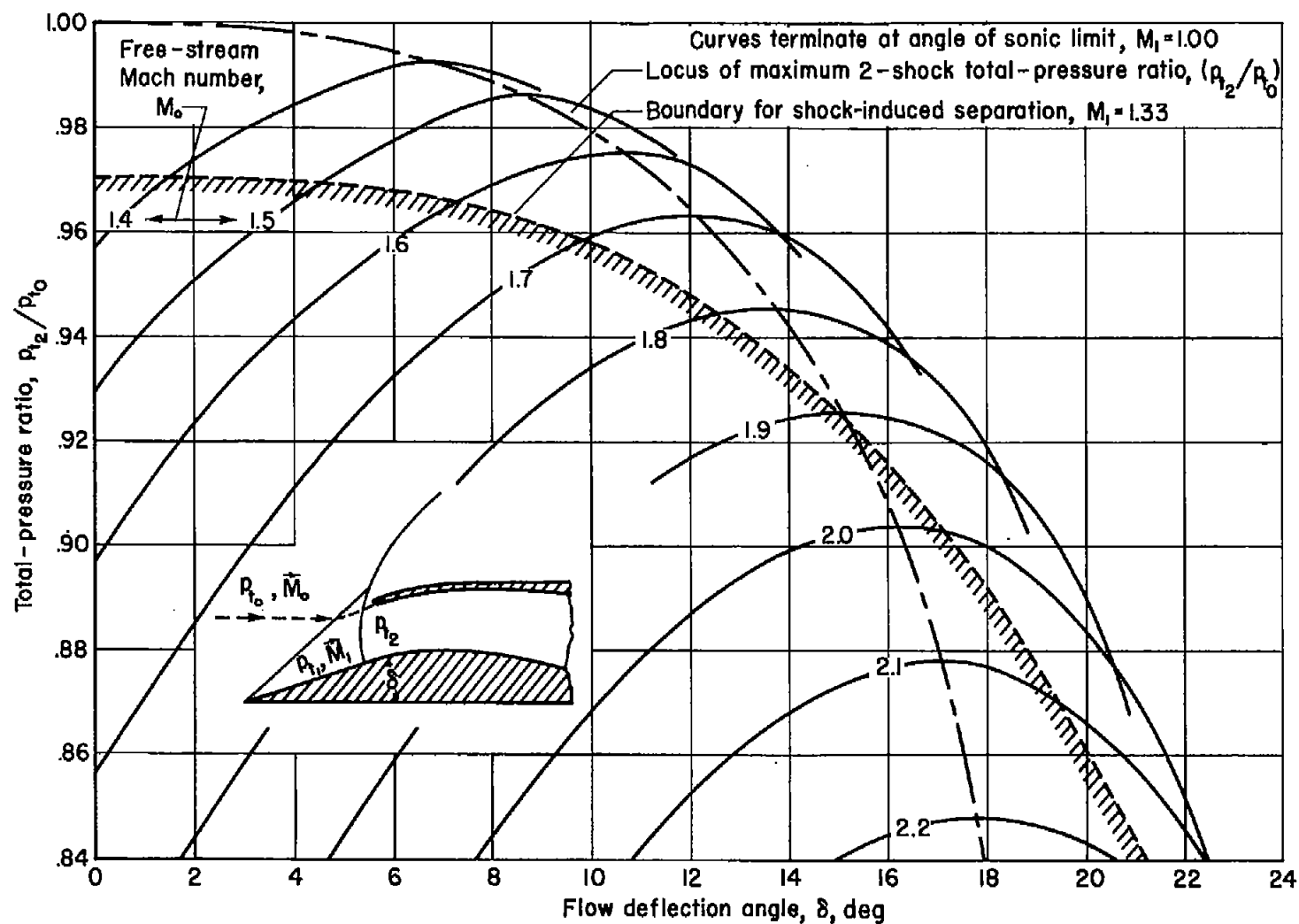


Figure 6.- Total-pressure ratios for two-dimensional two-shock compression.

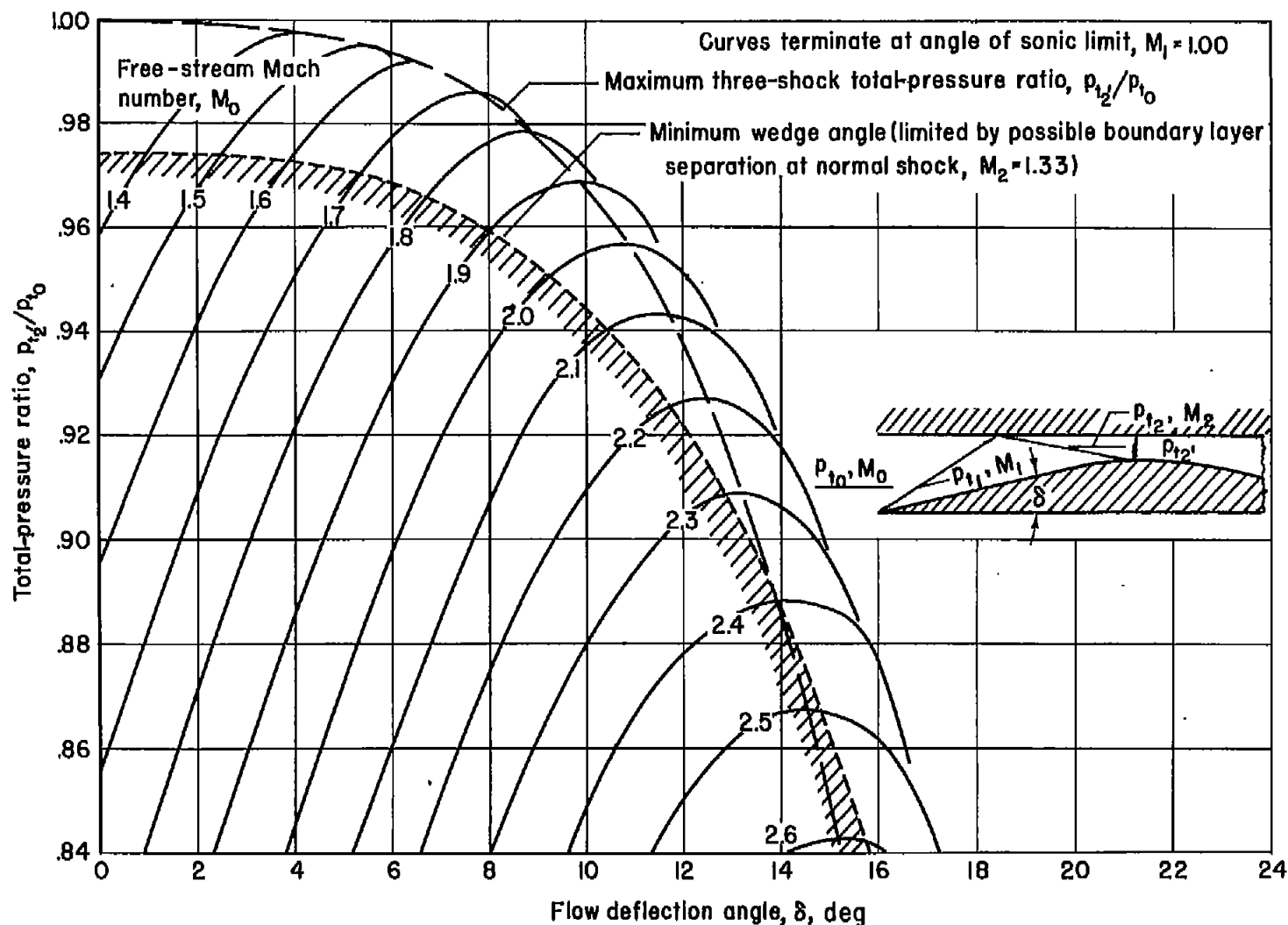


Figure 7.- Total-pressure ratios for conical two-dimensional three-shock compression.



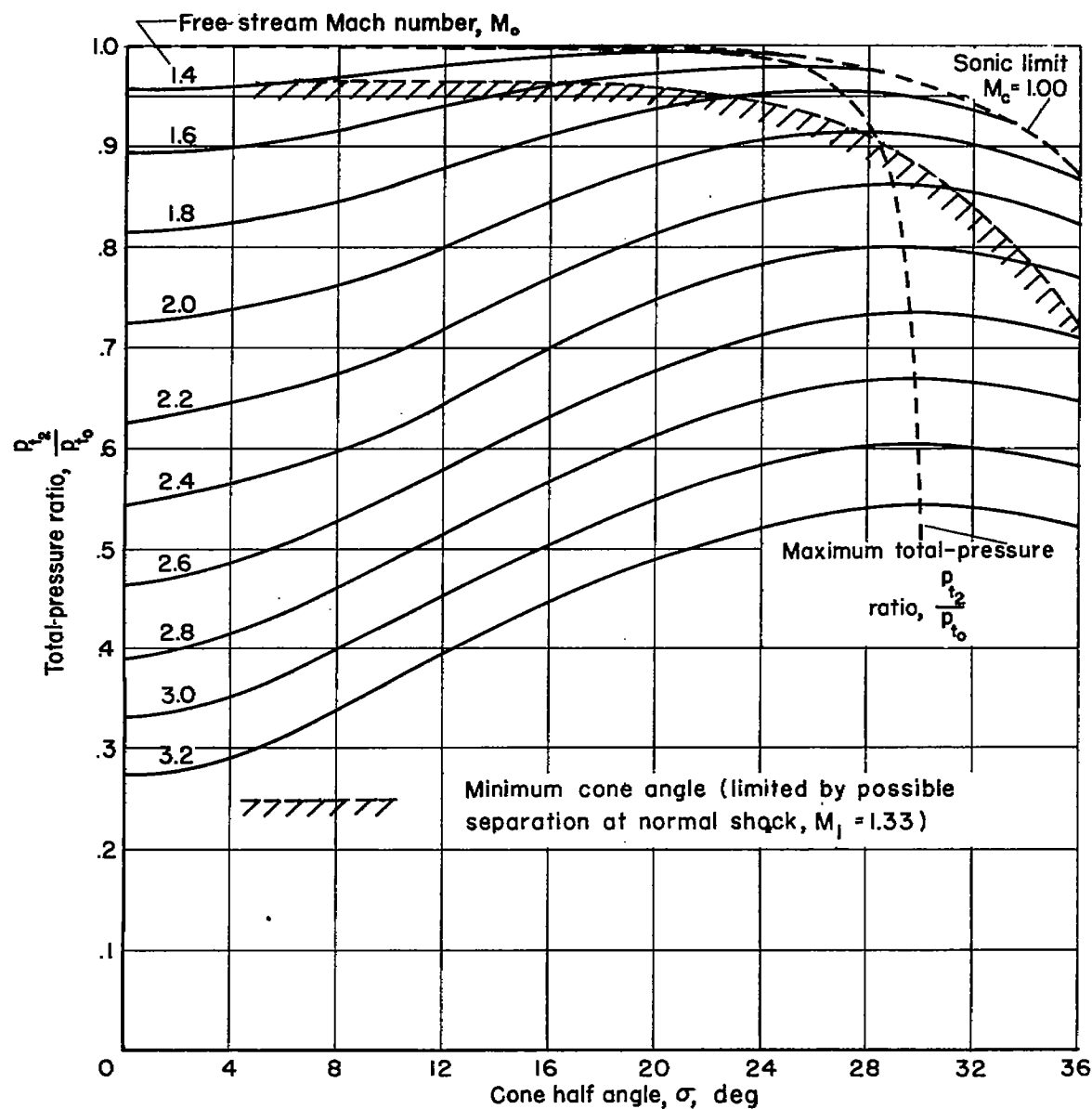


Figure 8.- Total-pressure ratios for conical two-shock compression.

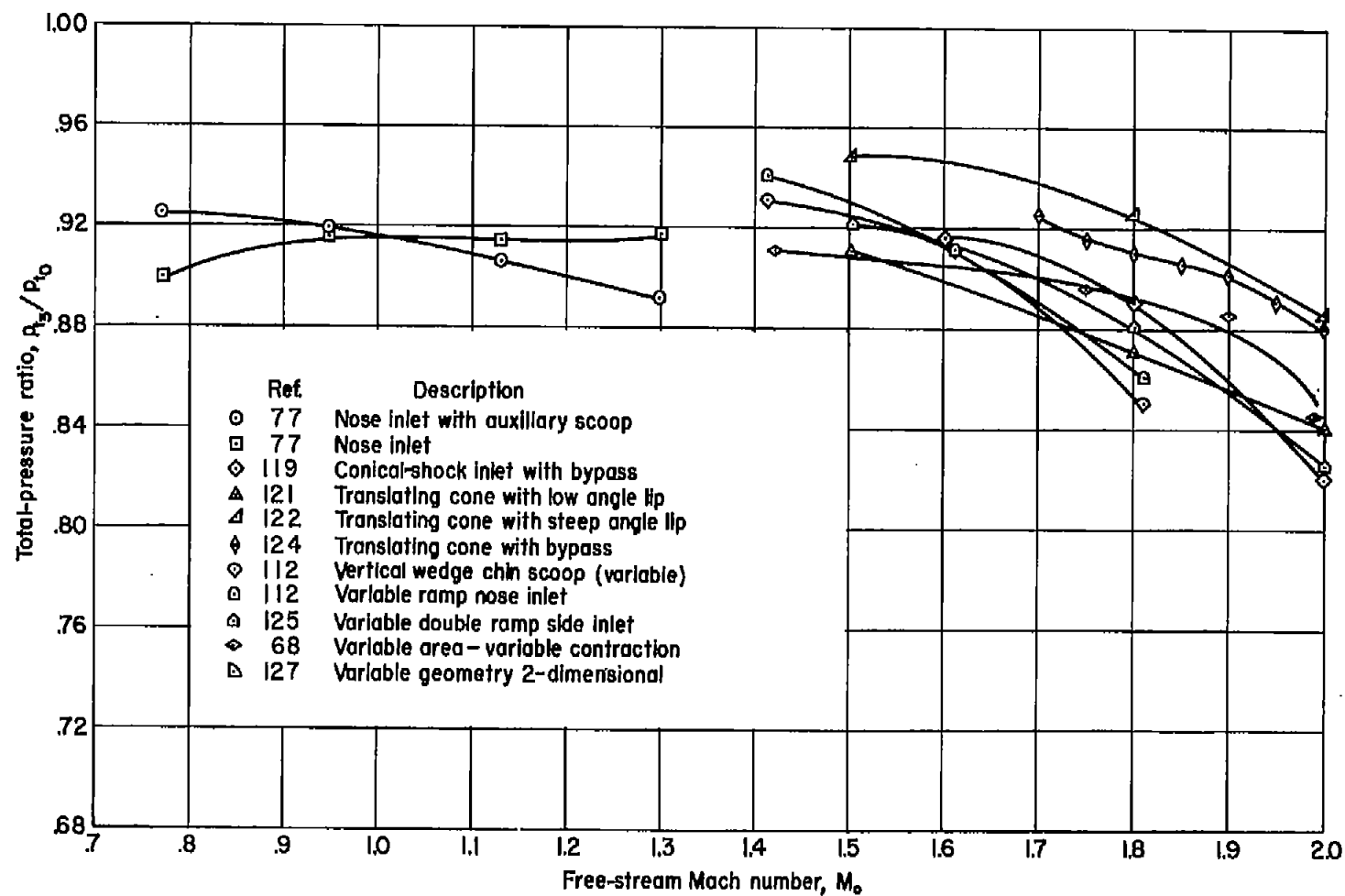


Figure 9.- Summary of data for various systems for maintaining high total-pressure ratios over a range of Mach numbers.

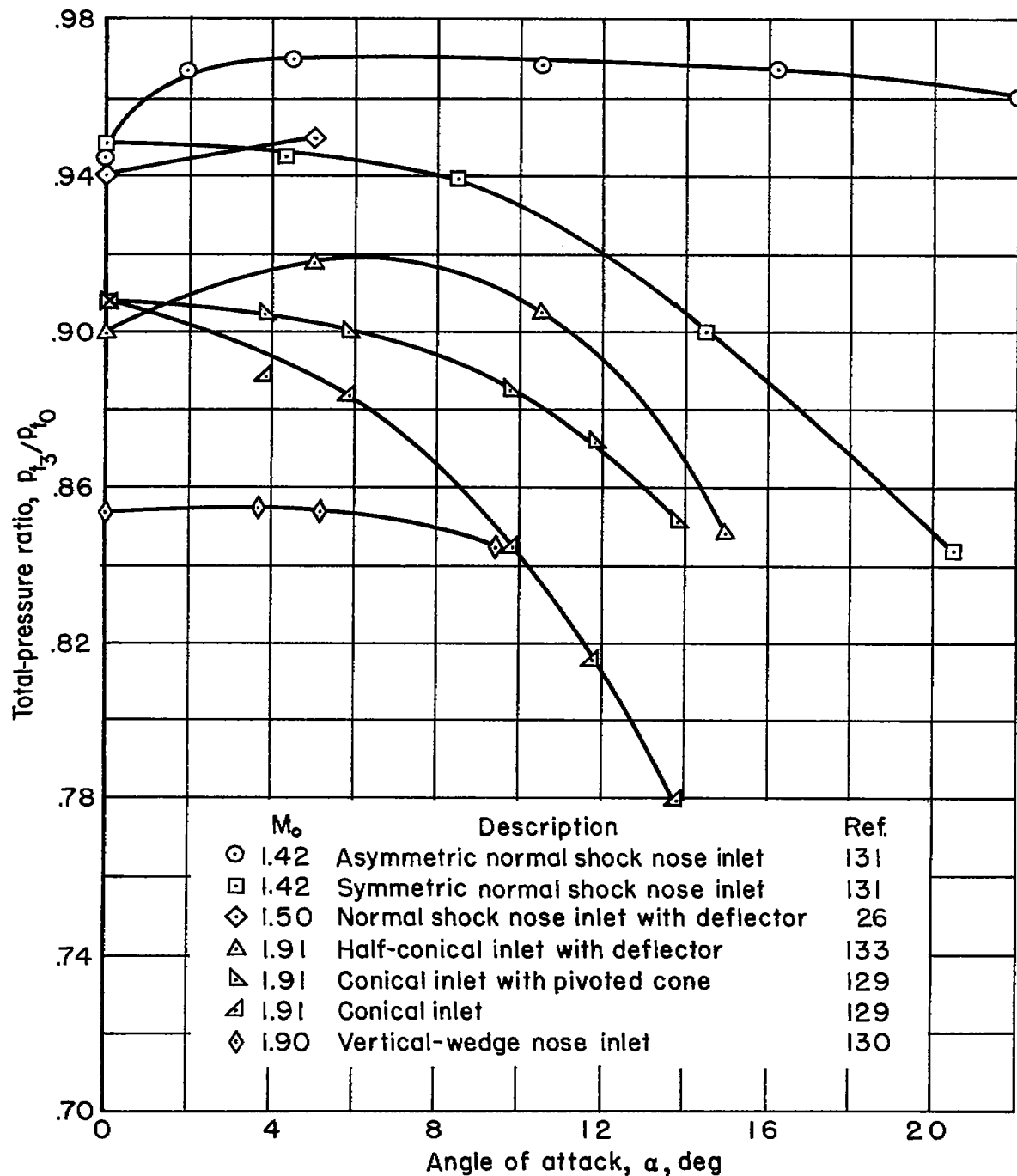


Figure 10.- Summary of data for the variation of total-pressure ratio with angle of attack.

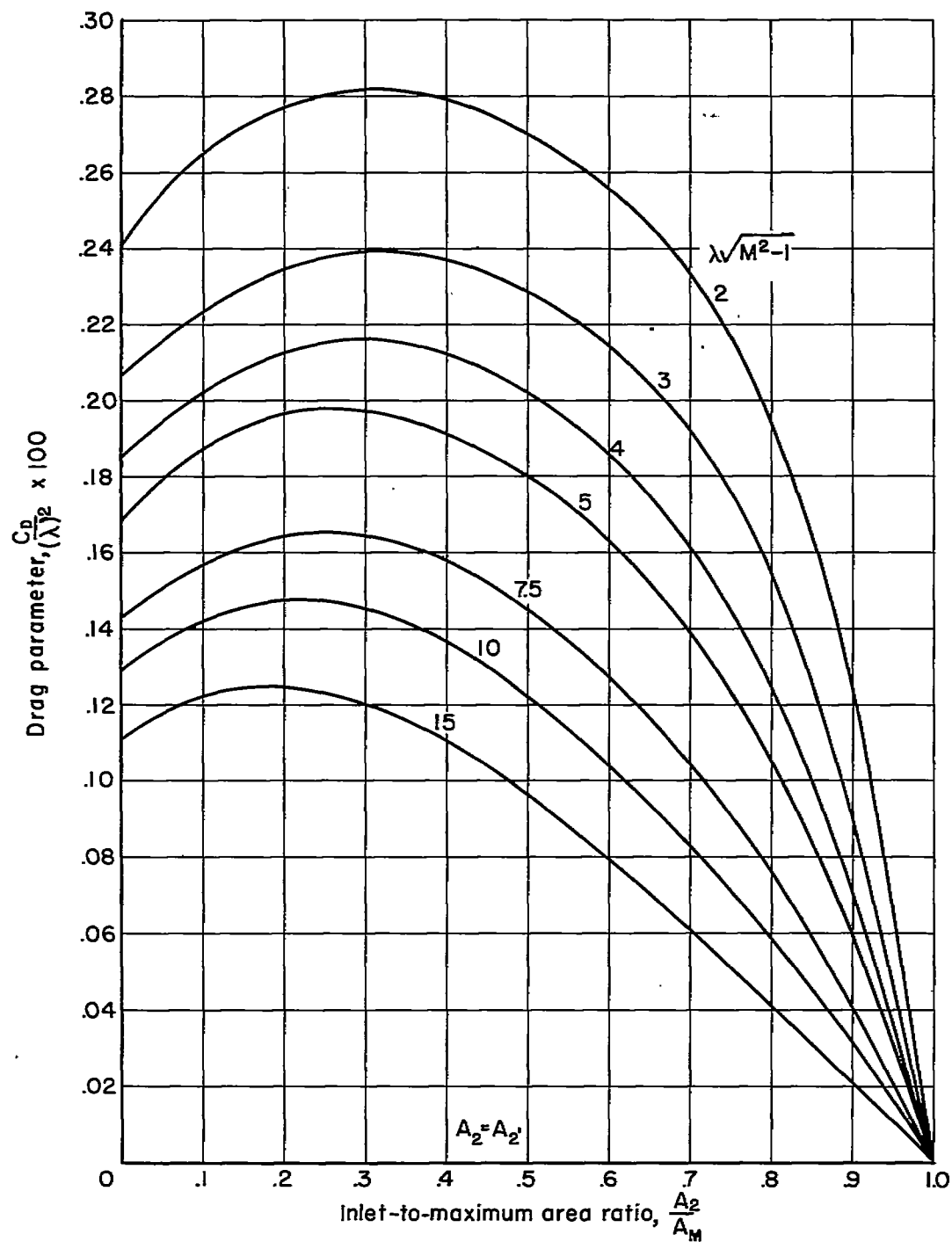


Figure 11.- Theoretical variation of drag coefficient with area ratio for conical cowls.

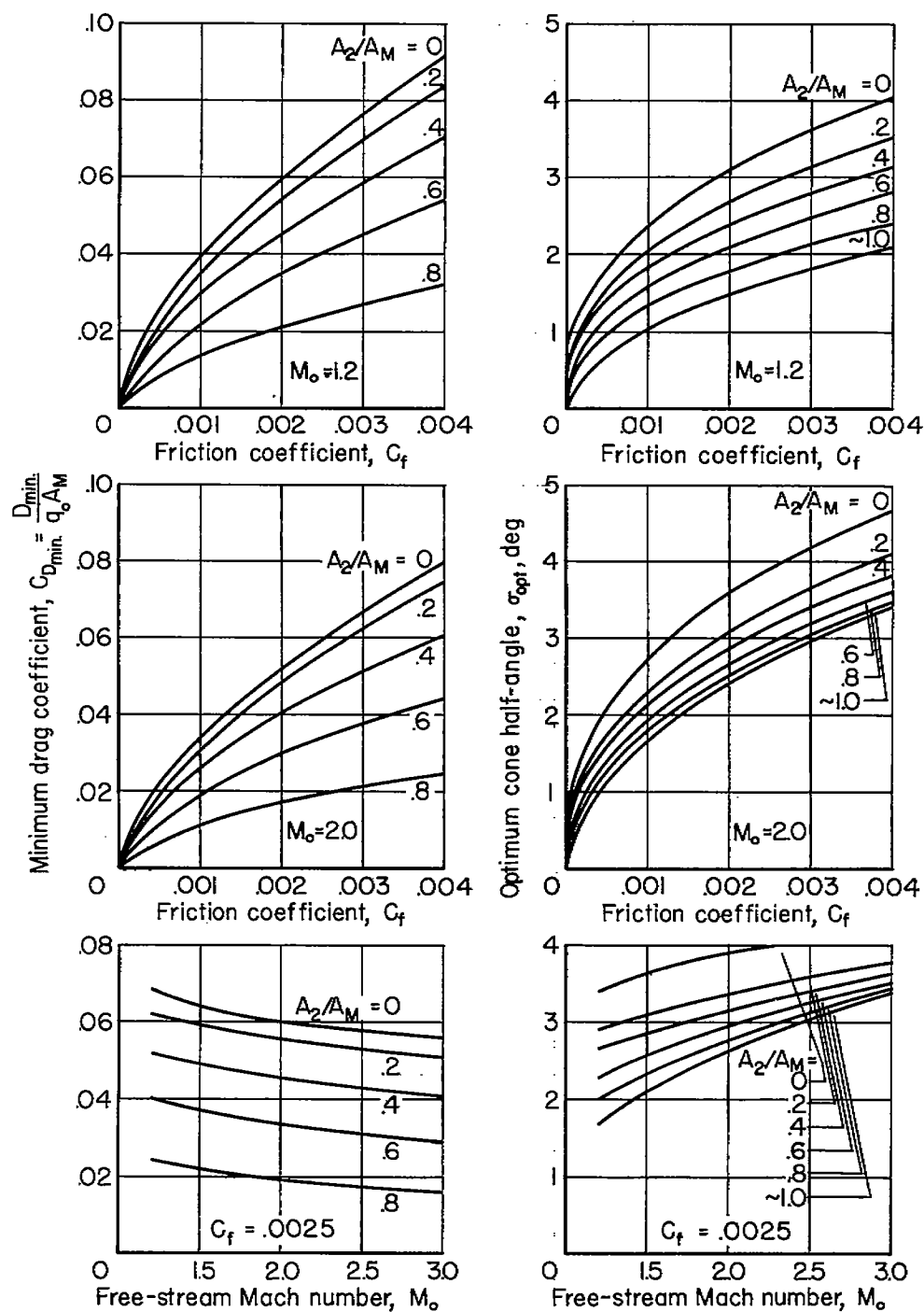


Figure 12.- Theoretical variation of minimum drag coefficient and optimum cone half-angle for conical cowls.

CONFIDENTIAL

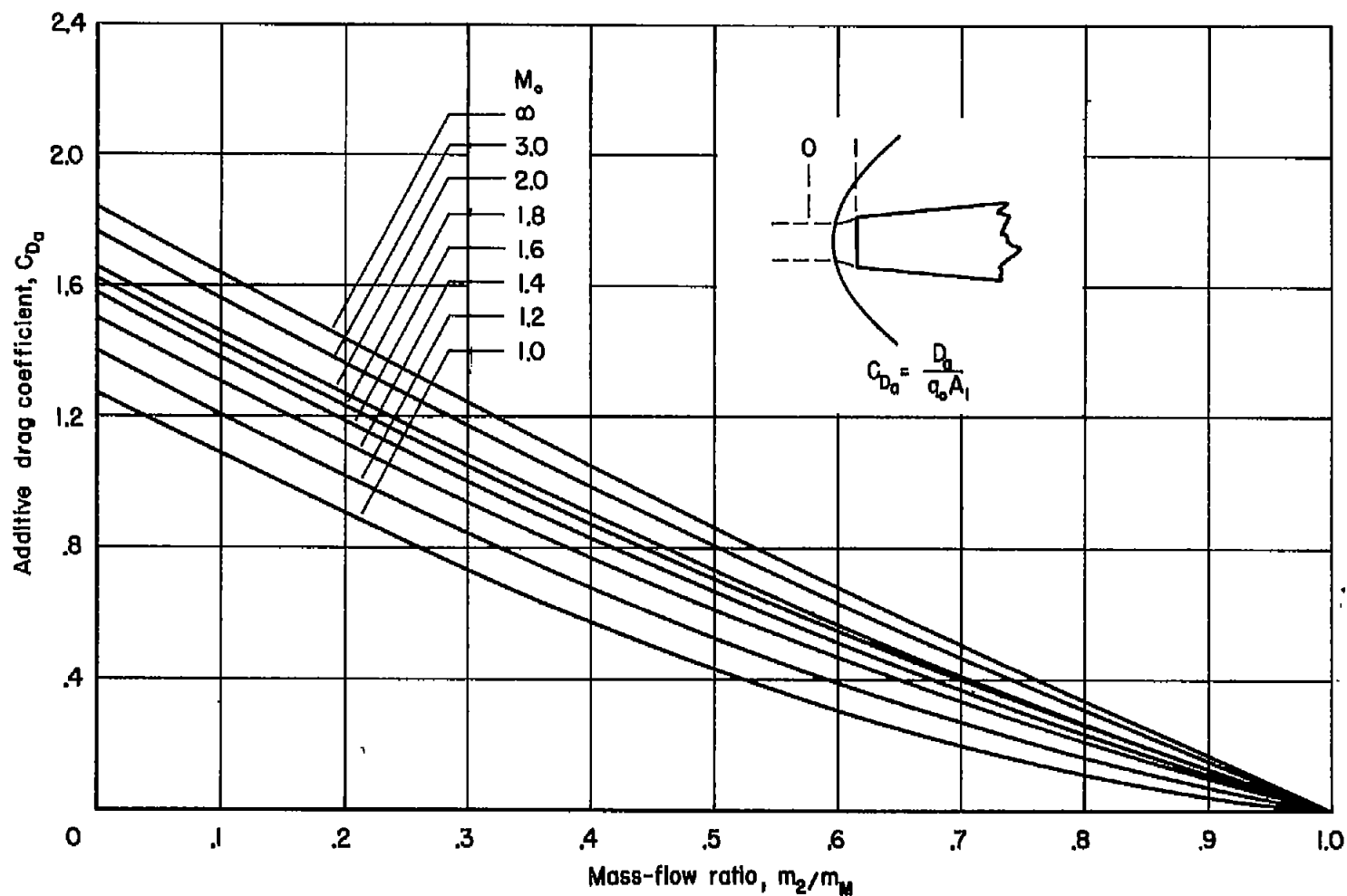


Figure 13.- Theoretical variation of additive drag coefficient for open-nose sharp-lip inlets.

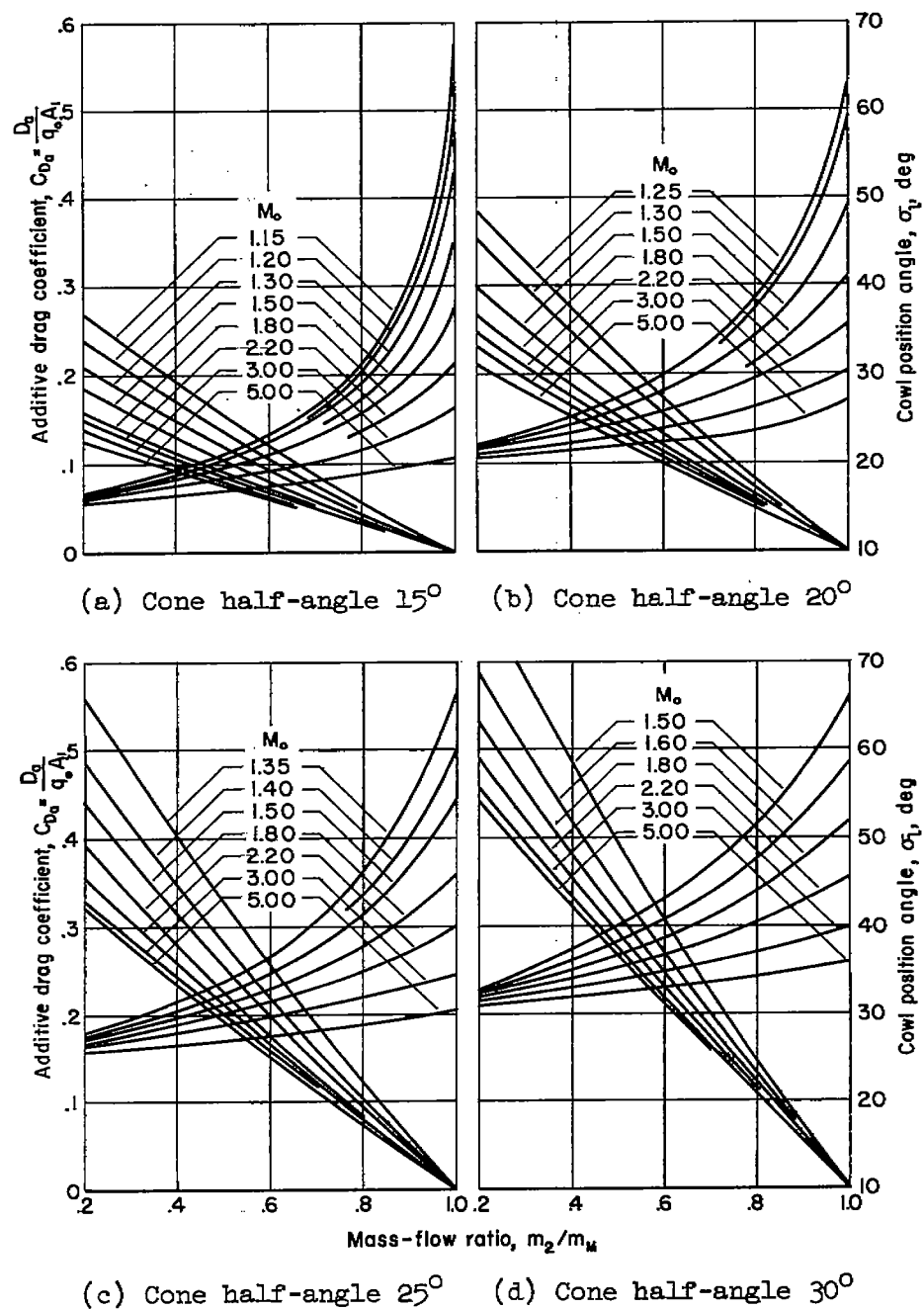


Figure 14.- Theoretical variation of additive drag coefficient and cowl position angle for conical-shock, sharp-lip inlets.

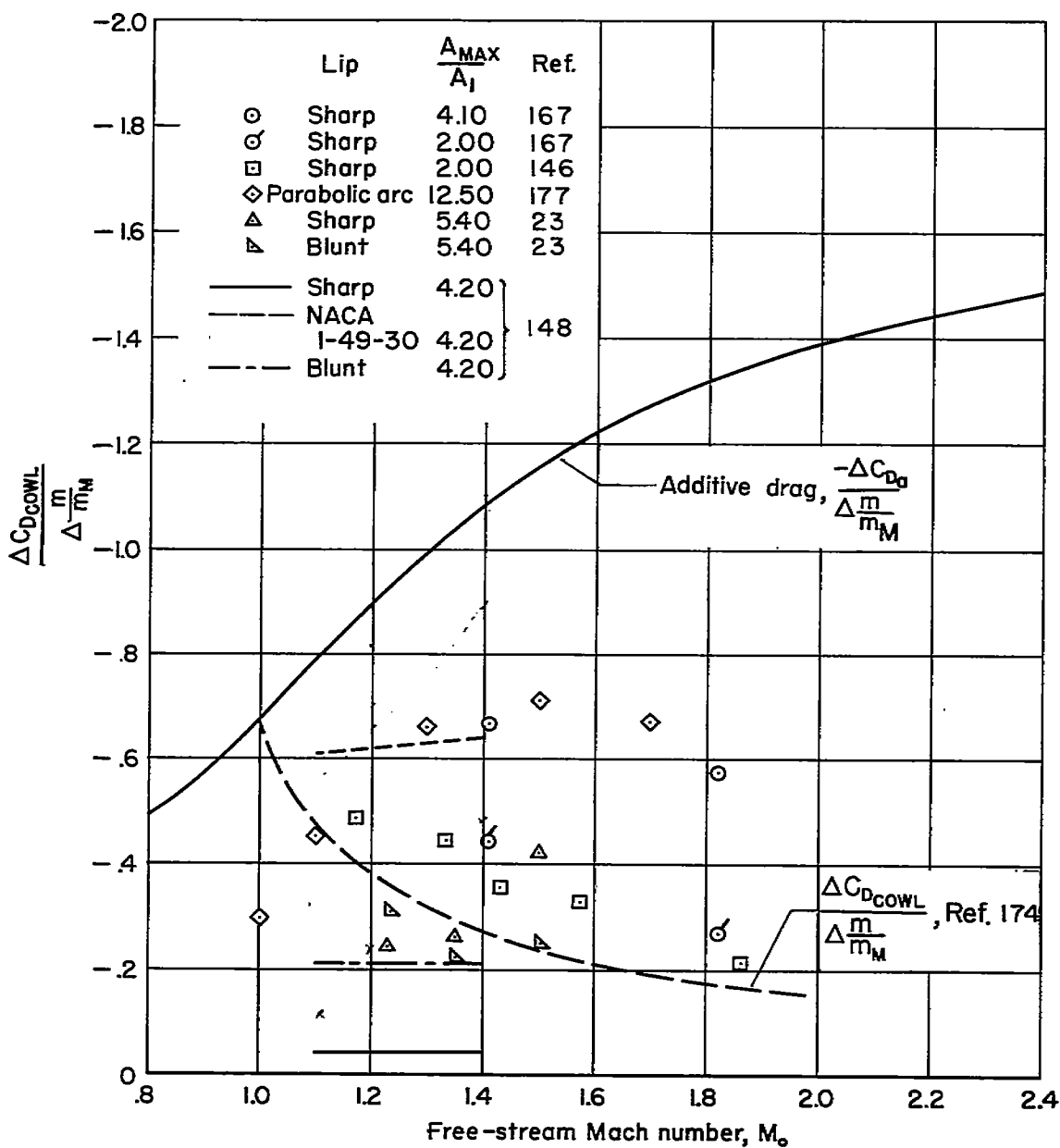


Figure 15.- Summary of data for cowl suction force and comparison with theory.